

AD-A199 375

DTIC FILE COPY

4

RADC-TR-88-30
Final Technical Report
May 1988



BISTATIC CLUTTER PHENOMENOLOGICAL MEASUREMENT/MODEL DEVELOPMENT

SRS Technologies

Sponsored by
Defense Advanced Research Projects Agency
DARPA Order No. 5462

DTIC
ELECTE
SEP 14 1988
S H D

APPROVED FOR PUBLIC RELEASE; DISTRIBUTION UNLIMITED.

The views and conclusions contained in this document are those of the authors and should not be interpreted as necessarily representing the official policies, either expressed or implied, of the Defense Advanced Research Projects Agency or the U.S. Government.

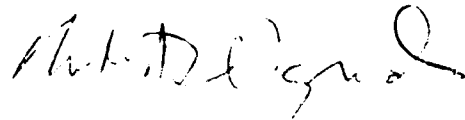
ROME AIR DEVELOPMENT CENTER
Air Force Systems Command
Griffiss AFB, NY 13441-5700

88 2 20 0 8

This report has been reviewed by the RADC Public Affairs Division (PA) and is releasable to the National Technical Information Service (NTIS). At NTIS it will be releasable to the general public, including foreign nations.

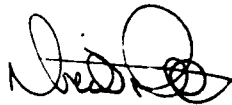
RADC-TR-88-30 has been reviewed and is approved for publication.

APPROVED:



ROBERT F. OGRODNIK
Project Engineer

APPROVED:



DAVID J. PRATT, Colonel, USAF
Director of Surveillance

FOR THE COMMANDER:



JOHN A. RITZ
Directorate of Plans & Programs

If your address has changed or if you wish to be removed from the RADC mailing list, or if the addressee is no longer employed by your organization, please notify RADC (OCTM) Griffiss AFB NY 13441-5700. This will assist us in maintaining a current mailing list.

Do not return copies of this report unless contractual obligations or notices on a specific document require that it be returned.

BISTATIC CLUTTER PHONOMENOLOGICAL
MEASUREMENT/MODEL DEVELOPMENT

Charles H. Hightower
David M. Maeschen
Catherine A. Sanders-Foster

Contractor: SRS Technologies
Contract Number: F30602-86-C-0045
Program Code Number: 5E20
Effective Date of Contract: 1 April 1986
Contract Expiration Date: 30 September 1987
Short Title of Work: Bistatic Clutter Phenomenological
Measurement/Model Development
Period of Work Covered: April 1986 - September 1987

Principal Investigator: Charles H. Hightower
Phone: (714) 250-4206

RADC Project Engineer: Robert F. Ogrodnik
Phone: (315) 330-4431

Approved for public release; distribution unlimited.

This research was supported by the Defense Advanced Research
Projects Agency of the Department of Defense and was monitored
by Robert F. Ogrodnik (OCTM), Griffiss AFB NY 13441-5700 under
Contract F30602-86-C-0045.

UNCLASSIFIED

SECURITY CLASSIFICATION OF THIS PAGE

REPORT DOCUMENTATION PAGE				Form Approved OMB No. 0704-0188	
1a. REPORT SECURITY CLASSIFICATION UNCLASSIFIED		1b. RESTRICTIVE MARKINGS N/A			
2a. SECURITY CLASSIFICATION AUTHORITY N/A		3. DISTRIBUTION/AVAILABILITY OF REPORT Approved for public release; distribution unlimited.			
2b. DECLASSIFICATION/DOWNGRADING SCHEDULE N/A					
4. PERFORMING ORGANIZATION REPORT NUMBER(S) SRS UR88-014		5. MONITORING ORGANIZATION REPORT NUMBER(S) RADC-TR-88-30			
6a. NAME OF PERFORMING ORGANIZATION SRS Technologies		6b. OFFICE SYMBOL (if applicable)	7a. NAME OF MONITORING ORGANIZATION Rome Air Development Center (OCTM)		
6c. ADDRESS (City, State, and ZIP Code) 17252 Armstrong Avenue Irvine CA 92714		7b. ADDRESS (City, State, and ZIP Code) Griffiss AFB NY 13441-5700			
8a. NAME OF FUNDING/SPONSORING ORGANIZATION Defense Advanced Research Projects Agency		8b. OFFICE SYMBOL (if applicable)	9. PROCUREMENT INSTRUMENT IDENTIFICATION NUMBER F30602-86-C-0045		
8c. ADDRESS (City, State, and ZIP Code) 1400 Wilson Blvd Arlington VA 22209		10. SOURCE OF FUNDING NUMBERS			
		PROGRAM ELEMENT NO. 62301E	PROJECT NO. E462	TASK NO. 00	WORK UNIT ACCESSION NO. 03
11. TITLE (Include Security Classification) BISTATIC CLUTTER PHENOMENOLOGICAL MEASUREMENT/MODEL DEVELOPMENT					
12. PERSONAL AUTHOR(S) Charles H. Hightower, David M. Maeschen, Catherine A. Sanders-Foster					
13a. TYPE OF REPORT Final		13b. TIME COVERED FROM Apr 86 to Sep 87	14. DATE OF REPORT (Year, Month, Day) May 1988		15. PAGE COUNT 316
16. SUPPLEMENTARY NOTATION N/A					
17. COSATI CODES			18. SUBJECT TERMS (Continue on reverse if necessary and identify by block number) HBR Assessment Clutter-to-Noise		
FIELD	GROUP	SUB-GROUP			
17	09				
09	06				
19. ABSTRACT (Continue on reverse if necessary and identify by block number) This program examines the scattering phenomenology of low grazing angle bistatic clutter, as well as specifies the required measurement techniques and instrumentation for its calibrated measurements. Clutter models are proposed for measurement validation techniques.					
20. DISTRIBUTION/AVAILABILITY OF ABSTRACT <input checked="" type="checkbox"/> UNCLASSIFIED/UNLIMITED <input type="checkbox"/> SAME AS RPT <input type="checkbox"/> DTIC USERS			21. ABSTRACT SECURITY CLASSIFICATION UNCLASSIFIED		
22a. NAME OF RESPONSIBLE INDIVIDUAL Robert F. Ogrodnik			22b. TELEPHONE (Include Area Code) (315) 330-4431		22c. OFFICE SYMBOL RADC (OCTM)

TABLE OF CONTENTS

Section	Title	Page
1.0	Introduction	
1.1	Program Steps	1
1.2	HBR Assessment Panel	1
1.3	Final Report Organization	1
2.0	HBR Assessment Panel Findings	3
2.1	Measurement System Design	3
2.1.1	Clutter-to-Noise Ratio	3
2.1.2	Receiver Bandpass Filter Design	4
2.1.3	Antenna Pattern Analysis and Requirements	4
2.1.4	Coherency Requirements	7
2.1.5	Antenna Beam Registration Analysis	7
2.1.6	Receiver Dynamic Range	8
2.2	Measurement System Accuracy	9
3.0	Clutter Model Definition	12
3.1	Mean Reflectivity Models	12
3.1.1	Kirchhoff Model	12
3.1.2	Perturbation Theory Model	13
3.1.3	Composite Model	13
3.1.4	Barton Model	13
3.2	Clutter Statistical Models	13
3.2.1	Beckmann's Statistical Model	14
3.2.2	Monte Carlo Statistical Fluctuation Model	14
3.3	Data Requirements	14
3.3.1	Estimation of the Mean	14
3.3.2	Hypothesis Testing	15
3.4	Clutter Workstation	16
4.0	Measurement System Description	17
4.1	ERIM Bistatic System	17
4.2	ERIM Monostatic System	18
4.3	Waveform and Channel Definition	18
4.4	Auxiliary Flight Data Collection Equipment	20
4.4.1	Aircraft Positioning System	20
4.4.2	Active Radar Calibrator (ARC) System	20
4.4.3	Antenna Pattern Measurement System	21
4.5	Ground Truth Instrumentation	21
4.5.1	Ground Truth Measurement Requirements	21
4.5.2	Ground Truth Measurement Equipment	22
5.0	Site Selection	24

5.1 Michigan Site	24
6.0 Signal Processing Software	27
6.1 Computer Compatible Tape Format Definition	27
6.1.1 Computer Compatible Tape Characteristics	27
6.1.2 Computer Compatible Tape Data Format	27
6.2 Signal Processing Software Description	28
6.2.1 Signal Processing Software Function Definition	29
References	31
SRS Technical Report Supplement	33

1.0 INTRODUCTION

This document is the Final Technical Report for the Bistatic Clutter Phenomenological Measurement/Model Development program sponsored by Rome Air Development Center (RADC) and the Defense Advanced Project Agency (DARPA) under Contract No. F30602-86-C-0045. The objectives of this program are to provide technical analyses, test planning, and participation in the collection of near-simultaneous bistatic and monostatic clutter data in support of the DARPA Hybrid Bistatic Radar (HBR) concept.

1.1 PROGRAM STEPS

The SRS Technologies effort was organized into four distinct steps by the Statement-of-Work. These steps included:

- Step I System Design and Analysis, Theoretical Modeling, and Test Plan and Schedule Development
- Step II Detailed Experiment and Flight Test Planning, Implementation of Data Processing and Theoretical Modeling, and Experimental Measurement System Integration Consultation
- Step III Analysis Tools Demonstration
- Step IV Flight Test Participation, Ground Truth Collection, and Data Analysis.

1.2 HBR ASSESSMENT PANEL ANALYSES

In addition to steps called for in the Statement-of-Work, SRS was directed early in the program to perform technical evaluation and analyses in support of a DARPA HBR Assessment Panel. The first HBR Assessment Panel meeting was held on 7 August 1986 at Decision Science Applications (DSA) offices in Arlington, Virginia under the direction of Mr. Neal Doherty of DARPA. Additional HBR Assessment Panel meetings were held on 3 September 1986, 22 September 1986, 8 October 1986, and 21 October 1986 (refer to SRS deliverables, Minutes of Formal Reviews, Inspections and Audits, ELIN A005 for minutes of these meetings).

The objectives of the Assessment study were (1) assess the adequacy of the Environmental Institute of Michigan (ERIM) proposed data collection equipment and procedures to provide data allowing the performance of HBR to be determined, and (2) assess the adequacy of ERIM equipment and procedures to characterize clutter phenomenology, especially as it pertained to HBR.

1.3 FINAL REPORT ORGANIZATION

This Final Report is organized as follows. Section 2.0 contains a summary of findings and technical recommendations made by SRS

Technologies during the HBR Assessment Panel period. Results of work on Steps I - III are presented in the remaining sections beginning with Clutter model definitions and associated issues in Section 3.0. A brief summary of the ERIM data collection system is contained in Section 4.0. Clutter data collection site recommendations and geometries are developed in Section 5.0. Due to the early redirection of the program involving the support of a DARPA HBR Assessment Panel, delays were caused in the development and integration of the ERIM data collection equipment. As a result, no flight data was made available to support Step IV of the present program. However, Section 6.0 concludes the Final Report with a description of the Computer Compatible Tape (CCT) format and signal processing software developed to support analysis when clutter data is eventually made available.

Numerous references to SRS Technologies documents created during this effort are found in the text. For ease of reference, we have included these documents in a supplement at the end of the Final Report.

2.0 HBR ASSESSMENT PANEL FINDINGS

As mentioned in the preceding section, there were two main objectives associated with the HBR Assessment Panel meetings and studies. SRS Technologies was principally involved with the second objective, namely, "assess the adequacy of ERIM equipment and procedures to characterize clutter phenomenology, especially as it pertained to HBR" because this issue directly impacted clutter modeling, test planning, and data analysis.

2.1 MEASUREMENT SYSTEM DESIGN

A number of critical measurement system design parameters were identified during the HBR Assessment Panel meetings which were investigated by SRS Technologies. A summary of the more significant analyses and results is presented in the following.

2.1.1 Clutter-to-Noise Ratio

One of the most critical parameters in the design of the ERIM data collection system is the Clutter-to-Noise Ratio (CNR) since this factor directly impacts the quality of the recorded data. Because ERIM data collection instrumentation is constrained by cost considerations to relatively modest modifications of existing hardware, the primary factors under control of the system designer influencing CNR are pulsewidth and measurement geometry. The latter is largely constrained by the requirement to simulate HBR geometries. Thus, the only significant system parameter that can be easily changed to increase CNR is the transmitted pulsewidth (with a concomitant adjustment in receiver bandwidth). The radar range equation shows that increasing pulsewidth will increase the clutter signal while narrowing the receiver noise bandwidth resulting in an improvement factor which is proportional to the square of the pulsewidth change.

Selection of an optimum pulsewidth for bistatic clutter measurements is complicated by conflicting requirements. First, illumination of a reasonably large clutter area is needed so that the clutter return will not be corrupted by receiver noise. This can be achieved by increasing the pulsewidth until a suitable CNR is obtained. However, the width of this pulse is severely limited by the low grazing angles associated with the bistatic geometry required to emulate HBR. This limit is due to the requirement that the direct path signal not interfere with the signal arriving from the desired clutter regions.

Examination of the Clutter Measurement Program measurement geometries proposed for HBR simulation (SRS UR86-199) indicated that a bistatic pulsewidth of 125 nanoseconds would provide a CNR of 22 dB for a clutter return of 23.3 dBsm and provide direct path isolation in excess of 76 nanoseconds for all measurement geometries. This was felt to be reasonable system design goal.

2.1.2 Receiver Bandpass Filter Design

The problem addressed in this analysis was the optimization of transmitter waveform and receiver matched filter design to achieve maximum CNR. This problem is complicated by the potentially large amplitude gradients in the clutter return which might cause matched filter "ringing" and inaccurate measurements of clutter radar cross section (RCS) between range gates. Discussions with ERIM and DSA personnel led to several assumptions for this analysis. First, it was felt that a second order Butterworth filter would be representative of filter performance in the actual system. Secondly, based on the foregoing analysis, a bistatic pulse duration of about 125 nanoseconds would provide a reasonable CNR for the expected experimental geometry.

The specific issue addressed was the determination of an optimum Butterworth filter bandwidth which minimized the clutter gradient ringing problem while preserving a high CNR. The analysis was based on computer simulation of the response of a two-pole Butterworth filter to a radar waveform provided by ERIM (the pulse was characterized by 50 nanosecond rise and fall times with a plateau duration of 75 nanoseconds). The conclusion of this analysis was that a Butterworth filter with an 8 MHz bandwidth be used for the bistatic return with an optimal range-gate sample interval of 160 nanoseconds. This combination of system parameters would provide approximately 30 dB isolation between range gates.

2.1.3 Antenna Pattern Analysis and Requirements

2.1.3.1 Antenna Pattern Analysis

An examination of antenna patterns made by Chu Associates for the existing dual feed, seven-element log-periodic L-X band antenna proposed for use for the bistatic receiver aircraft was conducted (SRS UR86-198). This examination indicated a severe distortion in the horizontal polarization mainbeam pattern along with abnormally high near-in sidelobes at L-band (the frequency used for clutter measurements). Simulations were run to compare the effect of these distortions with that of an ideal antenna. It was found that the ratio of sidelobe to mainbeam power for a typical out-of-plane CMP geometry was about -26 dB for the ideal antenna and only -5.6 dB for the simulated Chu antenna pattern. This indicated that the antenna would be unacceptable for accurate clutter measurements.

Because of this finding, the Naval Air Development Center (NADC) performed an independent set of antenna element and far-field pattern measurements. Their results indicated no major discrepancies with the feed elements and that the "distortion/null in the H-plane does not exist." Consequently, it was decided that the original measurements were in error and the antenna was suitable for CMP use.

2.1.3.2 Antenna Analysis and Requirements

The dual polarization L-band antenna described in Section 2.1.3.1 has a 17 dBi gain, 60 degree elevation beamwidth, and 10 degree azimuth beamwidth. Sidelobe levels for both polarizations in both the elevation and azimuthal cuts are on the order of -11 dB to -14 dB with polarization isolation around 20 dB. It was clear that these antennas were designed primarily for airborne side-looking imaging and not for precision measurement of clutter phenomenology. The large elevation beamwidth is intended to provide a wide range swath for imaging with the narrower azimuth beam processed to provide synthetic resolution in the cross-track direction. Thus, it was important to determine if there were any serious limitations imposed by this antenna when used for other purposes such as clutter data collection.

2.1.3.2.1 Mainbeam Gain

The antenna gain must be adequate to yield an adequate CNR for the design values of the remaining system parameters included in the bistatic range equation (SRS UR86-197). In arriving at the 22 dB CNR mentioned in paragraph 2.1.1, both the transmitter and receiver antenna gains were assumed to have gains of 16.5 dB. This figure appears to be conservative based on the original Chu Associates measurements which indicate this number is typical of the horizontal polarization with the vertical polarization gain one to two dB's higher.

2.1.3.2.2 Antenna Sidelobes

In determining clutter reflectivity from measured radar cross section (RCS) data, it is generally assumed that the received power is not contaminated by energy received through the sidelobes. Sidelobe power can be minimized by various aperture weighting techniques at the expense of gain and beamwidth. However, the ERIM antennas do not incorporate aperture weighting. Consequently, SRS explored the effect of unweighted sidelobes on clutter measurement accuracy (SRS UR86-197).

A computer simulation using diffraction limited antenna patterns conforming to ERIM provided antenna parameters was used to investigate this problem. The percentage of sidelobe power for nominal geometries at ranges of interest relative to the mainbeam power was computed taking into account the variation of bistatic range over the illuminated region. It was found that this ratio varied from -10.3 dB for a typical in-plane scenario to -26 dB for an out-of-plane geometry. The low value for the out-of-plane geometry can be attributed to the two-way bistatic antenna geometry where the majority of sidelobe energy results from the intersection of the mainbeam with only one set of near-in sidelobes of the opposite facing antenna. This is different than the in-plane geometry where the sidelobes intersect each other.

These ratios indicate that sidelobe interference is not negligible and could be exacerbated by geometries or terrain exhibiting high reflectivity in the sidelobe regions. This problem may be avoided by careful experiment planning. However, a more practical solution is to take advantage of the difference in doppler frequencies between the sidelobe and mainbeam clutter. Hence, it was recommended that the data be coherently processed to minimize the effect of sidelobe clutter on the clutter measurements.

2.1.3.2.3 Cross-Polarization Response

According to the Chu Associates data, the ERIM L-band antenna cross-polarization ratios varied with frequency in both elevation and horizontal cuts. In general, it appears likely that a polarization ratio better than 20 dB can be achieved, although values as low as 12.8 dB were measured at their facility. The lower values are probably due to the same problem that affected the overall pattern measurements and are not representative of actual antenna performance.

This parameter is of concern since it impacts validation of clutter models that predict both principal polarization and cross-polarization clutter levels. This is especially true for an in-plane geometry since physical optics scattering theory predicts no depolarization is possible. If this model is valid, then no cross-polarization return should be observed. This will not be the case for the ERIM antenna because of its finite polarization ratio. What will be observed, instead, is an image of the opposite polarization attenuated by the isolation ratio. This limitation must be kept in mind when analyzing the data.

Mitigating this effect somewhat is the limited out-of-plane region where little or no clutter depolarization is expected. Examination of physical optics clutter models indicate this region is about 10 degrees wide. Beyond this angle the principal and cross polarization returns begin to approach the same order of magnitude.

2.1.3.2.4 Antenna Calibration

Knowledge of the antenna patterns in two-dimensional space is needed to accurately convert the received signal to clutter reflectivity. An analysis was performed to examine the effect of mainbeam gain "ripple" on the conversion process. The mainlobe was modeled by a sinc pattern and perturbed with a sinusoidal ripple having a varying number of cycles across the mainbeam. It was found that mainbeam gain pattern ripple less than 1 dB did not affect reflectivity computation significantly. This conclusion may be somewhat optimistic since the zero-mean nature of the perturbing sinusoid may not be an accurate model of the real mainbeam gain variation. However, it should serve as a guideline for the accuracy of ERIM antenna pattern calibration techniques.

2.1.4 Coherency Requirements

From the discussion in the preceding paragraphs it is clear that reduction of sidelobe clutter is necessary to preserve clutter measurement accuracy for its intended purpose of reflectivity coefficient generation. Consequently, an analysis was performed to examine requirements for signal frequency stability and platform motion compensation; factors that affect coherent processing. The figure-of-merit used in the analysis was the restriction that the error source result in no more than a 10% shift of the processed doppler cell center frequency relative to the ideal doppler frequency during the processing interval.

The analysis approach was based on conventional synthetic aperture radar theory modified for bistatic geometry. Coherent processing requirements imposed on the measurement system were (1) a frequency stability of 1 part in 10^4 , (2) phase accuracy of $\lambda/10$, (3) aircraft velocity variation over the processing period of less than 0.3 m/s, and (4) aircraft platform acceleration over the same interval of less than 6.6 m/s^2 .

The first two requirements are exceeded by the proposed ERIM instrumentation. Discussions with ERIM personnel regarding items 3 and 4 indicate that these will not be exceeded in flight through relatively calm air. Since this may not always be the case, recording of the velocity and acceleration components of each platform was recommended.

2.1.5 Antenna Beam Registration Analysis

In the bistatic mode, clutter data will be obtained by pointing the transmitter and receiver antennas at a common point in a coordinate system moving with both platforms (i.e., beam registration). This ensures that the terrain illuminated can be later correlated with the recorded clutter data. Errors in beam registration will exist due to aircraft motion, Inertial Navigation System (INS) position and heading errors, servo system errors, and systematic errors associated with slight variations of the bistatic geometry.

Using a model of the bistatic measurement system, it was found that beam pointing accuracy of 1 degree or less and a position accuracy of 500 feet or less would limit the effect of beam registration errors on clutter measurement accuracy to less than 1 dB. Since the effect of these errors increases in a non-linear manner, they must not be allowed to exceed these values. In the ERIM system, special purpose signal processing software developed by SRS Technologies will be used in post mission processing to compensate for some of these errors.

2.1.6 Receiver Dynamic Range

SRS Technologies addressed the receiver dynamic range problem during the Assessment Panel period by examining potential bistatic clutter RCS variation and comparing these with limitations of the proposed ERIM instrumentation. It was found that an instantaneous dynamic range of about 73 dB was required to handle the expected range of clutter values over all polarizations. The assumption that the receiver noise is set just below the quantization level of the A/D convertor least significant bit for maximum sensitivity results in a requirement for a 25 bit A/D convertor (assuming linear quantization).

The existing ERIM system contains 6-bit A/D convertors which limit the maximum dynamic range achievable in the data collection system. With a 6-bit A/D convertor and noise set at the Least Significant Bit (LSB), the maximum dynamic range will be about 35 dB. Since this is less than the 73 dB requirement, a means to increase the system sensitivity was needed. SRS Technologies examined a number of alternatives including banks of flash A/D convertors, and logarithmic A/D conversion. One of the problems with these approaches was the ultra-short aperture time imposed by the signal 8 MHz bandwidth which inexpensive large word size A/D convertors do not possess. In addition, ERIM cost estimates for replacing the existing A/D convertors with a more suitable design were prohibitive.

A solution to this problem was suggested by Mr. Neil Doherty of DARPA and consisted of using "stepped gain" to provide increased system dynamic range. In this approach, the value of an attenuator in the receiver front-end is changed on alternate pulses for each channel. The attenuator's values are chosen to ensure that a signal within the desired dynamic range will be within the range of the 6-bit A/D convertor. Although this is a real-time adjustment, it should be possible to implement this technique during clutter data collection.

One of the risks associated with "stepped gain" is the possible loss of data in channels other than that used to set the attenuator. This will have to be considered during each mission and a reasonable compromise reached between system dynamic range and maximum data quantity.

Another consideration associated with limited dynamic range is clutter statistical fluctuation. For example, 90% of the time, Rayleigh clutter fluctuation will be limited to a range of 17 dB. However, since the "tails" of the probability density function are of interest, the receiver gain (or attenuation) must be set so that saturation does not occur when large clutter signals are received. On the other hand, the attenuation cannot be set so high as to place most signals near or into receiver noise. If clutter were Rayleigh, then an attenuation setting resulting in saturation less than 1% of the time would place the mean clutter power level at about 10 dB below the saturation level. Thus, with

a dynamic range of 35 dB (assuming noise is not the limiting factor), clutter levels 25 dB below the mean value could be recorded with the ERIM instrumentation.

2.2 MEASUREMENT SYSTEM ACCURACY

One of the most critical questions arising during the Assessment Panel Study was the accuracy of the ERIM data collection system. Of the numerous ways to address this problem, SRS chose to analyze the problem in terms of independent error sources in the expression for clutter reflectivity (σ^0). This expression is

$$\sigma_{p,q}^0 = \frac{P_{c,q}}{P_{t,p}} \frac{1}{KI}$$

where,

$P_{c,q}$ = received power on qth polarization

$P_{t,p}$ = power transmitted on pth polarization

and,

$$K = \frac{L_p L_q G_{A0} G_{B0} \lambda^2}{(4\pi)^2}$$

$$I = \int_{A_c} \frac{f_A(x,y) f_B(x,y)}{R_A^2 R_B^2} dx dy$$

where,

L_p, L_q = receiver and transmit path and system losses

G_{A0}, G_{B0} = receive and transmit antenna axial gains

λ = wavelength

$f_A(x, y), f_B(x, y)$ = antenna amplitude pattern at point x, y
 R_A, R_B = receiver and transmitter ranges from point x, y
 A_c = Illuminated clutter area.

It is clear from the formulation of the reflectivity expression that each of the terms is independent so that one can approximate the normalized error in reflectivity by the root-mean-square of the sum of the individual normalized error components or,

$$\frac{\Delta\sigma_{p,q}^o}{\sigma_{p,q}^o} = \sqrt{\left(\frac{\Delta P_{c,q}}{P_{c,q}}\right)^2 + \left(\frac{\Delta P_{t,p}}{P_{t,p}}\right)^2 + \left(\frac{\Delta K}{K}\right)^2 + \left(\frac{\Delta I}{I}\right)^2}$$

The terms on the right-hand side of this equation are seen to represent normalized errors in (1) the conversion of receiver voltage to receiver power in the qth polarization, (2) transmitted power in the pth polarization, (3) system propagation losses and mainbeam gains, and (4) clutter surface area integration weighted by antenna patterns, ranges, and clutter variation.

Discussions with ERIM and other independent analyses resulted in the system error budget contributions shown in Table 2-1.

Table 2-1 System Error Sources

Error Source	$\Delta P_{c,q}/P_{c,q}$	$\Delta P_{t,p}/P_{t,p}$	$\Delta K/K$	$\Delta I/I$
Rcvr Pwr Meas.	0.5 dB			
Rcvr Trans Gain	0.5 dB			
Rcvr Drift	0.5 dB			
Rcvr I&Q Channel				
Imbalance	0.5 dB			
Rcvr Nonlinearities	0.5 dB			
Rcvr Noise	0.5 dB			
ARC Calibration	2.0 dB			
Trans Pwr Meas		0.5 dB		
Trans Losses		1.0 dB		
Rcvr Ant Pattern			0.5dB	1.0 dB
Trans Ant Pattern			0.5 dB	1.0 dB
Beam Registration				1.0 dB

The worst case accuracy exists when the numbers in each column are correlated prior to the root-sum-square operation. If this is done, the resulting accuracy for the mean reflectivity coefficient is 4.0 dB. A more optimistic value is obtained if the above error

components are assumed uncorrelated; in this case the predicted system measurement system accuracy is 2.7 dB.

It must be emphasized that these predictions of system accuracy need to be updated when more information is available on the ERIM system. In particular, the error contributions due to the Active Radar Calibrator (ARC), receiver and transmitter antenna pattern measurements, and beam registration need to be updated when firm design information is available. They furthermore, assume that a number of systematic errors are removed by post-mission signal processing. However, the values used in Table 2-1 provide some insight into the anticipated accuracy of the ERIM instrumentation. The error range calculated is only slightly larger than that achieved under General Dynamics Large Bistatic Angle Radar Cross Section Measurements Program.

3.0 CLUTTER MODEL DEFINITION

The solution to the problem of modeling reflection of a plane wave at the boundary of an irregular and inhomogeneous surface has been attempted by many researchers over the past several decades (Beckmann 63; Ruck 70; Barton 74; Papa, RADC-TR-84-78; Lennon, RADC-TR-84-195) with various degrees of success. Such models range from simple curve fitting of empirical data to elegant mathematical solutions of Maxwell's equations. Models for sea, land, ice and vegetation covered terrain have been proposed and compared to available monostatic radar data with some success. However, little work has been accomplished in the comparison of bistatic radar data with theoretical predictions. Consequently, SRS Technologies, has identified a number of bistatic clutter models for subsequent comparison with clutter data collected under the Clutter Measurements Program (CMP) in support of the Hybrid Bistatic Radar Program.

These models are also valuable in planning CMP measurements even though they have not been validated since they will provide some idea of the clutter magnitude to be expected. This is important information because of the dynamic range issue described in Section 2.0. Consequently, SRS developed a computer workstation that incorporates these models including SRS extensions such as shadowing and layering.

3.1 MEAN REFLECTIVITY MODELS

Perhaps one of the most important functions of a clutter model is that it allows transformation of terrain physical and electrical properties (e.g., surface heights, correlation distances, permittivity, layering, etc.) into electrical parameters from which radar performance can be deduced. Because of this, those models which are developed from Maxwell's equations are extremely valuable. In this category are the Kirchhoff (Physical Optics) and Perturbation theory models. These are sometimes referred to as "large-scale" and "small-scale" clutter models by RADC personnel at Griffis Air Force Base. These models have been documented in (SRS TM86-103 and TM87-005).

3.1.1 Kirchhoff Model

Models derived from the Kirchhoff integral, which is a simplified form of the Vector Green's Theorem, for scattering from a boundary have been shown to agree fairly well with measured backscatter data (Beckmann 63). Consequently, they may also be applicable to the bistatic case and certainly should be candidates for examination. These models are applicable for terrain where the RMS surface height fluctuation is much larger than the wavelength of interest. Variations of the model are possible by assuming different forms of the terrain surface height correlation function.

3.1.2 Perturbation Theory Model

Another model based on Kirchhoff's Integral exists for the condition where the surface height standard deviation and correlation length are smaller than a wavelength (SRS TM86-103). These models are based on the assumption that the surface can be described by a random surface which is Fourier-transformable. Variations of the model are possible by assuming different forms of the terrain surface height correlation function.

3.1.3 Composite Model

The Kirchhoff model and Perturbation models represent scattering from two classes of surfaces. Namely, those that are rough compared to a wavelength and those that are fairly smooth in relation to a wavelength. In addition, the derivations for both models neglect the effect of incident and reflected wave blockage by undulations of the surface (i.e., shadowing) which are of importance at low grazing angles. Since actual terrain may consist of both types of surfaces, it is natural to formulate a model which is the weighted sum of the two models with each model including an appropriate shadow function. This has been accomplished by SRS through extension of Sancer's (Sancer 69) approach for shadowing from a randomly rough surface.

It is possible to include layering effects in these models through the modification of the complex surface permittivity inherent in the models. Thus, surfaces covered with vegetation may be modeled as can ice covered water, among others. This was done by SRS for the Kirchhoff large-scale model since it was felt that modeling of vegetation or ice-covered trundra or sea water were important for HBR feasibility studies.

3.1.4 Barton Model

The Barton Model (Barton 74) is a relatively simple intuitive model of clutter scattering that can be applied to bistatic geometry. Its intended use was to aid in the evaluation of diffuse scattering from rough terrain on low-angle radar tracking systems. Barton's model divides clutter scattering into two distinct regions as a function of bistatic angle. The first region exists when the bistatic bisector is less than the RMS surface slope. This is called the "glistening region." Outside this region, Barton's model is given by the geometrical mean of the monostatic backscattering coefficients which would exist at the receiver and transmitter sites independently. It appears that the Barton model is an experimental confirmation of the theory underlying the composite model described previously.

3.2 CLUTTER STATISTICAL MODELS

Clutter models described in the previous paragraphs are limited to the determination of the mean clutter reflectivity coefficient and do not provide any information on the statistical nature of the

coefficient. As before, a candidate model with a sound analytical basis is desirable in contrast to the assumption of an ad hoc probability density function.

3.2.1 Beckmann's Statistical Model

This problem has been addressed by Beckmann (Beckmann 63) in some detail. Beckmann based his analysis on the premise that the clutter signal is composed of an infinite sum of plane waves arriving at the receiver with random amplitudes and phases. He shows that under fairly general conditions for the nature of the amplitude and phase variations of the plane waves, that the resulting amplitude will be Rayleigh in nature.

Beckmann also examined the problem for the case where not all wave amplitudes were independent and the phases were not uniformly distributed. The resulting amplitude density function is fairly complex but has the attribute that it can be calculated given the mean and variance of the clutter amplitude. Therefore, this is an excellent candidate for examination by this program since these parameters can be computed from the measured data.

3.2.2 Monte Carlo Statistical Fluctuation Model

A more complex and direct approach for determination of reflection coefficient fluctuation behavior begins with the mathematical expression for the scattering coefficient based on the Helmholtz integral. This approach is desirable since characteristics of the radar system can be incorporated into the integral's evaluation and the variation of the actual received signal computed. This can be accomplished by creating a random surface with desired electrical and surface height characteristics and restricting the evaluation of the integral to the area illuminated by the system as determined from the antenna patterns and pulse width. This model has been implemented by SRS Technologies for comparison with the clutter data. However, because the integral contains a phase term that restricts the surface area increment size, its computation for realistic beam areas can be rather time-consuming.

3.3 DATA REQUIREMENTS

In order to test the mean reflectivity models mentioned above, it will be necessary to estimate their the mean values from sampled data and compare these values to predicted results. Similarly, probability density functions can be tested using various hypothesis tests. Hypothesis testing may also alleviate the problem of missing the "tails" of a distribution in the data due to limited dynamic range.

3.3.1 Estimation of the Mean

Given n independent samples $\{x\}$, it can be shown that the sample mean will exhibit a nearly Gaussian distribution (Central Limit Theorem). If we assume that an estimate of the mean value within

10% of its true value with a 95% confidence factor is adequate, then the number of samples needed to estimate the mean is given by

$$n \geq \left[19.6 \frac{\sigma(x)}{|E\{x\}|} \right]^2$$

For a exponential probability density function, the ratio in the above expression is equal to unity, so that $n \geq 384$. An upper bound on n can be estimated using the Chebyshev inequality (Parzen 67) as well. This results in $n \geq 2,204$. Hopefully, the scattering statistics will be nearer to an exponential density (i.e., Rayleigh amplitude) so that the measured data will provide even more accurate mean reflectivity values.

During data collection, a large number of pulses will be transmitted and recorded for ground processing. For the above analysis to be valid, each sample x must be independent. Independence can only be ensured when the processed data is obtained from clutter patches separated by at least one beamwidth on the ground. In general, it will be difficult to meet this requirement because of the rather large azimuth beamwidths proposed by ERIM. For example, an aircraft flying at 220 Knots for 5 minutes will illuminate about 20 Nmi of terrain. For a nominal aim point range of 25,000 feet, a 10 degree beamwidth will be about 0.7 Nmi wide on the ground. Thus, a little over 25 separate beamwidths will exist during a 5 minute flight.

It will be possible to increase the number of independent samples by coherently processing the data to provide additional azimuthal resolution (at least for low out-of-plane angle geometries). This improvement is a complex factor of PRF, processing time, and radar platform geometry. It is recommended that the requirement for independent data be considered when selecting coherent processing parameters.

3.3.2 Hypothesis Testing

Another data analysis objective is to estimate the probability density function which characterizes the clutter data base. This can be achieved by comparing binned reflectivity data to a known distribution (Press 86). The accepted test for differences between binned distributions is the chi-square test. That is, bin sizes are selected to yield a reasonable number of samples in each bin (e.g., five or more) and the difference between the observed number and the number predicted by the test distribution computed to form the chi-squared statistic. If this statistic results in a low significance probability, then the two distributions are

unlikely to be related. However, if the significance statistic is large, then they are likely to be related.

In this manner, a priori statistical models may be compared with the clutter data base for likely matches. Thus, even though the system dynamic range is limited, it may be possible to use this approach to estimate the "tails" of the distribution since the major chi-squared statistic terms come from data below the tails. Some of the density functions that will be tested include (1) Exponential, (2) Gamma, (3) Gaussian, (4) K Distribution, (5) Log Normal, and (5) the Weibull. These probability density functions are described in SRS UR86-173.

3.4 CLUTTER WORKSTATION

SRS Technologies has developed a radar clutter workstation that provides information about clutter behavior on radar system performance. The workstation incorporates the mean reflectivity models described in the above paragraphs. The workstation provides information for both monostatic and bistatic radar system configurations. Graphical output is organized into three categories (1) geometrical, (2) clutter phenomenology, and (3) system performance. The clutter models include the Kirchhoff, perturbation, and composite. The latter includes shadowing. Scattering is computed for various terrain types which may be represented by exponential or Gaussian surface height correlation functions having specified correlation lengths, orientations, mean surface height, and surface height standard deviation. Electrical properties of the terrain including complex permittivity and permeability can also be specified. The effect of vegetation and foliage can be accounted for by selecting a layered Kirchhoff model formulation.

This workstation has been utilized extensively to predict signal levels that can be expected during the CMP data collection missions. It also serves as a repository of clutter model information for future data analysis. The workstation is described in (SRS TM87-005) and an operator's manual in (SRS TM87-009).

4.0 MEASUREMENT SYSTEM DESCRIPTION

Clutter data collection equipment for the Clutter Measurements Program (CMP) in support of the Hybrid Bistatic Radar (HBR) concept feasibility effort is under development by the Environmental Research Institute of Michigan (ERIM). ERIM is being supported by RADC and DARPA under contract F30602-86-C-0055. The measurement system will consist of two aircraft platforms. The first will carry the bistatic radar transmitter. The second aircraft will carry a receiver that will record the bistatic transmissions. In addition, the second aircraft will have its own transmitter and utilize the same receiver in a time-multiplexed mode for reception of monostatic (backscatter) transmissions. Both transmitters will operate at L-band (approximately 1.25 GHz) and their transmissions synchronized by atomic clocks on each aircraft.

A detailed description of the ERIM equipment can be found in Reference (ERIM Design Plan, 87) and only its pertinent features summarized here. Since SRS Technologies will collect ground truth data during the measurement flights and later analyze the data, these aspects of the measurement system will be included in this section. Of particular importance is the signal processing software developed by SRS Technologies which greatly improves the accuracy of the ERIM instrumentation and is discussed in Section 6.0.

4.1 ERIM BISTATIC SYSTEM

The ERIM bistatic data collection transmitter parameters as of November 1987 are summarized in Table 4-1. Common receiver parameters are shown in Table 4-2. It should be noted that the receiver system receives one linear polarization at a time.

Table 4-1 ERIM Bistatic Transmitter System Parameters

PULSE WIDTH	125 nanoseconds
BANDWIDTH	8 MHz
WAVEFORM	Pulsed Carrier
TRANSMITTED POWER	5 KW
CARRIER FREQUENCY	1250 MHz
TRANSMITTER PRF	2000 Hz
TRANSMIT POLARIZATIONS	V, H
ANTENNA GAIN	16.5 dB
ANTENNA BEAMWIDTH	10 x 60 degrees

Table 4-2 ERIM Common System Parameters

CHANNEL PRF (8 CHANNELS)	500 Hz
SAMPLES PER PULSE	40
STEPPED GAIN	Up to Four Steps
SAMPLE WORD LENGTH	6 bits I and 6 bits Q
SAMPLE TYPE	Complex
INSTANTANEOUS DYNAMIC RANGE	29 dB with 10 dB CNR
MANUAL DYNAMIC RANGE	>40 dB
TOTAL POTENTIAL DYNAMIC RANGE	70 dB
HIGH DENSITY DATA TAPE RECORDER CAPACITY	>5 Hours
COHERENCE TIME	100 milliseconds
SYSTEM TIMING ACCURACY	1 part in 10^{12}
RECEIVER POLARIZATIONS	Vertical, Horizontal
RECEIVER ANTENNA	Same as Monostatic Source
AIRCRAFT NAVIGATION	Ground Beacons

4.2 ERIM MONOSTATIC SYSTEM

The ERIM monostatic data collection transmitter parameters as of November 1987 are summarized in Table 4-3. The common parameters in Table 4-2 are also applicable to the monostatic system.

Table 4-3 ERIM Monostatic Transmitter System Parameters

PULSE WIDTH	4 microseconds
BANDWIDTH	250 KHz
WAVEFORM	Pulsed Carrier
TRANSMITTED POWER	5 KW
CARRIER FREQUENCY	1250 MHz
TRANSMITTER PRF	2000 Hz
TRANSMIT POLARIZATIONS	Vertical, Horizontal
ANTENNA GAIN	16.5 dB
ANTENNA BEAMWIDTH	10 x 60 degrees

4.3 WAVEFORM AND CHANNEL DEFINITION

A typical waveform showing the relationship between the bistatic and monostatic pulses and the corresponding polarization combinations is shown in Figure 4-1.

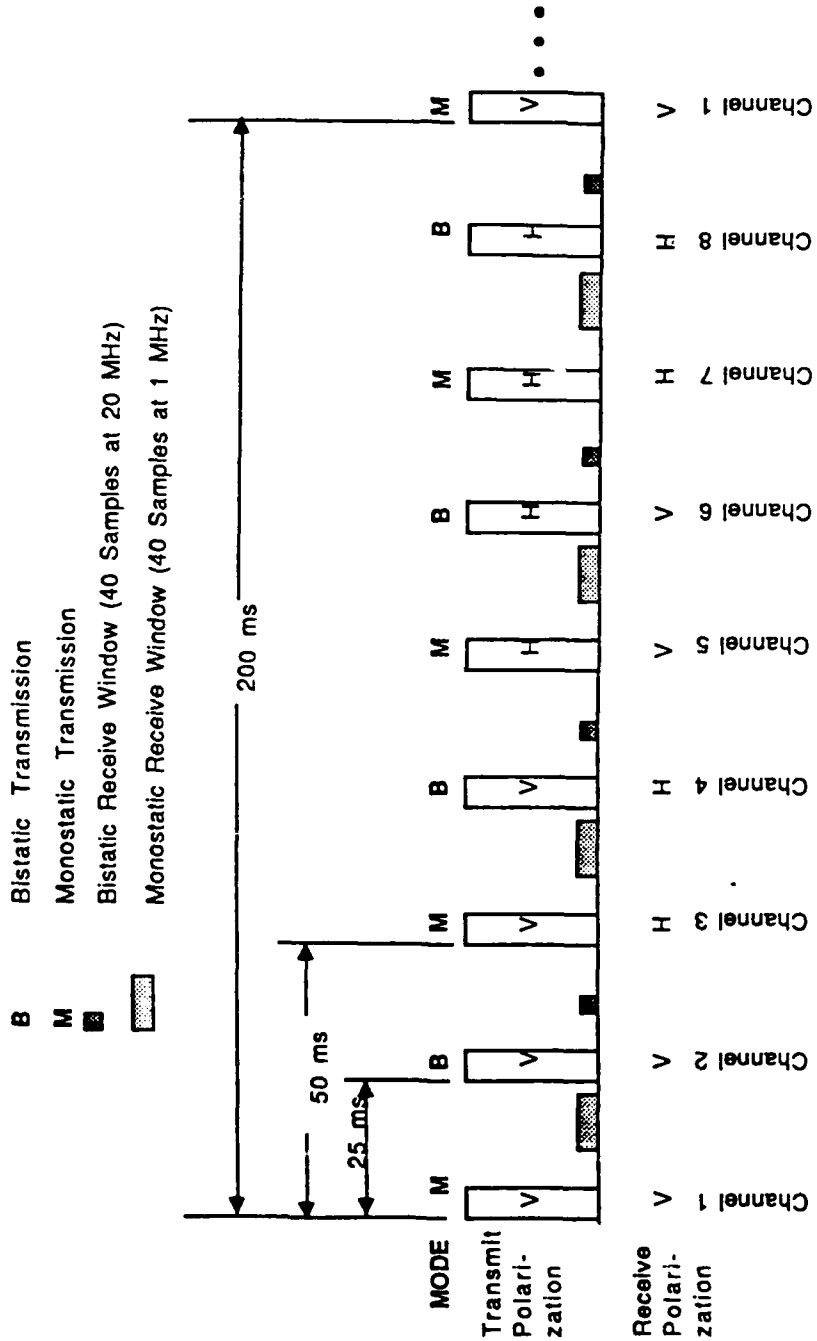


Figure 4-1 ERIM Data Collection Waveform

4.4 AUXILIARY FLIGHT DATA COLLECTION EQUIPMENT

In addition to the airborne instrumentation equipment under development by ERIM, there are a number of ground support systems required for mission support. These include (1) a beacon positioning system, (2) Active Radar Calibrators (ARC's), and (3) an antenna gain measurement system.

4.4.1 Aircraft Positioning System

ERIM originally proposed that the position of each aircraft during a data collection mission be determined by on-board Global Positioning System (GPS) receivers. The use of differential GPS techniques would have provided position accuracies on the order of 10 meters CEP (circular error probability) in the horizontal plane and 60 feet in altitude.

At the present time it appears that this approach is not viable due to insufficient coverage by the existing constellation of GPS satellites. Consequently, ERIM has proposed the use of ground-located beacons for positioning. ERIM estimates that aircraft position using the on-board Inertial Navigation System (INS) updated by the ground beacons will provide a horizontal CEP of 45 meters and an altitude accuracy of 300 feet. This accuracy is acceptable for pointing the antennas at specified points on the ground but is not adequate for precision clutter reflectivity measurements because of their extreme sensitivity to geometric factors.

4.4.2 Active Radar Calibrator (ARC) System

Because of the sensitivity of bistatic clutter reflectivity coefficient measurements to geometry noted above, and the need to provide accurate calibration of the power received, ERIM will utilize another set of extremely precise repeaters located at surveyed ground sites. These repeaters are referred to as Active Radar Calibrators or ARC's. Similar devices proved useful during the Shuttle Imaging Radar B (SIR-B) experiments several years ago.

The ARC's will provide a calibration reference for both the bistatic and monostatic system data. They will also provide an extremely accurate range update which can be used to augment the INS/Ground Beacon positioning system data. Since the ARC's will maintain signal coherence, they can also provide precise doppler offset information. The latter information will be utilized in by SRS Technologies signal processing software in the conversion of digitized data to clutter reflectivity coefficient.

SRS Technologies and ERIM prepared a specification (SRS UR87-044) for these ARC's during the program and a prototype of the device is undergoing testing at this time. The effective bistatic RCS of an ARC will be 55 dBsm and 50 dBsm for a monostatic ARC. The

ARC's will both delay and doppler offset the repeated signal to help reduce interfering clutter effects.

4.4.3 Antenna Pattern Measurement System

As discussed in Section 2.0, measurement system accuracy is a function of the combined antenna patterns in the bistatic case. In fact, small antenna gain errors cause proportionate errors in determination of the clutter reflectivity coefficient from recorded data. Because of this, ERIM has investigated several antenna pattern measurement concepts. The first consists of a linear array of calibrated receivers which record the amplitude of the signal as the beam is flown past the array. ERIM has estimated the accuracy of this approach at about 0.5 dB relative accuracy and 0.5 dB absolute accuracy. An alternate approach is the use of an existing antenna pattern measurement range located near RADC in Rome, New York. No decision has been made on either approach at this time.

4.5 GROUND TRUTH INSTRUMENTATION

Examination of the Kirchhoff Integral related clutter models described in Section 3.0 shows that scattering is strongly influenced by physical and electrical properties of the underlying terrain. Physical characteristics describe the roughness of the surfaces, how they vary over the region of interest, and any layering that may be significant. Electrical properties include the complex dielectric constant (sometimes called the complex permittivity) of the surface material and underlying layers and its permeability. Measurements of these quantities are called "Ground Truth Measurements" and must be made in conjunction with flight measurements in order to validate the models. Without good ground truth data, the utility of the flight data is significantly reduced since there is no foundation for extrapolation of the flight data to other types of terrains.

4.5.1 Ground Truth Measurement Requirements

4.5.1.1 Surface Height Data

Reference (SRS UR87-060) contains a more detailed discussion of ground truth requirements and is summarized in the following paragraphs. Surface height measurements of the terrain are needed so that the surface height and surface slope probability density functions can be estimated. Measurement of this information must be performed with sufficient accuracy to determine the composite (two-scale) model parameters. The large-scale model (Kirchhoff model) surface height parameters can be estimated using topographical map data. However, the small-scale (perturbation) model requires surface height measurements with an accuracy of 0.1 wavelength or less (about 3 cm at L-band). In addition, the horizontal spacing of these measurements should be on the order of 0.5 wavelengths (15 cm at L-band). Because of the latter requirement, it is likely that only a limited number of regions

within the data collection region can be sampled in a reasonable time. Thus, some care should be taken in their location so that they are representative of the terrain in the overall data collection area.

4.5.1.2 Terrain Electrical Characteristics

The principal electrical parameter required for model validation is the complex permittivity of the surface and any significant layers. The value of the dielectric constant is almost entirely determined by the terrain's water content and there are complex formulations relating water content and material composition to dielectric constant. However, since instrumentation exists to measure the relative dielectric constant (i.e., relative to the permittivity of free-space) directly, the direct approach is preferred. In this case, the real part of the dielectric constant may range from 1 to 80 for material of interest and the imaginary part from 0.01 to 20. The dielectric constant should be measured at varying depths below the surface with the deepest depth determined by its extinction coefficient at L-band (this can be computed in the field). In addition, the dielectric constant of any vegetation covering the surface should also be recorded and its density.

Since most materials are non-magnetic, they will be characterized by the permeability of free-space. Consequently, this parameter will not need to be measured.

4.5.2 Ground Truth Measurement Equipment

Procedures for collection of ground truth data are described in SRS UR87-112 and are summarized here. Large-scale surface height data can be obtained from U.S Geological Survey Service maps or digitized tapes for the regions of interest (digitized data is not available for most of Michigan). Small-scale surface height data will be measured with an acoustic ranging system moving along a horizontal track. The track will be oriented in several directions to provide a measure of the spatial characteristics of the small-scale height data. Logistical considerations limit the amount of terrain which can be measured in this manner. As a minimum, these measurements should be made at the beginning, middle, and end of the data collection ground track (i.e., about 9 Nmi apart). At least 30 feet of data should be collected in the selected directions. An alternative approach is the use of a carpenter's tool called a "Formit" which consists of a row of wires held in place by friction between two plates. When the row ends are pressed against an irregular surface, the individual wires will adjust to reproduce the irregular contour form. The surface roughness can be transferred by tracing the contour with a pencil on a piece of paper.

At L-band frequencies, penetration of the surface can occur up to several wavelengths depending on the moisture content and composition of the surface. Foliage type, density, and height

above the surface should be recorded. Similarly ice or snow covering should be described and measured. A tubular soil sampler (e.g., Lord Model 225) can be inserted into the ground and visual determination of the soil profiles made.

To avoid the use of soil mixture models and water content measurements, direct measurement of the surface (and subsurface) complex permittivity will be made. This will occur at the surface roughness measurement sites. A specification for this tool was prepared by SRS Technologies (SRS UR87-045). A device which satisfies these requirements is available from Applied Microwave Corporation (AMC). The sensor head is merely pressed against the surface to be measured and the real and imaginary parts of the dielectric constant recorded. This instrument will work with both fresh water and sea water.

A video recording of the test area should be made within two hours of the data collection flights. Any unusual geological features, surface cover, topology, or man-made features should be recorded and their locations accurately measured.

5.0 SITE SELECTION

SRS Technologies site selection efforts initially examined locations that were similar to those proposed for an operational Hybrid Bistatic Radar (HBR) system. The rationale for this approach was to ensure utility of the resulting bistatic and monostatic clutter data base for HBR feasibility analyses. Proposed HBR operation areas can be categorized into two major classes. The first includes a 200 Nmi wide defensive semi-circular ring around the continental United States (including both coasts and the northern border but excluding the southern border). This is shown in Figure 5-1. The second operational area is provides naval protection and consists of isolated ocean regions centered on Fleet locations and is illustrated in Figure 5-2. It was concluded that CMP collection sites should encompass nearly equal amounts of ocean and land. Ocean areas should be within 200 NMI of both coasts and the land area should be representative of the Canadian Arctic.

As the Clutter Measurements Program unfolded, the extensive geographical data collection program that would be needed to fully support HBR concept evaluation was reduced in scale because of funding limitations and uncertainties in ERIM aircraft availability. Consequently, SRS Technologies was tasked to identify specific sites in California and Michigan for data collection flights which would offer maximum HBR utility. This activity resulted in the identification of the Pacific Missile Test Center located at Point Mugu, California as a base for ocean clutter data collection flights. In addition, desert areas near Edwards Air Force base, California were proposed as additional data collection sites. The latter sites were included since dry sand and ice exhibit nearly identical scattering behavior at L-band and would provide scattering behavior similar to the Arctic region. Since the main purpose of the Michigan flight is to validate data collection system performance and provide pilot and crew training, the Michigan site selected was near the Willow Run airport where ERIM aircraft are based.

At the current time, SRS Technologies has been directed to address test planning only at the Michigan site. It is assumed that more comprehensive measurements will be made in a future program after ERIM data collection system performance has been demonstrated.

5.1 MICHIGAN SITE

A detailed Test Plan and Procedures document for clutter data collection in Michigan was delivered to the Government as SRS UR87-112. This comprehensive document defines (1) data collection objectives, (2) participants and responsibilities, (3) mission plans, (4) communications plan, (5) ground support activities, (6) mission description, (7) waypoint description, and (8) contingency planning. The scope of the data collection at this site was limited to about three hours since only 12 hours of total flight

time was scheduled by ERIM and the balance of the time was devoted to system checkout and crew training.

Because of the system validation aspects of these flights and concerns regarding potential ARC multipath interference associated with low grazing angles, a test geometry that avoided the multipath problem was proposed by SRS Technologies (SRS UR87-112) for a discussion of this problem). A site located at 84 degrees 12 minutes west longitude and 42 degrees 25 minutes north latitude was chosen because of its close proximity to Willow Run Airport and relatively well-behaved terrain. A capsule summary of the data collection geometry for this site and series of tests is given in Table 5-1.

Table 5-1 Michigan Data Collection Flight Geometry

Bistatic Receiver/Monostatic Radar

Altitude	12,000 feet AGL
Grazing Angle	20 degrees
Speed	220 Knots
Heading	true north
Flight Path	race track
Out-of-Plane Angle	0 degrees, 5 degrees, 10 degrees, 20 degrees, and 35 degrees

Bistatic Illuminator

Altitude	12,000 feet AGL
Grazing Angle	35 degrees
Speed	220 Knots
Heading	true north
Flight Path	race track

Because of the short time available, the proposed number of out-of-plane angles may not be accomplished. In this case, the in-plane (i.e., 0 degree out-of-plane angle) geometry should be attempted first since interpretation of clutter data for this geometry is more straight-forward than the other cases. Note that platform altitude is specified as Above Ground Level (AGL) to ensure the desired grazing angles are achieved on the ground.

Although the SRS Technologies radar clutter workstation predicted substantial bistatic clutter returns for the above in-plane geometry, it appears likely that the monostatic return may be so low as to be undetectable. This results from the extremely low backscatter clutter reflectivity coefficient expected at small grazing angles. (SRS UR87-059) discusses this issue in more detail. As a consequence, it may be desirable to reallocate monostatic data channels to the collection of additional bistatic data.

Consequently, it is recommended that at least one data collection pass be made to confirm monostatic clutter signal strength is below the receiver noise level. If this is confirmed, then the

remaining passes should concentrate on collection of bistatic clutter data.

6.0 SIGNAL PROCESSING SOFTWARE

SRS Technologies will be responsible for processing and analyzing clutter data collected by the ERIM instrumentation. Clutter data for a given mission will be stored on a High Density Data Tape (HDDT) in real-time and converted to a Computer Compatible Tape (CCT) during post-mission processing. The CCT will be compatible with most general purpose tape devices. During this program, SRS Technologies participated in the definition of the CCT format. Since it was recognized that the ERIM instrumentation could not, by itself, provide accurately calibrated clutter data, SRS Technologies developed the necessary signal processing software to accomplish this using data recorded on the CCT. Thus, the signal processing software can be viewed as an extension to the ERIM data collection instrumentation. It is anticipated that SRS Technologies will perform software development for clutter data analysis software in a future effort. Data analysis software will perform statistical analyses and evaluate various clutter model candidates.

6.1 COMPUTER COMPATIBLE TAPE FORMAT DEFINITION

A detailed CCT interface specification was prepared as (SRS UR87-014) over the course of this program. This specification was reviewed by both ERIM and DSA and was revised five times based on comments received from these organizations. Since each data collection pass (about 5 minutes of clutter data recording) will result in an enormous amount of raw data, the format for the CCT was designed to minimize the number of magnetic tapes holding this data. The CCT format selected will result in data from a single pass being stored on two and one-half, 2400 feet, 1600 BPI tapes.

6.1.1 Computer Compatible Tape Characteristics

In order to be compatible with the majority of computer tape drives, the CCT will conform to level 3 of the ANSI standard (American Standard X3.27-1978) for labeled magnetic tapes. The salient features of this standard include (1) nine tracks per tape, (2) 1600 bits per inch, (3) one file per pass, (4) and 1964 bytes per record.

6.1.2 Computer Compatible Tape Data Format

The data on each CCT representing one pass of a many pass mission will include (1) pass identification data, (2) calibration data, (3) pass characteristic data, (4) location data, and (5) radar channel data. This data will be written on the CCT using a standard record format of 1964 bytes. The six types of records are (1) Pass-Header Record, (2) Attenuation Record, (3) antenna Pattern Calibration Record 1, (4) antenna Calibration Record 2, (5) Auxiliary Data Record, and (6) Channel Data Record.

6.1.2.1 Standard Header Record

The first four bytes of the each record are the record header which indicates the type of record. The next eight bytes of the header contain a unique number identifying the record. The remaining 1952 bytes contain the data characteristic of the record type.

6.1.2.2 Pass-Header Record

The Pass-Header Record will contain mission and pass identification information, ARC locations, synchronization information, channel polarization definitions, and attenuator setting data. This record will contain the location of the aircraft waypoints and detailed data on the radar waveforms.

6.1.2.3 Attenuation Record

This record contains six-bit samples of receiver output in $I^2 + Q^2$ form corresponding to known power levels injected into the receiver front end after each pass.

6.1.2.4 Antenna Pattern Records

This record contains antenna pattern calibration data that will be used in the determination of the reflectivity coefficient. It was felt that this data should be included on each set of pass CCT's so that they a set could be processed independently. There will be a record for each antenna.

6.1.2.5 Auxiliary Data Record

Information stored on this record will include position location beacon coordinates, aircraft true heading and altitude, velocity, and acceleration, power meter readings, commanded antenna pointing angles, and the servo loop correction angles.

6.1.2.6 Channel Data Record

This record consists of four 488 byte subrecords and contains the digitized channel I and Q data. The first eight bytes of each subrecord are the pass pulse number. The remaining 480 bytes are divided into 60 byte parts, each part corresponding to one receiver channel. Each 60 byte part contains eighty, six-bit digital samples (40 in-phase and 40 quadrature) for a channel corresponding the system's 40 range gates.

6.2 SIGNAL PROCESSING SOFTWARE DESCRIPTION

At the time this report was written, a CMP data collection mission was envisioned to consist of a number of passes over a selected region with each pass corresponding to a geometry of importance to HBR. In addition, because of multipath effects on the ARC signals

at low grazing angles, a separate pass at higher grazing angles will be flown to collect uncorrupted ARC data. After each pass, the receiver transfer function will be calibrated by injecting signals of various levels into its front end.

During each pass (including the ARC passes) each of eight channels of linearly polarized monostatic and bistatic signal data will be coherently sampled and recorded. Each channel will be sampled with forty range gates centered about the time-of-arrival of the nominal beam aim point. Position, velocity, and acceleration of each platform are also recorded as auxiliary data.

The purpose of the signal processing software developed by SRS Technologies is to derive a time series of calibrated clutter reflectivity coefficients from the digitized data for later data analysis. This is a complex process because of instrumentation system characteristics and the unusual nature of bistatic radar range-doppler cell features.

6.2.1 Signal Processing Software Functional Definition

Signal processing has been organized into two major functions. These are: (1) ARC pass calibration, and (2) clutter reflectivity coefficient computation.

6.2.1.1 ARC Pass Calibration

This signal processing function utilizes the internal receiver calibration data to determine the transfer function of the receiver for given channel attenuator settings. External ARC calibration signals are then used to relate this curve to an absolute RCS level. A scale factor will be derived from the detected ARC signal and used later for conversion of digitized clutter data to RCS in square meters. ARC detection involves coherent processing and searching range and doppler bins for the desired calibration signal. Auxiliary channel data will be used to determine the most likely times on the data tape to search for the ARC signals.

6.2.1.2 Clutter Data Processing

Clutter data processing involves prediction of platform positions, locating the aimpoint range gate, calibrating the data, interpolating sample levels between range gates, accumulating a number of time samples for each channel, performing coherent processing, and sampling the aimpoint doppler frequency bin. Only the range doppler cell corresponding to the center of the range gate will be utilized.

Because of the sensitivity to aircraft position errors in the bistatic system, ARC data embedded in the clutter pass will be used to compensate for this error source. Finally, antenna pattern calibration data will be used in the computation of the clutter reflectivity coefficient from the recorded data. A more

detailed description of these functions can be found in (SRS UR87-116).

REFERENCES

Beckmann, P., The Scattering of Electromagnetic Waves from Rough Surfaces, Pergamon Press, Oxford, 1963.

Papa, R.J., An Analysis of Physical Optics Models for Rough Surface Scattering, Rome Air Development Center, Griffiss Air Force Base, NY, RADC-TR-84-195, Sept. 1984.

*Lennon, J.F., A Survey of Terrain Scattering Theory and Measurements for Air Force Systems, Rome Air Development Center, Griffiss Air Force Base, NY, RADC-TR-84-78, April 1984.

Parzen, E., Modern Probability Theory and its Applications, John Wiley and Sons, NY, 1960.

Press, W. H., Numerical Recipes, Cambridge University Press, Cambridge, 1986.

Barton, D. K., Low-Angle Radar Tracking, Proceedings of the IEEE, Vol. 62, No. 6, June 1974.

Ruck, G. T., Radar Cross Section Handbook, Vol. 2, Plenum Press NY, 1970.

Calabretta, R. A., Bistatic Terrain Clutter Reflectivity Modeling, SRS TM86-103, 19 August 1986.

Sancer, M., Shadow-Corrected Electromagnetic Scattering from a Randomly Rough Surface, IEEE Trans. Antennas and Propagation, Vol. AP-17, Sept. 1969.

ERIM, Design Plan for Hybrid Bistatic Radar Clutter Measurements Program, Environmental Research Institute of Michigan, Contract F30602-86-C-0055, Preliminary Draft, 16 January 1987.

*Although the above * document is a limited document, no limited information has been extracted.

SRS TECHNICAL REPORT SUPPLEMENT

THIS PAGE INTENTIONALLY LEFT BLANK.

SRS TECHNICAL REPORT SUPPLEMENT CONTENTS

1. SRS UR86-199, Charles H. Hightower, "Design Plan, Clutter Measurement Radar Pulsewidth Tradeoff Analysis," ELIN A003, 19 August 1986.
2. SRS UR86-198, Charles H. Hightower, "Design Plan, Antenna Pattern Measurements Analyses, ELIN A003, 14 August 1986."
3. SRS UR86-197, Charles H. Hightower, "Design Plan, Antenna Analysis and Requirements," ELIN A003, 14 August 1986.
4. SRS UR86-202, Charles H. Hightower, "Design Plan, Antenna Beam Registration Analysis and Requirements," ELIN A003, 14 August 1986.
5. SRS UR87-089, Charles H. Hightower, "Design Plan, CMP Doppler Spread Analysis," ELIN A003, 15 April 1987.
6. SRS TM-005, Catherine Sanders-Foster, "Hybrid Bistatic Radar Clutter Measurements Program SRS Clutter Workstation," 27 February 1987.
7. SRS UR86-173, Charles H. Hightower, "Candidate Bistatic Clutter Models," 28 June 1987.
8. SRS TM87-009, C. Foster, "SRS Clutter Workstation User's Manual," 21 April 1987.
9. SRS UR87-052, Charles H. Hightower, "Design Plan, Active Radar Calibrator (ARC) Specification - Revision 1," ELIN A003, 7 January 1987.
10. SRS UR87-060, Charles H. Hightower, "Hybrid Bistatic Radar (HBR) Clutter Measurements Program (CMP)," ELIN A003, 20 March 1987.
11. SRS UR87-112, Charles H. Hightower, "Test Plan/Procedures - Phase 1 Data Collection," ELIN A002, 4 June 1987.
12. SRS UR87-045, Charles H. Hightower, "Design Plan, Complex Permittivity Measurement Device Specification," ELIN A003, 9 December 1987.
13. SRS UR87-059, Charles H. Hightower, "Design Plan, Comparison of Bistatic and Monostatic Normalized Scattering Coefficient," ELIN A003, 16 March 1987.
14. SRS UR87-091, Charles H. Hightower, "Design Plan, ERIM Measurement System Calibration Accuracy and Multipath Mitigation Analysis Summary," ELIN A003, 17 April 1987.

15. SRS UR87-120, Charles H. Hightower, "Design Plan, Signal Processing Module Development Schedule," ELIN A003, 1 July 1987.

16. SRS UR87-014, Catherine Sanders-Foster, "Design Plan, Computer Compatible Tape Interface Specification," ELIN A003, 17 August 1987.

17. SRS UR87-116, David M. Maeschen, "Design Plan, Flight Data Processing Software Functional Specification," ELIN A003, 15 June 1987.

DESIGN PLAN
CLUTTER MEASUREMENT RADAR
PULSEWIDTH TRADEOFF ANALYSIS
ELIN A003

CONTRACT TITLE: BISTATIC CLUTTER PHENOMENOLOGICAL
MEASUREMENT/MODEL DEVELOPMENT

CONTRACT NUMBER: F30602-86-C-0045

CONTRACT PERIOD: 1 APRIL 1986 - 31 SEPTEMBER 1987

PREPARED BY: CHARLES H. HIGHTOWER

DATE: 19 AUGUST 1986

Prepared for:

ROME AIR DEVELOPMENT CENTER
GRIFFISS AIR FORCE BASE
NEW YORK 13441-5700

SRS

TECHNOLOGIES

ADVANCED TECHNOLOGY DIVISION
17252 ARMSTRONG AVENUE
IRVINE, CALIFORNIA 92714
(714) 250-4206

1.0 INTRODUCTION

One of the most critical design parameters for the HBR bistatic CMP radar is pulse width since the bistatic range equation shows that the square of the pulse width affects the expected Clutter-to-Noise Ratio (CNR). That is, as pulse width increases, illuminated ground area increases proportionally causing an increase in received clutter power. Similarly, as pulse width increases (signal bandwidth decreases) receiver if bandwidth can be reduced resulting in less noise power competing with the clutter signal. The net result is a dramatic increase on CNR.

Selection of an optimum pulse width for bistatic clutter measurements is complicated by several opposing factors. First, of course, is illumination of a reasonably large clutter area so that the clutter return (which exhibits statistical fluctuations) can be measured without corruption by receiver noise. This requirement is achieved by increasing the pulse width until a suitable CNR has been achieved. In contrast, the pulse width must be made short enough so that the direct path signal does not interfere with the signal arriving from the desired clutter patch(es). Finally, the pulse width must satisfy similar requirements for the companion monostatic radar since cost and complexity considerations constrain the bistatic and monostatic pulse widths to be identical.

2.0 BISTATIC PULSE WIDTH C/N AND DIRECT PATH OVERLAP TRADEOFF

To date, ERIM has proposed two pulse widths for the bistatic radar. These are 0.5 microseconds and 50 nanoseconds. ERIM has calculated a CNR corresponding to the 50 nanosecond pulse for nominal system geometries and a clutter reflectivity of 0 dB. Adjusting the ERIM CNR of 43 dB for a more realistic -30 dB, results in a CNR of only 13 dB. This value is marginal in the sense that the statistical variation in clutter reflectivity will mean that the clutter return will be below the receiver noise level much of the time. For example, assuming that the clutter amplitude is Rayleigh distributed (exponential power), means that the clutter return would be below the average receiver noise level about 30 percent of the time. ERIM has also shown that a 50 nanosecond pulse will provide approximately 26 nanoseconds temporal separation between the direct path signal and the minimum bounce path signal for an in-plane large bistatic angle geometry (i.e., a transmitter grazing angle of 10 degrees, a receiver grazing angle of 1 degree, and the transmitter, clutter patch, and receiver all in the same vertical plane.). It can be shown that the minimum bounce occurs on the surface where the transmitter and receiver grazing angles are equal (i.e., the incident angles are equal). Since this location only corresponds to the desired clutter patch location when the bistatic transmitter and receiver platforms are at the same altitude (identical grazing angles), it may be possible to increase the 50 nanosecond pulse width in the large bistatic angle case substantially resulting in a significantly improved CNR ratio.

Calculations indicate that for the nominal ERIM in-plane geometry described above (with the slant ranges from the transmitter and receiver platforms to the clutter patch fixed at at 25,000 feet) that the leading edge of the minimum path signal will arrive at the receiver 76 nanoseconds after the leading edge of the direct path transmitted signal arrives at the receiver. Thus, a 50 nanosecond pulse will provide 26 nanoseconds margin for receiver

recovery after the trailing edge of the direct path signal and arrival of the leading edge of the minimum bounce pulse. However, measurement of clutter from the minimum bounce region is not what is desired for this geometry since its bistatic and grazing angles are different than the 10 degree, 1 degree desired. It can be shown that the leading edge of the pulse reflected from the desired clutter region arrives at the receiver 231 nanoseconds after the leading edge of the direct path signal or 155 nanoseconds after the minimum path signal. Hence, if the minimum path clutter reflectivity is on the order of the desired clutter patch reflectivity (i.e., so receiver sensitivity is not affected), then the transmitted pulse could be as large as 200 nanoseconds; leaving a 31 nanosecond margin between the trailing edge of the direct path pulse at the receiver and the arrival of the leading edge of the pulse from the desired region. Of course, the minimum path signal and direct path signal would overlap for 124 nanoseconds. Increasing the pulse width from 50 nanoseconds to 200 nanoseconds in this way would result in a CNR improvement of 12 dB.

On the other hand, if the minimum path signal is very large (e.g., the region behaves as a smooth specular reflector), then the return from the desired clutter patch could be masked by the large specular return causing a large receiver AGC signal which had not decayed significantly by the time the desired pulse arrived at the receiver. This problem can be solved by blanking the receiver front-end for some time after the specular (minimum path) pulse trailing edge arrives at the receiver. Assuming a 30 nanosecond delay is adequate for these purposes as in the previous example, the transmitted pulse could be as large as 125 nanoseconds (155 nanoseconds - 30 nanoseconds). This would result in a CNR improvement of 8 dB compared with a 50 nanosecond pulse.

Consequently, in either of the cases discussed above, considerable improvement in CNR is achievable by choosing a pulse width in the 125 to 200 nanosecond region.

3.0 MONOSTATIC RADAR PULSE WIDTH COMPATIBILITY

The monostatic single pulse bandwidth limited CNR has been calculated based on parameters provided by ERIM for the bistatic radar. In this case, the illuminated area is about 1.9 million square feet. Using these values with a monostatic clutter reflectivity coefficient of -30 dB at a range of 25,000 feet, results in a CNR of 19.9 dB for a 125 nanosecond pulse. The CNR becomes 22.4 dB for a 200 nanosecond pulse. These CNR can be contrasted to that for a 50 nanosecond pulse or 11.9 dB. Clearly the larger pulse widths are desirable for both the bistatic and monostatic radars.

Since the two-way range resolution for the 125 nanosecond and 200 nanosecond pulses are 61 feet and 98 feet, respectively, the receiver may be blanked for a sufficient time to ensure adequate sensitivity for the reception of these pulses from the desired clutter areas.

4.0 CONCLUSIONS

The analyses in the above paragraphs lead to the conclusion that the optimum bistatic and monostatic pulse width is on the order of 125 to 200 nanoseconds. pulse widths in this range will provide adequate CNR's for both the bistatic

and monostatic radars under difficult geometry and clutter reflectivity conditions. In addition, the direct pulse return will not overlap the desired clutter signal. Similarly, the monostatic return will be free of a similar problem. Consequently, it is concluded that the minimum ERIM CMP radar pulse width should be at least 125 nanoseconds and that the bistatic receiver be blanked from pulse transmission until 30 nanoseconds prior to reception of the signal from the in-plane high bistatic geometry area to alleviate receiver saturation problems.

DESIGN PLAN
ANTENNA PATTERN MEASUREMENTS ANALYSIS
ELIN A003

CONTRACT TITLE: BISTATIC CLUTTER PHENOMENOLOGICAL
MEASUREMENT/MODEL DEVELOPMENT

CONTRACT NUMBER: F30602-86-C-0045

CONTRACT PERIOD: 1 APRIL 1986 - 31 SEPTEMBER 1987

PREPARED BY: CHARLES H. HIGHTOWER

DATE: 14 AUGUST 1986

Prepared for:
ROME AIR DEVELOPMENT CENTER
GRIFFISS AIR FORCE BASE
NEW YORK 13441-5700



ADVANCED TECHNOLOGY DIVISION
17252 ARMSTRONG AVENUE
IRVINE, CALIFORNIA 92714
(714) 250-4206

1.0 INTRODUCTION

This report presents the results of a brief examination of pattern measurements made by Chu Associates in April 1986 of an L-X Band antenna ERIM has proposed for the Hybrid Bistatic Radar (HBR) Clutter Measurements Program (CMP). This antenna will be installed in the SARLAB aircraft. This data was provided by Rome Air Development Center as part of contract F30602-86-C-0045. Emphasis was placed on examination of the L-Band patterns since the proposed CMP baseline bistatic clutter measurements system will operate at this frequency.

2.0 TEST RANGE RESULT ANALYSIS

Chu Associates made L-Band antenna measurements for the range of test parameters shown in Table 2-1. The antenna was rotated through 360 degrees with zero degrees as the boresight reference. The matrix patterns were measured at three frequencies: 1.195 GHz; 1.245 GHz; and 1.295 GHz.

TABLE 2-1 TEST MEASUREMENT CENTER

<u>PLANE</u>	<u>SOURCE POLARIZATION</u>	<u>TEST ARTICLE PATTERNS</u>
Azimuth	Vertical	Vertical
	Vertical	Horizontal
	Horizontal	Horizontal
	Horizontal	Vertical
Elevation	Vertical	Vertical
	Vertical	Horizontal
	Horizontal	Horizontal
	Horizontal	Vertical

Unfortunately, drawings or photographs of the antenna were not included in the data package. It is stated that the test was conducted with the X and L-Band arrays positioned as close as possible to each other in the elevation plane. The L-Band antenna is referred to as a "log-periodic array." Whether or not the proximity of the X and L-Band arrays resulted in the anomalous behavior described below is not known but should be investigated.

2.1 COMMENTS ON MAIN BEAM SHAPE

Examination of the measured azimuth and elevation patterns reveals a symmetrically shaped smoothly varying main beam for vertical polarization. In contrast, the horizontal polarization main beam shape in both cuts is relatively distorted and deviates about 1-2 dB from a smooth pattern.

2.2 BEAMWIDTH RESULTS

The 3 dB beamwidths measured by Chu Associates lie with 1-2 degrees of that expected for a uniformly illuminated aperture in the azimuth plane but appear about 10 to 30 degrees wider in the elevation plane. This may be due to the

difference in aperture efficiency between the uniformly illuminated model and the actual radiating elements.

2.3 SIDELOBE LEVELS

Again, vertically polarized sidelobes behave nicely and are below those of an equivalent uniformly illuminated aperture in both the azimuth and elevation cuts. However, the horizontally polarized sidelobe levels for both cuts exhibit anomalous behavior. That is, the horizontally polarized azimuth pattern shows the first two sidelobes about 3-4 dB higher than those expected for a diffraction limited antenna and generally more pronounced than for the corresponding vertical polarization. The same is true of the horizontal polarization sidelobes in the elevation plane.

2.4 ON-AXIS GAIN

The Chu test report indicates the gain for horizontal polarization is about 2-4 dB less than for the vertical polarization and does not meet the 17 dB goal. In general, the design goal of 17 dB is exceeded in the vertical polarization for the frequencies tested.

2.5 CROSS-POLARIZATION RESPONSE

Polarization isolation of 20 dB is generally not achieved in the azimuth plane for both horizontal and vertical cross polarizations. The elevation plane polarization isolation generally exceeds 20 dB except for one case that may be explained by antenna misalignment.

3.0 CONCLUSION

This analysis of Chu Associates data supports the contention that the L-Band horizontal polarization patterns are indicative of a problem in the antenna. The impact on clutter measurements may be significant if the problem is a fundamental design issue and cannot be fixed. Specifically, the non-linearly of the elevation pattern coupled with large, near-in sidelobes may cause a relatively large error in clutter RCS measurement and its inversion to reflectivity coefficient; especially, for horizontally polarized data. A computer simulation comparing the ratio of sidelobe power to main beam power for the ideal antenna and one with abnormal sidelobes was performed to examine this issue. For the ERIM out-of-plane geometry this ratio was -26 dB along a constant bistatic range cell for the ideal antenna. The simulated abnormal sidelobe pattern degraded this ratio to -5.4 dB. Thus, about 28.8 percent of the received power is due mainly to abnormal sidelobe contributions. This is a worst case figure since the clutter reflectivity coefficient was assumed constant over the entire illuminated area. It does, however, emphasize the need to understand and correct the ERIM antenna sidelobe problem.

DESIGN PLAN
ANTENNA ANALYSIS AND REQUIREMENTS
ELIN A003

CONTRACT TITLE: BISTATIC CLUTTER PHENOMENOLOGICAL
MEASUREMENT/MODEL DEVELOPMENT

CONTRACT NUMBER: F30602-86-C-0045

CONTRACT PERIOD: 1 APRIL 1986 - 31 SEPTEMBER 1987

PREPARED BY: CHARLES H. HIGHTOWER

DATE: 14 AUGUST 1986

Prepared for:
ROME AIR DEVELOPMENT CENTER
GRIFFISS AIR FORCE BASE
NEW YORK 13441-5700



ADVANCED TECHNOLOGY DIVISION
17252 ARMSTRONG AVENUE
IRVINE, CALIFORNIA 92714
(714) 250-4206

1.0 INTRODUCTION

This report has been prepared under Contract Number F30602-86-C-0045, as part of the Design Plan called for by ELIN A003. In particular, this report explores the adequacy of the Environmental Research Institute of Michigan's (ERIM) proposed antennas for the Hybrid Bistatic Radar (HBR) Clutter Measurements Program (CMP) monostatic and bistatic instrumentation radars. The antenna issue is critical because it is considered to be a "long lead time item" and any deficiencies found in its design might jeopardize the overall CMP in terms of cost, schedule, and performance.

This report is organized in the following manner. Section 2.0 discusses the ideal antenna model used to assess the performance of the ERIM antenna for measurement of clutter data. Section 3.0 utilizes this model and other information to assess the antenna's ability to provide meaningful clutter phenomenology data and derive reasonable requirements for the actual antenna. Lastly, Section 4.0 summarizes the results of this analysis and comments on the impact of differences between the ideal antenna model and recent test measurements of an existing ERIM L-band antenna similar to those proposed for the Clutter Measurements Program.

2.0 ERIM ANTENNA DESCRIPTION

ERIM has proposed the use of two nearly identical antennas for their HBR CMP bistatic instrumentation. The first of these antennas will be mounted on the bistatic receiver/monostatic radar aircraft and the second on the illuminator aircraft. The antenna on the bistatic receiver/monostatic platform will also act as the monostatic radar antenna. The design goals of the L-band antennas are shown in Table 2-1.

Table 2-1 ERIM Antenna Characteristics

<u>Parameter</u>	<u>Goal</u>
Elevation Beamwidth	60 degrees
Azimuth Beamwidth	10 degrees
Gain	17 dBi
Polarization	Vertical and Horizontal
Elevation Sidelobes	
First - Vertical	-11 dB
First - Horizontal	-13 dB
Azimuth Sidelobes	
First - Vertical	-14 dB
First - Horizontal	-13 dB
Polarization Isolation	20 dB
Dimensions	
Length	5 feet
Height	1 foot

The analyses in the body of this report require a model of the proposed ERIM antenna in many instances. The model used for these purposes is based on the Fresnel-Kirchhoff diffraction integral. It is assumed that the aperture is rectangular and uniformly illuminated. In the far field, the resulting

pattern for field intensity yields the product of $\sin(x)/x$ terms representing the horizontal and vertical patterns. The first sidelobes in each plane are 13 dB below the on-axis gain. The on-axis gain is adjusted to match the design goal value. Since the model behavior is nearly identical to the ERIM design goals, it should provide reasonable insight into the performance of the actual antenna. A more realistic model would integrate the contributions of a single antenna element so that "grating lobe" effects and individual feed phase and amplitudes difference could be observed. Section 4.0 discusses antenna pattern measurements recently made available and their impact on the conclusions based on the ideal model.

3.0 ANTENNA PERFORMANCE ANALYSIS

It is clear that the ERIM L-band antennas were designed primarily for airborne side-looking imaging and not for precision measurement of clutter phenomenology. The large elevation beamwidth is intended to provide a wide range swath for imaging with the narrower azimuth beam processed to provide synthetic resolution in the cross-track direction. Thus, it is important to determine if there are any serious limitations imposed by these antennas when used for other purposes such as gathering clutter data. The paragraphs that follow address this important topic.

3.1 Clutter-to-Noise Ratio

The most important figure-of-merit for the proposed ERIM clutter measurement instrumentation system is the clutter-to-noise ratio (C/N). Without an adequate C/N, clutter model validation is seriously compromised in two ways. First, the variations in mean clutter reflectivity predicted by candidate physical models cannot be measured with confidence. Secondly, the statistical variation of the reflectivity coefficient (which is needed for detection probability and false alarm probability calculations by the HBR system designer) cannot be accurately determined. The antenna parameter affecting C/N most directly is its gain since gain enters the bistatic radar equation as a squared term (i.e., as the product of the transmit gain and receive gain).

The antenna gain must be adequate to yield a C/N for the expected values of the remaining system parameters included in the bistatic range equation. Table 3-1 shows C/N calculations for the ERIM system as proposed at the CMP Kickoff Meeting and in early August of 1986. A mean reflectivity of -30 dB was used in these calculations corresponding to estimates provided by candidate reflectivity models for out-of-plane geometries (i.e., illuminator, target clutter patch, and receiver not in the same plane). Assuming that bistatic clutter exhibits Rayleigh amplitude statistics (exponential power) leads to the observation that the clutter signal would be below the mean receiver noise level less than 0.25% of the time for a C/N of 26.2 dB and about 11% of the time for a C/N of 9.2 dB. Clearly, the larger C/N is desirable since the sampled clutter data will be significantly less corrupted by receiver noise. Since the larger C/N was obtained with the antenna gains given in Table 2-1, it is concluded that the ERIM antenna is adequate for the measurement program provided other system parameters are appropriately chosen.

Furthermore, for clutter model validation, a capability to accurately measure reflectivity to the -30 dB level appears to be sufficient. That is, clutter



Table 3-1 SINGLE PULSE CLUTTER-TO-NOISE RATIO
COMPARISON

PARAMETER	PROPOSAL 25 JAN 1985	K/O MEETING 10 JULY 1986	LATEST 1 AUG 1986
FREQUENCY	1.275 GHz	1.2-1.4 GHz	1.2-1.4 GHz
WAVEFORM	LINEAR FM	PULSED CARRIER	PULSED CARRIER
PEAK POWER	5000W	5000W	5000W
PULSEWIDTH	1.2 μ s	0.5 μ s	50ns
BANDWIDTH	40MHz	2MHz	20MHz
XMTR GAIN	16.5 dB	17dB	17dB
RCVR GAIN	16.5 dB	17dB	17dB
CLUTTER CELL AREA	0.9 X 10 ⁶ SQ FT	4.4 X 10 ⁶ SQ FT	4.4 X 10 ⁶ SQ FT
CLUTTER REFLECTIVITY	-30dB	-30dB	-30dB
LOSSES	6dB	6dB	6dB
NOISE FIGURE	6dB	6dB	3dB
BISTATIC ANGLE	150°	150°	160°
C/N	22.2dB	26.2dB	9.2dB

A-3301

model validation can be achieved by planning experiments (through terrain and geometry selection) that will result in predicted levels in excess of -30 dB.

3.2 Antenna Sidelobes

In determining clutter reflectivity from measured radar cross section (RCS) data, it is generally assumed that the received power is not contaminated by the sidelobes. Sidelobe power can be minimized by various aperture weighting techniques at the expense of gain and beamwidth. However, the ERIM antenna does not incorporate aperture weighting. Consequently, its sidelobes levels will be very close to those shown in Table 2-1. The percentage of sidelobe power for nominal geometries at ranges of interest relative to the mainbeam power has been computed using the antenna model described above taking into account the variation of bistatic range over the constant range contour. It has been found that the ratio of sidelobe power to mainbeam power along constant bistatic range contours ranges from -10.3 dB for a typical in-plane geometry to -26 dB for an out-of-plane geometry. The low value for the out-of-plane geometry can be attributed to the two-way bistatic antenna geometry where the majority of sidelobe energy comes from the intersection of the mainbeam with only one set of near-in sidelobes of the opposite facing antenna. This is different than the in-plane geometry where the sidelobes intersect each other.

These preliminary integrated sidelobe to mainbeam power ratios indicate that sidelobe interference is not negligible. This problem would be exacerbated by selecting geometries where the reflectivity in the sidelobe regions along a constant bistatic range was much greater than in the corresponding mainbeam region. Similarly, if large specular scatterers appear in the sidelobe region, sidelobe energy at the bistatic range of interest may be a problem. Circumvention of this problem may be possible by carefully planning the experiment to avoid such conditions. In addition, real-time data processing would provide warning when this situation occurred and the geometry or test conditions modified immediately. The latter situation would be most likely to occur in the presence of man-made clutter or when examining very low regions of reflectivity with the mainbeams.

3.3 Antenna Beam Patterns

An ideal clutter measurement radar antenna would restrict the illuminated clutter patch to a region over which the measured phenomenon would be essentially homogeneous. This greatly simplifies the inversion of radar cross section (RCS) to reflectivity coefficient and would significantly increase confidence in the resulting data. Unfortunately, with today's limited understanding of clutter behavior (particularly bistatic clutter) it is difficult to predict the size of this ideal region. Secondly, if the ideal clutter patch is very small, the antenna azimuth and elevation beamwidths must be made correspondingly small. Since beamwidth is inversely related to antenna size, this calls for an increase in antenna dimensions which may impose severe limitations on the airborne platform installation. In addition, development of a new antenna specifically for the HBR Clutter Measurement Program driven by such a requirement would undoubtedly be prohibited by available funding and schedule constraints. In this context, the capabilities of the proposed ERIM antenna, its limitations, and possible work-arounds to the limitations are addressed next.

3.3.1 Azimuthal Beam Pattern Effects on Reflectivity Measurement

To explore the variation of clutter reflectivity that can be expected within an ERIM antenna beam, a clutter model was chosen that was known to exhibit nonuniform behavior over a planar rough surface as well as interesting polarization effects. This model can be considered to fall into the "worst-case" category of reflectivity models for these reasons. The basis for this model is a solution of an integral equation representing the bistatic scattered field using the tangent plane approximation, i.e., the field at every point on the rough surface is related to the incident field by the Fresnel reflection coefficients. In essence, this model is based on the contention that all of the scattering from a very rough surface comes from areas which specularly reflect. Specific parameters chosen for the model were a relative permittivity of 10 and an RMS slope of 35 degrees. The former represents terrain with about 10 to 15% moisture content. The RMS slope is characteristic of very rough terrain where shadowing effects can be expected to be significant.

Shadowing effects are modeled separately for this case and represent the probability that the facet angle of incidence and reflection are oriented to scatter energy from the transmitter to the receiver.

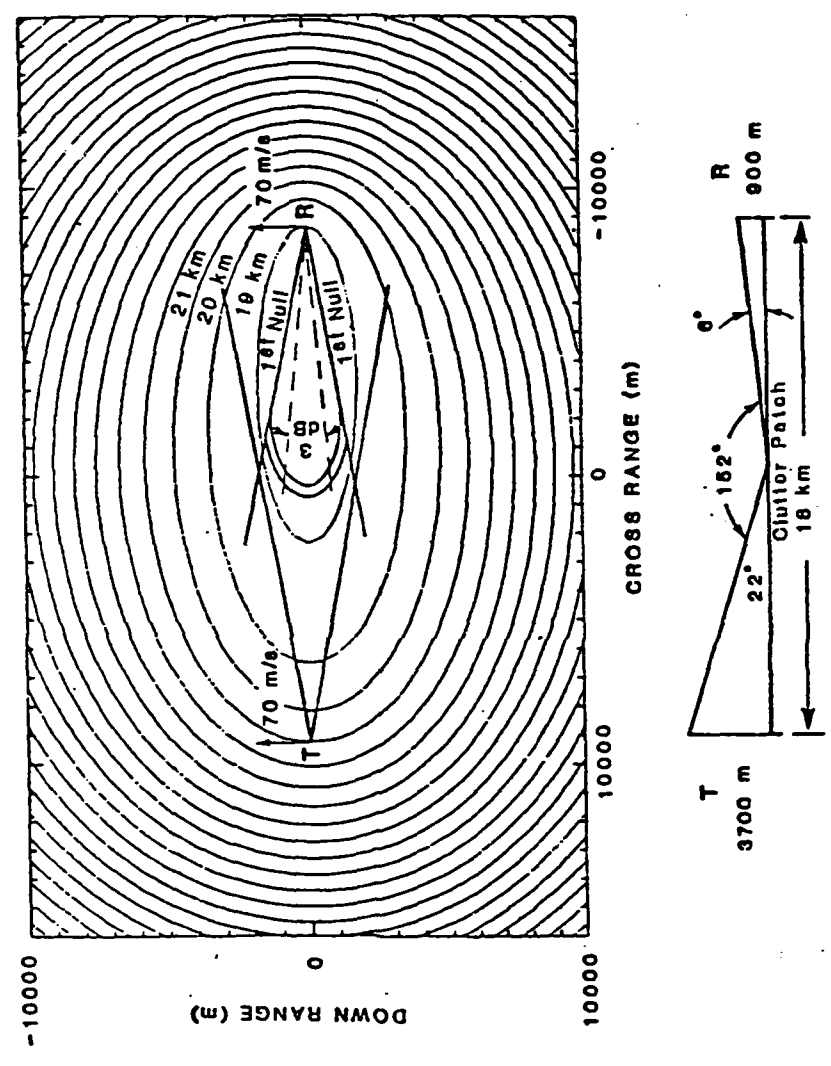
Reflectivity contours have been plotted for two representative CMP geometries. The geometries are (1) in-plane, and (2) out-of-plane. The location of receiver and transmitter platforms are shown in Figures 3-1 and 3-2 superimposed on constant bistatic range contours. The bistatic range cell centered on the clutter patch of interest is also shown on the figures. Since the antenna azimuthal beamwidth attenuates the clutter power along the constant range contour, the null-to-null and 3 dB beamwidth effects are also shown. The width of the range cell is determined by the pulse length and other geometric parameters.

The resulting reflectivity contours (horizontal-horizontal polarization) for the in-plane and out-of-plane cases are shown in Figures 3-3 and 3-4 respectively. The unusual diamond-like patterns are an artifact of the contouring program used to generate these plots. The region where this effect occurs is actually a deep valley separating the plane into interior and exterior regions. This behavior is unlike simple clutter scattering models that vary uniformly over the surface and is probably more nearly like the real-world. It has also been observed that within the interior region, the horizontal-horizontal (HH) coefficient is greater than the vertical-vertical (VV) coefficient and in the exterior region the opposite relationship is true.

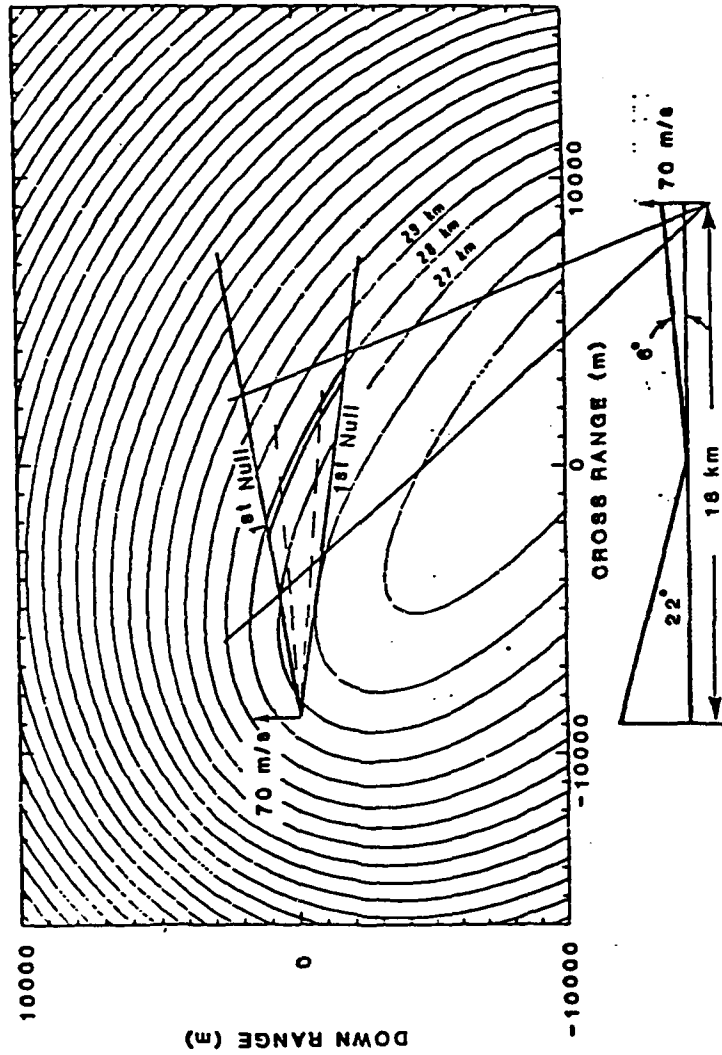
Examination of the variation of reflectivity values for the HH polarization over the bistatic range cell of Figure 3-3 indicates a variation from +3dB to about -3 dB over the antenna null-to-null length or +3 dB to 0 dB between the combined bistatic antenna pattern 3 dB width. Therefore, for this in-plane geometry, the variation of reflectivity is on the order of or less than the expected calibration accuracy of the ERIM radar (about 5 dB) and probably would not be detectable. In marked contrast, Figure 3-4 shows a much larger variation over the desired clutter patch. In this case, the coefficient ranges from -33 dB to -63 dB over the null-to-null beamwidth and from -38 dB to -55 dB for the 3 dB beamwidth. Such a wide range of variation is clearly not desirable. However, this situation is mitigated by the fact that the

**IN-PLANE GEOMETRY -
BISTATIC RANGE CELL ($\beta = 150^\circ$)**

Figure 3-1



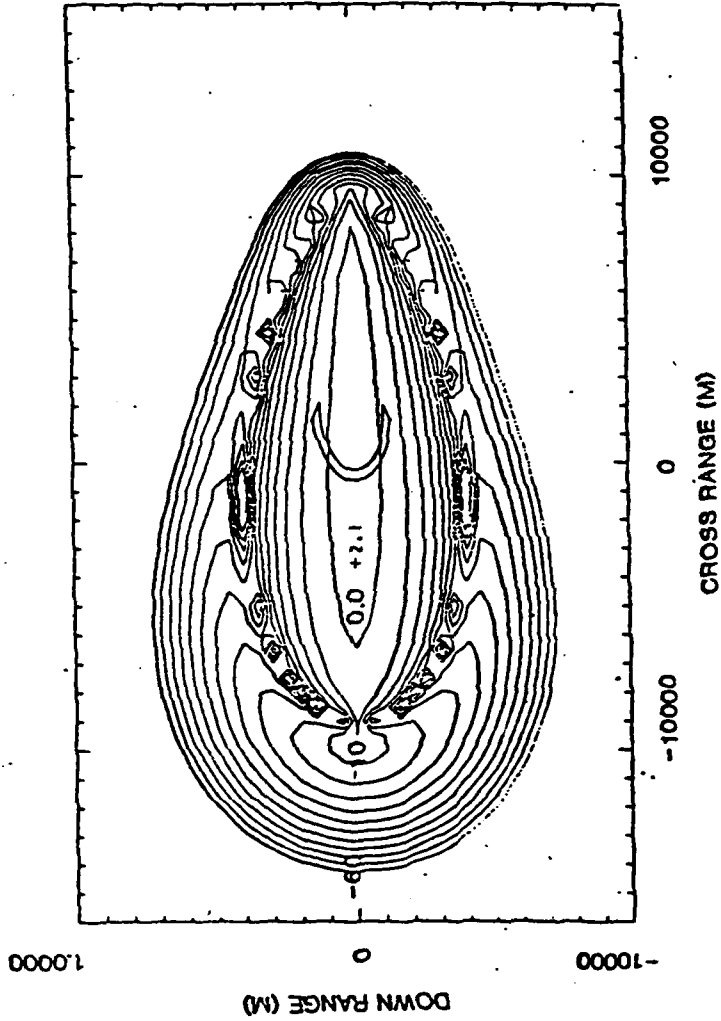
A-3404



**IN-PLANE GEOMETRY - VERY ROUGH TERRAIN
HH POLARIZATION**

Figure 3-3

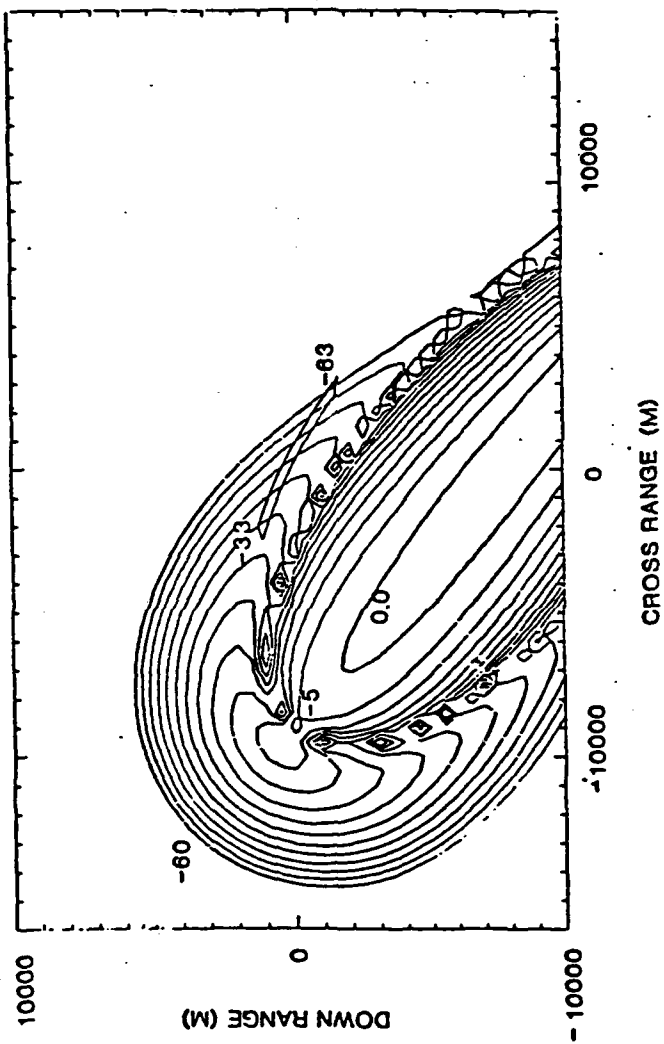
SRS
TECHNOLOGIES



4-9-83

OUT-OF-PLANE GEOMETRY - VERY ROUGH TERRAIN
HH POLARIZATION

Figure 3-4



reflectivity values are so low that they are probably well below the sensitivity of the ERIM radar.

It is also quite simple to overcome this limitation and provide sufficient information to validate this model by careful experiment design. In the out-of-plane case, data from range cells inside the valley would be compared with data outside the valley in both polarizations. Inside the valley, the HH reflectivity coefficient should be higher than the VV coefficient. Similarly, outside the valley, the situation should be reversed and the absolute levels of the reflectivity lower. Furthermore, since the model predicts the variation of reflectivity over the range cell, compensation for this effect would be possible during the inversion from absolute radar cross section (RCS) to reflectivity coefficient. Even more simply, the HH RCS of each range gate ranging from the interior of the valley to the exterior could be examined to see if the return decreased to the receiver noise level and then emerged from the noise for a limited (but predictable) extent. This test combined with a reversal of the relative amplitudes between the HH and VV polarizations would lend a great deal of credence to the validity of this model. On the other hand, if neither effect was observed, model predictions would clearly be in error.

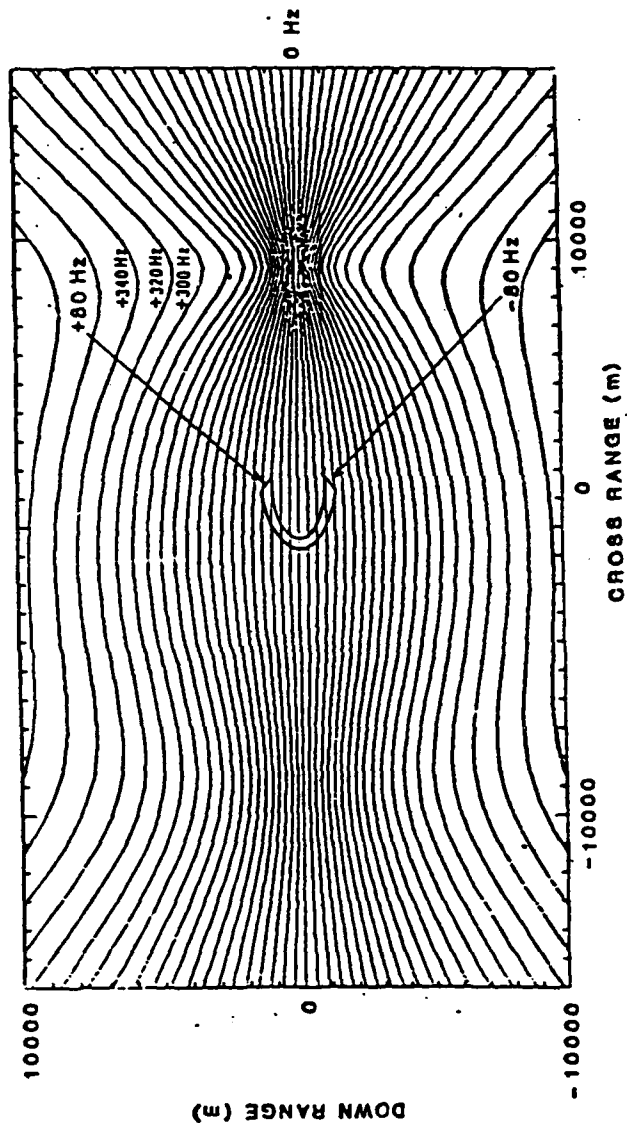
3.3.2 Coherent Processing For Synthetic Azimuth Beam Sharpening

In addition to the test planning approach mentioned above to overcome the limitations imposed by the azimuth extent of the ERIM antenna, signal processing techniques based on synthetic aperture processing could be utilized to provide better azimuth resolution. Of course, it is necessary to record clutter data coherently to achieve this capability. This possibility is illustrated for the in-plane and out-of-plane cases in Figures 3-5 and 3-6. Note a Doppler spread of +80 to -80 Hz occurs over the null-to-null bistatic range cell in the in-plane case (Figure 3-5). The out-of-plane case provides a smaller but significant spread of 60 Hz. Doppler resolution (and hence, synthetic beam formation) is limited by the reciprocal of the time a clutter patch remains within the antenna beam and bistatic range cell. For the in-plane case with a pulsewidth of 0.5 microseconds, this corresponds to the time the bistatic range cell moves about 2000 m. Since the cell is moving at the platform velocity with respect to the ground (70 m/s), this time is equal to 28 seconds. Thus, a Doppler resolution of 1/28 Hz is theoretically possible. Since the total Doppler spread is 160 Hz, the antenna azimuth could then be synthetically improved by a factor 4,480. This is not achievable in practice due to phase errors associated with platform motion and other effects occurring during the processing interval. An analysis of platform motion induced velocity and acceleration phase errors has shown that synthetically processing the beam into about 10 parts would be possible without requiring platform motion compensation. Although this is well below the theoretical maximum, it would favorably improve clutter resolution and allow more precise spatial reflectivity measurements.

In the out-of-plane case, the bistatic range cell normal to its motion over the ground is not nearly as wide as for the in-plane case. In this case, the bistatic range cell is only about 200 m wide. Thus, the clutter patch remains coherent for only about three seconds. However, this still yields a theoretical improvement in azimuth resolution of over 180. As before, it

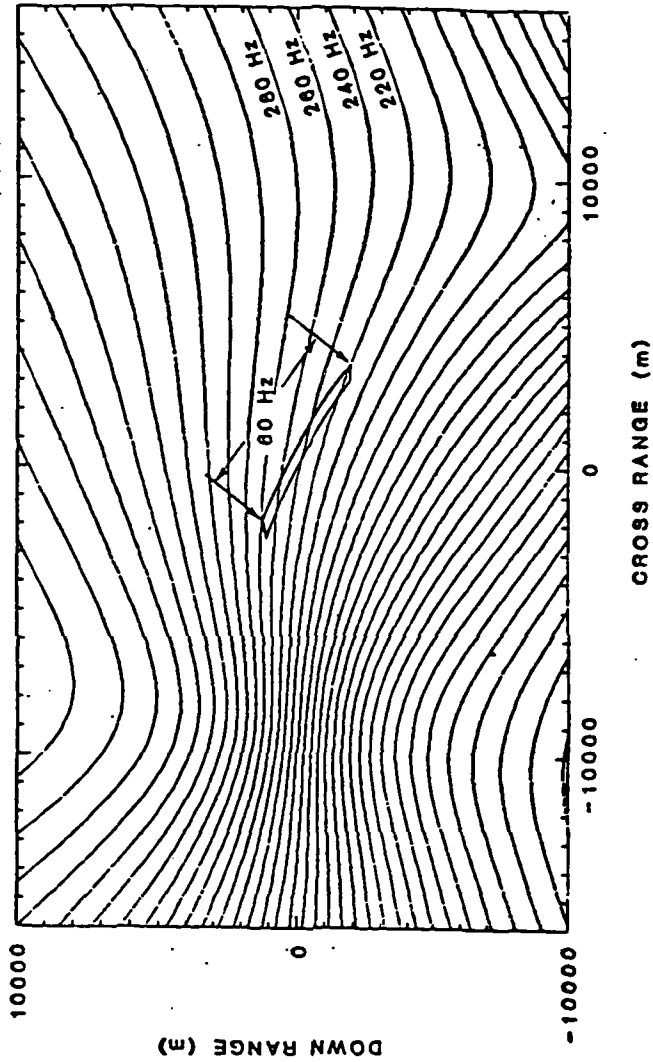
**IN-PLANE GEOMETRY -
BISTATIC DOPPLER CONTOURS**

Figure 3-5



A-3300

Figure 3-6 **OUT-OF-PLANE GEOMETRY -
BISTATIC DOPPLER CONTOURS**



A-3393

appears likely that the beam could be synthetically resolved into at least 10 parts without requiring aircraft motion compensation.

The above discussion assumes that the pulse repetition frequency (PRF) of the channel being coherently processed is at least equal to the Doppler spread expected in the bistatic range cell. This is necessary to prevent "foldover" or "aliasing" of clutter power at higher Doppler frequencies into the lower frequencies. Thus, for the in-plane case, a PRF for one channel should be at least 160 Hz. This is above the currently envisioned 119 Hz PRF so that the proposed waveform may need to be modified. The 119 Hz PRF is adequate for the out-of-plane example.

3.4 Antenna Polarization

Model validation requires measurement of clutter scattering polarization effects. This includes the principal polarizations HH and VV along with their corresponding cross polarizations HV and VH. As mentioned previously, clutter models predict substantially different behavior for HH and VV. The same is true for the cross polarization reflectivity.

Polarization isolation is a significant antenna requirement if accurate cross polarization reflectivity measurements are to be made. That is, if transmission polarization is horizontal and the receive polarization is horizontal, the resulting received energy is referred to as HH. Any depolarization caused by the clutter or antenna orientation would appear in the receiver's vertically polarized antenna elements and is called VH. Consequently, the vertical elements of the antenna should not respond to a horizontal electric field in this example or the depolarization phenomenon would be masked. In practice there is always some coupling between the antenna elements in different polarizations. This coupling limits the minimum sensitivity of the cross polarization channel. This is of particular significance for the in-plane geometry since theory predicts no depolarization is to be expected. As the out-of-plane angle increases, the cross polarization return increases. Analysis of this effect indicates that the cross polarization is about 20 dB below the principal polarization return when the out-of-plane angle reaches 10 degrees. Thus, the ERIM antenna, with a design goal of 20 dB isolation, would allow model prediction of cross polarization to principal polarization ratios for out-of-plane angles exceeding 10 degrees. Within the 10 degree limit, model validation would be demonstrated by the cross polarization data channels indicating receiver noise output only.

3.5 Antenna Calibration

A priori knowledge of the antenna patterns in two dimensional space is needed to accurately invert RCS to reflectivity. This is particularly true if the reflectivity is expected to vary over the bistatic range cell of interest. If this is not the case, then calibration of the entire system using a ground based repeater may provide sufficient accuracy. Since ERIM antenna measurements will be limited to the cardinal planes (horizontal and vertical cuts), the necessary spatial antenna patterns will not be available. Based on limited analysis of the effect of sidelobes on RCS measurement using ideal antenna patterns, it appears that only calibration of the mainbeam region

would be required. In this region, knowledge of the antenna's gain within 1 dB would seem adequate considering the overall system accuracy.

3.6 Other Antenna Considerations

The factors mentioned previously have the greatest impact on clutter measurement accuracy. However, there are other effects that will also limit accuracy even if the above error contributors were nonexistent. Two of these second order effects are (1) pattern distortion due to reflected energy interacting with the aircraft fuselage, wings, etc., and (2) radome attenuation. Aircraft and antenna interaction is most severe in low sidelobe antennas. Since the ERIM antenna aperture is uniformly illuminated, it does not produce extremely low sidelobes and the impact of this interaction should be small. Similarly, the radome impact on antenna patterns should be small as well. Based on the overall system accuracy, requirements for these effects to be less than 0.5 dB on the mainbeam gain and 1.0 dB in the sidelobe region (in both polarizations) seems sufficient to ensure their effects are negligible.

4.0 SUMMARY AND PRELIMINARY COMMENTS ON ERIM ANTENNA MEASUREMENTS

Based on the analyses performed to date with ideal antenna models over a limited set of geometries and worst case reflectivity behavior, the following conclusions can be drawn:

1. ERIM's antenna design goals will provide adequate C/N for regions of interest.
2. Sidelobe interference is possible but can be avoided by selection of favorable geometries. It is also recommended that real-time processing be performed to monitor this problem.
3. The relatively large azimuth beamwidth of the proposed antennas will result in significant variation of reflectivity over a bistatic range cell. However, test planning, geometry selection, and coherent processing will mitigate this effect.
4. Polarization isolation of 20 dB appears to be adequate for clutter model validation.
5. Calibration of the mainbeam pattern should be performed.
6. Second order effects should be restricted to 0.5 dB in the mainbeam region and to less than 1 dB in the sidelobe regions.

Recently received data from RADC showing L-band antenna pattern measurements made by Chu Associates for an antenna very similar to that proposed by ERIM for CMP indicates that mainbeam behavior in the horizontal and vertical planes is very near the ideal model described above for both the azimuth and elevation planes. The sidelobe levels also appear reasonably consistent with the ideal model for vertical polarization in both planes. However, there is significant disagreement between the model sidelobe levels and the measured horizontal polarization sidelobes in both planes. In particular, the L-band

azimuth horizontal polarization patterns exhibit very wide near-in sidelobes with amplitudes at about the -10 dB level. Chu Associates indicates this may be caused by an error in cabling, a bad cable, or other feed errors. This is a serious problem since the foregoing analysis indicated that the ideal model sidelobe levels (which are narrower and lower) may introduce errors into the measurements under some conditions. These anomolous sidelobe levels were included in the model and geometry in Section 3.2 and found to seriously affect the sidelobe to main beam power ratio along a constant bistatic range contour. The side-lobe to main-beam clutter ratio decreased from -10.3 dB to -8.7 dB for the in-plane case. The most severe change was from -26 dB to -5.4 dB for the out-of-plane case. As a result, it is strongly recommended that the reason for the anomalous behavior of the test article be investigated and remedied so it does not impact CMP clutter measurements.

This report focused on bistatic clutter measurement antenna related issues. In the future, a similar analysis will be performed for the proposed ERIM antenna as part of the monostatic radar.

DESIGN PLAN
ANTENNA BEAM REGISTRATION ANALYSIS AND REQUIREMENTS

ELIN A003

CONTRACT TITLE: BISTATIC CLUTTER PHENOMENOLOGICAL
MEASUREMENT/MODEL DEVELOPMENT

CONTRACT NUMBER: F30602-86-C-0045

CONTRACT PERIOD: 1 APRIL 1986 TO 31 SEPTEMBER 1987

PREPARED BY: CHARLES H. HIGHTOWER

DATE: 14 AUGUST 1986

Prepared for:

ROME AIR DEVELOPMENT CENTER
GRIFFISS AIR FORCE BASE
NEW YORK 13441-5700

SRS

TECHNOLOGIES

ADVANCED TECHNOLOGY DIVISION
17252 ARMSTRONG AVENUE
IRVINE, CALIFORNIA 92714
(714) 250-4206

1.0 INTRODUCTION

This report has been prepared under Contract Number F30602-86-0045 as part of the Design Plan called for by ELIN A003 in support of the Hybrid Bistatic Radar (HBR) Clutter Measurements Program (CMP) Assessment Study. The issue addressed in this report is beam registration. Beam registration in the bistatic experiment is accomplished by pointing or aiming the transmitter and receiver antennas at the same point in a coordinate system moving with both platforms. This ensures the ground area illuminated can be later correlated with the recorded clutter data. Secondly, beam registration is needed to maintain a fixed orientation between the two antennas so that antenna gain and range effects can be removed in the conversion of clutter Radar Cross Section (RCS) to clutter reflectivity. Since aircraft motion, Inertial Navigation System (INS) position and heading, and servo system characteristics are not ideal, it can be expected that the antenna beams will not be perfectly registered at all times.

The effect of errors in beam registration can be assessed by examining (1) the resulting variation in illuminated area, and (2) the perturbation of the combined bistatic antenna pattern over the illuminated region. The impact of beam misalignment on these two parameters is discussed in the following paragraphs.

2.0 VARIATION IN ILLUMINATED AREA DUE TO ERRORS IN BEAM REGISTRATION

For the out-of-plane HBR CMP geometry with low grazing angles, it can be shown that the bistatic range cell area (A_c) is given by the expression

$$A_c = R \times \Theta \times (c \times \tau / 2) \times \sec^2(\beta / 2) \quad (1)$$

where,

- R = range to transmitter or receiver
- Θ = antenna one-way 3 dB beamwidth
- c = speed of light
- τ = pulsewidth
- β = bistatic angle.

This equation assumes that the difference of the distances between the transmitter-clutter patch-receiver path and the transmitter-to-receiver line-of-sight (LOS) path is much greater than the pulsewidth. Under these conditions, an error in beam registration is equivalent to an error in bistatic angle. Thus, (1) can be differentiated with respect to β and the resulting sensitivity of A_c found. The normalized result is given by (2).

$$\Delta A_c / A_c = \Delta \beta \times \tan(\beta / 2) \quad (2)$$

The effect of a one degree error in bistatic angle in the vicinity of various bistatic angles is shown in Table 2-1. The one degree error may be thought of as the combined transmitter and receiver antenna pointing angle error or the

combined platform position error divided by the range to the target. In the latter case, for a range of 25,000 feet to the clutter patch, the combined platform position error corresponding to one degree is 436 feet.

Table 2-1 Beam Registration Angle Error Versus Bistatic Angle -

<u>Bistatic Angle</u> (Degrees)	$\Delta A_c / A_c$ (dB)	$(A_c + \Delta A_c) / A_c$ (dB)
120	-15.2	0.13
130	-14.3	0.16
140	-13.2	0.19
150	-11.9	0.27
160	-10.0	0.41
170	- 7.0	0.79

The right hand column of Table 2-1 shows the effect of a one degree beam registration error on the total area within a bistatic range cell for the given nominal bistatic angle. Clearly, errors of this magnitude on RCS measurement are insignificant compared with overall system calibration accuracy.

3.0 Bistatic Beam Pattern Perturbation Due to Beam Registration Errors

The effect of beam misalignment on the gain/range pattern over the illuminated clutter region was investigated by simulation since it is virtually impossible to find a closed form solution for this function. In particular, the -3dB and -20 dB contours of the combined antenna gain and bistatic range parameters for no misalignment were compared with the case when the receiver pointing angle was one degree in error. The resulting contours are shown in Figure 3-1. Note that these contours shift in the direction of the beam error as would be expected. The most significant effect of the misalignment is associated with the -3 dB contour since the difference in the -20 dB contours is relatively small. The new area illuminated within the -3 dB contour is approximately equal to 12.5 percent of the original area. By properly choosing the test sites so that the general terrain type examined does not change dramatically over the uncertainty in error caused by misregistration, this effect can be mitigated.

The difference in bistatic gain/range between the perfectly aligned case and the misaligned case at the true aimpoint (point 1) is 0.07 dB and about 2 dB at point 2 on Figure 3-1. Thus, it is expected that numerical integration of the combined gain/range patterns bounded by the two contours would yield results within 2 dB of each other. This is particularly true when integrating along a line of constant bistatic range. Therefore, it is concluded that one degree error in beam registration (caused either by combined platform position error or combined antenna pointing error) will not significantly affect the accuracy of the reflectivity measurement due to antenna gain/range variation considering the overall system accuracy predicted by ERIM (on the order of 3 to 5 dB).

4.0 CONCLUSIONS

It is concluded that beam registration effects on reflectivity measurement can be controlled by constraining the combined bistatic platform position errors and antenna pointing errors. The results of this analysis indicate that sufficient values for these parameters are 463 feet and one degree, respectively, assuming the ranges from the transmitter and the receiver to the illuminated clutter patch are 25,000 feet. For longer ranges a larger position error can be tolerated but the pointing angle must be proportionally smaller. Additional analysis effort may be required if these values impose impractical or costly requirements on HBR CMP instrumentation.

DESIGN PLAN
CMP DOPPLER SPREAD ANALYSIS
ELIN A003
SRS UR87-089

CONTRACT: BISTATIC CLUTTER
PHENOMENOLOGICAL
MEASUREMENT/MODEL DEVELOPMENT

CONTRACT NUMBER: F30602-86-C-0045

CONTRACT PERIOD: 1 APRIL 1986 TO 31 SEPTEMBER
1987

PREPARED BY: CHARLES H. HIGHTOWER

DATE: 15 APRIL 1987

Prepared For:
ROME AIR DEVELOPMENT CENTER
GRIFFISS AIR FORCE BASE
NEW YORK 13441-5700

SRS

TECHNOLOGIES

CORPORATE HEADQUARTERS
1500 QUAIL STREET, SUITE 350
P.O. BOX 9219
NEWPORT BEACH, CALIFORNIA 92660
(714) 833-9088

1.0 INTRODUCTION

This report has been prepared in response to the Action Item assigned SRS Technologies by RADC resulting from the 25 to 26 March 1987 Clutter Measurements Program Quarterly Review Meeting (QRM) held at ERIM facilities in Ann Arbor, Michigan. The Action Item is described in an RADC letter dated 9 April 1987 on page 3, item 1. The Action Item is concerned with the aimpoint range-gate Doppler spreads predicted for various CMP test matrix cases. Specific questions addressed are:

1. Are the results to date correct?
2. Can performance be improved?

2.0 THEORETICAL BACKGROUND

The Doppler frequency of any point on a fixed surface for a bistatic system with moving platforms can be calculated using the vector expression given in Equation 2.1.

$$f_d = (\mathbf{v}_r \cdot \mathbf{r}_r + \mathbf{v}_t \cdot \mathbf{r}_t) / \lambda \quad 2.1$$

where,

f_d = Doppler frequency at point (x, y, z)

\mathbf{r}_r = a unit vector pointing from platform r to the point (x, y, z)

\mathbf{r}_t = a unit vector pointing from platform t to the point (x, y, z)

\mathbf{v}_r = platform r velocity

\mathbf{v}_t = platform t velocity.

The geometry associated with this expression is shown in Figure 2-1.

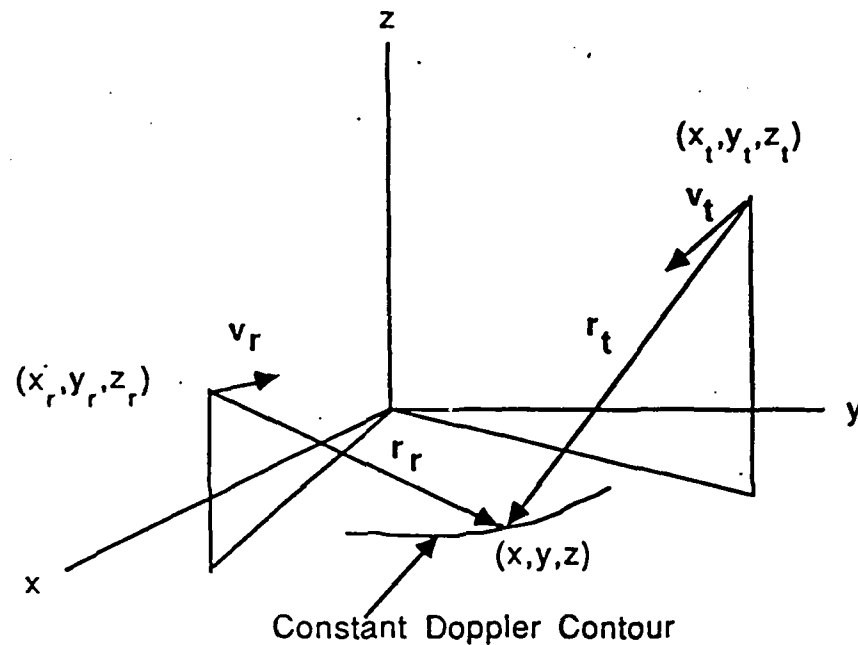


Figure 2-1 Doppler Frequency Calculation Geometry

During CMP data collection, the vectors v_r and v_t are parallel and point in the same direction (along track). Each aircraft will maintain a constant airspeed of about 215 Knots (113 m/s). Thus, the maximum Doppler frequency possible would be for a point infinitely far from the aircraft where the unit vectors r_r and r_t are parallel to the velocity vectors. In this case, the maximum bistatic Doppler frequency at a wavelength of 25 cm is

$$f_d = (113 + 113) / 0.25 = 904 \text{ Hz.}$$

In principle, the maximum Doppler spread would be twice this

value or 1,808 Hz resulting from points infinitely far ahead and behind the aircraft platforms being illuminated by the antenna.

Of course, this is an impossible condition since the CMP aircraft antennas are highly directional.

3.0 CMP DOPPLER SPREAD ANALYSIS

At the 25 March CMP Quarterly Review Meeting, Doppler spreads for 28 candidate data collection geometries were shown. The calculations were made using Equation 2.1 for each case and are repeated in Table 3-1 (fifth column). Note that the maximum Doppler spread occurs for Case B-10. In this case, the Doppler frequency across the bistatic range cells of interest ranged from -640 Hz to +340 for a total Doppler spread of 980 Hz. This Doppler spread corresponds to the maximum and minimum Doppler frequencies across 16 range gates centered on the aim point, not just the aimpoint as the column heading indicates. Antenna weighting was not considered nor was the relative strength of the high Doppler regions. These results led to the conclusion that a 500 Hz PRF would not provide adequate clutter aliasing protection.

Since the CMP waveform and PRF are relatively invariant, this problem was explored in more detail after the QRM. It was found that reducing the size of the area examined from 16 to four range gates did not significantly change the results. However, upon further analysis, it was observed that the areas responsible for the extreme Doppler values were located very near the lower altitude aircraft on either side. This occurs because of a "cusping" of the isodoppler contours relative to the isorange contours in these regions. This is unlike the situation near the aim point of the two antennas where the isorange and isodoppler contours are nearly parallel.

The relative magnitude of clutter power occurring at the extreme Doppler frequencies was then examined. The size of these regions compared to the total area of a bistatic range contour was found to be very small. In addition, these areas are heavily weighted by the bistatic antenna gain pattern. The SRS Radar Clutter Workstation was used to examine the effect of these factors on

TABLE 3-1

* over 16 range gates

CASE NUMBER	AIM POINT BISTATIC ANGLE (DEG)	BISTATIC ANGLE VARIATION (DEG) *	DIMENSIONS OF MAINBEAM ON GROUND (NMI x NMI) *	AIMPOINT RANGE GATE DOPPLER SPREAD (HZ)*	AIMPOINT ARRIVAL RELATIVE TO DIRECT PATH (GATES)	CAN SIDELOBE EFFECTS BE ELIMINATED BY DOPPLER PROCESSING? RANGE GATE/ DOPPLER PROC.
A-1	150°	136° to 150°	0.65 x 4.11	-200 to 200	16.17	N Y
A-2	148.4°	132° to 148.4°	1.15 x 5.10	-300 to 300	17.9	N Y
A-3	156°	136° to 156°	0.99 x 3.54	-360 to 360	8.64	N Y
A-4	154.1°	142° to 158°	1.0 x 4.11	-420 to 420	10.08	N Y
A-5	138.1°	130° to 140°	1.39 x 2.96	-520 to 500	26.10	N S
A-6	158°	140° to 158°	1.32 x 4.39	-480 to 480	10.79	N Y
A-7	157.5°	140° to 157.5°	1.56 x 5.10	-500 to 500	11.33	N Y
A-8	155.9°	140° to 155.9°	1.40 x 5.51	-520 to 500	12.93	N S
A-9	150.5°	132° to 150.5°	1.23 x 6.17	-500 to 400	19.33	N S
A-10	139.2°	129° to 139.2°	1.22 x 4.44	-600 to 360	36.79	N S
A-11	159.5°	132° to 161°	2.47 x 5.02	-420 to 420	14.69	N Y
A-12	157.3°	140° to 162°	0.25 x 14.86	-500 to 300	18.02	N Y
A-13	170.1°	130° to 170°	3.29 x 24.18	-440 to 440	3.29	Y Y
A-14	170°	152° to 170°	2.14 x 12.99	-360 to 360	2.66	N Y
B-1	135°	120° to 135°	0.66 x 1.65	-360 to 360	28.16	Y Y
B-2	134°	120° to 134°	0.99 x 2.13	-300 to 360	29.42	Y S
B-3	141°	126° to 141°	0.66 x 1.56	-460 to 460	18.38	Y Y
B-4	139.9°	123° to 140°	0.91 x 1.09	-500 to 440	19.44	Y S
B-5	129°	117° to 129°	0.50 x 2.30	-600 to 400	31.21	N S
B-6	143°	126° to 143°	1.15 x 1.65	-500 to 500	22.46	Y Y
B-7	142.7°	127° to 143°	1.09 x 2.06	-540 to 540	22.82	Y S
B-8	141°	125° to 141°	0.99 x 2.55	-500 to 520	23.08	Y S
B-9	130.5°	121° to 140°	1.02 x 3.29	-600 to 440	20.14	N S
B-10	130.6°	112° to 133°	0.02 x 3.45	-640 to 340	39.72	S S
B-11	144.5°	130° to 145°	0.62 x 1.64	-440 to 440	20.0	Y Y
B-12	143.3°	116° to 135°	0.62 x 2.30	-480 to 380	29.9	N Y
B-13	100°	02° to 100°	0.99 x 3.04	-300 to 300	67.0	no sidelobe activity
B-14	100°	02° to 100°	0.99 x 3.04	-300 to 300	67.21.....	no sidelobe activity

Doppler spread. The results are shown in the right-hand column of Table 3-2 using a -20 dB threshold for antenna pattern cutoff. Note the significant reduction in Doppler spread obtained. For example, the Doppler spread for Case B-10 has been reduced from 980 Hz to 180 Hz, well below the 500 Hz PRF. However, it should be pointed out that clutter energy at the higher frequencies in this region will appear in the received data due to antenna sidelobes. This will limit coherent processing gain to that of the relative sidelobe levels.

4.0 SUMMARY

Based on the analyses performed in the preparation of this report, it is concluded that the Doppler spread information presented at the QRM was properly computed. However, several important factors were not considered in that analysis which were incorporated in this report. These factors included both relative area and beam weighting. The results indicate the system PRF is adequate and no improvement is necessary.

TABLE 3--2

* over four range gates

CASE NUMBER	AIMPOINT ELEVATION ANGLES (DEGREES)				POTENTIAL PEAK RANGE GATE MEAN RCS VARIATION (DBSM)	POTENTIAL CLUTTER-TO-NOISE RATIO VARIATION (DB)	POTENTIAL ARC SIGNAL-TO-CLUTTER RATIO VARIATION (DB)	DOPPLER SPREAD ACROSS COMBINED BEAM PATTERN (HZ)
	RCVR/ILLUMINATOR							
	θ_1	θ_2	θ_1	θ_2				
A-1	-4°	2°	3°	-3°	42 to 80	52 to 58.3	13 to -25	-100 to 100
A-2	-9°	2°	5°	-6°	40 to 72	-8 to 50	15 to -17	-20 to 160
A-3	-1°	1°	2°	-3°	43 to 80	55 to 85	12 to -25	-100 to 100
A-4	-2°	1°	2°	-5°	40 to 70	-34 to 41	15 to -15	-40 to 140
A-5	-2°	1°	3°	-7°	-27 to 34.5	-119.9 to -119.9	82 to 20.5	220 to 320
A-6	-1°	1°	4°	-3°	33 to 72	50 to 81	22 to -17	-100 to 100
A-7	-1°	1°	5°	-4°	32 to 73	20 to 45	23 to -18	-60 to 140
A-8	-1°	1°	6°	-6°	30 to 62	-44 to 31	25 to -7	-40 to 180
A-9	-1°	1°	6°	-14°	-5 to 52	-25 to -17	60 to 3	50 to 220
A-10	-1°	1°	5°	-15°	-38 to 34.4	-119.9 to -119.9	93 to 20.6	220 to 280
A-11	-1°	1°	5°	-3°	19 to 69	24 to 67	36 to -14	-100 to 100
A-12	-1°	1°	13°	-8°	18 to 61	-57 to 10	37 to -6	-20 to 140
A-13	-2°	1°	7°	-3°	22 to 80	22 to 71	33 to -25	-100 to 100
A-14	-8°	1°	1°	-18°	30 to 75	-80 to 30	25 to -20	40 to 140
B-1	-1°	1°	3°	-4°	45 to 75	65 to 82	10 to -20	-100 to 100
B-2	-2°	1°	7°	-5°	41 to 70	18 to 48	14 to -15	-20 to 200
B-3	-1°	1°	3°	-3°	43 to 67	55 to 77	12 to -12	-100 to 100
B-4	-1°	1°	5°	-5°	31.5 to 60	-16 to 39	23.5 to -5	-20 to 200
B-5	-1°	1°	0°	-12°	-30 to 39.5	-119.0 to -118.4	85 to 15.5	200 to 360
B-6	-1°	1°	4°	-4°	32 to 57.4	33 to 57	23 to -2.4	-100 to 100
B-7	-1°	1°	7°	4°	23 to 50.8	11 to 43	32 to -3.8	-60 to 160
B-8	-1°	1°	9°	-7°	10 to 56.2	-35 to 27	45 to -1.2	-20 to 200
B-9	-1°	1°	11°	-12°	-16 to 51.2	-119.3 to -19	71 to 3.8	40 to 240
B-10	-1°	1°	10°	-21°	-69 to 41.4	-120 to -119.8	124 to 13.6	140 to 320
B-11	-1°	1°	3°	-3°	19 to 59.2	10 to 40	36 to -4.2	-100 to 100

HYBRID BISTATIC RADAR
CLUTTER MEASUREMENTS PROGRAM
SRS CLUTTER WORKSTATION

27 FEBRUARY 1987

Contract Number:
F30602-86-C-0045

Prepared for:
Charles Hightower

Prepared by:
Catherine Sanders-Foster

TABLE OF CONTENTS

- 1.0 INTRODUCTION
- 2.0 GEOMETRY
 - 2.1 Bistatic Range Contours
 - 2.2 Bistatic Doppler Contours
 - 2.3 Bistatic Angle Contours
 - 2.4 Area Contours
 - 2.5 Normalized Range-Gain Contours
 - 2.6 Digitized Antenna Patterns
- 3.0 CLUTTER PHENOMENOLOGY
 - 3.1 Coherent Specular Scattering
 - 3.2 Incoherent Diffuse and Specular Scattering
 - 3.3 Shadowing Contours
- 4.0 SYSTEM PERFORMANCE
 - 4.1 Range-Doppler Cell of Interest
 - 4.2 Pulse Area vs. Bistatic Range
 - 4.3 Clutter To Noise Ratio (CNR) vs. Bistatic Range
- 5.0 PLOT OPTIONS
- 6.0 SYSTEM HARDWARE
- 7.0 SUMMARY

SRS CLUTTER WORKSTATION DESCRIPTION

1.0 INTRODUCTION

A Radar Workstation has been developed to support the clutter measurements project. A bistatic clutter prediction program is now available, which is capable of computing and plotting the following values, for an arbitrary bistatic system:

- 1) Bistatic Range
- 2) Doppler
- 3) Bistatic Angle
- 4) Area
- 5) Beam Patterns
- 6) Coherent Specular Scattering (Polarizations HH/VH/HV/VV)
- 7) Incoherent Diffuse Scattering (Polarizations HH/VH/HV/VV)
- 8) Incoherent Specular Scattering (Polarizations HH/VH/HV/VV)
- 9) Shadowing Contours (Slightly Rough & Very Rough Terrain)

The scattering may be computed in the spatial domain of along track and cross track, or it may be transformed to the time domain of range and doppler. The values listed above are divided into two groups. The first five are concerned with the geometry of the system. The last four involve clutter phenomenology.

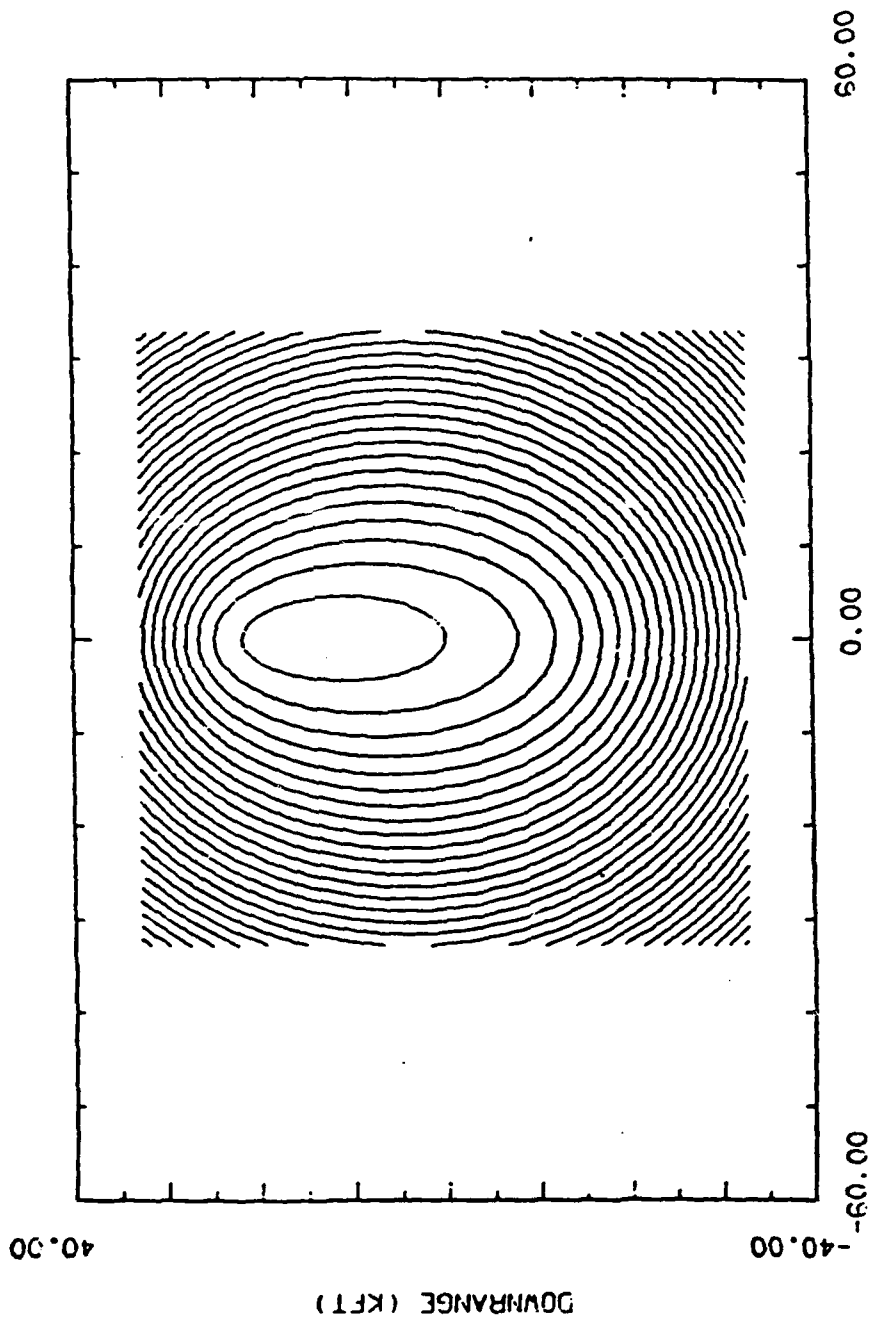
2.0 GEOMETRY

There are five plots generated by this workstation which provide the necessary geometrical information. They are bistatic range, doppler, bistatic angle, area and beam pattern. Each will be addressed separately in this section. The basic calculation of each variable and the information provided by the plot will be discussed.

2.1 Bistatic Range Contours

The Bistatic Range is the total distance from the transmitter to the ground to the receiver. The calculations involve determining the magnitude of the distance between the transmitter and the point on the ground, the same magnitude for the receiver, and summing the two magnitudes. The bistatic range contours display ellipses representing range gates of various constant ranges. (Figure 2-1) The inside contour represents half the bistatic range to the ground point. Each subsequent contour is incremented by 123 ft.

RISTATIC RANGE



CROSSRANGE (KFT)

FIGURE 2-1

17:08:44 18-DEC-86 98-330-81 4180121

2.2 Bistatic Doppler Contours

The Doppler frequency shift induced by system motion is the sum of the dot products of the velocity and unit range products for both transmitter and receiver, divided by the wavelength. The doppler contours are plotted in the spatial domain. See Figure 2-2. The main concerns are doppler width of the beam and whether sidelobe power can be discriminated, using the doppler frequency shift. A target can be discriminated if the doppler shift is significantly different from the terrain. The doppler frequency of the center contour is 0 Hz for the in-plane cases. For the out-of-plane cases, this value varies from case to case. Subsequent contours to the right are incremented by 20 Hz. Conversely, to the left, they are decremented by 20 Hz.

2.3 Bistatic Angle Contours

The Bistatic Angle is calculated by taking the arccosine of the dot product of the two unit range vectors calculated for the bistatic range. The projected bistatic angle is calculated by taking the arccosine of the dot product of the related unit projected range vectors. However, only the bistatic angle plots are currently generated. Refer to Figure 2-3 for a sample output. The bistatic angle contours help identify the geometric variations over various scattering areas. It also provides information on inputs for other variables. The bistatic angle of the center contour is listed on each case's description. The remaining contours are each 10 degrees less than the previous contour.

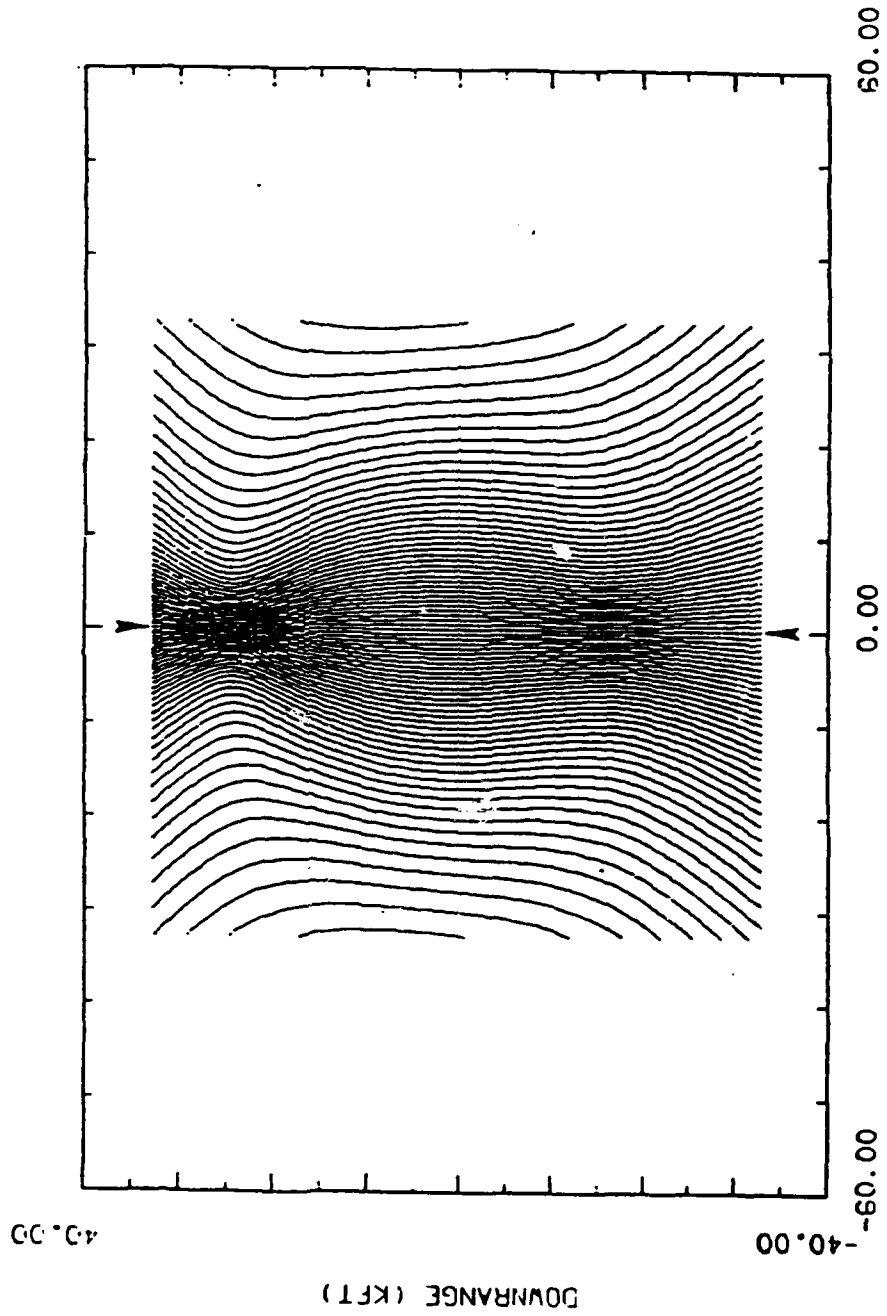
2.4 Area Contours

The Area of a cell can be calculated by dividing the product of x and y that were specified in the ground plane definition, by the dot product of the local and global plane normals. It is used for simulated terrains with facets tilted from the normal. It gives an indication of how much the ground is tilted. (Figure 2-4) The area plot represents a measure of the magnitude of local slopes, with mountainous terrains being a high slope and flat terrains equaling unity. These calculations are not radar system dependent. They depend purely on the elevation contours. Figure 2-5 is an elevation contour of the simulated terrain used to generate the beam area contours and represents a 10 meter contour of the surface elevations. The transformed area plots represent the range- doppler cell area.

2.5 Normalized Range-Gain Contours

Normalized Range-Gain Contours are generated by calculating the scalar field gain for a point within the antenna's view, for both the transmitter and

DOPPLER

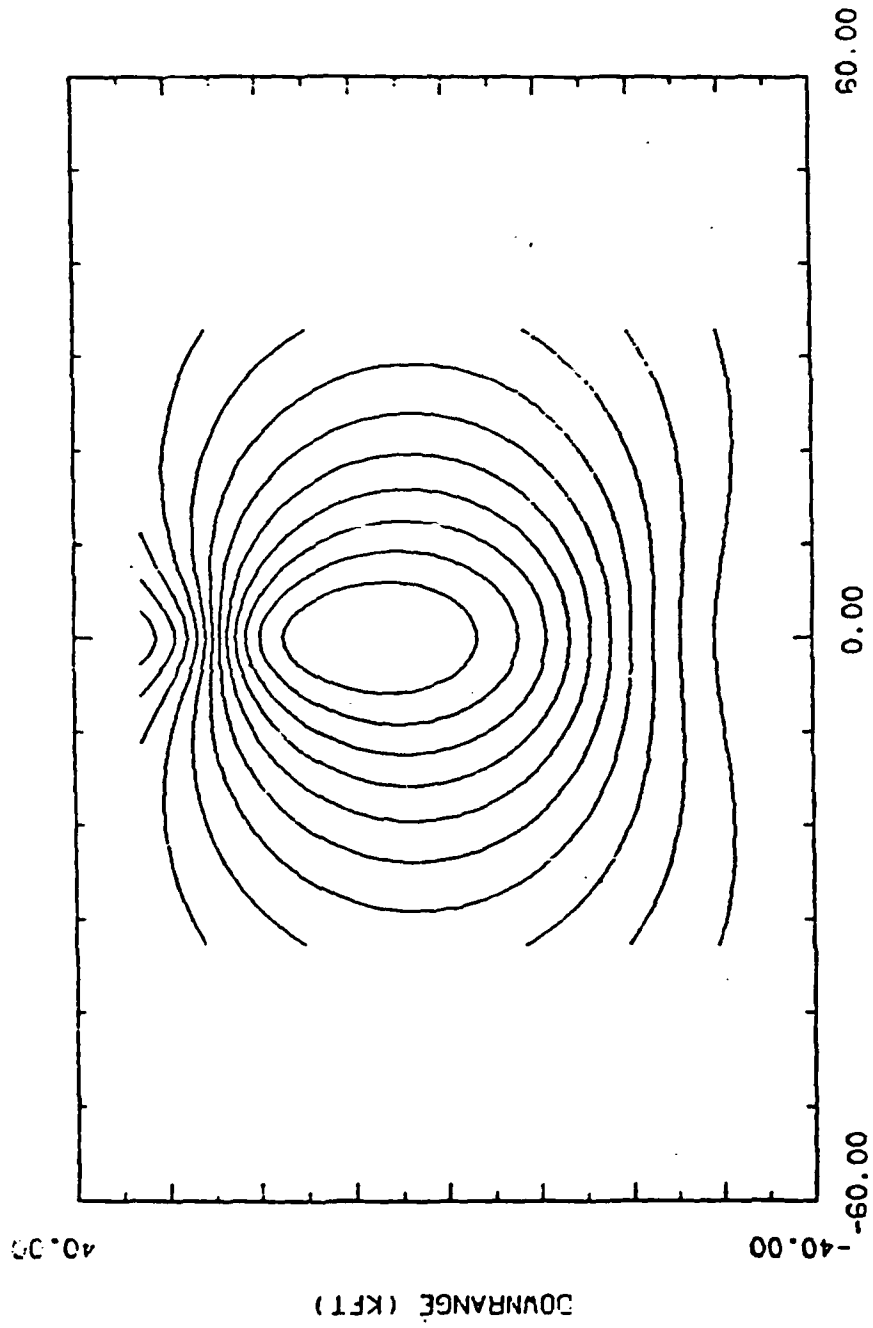


CROSSRANGE (KFT)

FIGURE 2-2

88-030-81 8C1C1171

RISTATIC ANGLE



CROSSRANGE (KFT)

FIGURE 2-3

17119120 18-DEC-88

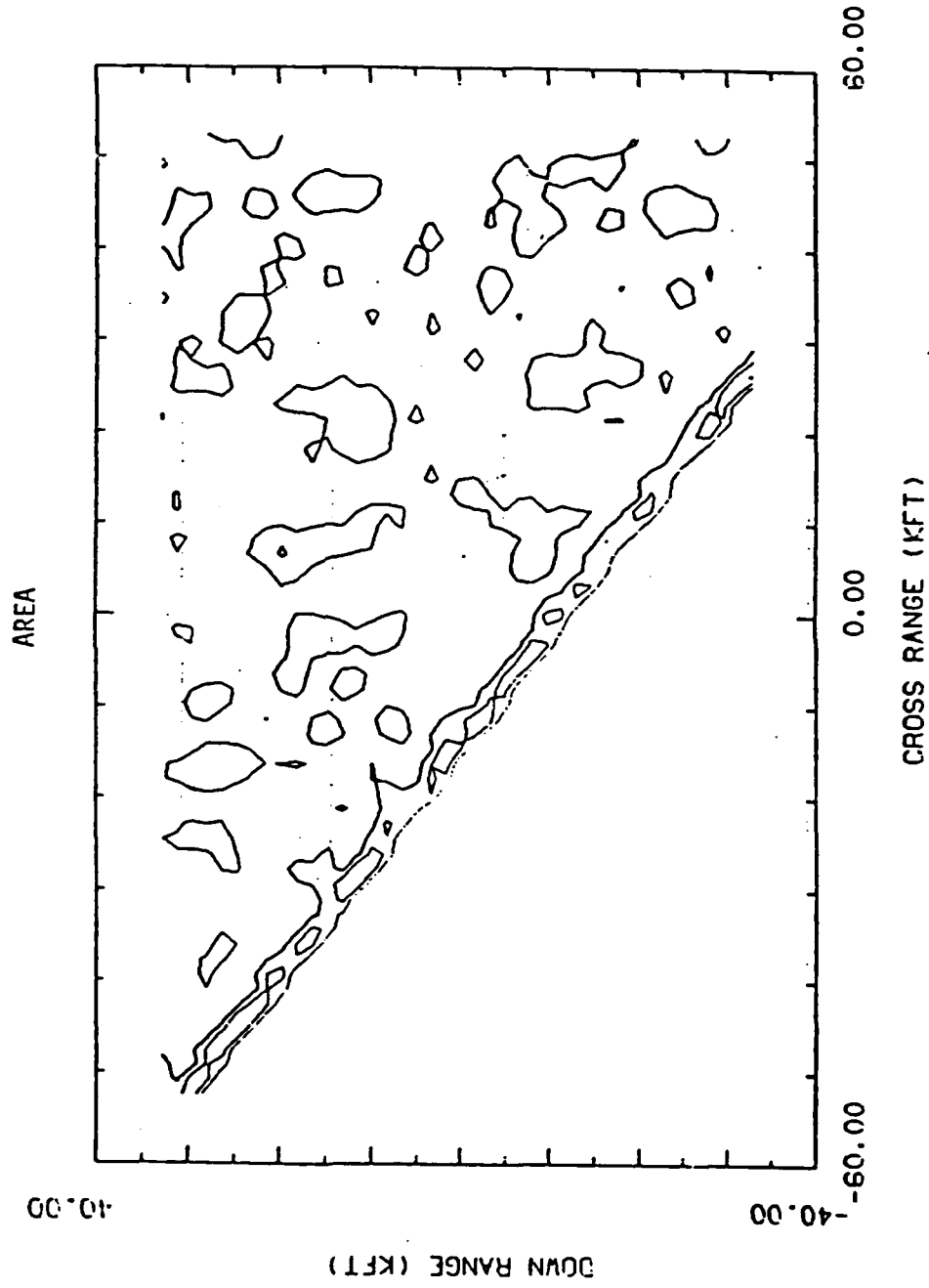


FIGURE 2-4

TERRAIN ELEVATION CONTOUR

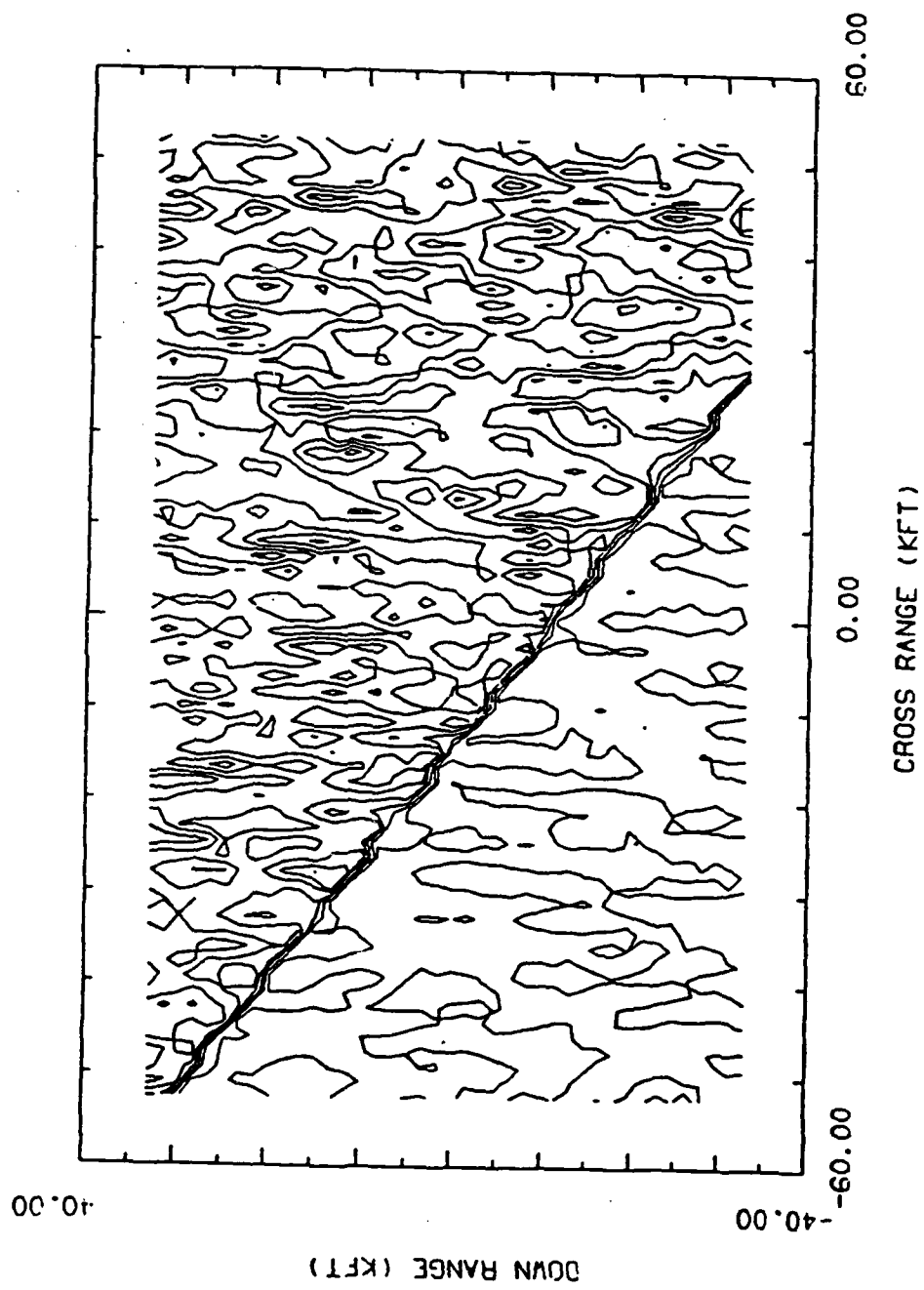


FIGURE 2-5

receiver, using the following ideal representation of the antenna amplitude rectangular diffraction pattern:

$$F(\theta, \phi) = \frac{\sin((\pi a/\lambda) \alpha)}{(\pi a/\lambda) \alpha} \frac{\sin((\pi b/\lambda) \beta)}{(\pi b/\lambda) \beta}$$

where $\alpha = \sin(\tan^{-1}(\tan \theta \cos \phi))$ and $\beta = \sin(\tan^{-1}(\tan \theta \sin \phi))$. Theta is the angle between the point vector (\vec{PT}) (the vector from the antenna origin to the point on the plane) and the Z axis in the antenna coordinate system, and Phi is the angle between the point vector (\vec{PT}) projection in the antenna X-Y plane and the X axis in the antenna coordinate system. The antenna height is "a" and the antenna length is "b". The two individual scalar field gains are then multiplied, squared and normalized with respect to the antenna-beam point ranges and the antenna-ground point ranges. This value is then converted to dB and stored. This procedure is repeated as the ground point is moved throughout a plane of specified size, thus generating enough data to produce contours, each representing a constant total field gain.

2.6 Digitized Antenna Patterns

A more realistic approach was also incorporated, using digitized elevation patterns and azimuthal angle calculations. The elevation angle is the angle between the vector from the receiver to the point and its projection into the Y-Z plane. It's calculated using previously calculated values of theta and phi and the following equation: $\tan^{-1}(\cos \phi \tan \theta)$. The azimuthal angle is the angle between the vector from the receiver to the point, and its projection in the X-Z plane. The equation is: $\tan^{-1}(\sin \phi \tan \theta)$. The range-gain contours allow the operator to identify different levels of power gain within the main beam. (See Figure 2-6) When these contours are overlaid with the Bistatic Range contours, the range gates at which main and sidelobes contribute to the power gain can be identified (Figure 2-7). When the beam pattern is transformed to the range-doppler domain, it identifies the maximum clutter power as a function of range with a fixed doppler frequency. Figure 2-8 represents a typical transformation. Figure 2-9 shows the beam area contours as a function of both range and doppler frequency. For both the normalized range-gain contours and the digitized antenna patterns, the inside contour is 0 dB, unless otherwise indicated on the case description. The remaining contours are in decrements of 3 dB, out to -21 dB.

BEAM PATTERN

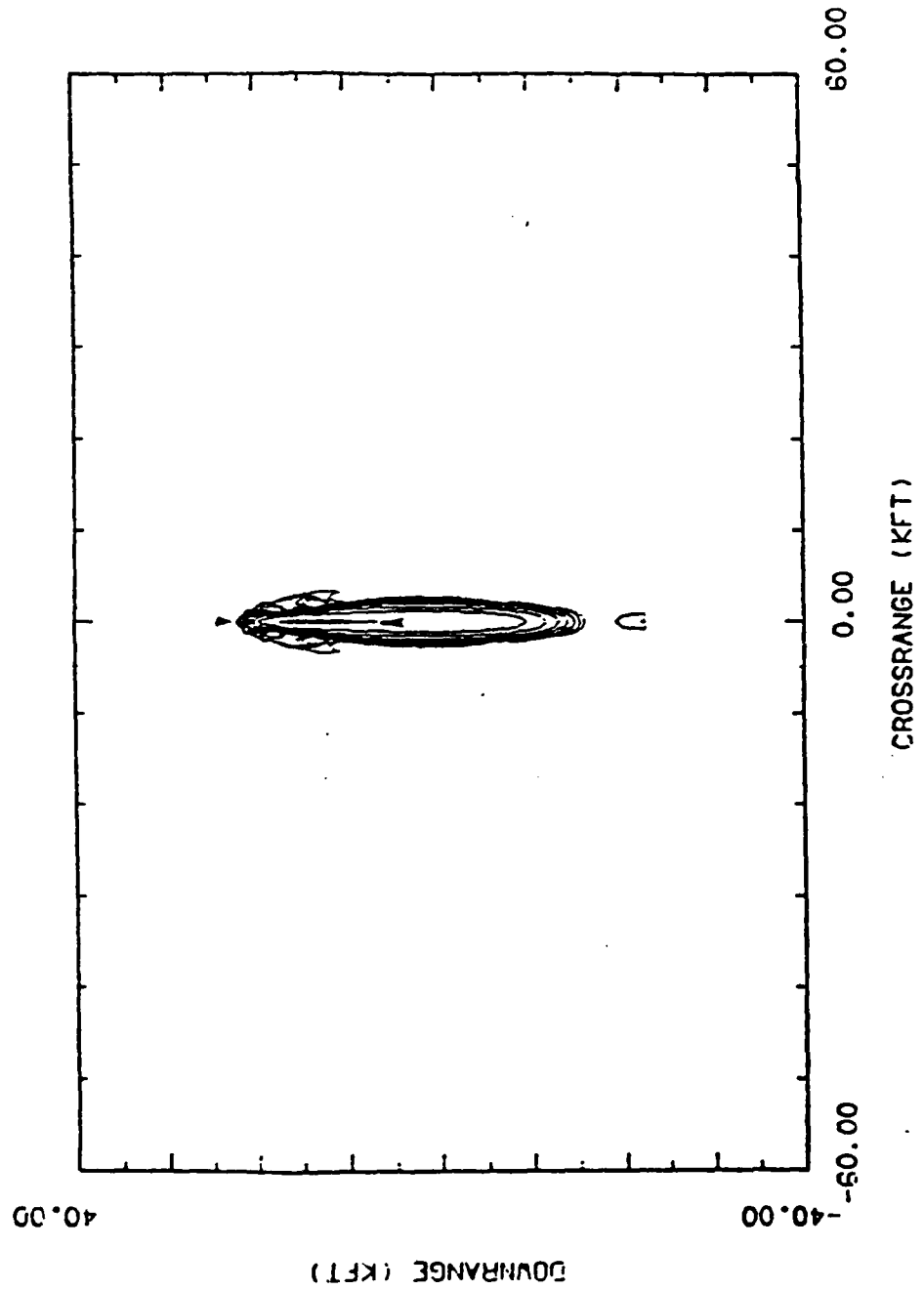
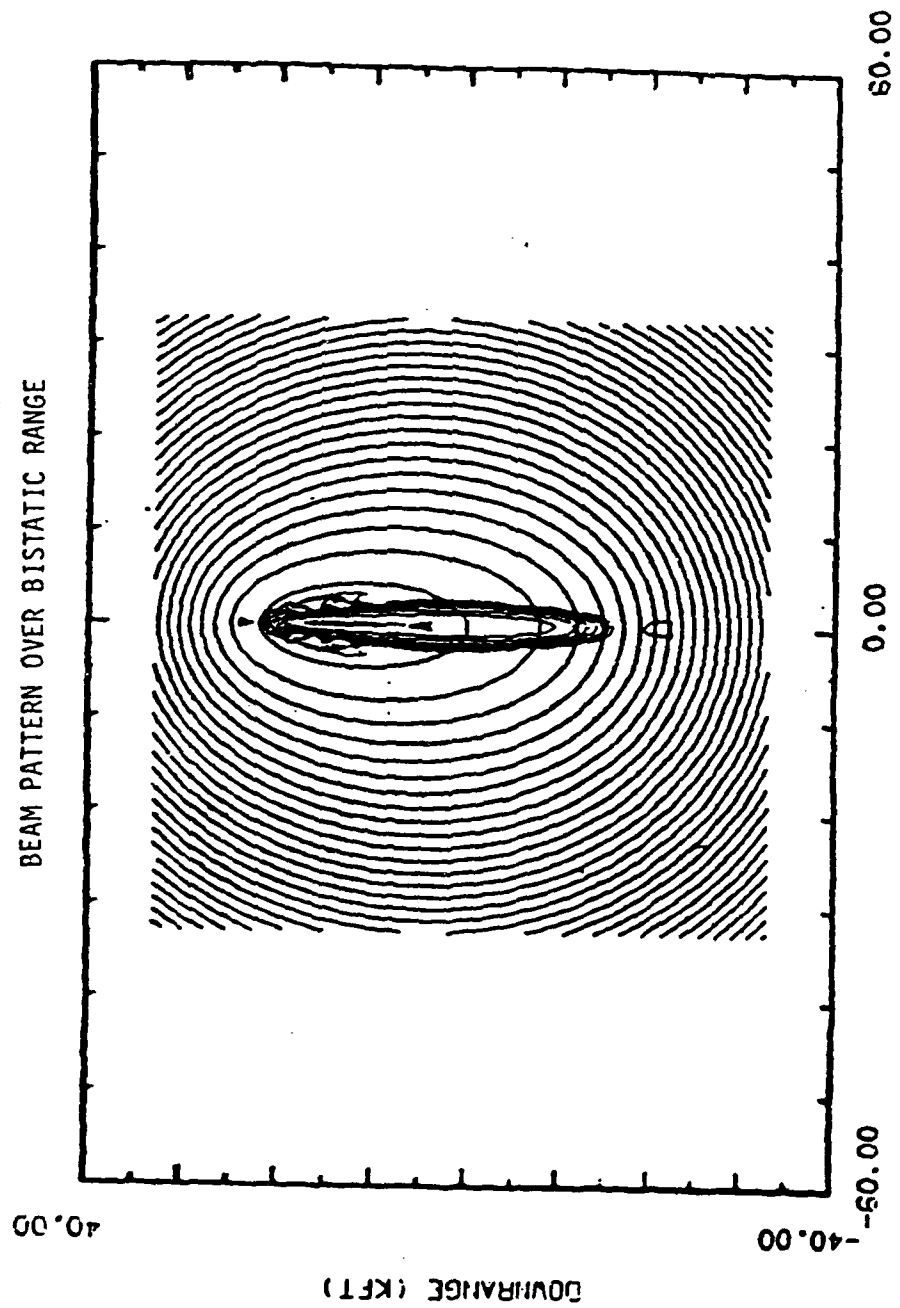


FIGURE 2-6

88-030-81 8112171

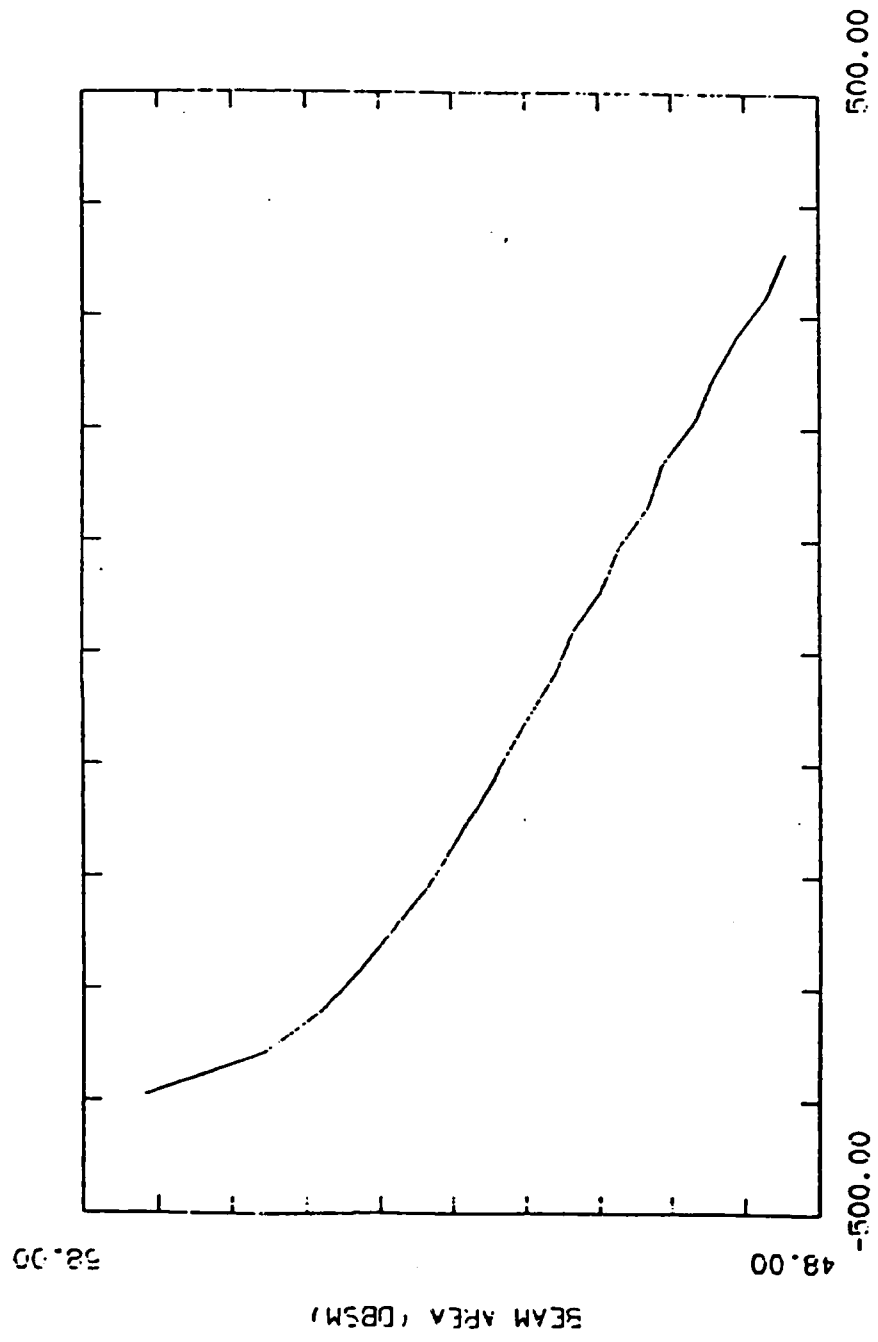
BEAM PATTERN OVER BISTATIC RANGE



CROSSRANGE (KFT)

FIGURE 2-7

88-330-01 81:12:71



BISTATIC RANGE (M)

FIGURE 2-8

98-230-0C BCIC1180

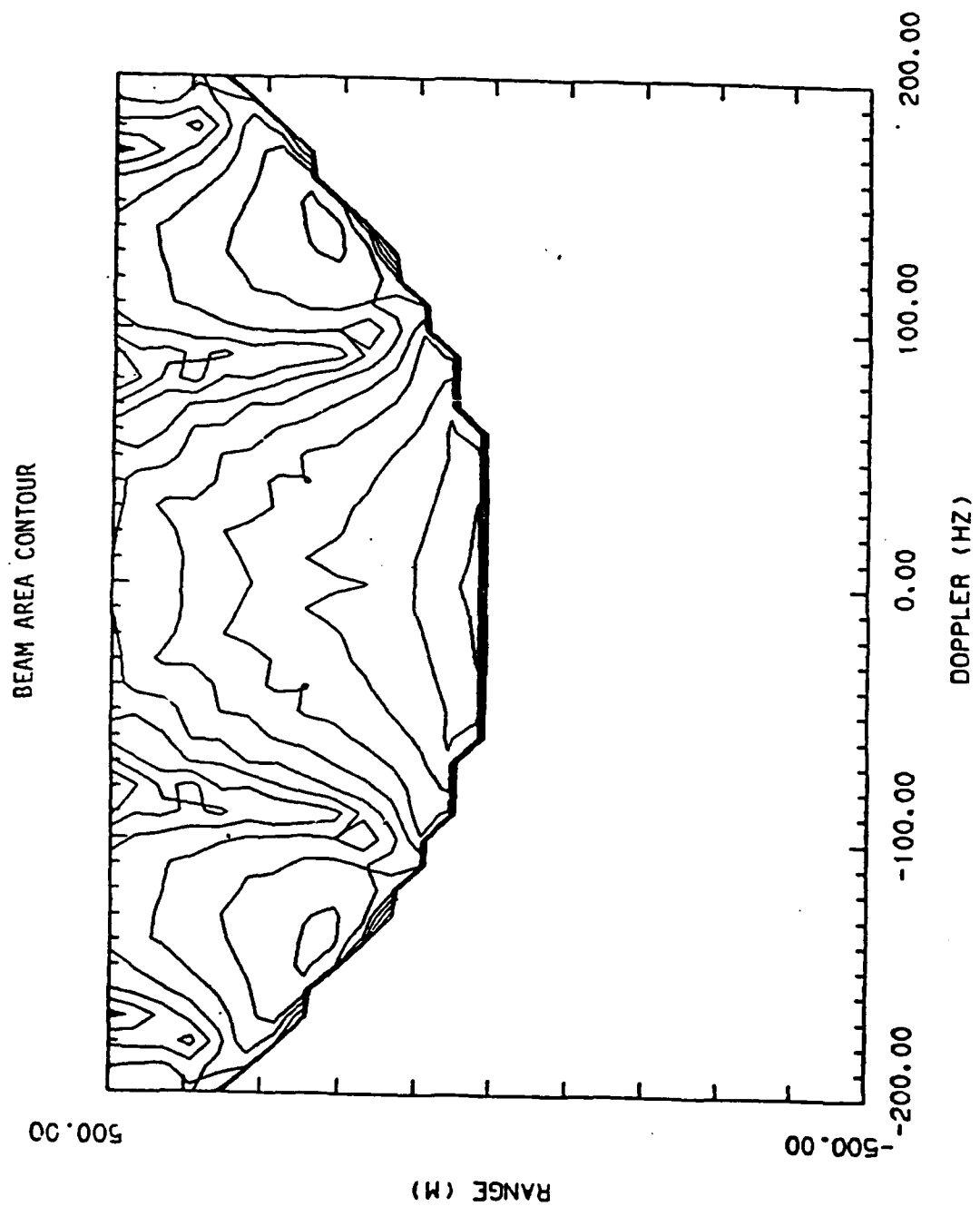


FIGURE 2-9

3.0 CLUTTER PHENOMENOLOGY

The range areas, illuminated areas, bistatic angles, doppler regions and beam limits are calculated by the geometrical portion of this program. But they are not sufficient to understand how the radar system will realistically perform in the environment. Therefore, the geometrical information must be converted to actual scattering plots using various clutter models. These models and their uses are discussed in this section.

Average surface scattering can be predicted for slightly rough and very rough surfaces of different polarizations for:

- Coherent specular scattering from slightly rough terrain using a tangent plane approximation
- Incoherent diffuse scattering from slightly rough terrain
- Incoherent specular scattering from very rough terrain using a tangent plane approximation for areas large w/respect to a correlation length.

These predictions assume an exponential or Gaussian elevation correlation function. These are functions of incident, scattered and out-of-plane angles, rms heights and slopes, ground permittivity and permeability. Coherent scattering decreases exponentially with the square of the surface roughness height in wavelengths. Slightly rough terrain results in broad diffuse scatter. Very rough terrain results in specular scattering from suitably oriented microfacets.

Slightly rough terrain HH has a null at $\pi/2$ bistatic angle due to polarization loss. All cross polarizations have a null in the system plane. The VV polarizations have a null at the Brewster angle in plane. The larger the permittivity, the greater the difference in cross polarizations.

Terrain scattering cross sections can be calculated based upon the physical properties and statistical characteristics of the local terrain. A flat, simulated, or real terrain may be used. The flat terrain model represents homogeneous isotropic areas large enough for the expected normal to be vertical. Terrain may be simulated with exponential or Gaussian correlated elevations, having specified correlation lengths, orientation, and mean and standard deviation elevations. Composite terrains may be formed from several different realizations, each having its own roughness, permittivity, and permeability. Or a real terrain map of terrain type and elevation may be input. Shadowing may be determined from orientation and obscuration.

3.1 Coherent Specular Scattering

Coherent reflectivities are calculated treating the ground plane as a mirror. The contours portray the scattering as it would be from a mirror surface. These contours become more useful as wavelength increases (See Figure 3-1).

3.2 Incoherent Diffuse and Specular Scattering

The incoherent diffuse scattering and incoherent specular scattering are calculated using various terrain models. The contours tell what the mean reflectivity of any polarization is at a given point. Figures 3-2 and 3-3 are examples of incoherent scattering. Both coherent and incoherent reflectivities may be generated for various polarizations, including two principle (VV and HH) and two cross (VH and HV) polarizations.

3.3 Shadowing Contours

Shadowing contours are statistical measures of the amount of shadowing by slightly rough and very rough terrain. Mean reflectivities can be weighted by shadowing factors to obtain a more accurate reflectivity. Figures 3-4 and 3-5 are samples of slightly rough and very rough terrain shadowing contours, respectively.

4.0 SYSTEM PERFORMANCE

Combinations of various plots discussed in the geometry section and transformation of the scattering plots discussed in the clutter phenomenology section provide some indications of the quality of system performance.

4.1 Range-Doppler Cell of Interest

The Range-Doppler cell of interest is delineated by taking the intersection of the Range and Doppler curves(See Figure 4-1). The beam pattern tells how much energy comes from the cell of interest. This value can also be weighted with mean reflectivities and shadowing to obtain a more accurate estimate.

4.2 Pulse Area vs. Bistatic Range

The pulse area vs. bistatic range is useful in removing the beam weighting and allowing fundamental unit measurement. The Range-Doppler transform corresponds to integration over various range-doppler cell areas (Figure 4-2). It provides the area without beam weighting.

4.3 Clutter to Noise Ratio (CNR) vs. Bistatic Range

The Clutter to Noise ratio (CNR) is calculated by dividing the clutter power by the receiver noise level. The clutter power is the sum of scattering computed over the beam area in dB relative to a square meter at the aim point for the given

COHERENT HH POLARIZATION

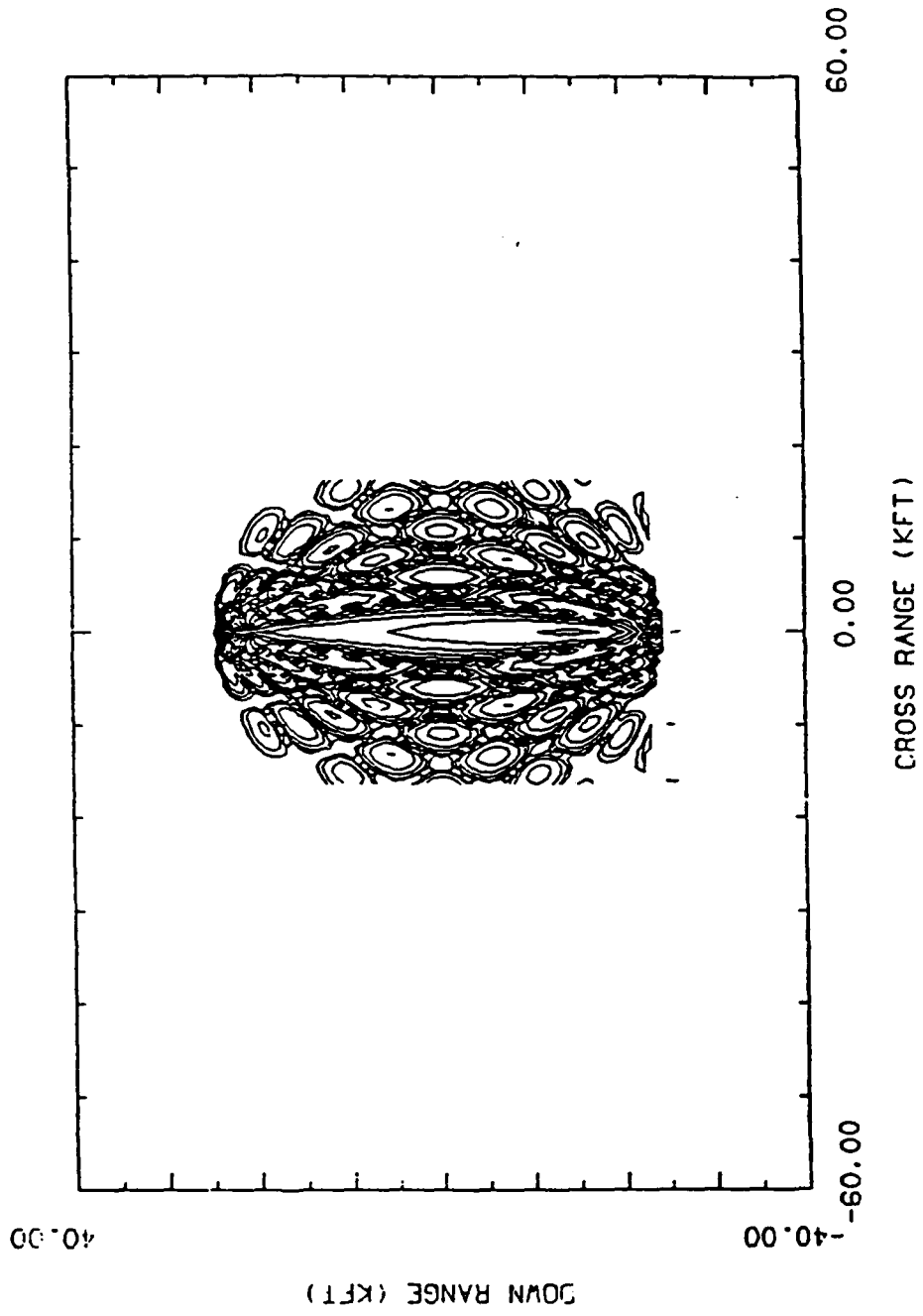


FIGURE 3-1

INCOHERENT DIFFUSE SCATTERING

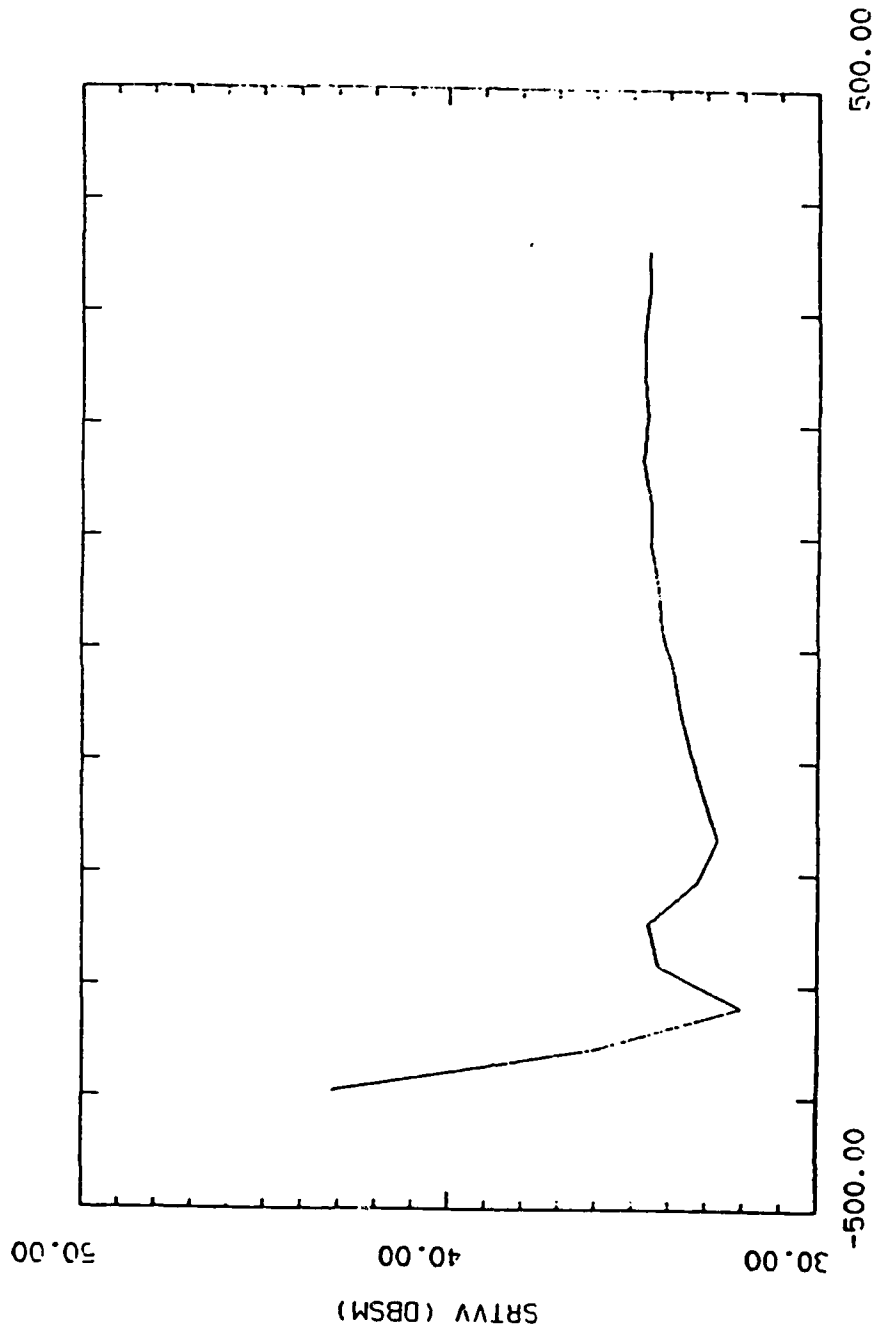
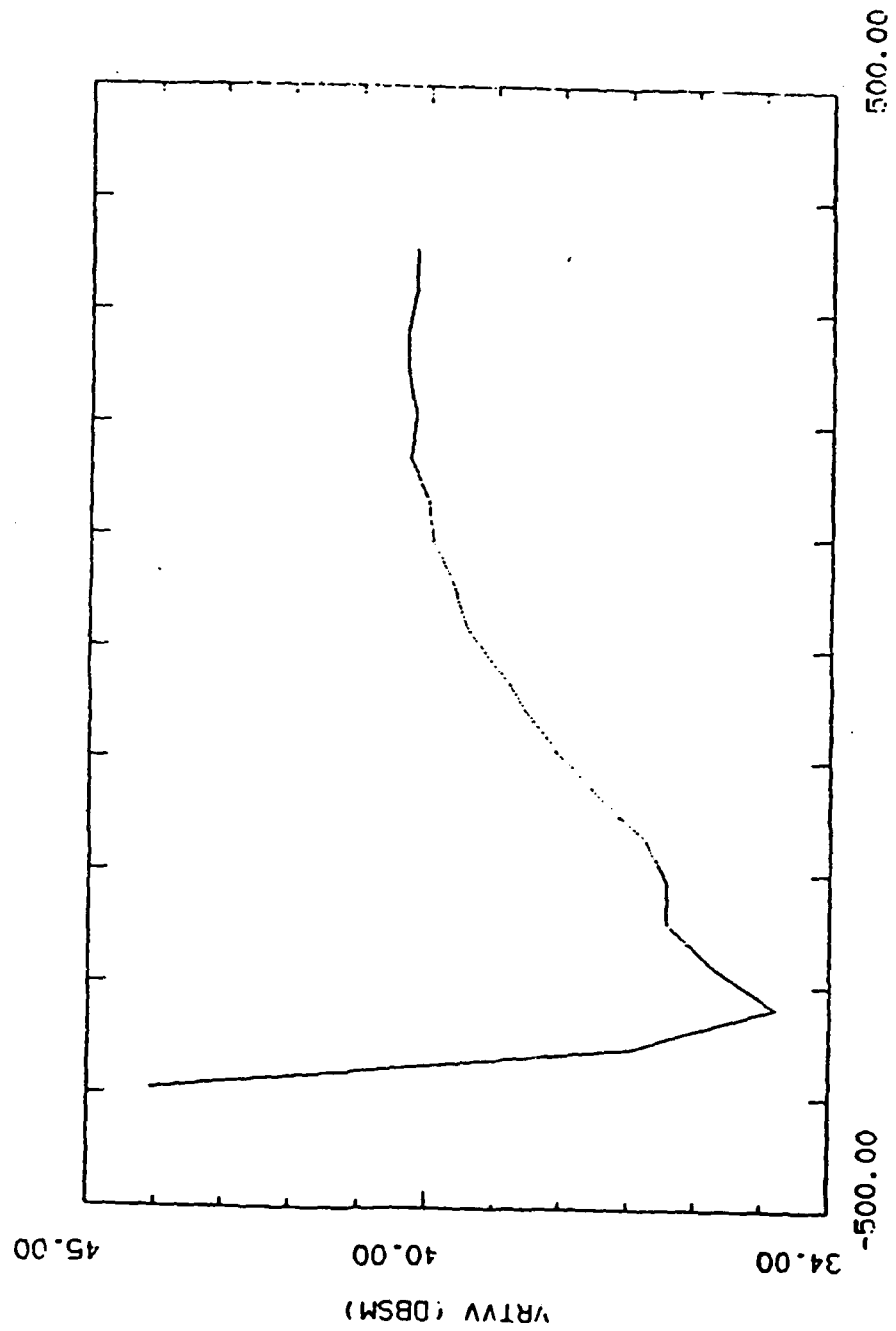


FIGURE 3-2

88-330-0C 41:04:11

INCOHERENT SPECULAR SCATTERING



BISTATIC RANGE (M)

FIGURE 3-3

88-330-0C C8104171

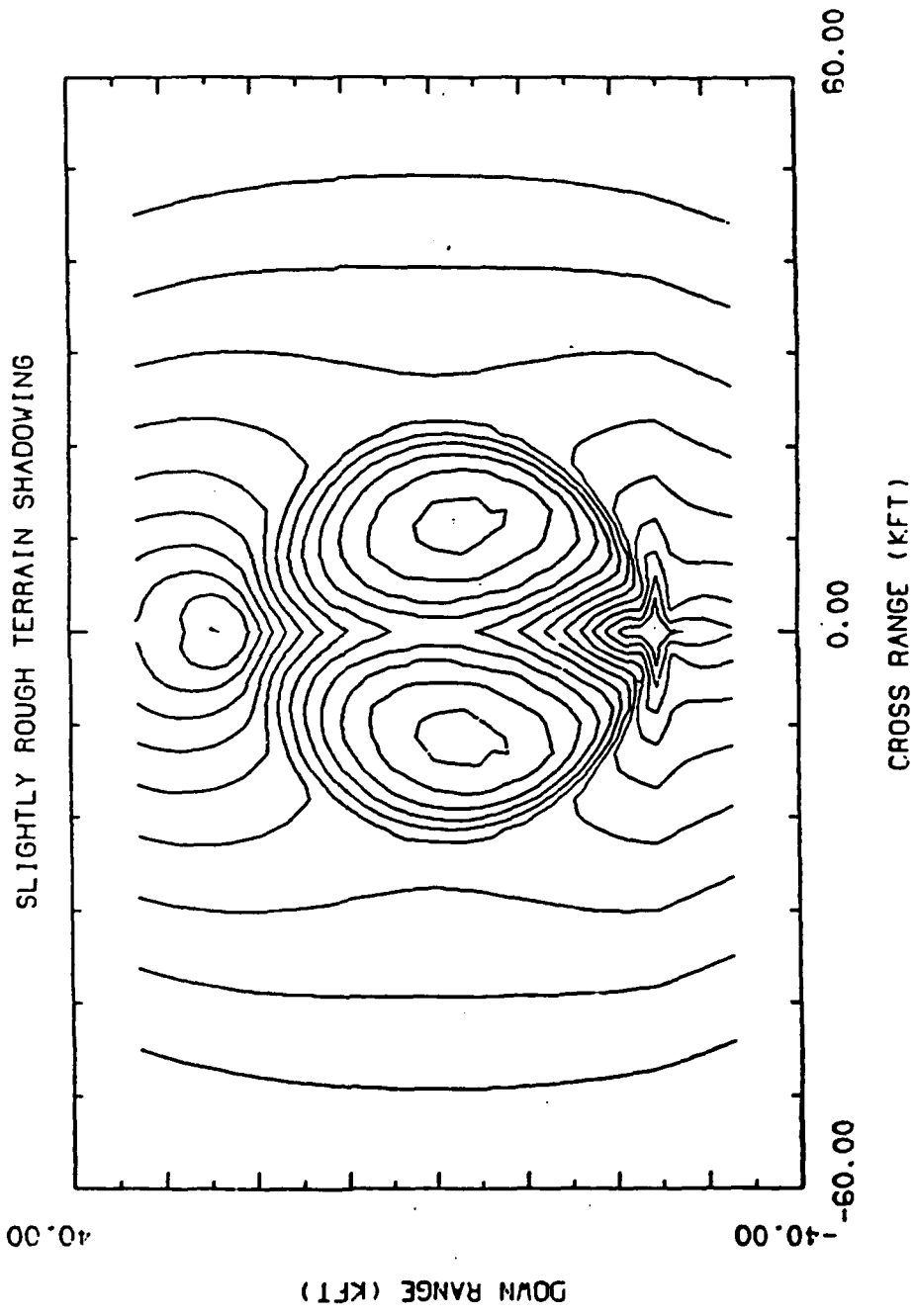


FIGURE 3-4

VERY ROUGH TERRAIN SHADOWING

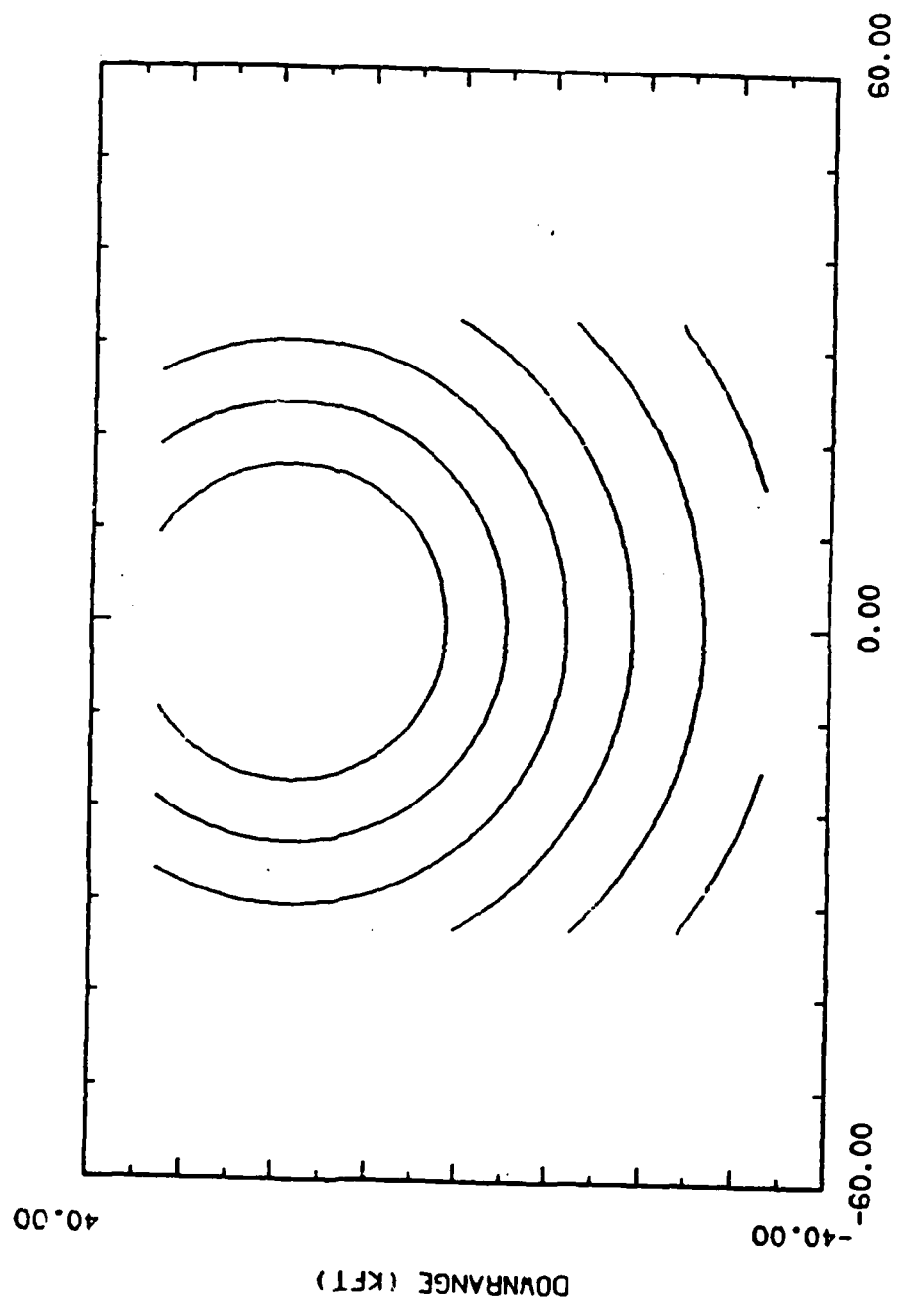


FIGURE 3-5

02:48:48 21-JAN-87

RANGE-DOPPLER CELL

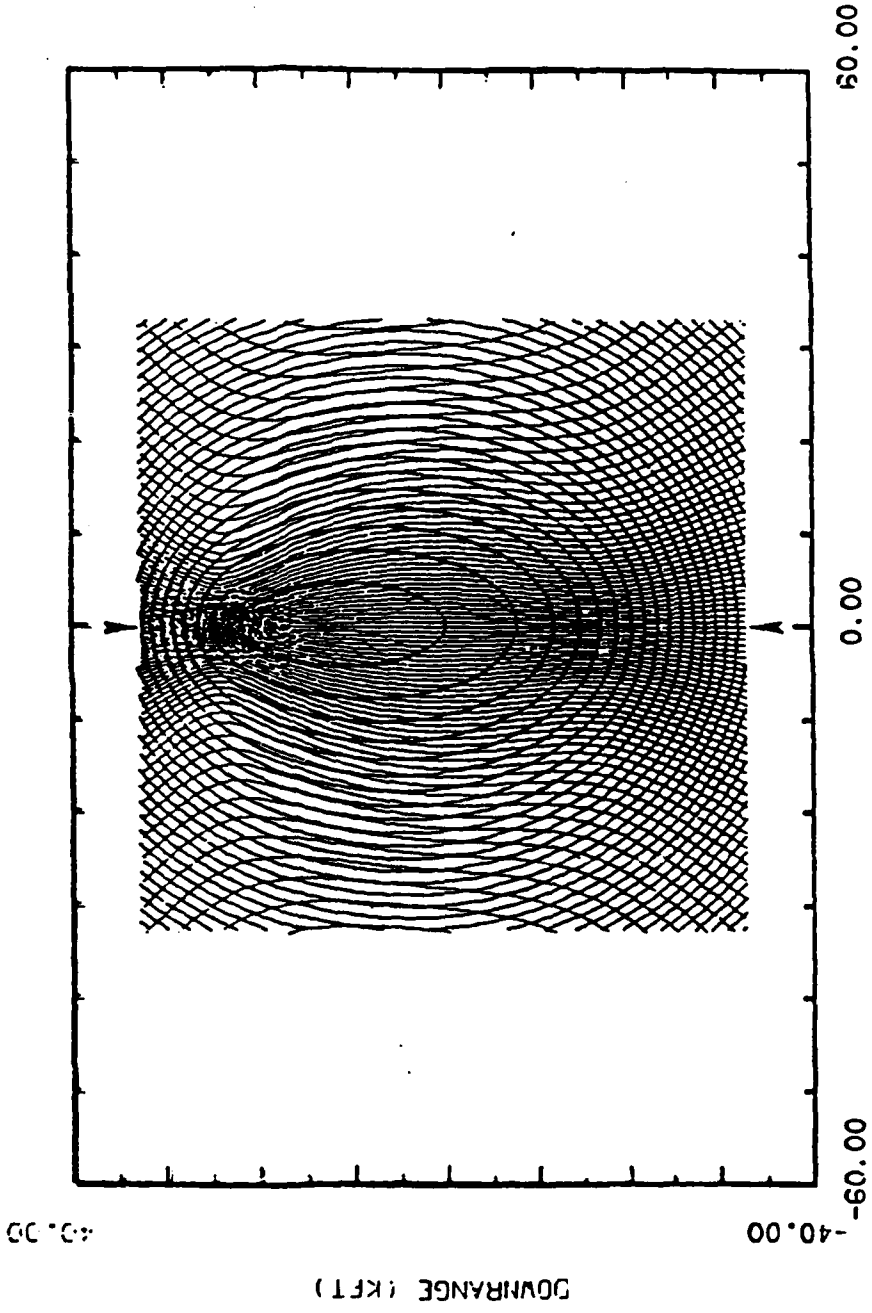
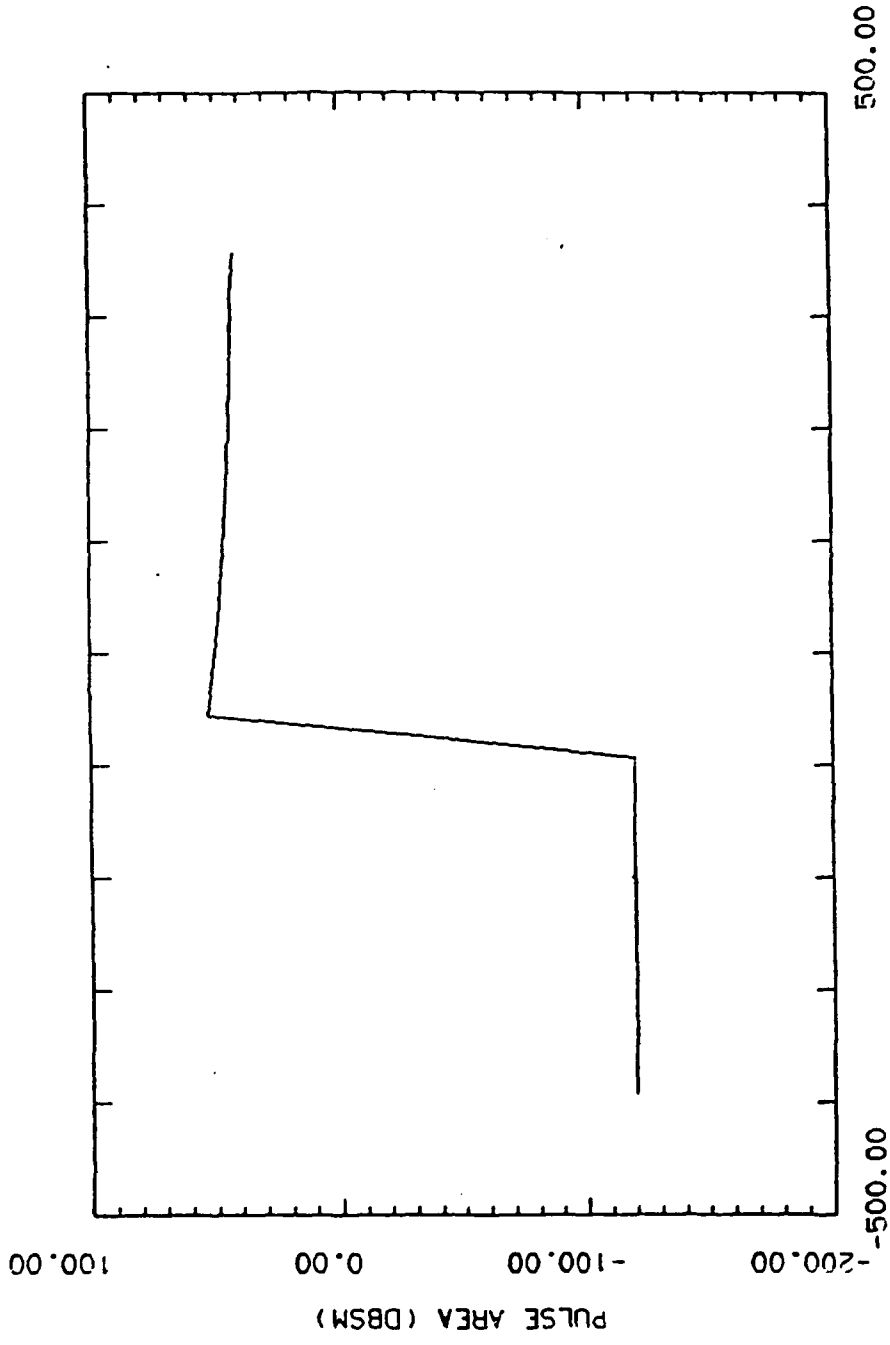


FIGURE 4-1

88-230-81 8C1C1171

PULSE AREA



BISTATIC RANGE (M)

TGA- 0.0. T.OPA-0. RGA-20.0. R.OPA- 0.0

13:39:48 5-FEB-87

FIGURE 4-2

point. The CNR plots give the CNR for various range gates, usually between -10 and 10 gates relative to the beam center. An example of these plots is shown in Figure 4-3. To validate scattering models, the CNR ratio must remain significant. Otherwise, only noise is being measured. Once the model is validated, it is important to reduce the ratio, to eliminate the clutter noise. If doppler curves are drawn on top of range rings, resolution is improved and smaller areas are examined. A higher resolution of ground scattering is obtained with doppler processing. The maximum resolution for a specified pulse length and doppler filter can be derived.

5.0 PLOT OPTIONS

Several variations of the standard plots illustrated here are available. These options are controlled by operator input and include:

- Large scale (not used with time domain)

- Small scale

- Window size (not used with time domain or large scale)

- Contour level range (not used with time domain or large scale)

- Contour level increment (not used with time domain or large scale)

- Axes lengths

- Axes rotations

- Color filled contours (not used with time domain)

A large scale or blown-up version of the standard plots (small scale) is available. If the large scale is selected, the window size, axes lengths and rotations should not be set manually. Rather, they should be allowed to be automatically set. The large scale option is available only in the spatial domain. Therefore, it should not be selected when plotting clutter phenomenology prediction plots.

The next option available involves the selection of window size, contour level range and contour level increment. If the choice is made to manually enter the window size, the contour level range and increment must also be entered. Again, these selections should only be made for plots in the spatial domain.

The next option available is manual entry of axes lengths and rotations. If chosen, axes lengths and rotations must be entered for all three axes in a three dimensional system (e.g., x, y and z axes).

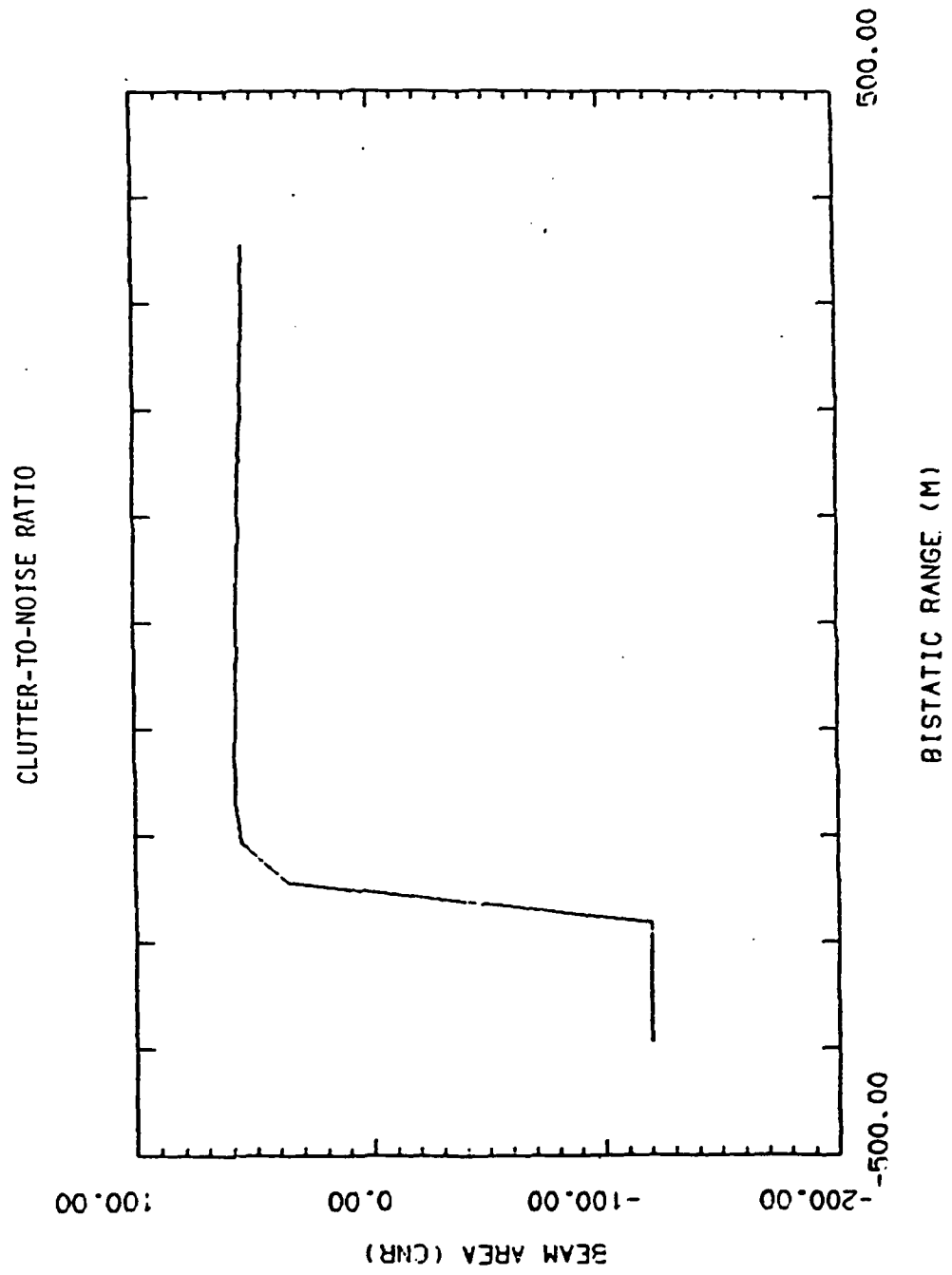


FIGURE 4-3

18147108 12-JAN-87

The final option available provides for color filled contour levels. This option is also only available in the spatial domain. The colored contours are alternated with white filled contours to allow a greater number of contour levels before color repetition begins. Figure 5-1 and 5-2 are two examples of color filled contours. Figure 5-2 has a contour level range twice as wide as that in Figure 5-1, with the same size contour level increment. All of the above options and necessary inputs are more fully described in the User's Manual for this workstation.

6.0 SYSTEM HARDWARE

The bistatic clutter prediction program is resident on a VAX 11/750. The program is written in Fortran 77. Upon completion of calculations and generation of the necessary data files, the plots are first generated on the Ramtek 9465 Graphic Display System. It is a raster-scan display system with a color CRT monitor, capable of single or multichannel operation. The plot on the Ramtek monitor is then sent to the D-Scan CH5201, where a hard copy of the plot is produced. Local intelligence in the copier moves software intensive functions such as multiple color and independent color assignment from the display terminal to the copier. Output is produced in approximately 60 seconds. A full frame buffer allows copies to be produced unattended. Image download time is less than six seconds. Versatility is enhanced through a choice of plain paper or transparency media, and a choice of color or monochrome.

7.0 SUMMARY

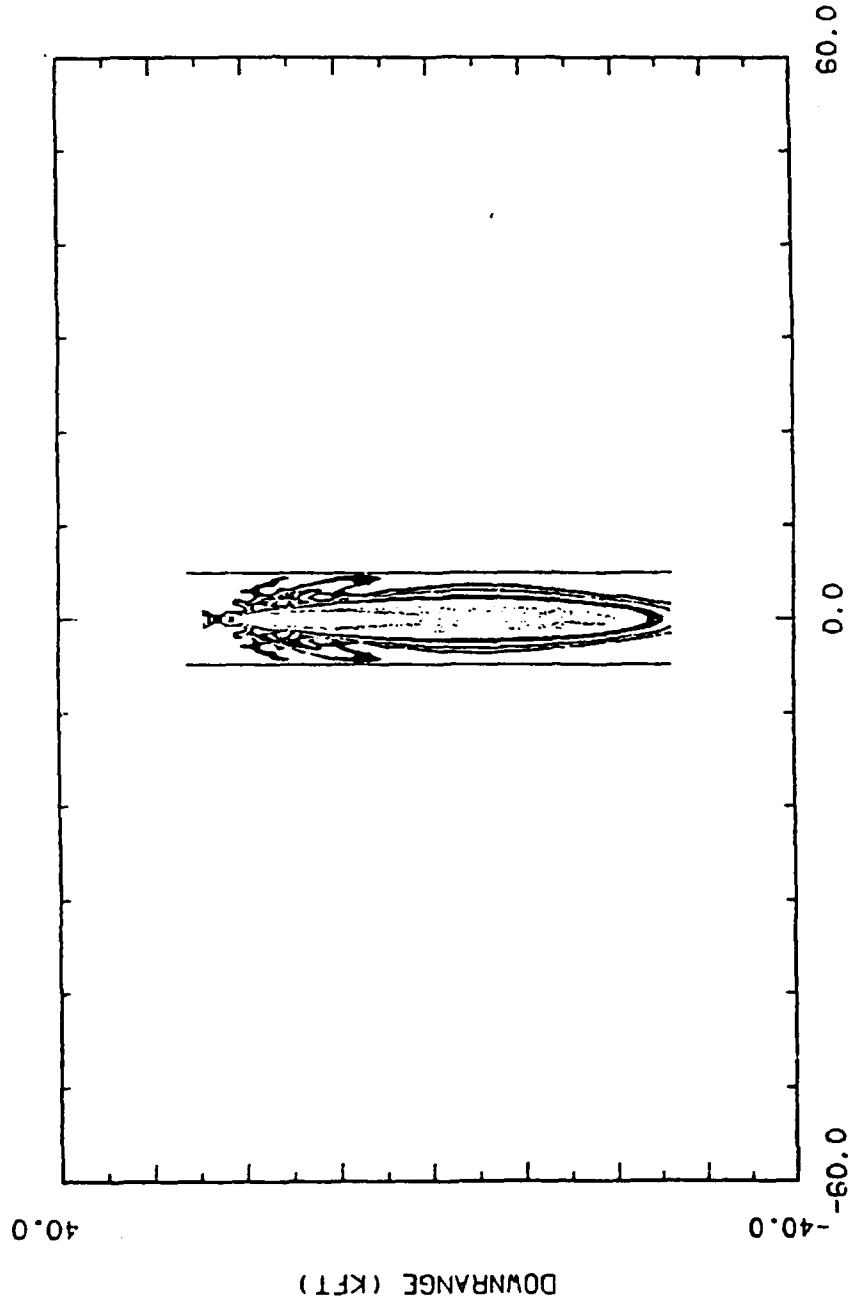
The capabilities of this program are diverse. Bistatic range, doppler, bistatic angle, pulse area, and beam patterns, using simulated or realistic elevation patterns, may be computed for an arbitrary bistatic system. The capabilities also include shadowing and different polarization mean reflectivity predictions. A flat, simulated, or real terrain may be used, and a transformation from the spatial domain to the time domain may be performed.

Limitations of the model which should be considered are:

- 1) an underlying flat earth model is used
- 2) only average surface scattering is modeled, subject to roughness limitations
- 3) no statistical, volumetric, or ambient scattering or attenuation is present
- 4) multiple scattering is currently ignored
- 5) aliasing of returns is neglected.

FIGURE 5-1

BEAM PATTERN

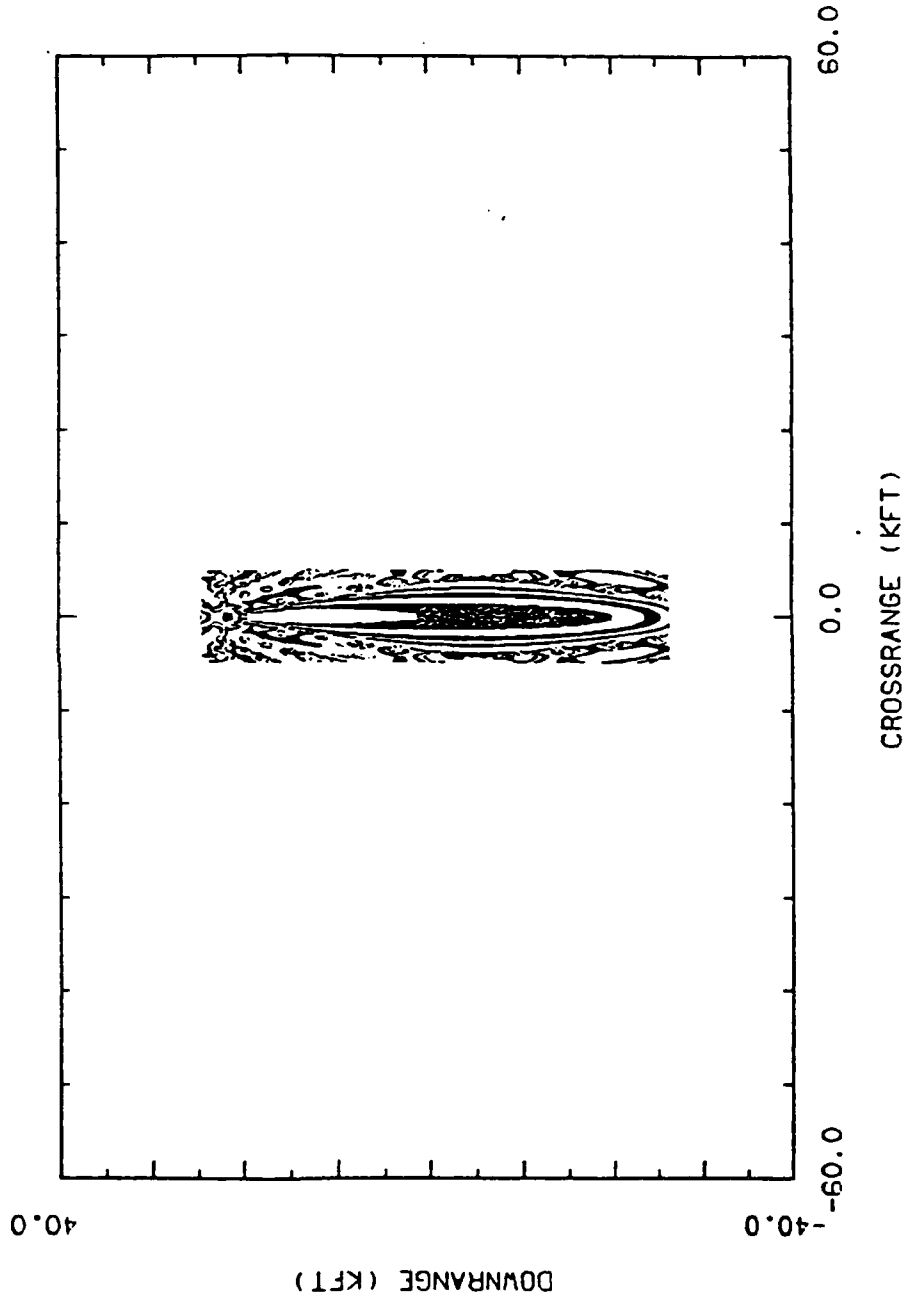


CROSSRANGE (KFT)

TEA=20.0. T.OPA=0. REA=10.0. R.OPA= 0.0

14:45:05 27-MAR-87

FIGURE 5-2
BEAM PATTERN



15:15:27 27-MAR-87

TEA=20.0. T.OPA=0. RBA=10.0. R.OPA= 0.0

Additional capabilities have been added, allowing model selection and parameter inputs to be fully automatic or manual, subject to the operator's current needs. Once the bistatic system has been defined and the model selection made, the process becomes automatic, generating the necessary command files and data files needed to calculate and plot the variables selected in the model selection. Plot options, analytical tools and an audit trail are also features of this program.

CANDIDATE BISTATIC CLUTTER STATISTICAL MODELS

28 June 1986

Contract No. F30602-86-C-0045

Prepared by: Charles H. Hightower

Prepared for

ROBERT OGDONIK
ROME AIR DEVELOPMENT CENTER
GRIFFISS AIR FORCE BASE
NEW YORK 13441



CORPORATE HEADQUARTERS

1811 QUAIL STREET
NEWPORT BEACH, CALIFORNIA 92660
(714) 833-9088

CANDIDATE BISTATIC CLUTTER STATISTICAL MODELS

1.0 INTRODUCTION

In recent years, various statistical descriptions of clutter return have been postulated and attempts made to fit these distributions to measured data. Some success has been realized for back scatter clutter but little work has been devoted to bistatic clutter statistics. The paper presents candidate statistical descriptions (in the form of probability densities) for the reflectivity coefficient characterizing bistatic clutter returns. Since the reflectivity coefficient is proportional to the radar cross section (RCS), both will have the same probability density functions. It is assumed in this paper that the clutter statistics are stationary at least over the period of observation. Also discussed are the implications on radar design under the assumption that bistatic clutter obeys these models under suitable conditions. This discussion is the first of a series of papers dealing with this topic. Following papers will deal with doppler spectra, electromagnetic modeling and shadowing in a bistatic geometry.

2.0 CANDIDATE STATISTICAL MODELS

Candidate statistical models discussed in this paper include:

1. Rayleigh Density (Exponential)
2. Rice and Chi Density
3. Contaminated-Normal Density
4. K Density
5. Gamma Density
6. Weibull Density
7. Log-Normal Density

2.1 Rayleigh Density (Exponential)

The Rayleigh probability density function is applicable to the case where the area illuminated by the radar is relative large. The signal return may be thought of as being the vector sum of randomly-phased components from a large number of independent scatterers. The consequence of applying the Central Limit Theorem results in a Rayleigh distribution for the envelope (amplitude) of the signal return. Since radar cross section (RCS) is proportional to the

square of the amplitude return, the resulting probability density function for the RCS is exponential.

The Rayleigh and exponential distributions have only one parameter. Therefore, only the mean, median, standard deviation or variance is needed to define the probability density. Consequently, if the clutter return were known a priori to be Rayleigh distributed, the measurement radar would only have to be designed to accurately measure one of these parameters.

The Rayleigh and exponential probability density functions are shown in Table 2-1.

2.2 Rice Distribution and Chi Densities

Measurements of sea clutter (Trunk) at low grazing angles with a high resolution radar have indicated the sea clutter RCS was not exponential but could be a Chi distribution. There does not appear to be a physical mechanism that would generate a Chi density although the Chi random variable can be shown to result from the square root of the reciprocal of n times the sum of the squares of n normally distributed independent random variables (Parzen).

The Rice density function is a good approximation to the Chi density and has a reasonable physical interpretation that may explain Trunk's results. The Rice density function describes the amplitude of a signal which contains a steady signal plus many independent random signals which by themselves produce a Rayleigh amplitude density function (Thomas). Thus, the Rice density function can be thought of as representing a steady or dominant scatterer in the midst of many independent scatterers.

The Rice density function contains two parameters; the first of which is the amplitude of the dominant scatterer and the second is the standard deviation of the Rayleigh noise. The Rice density function approaches a Gaussian density when the ratio of the dominant scatterer amplitude is large relative to the standard deviation of the noise with a mean amplitude given by the amplitude of the dominant scatterer and with a standard deviation given by the standard deviation of the random signal component.

Consequently, the Rice density function appears to be representative of the situation when the geometry of the bistatic receiver and transmitter are such that the specular reflection is included in the commonly viewed region. The Rice and Chi distributions are tabulated in Table 2-1.

2.3 Contaminated-Normal Density

The contaminated-normal probability density represents the sum of two Gaussian probability densities with different variances but the same mean. Hence, it is a three parameter probability density function. This distribution has no physical interpretation but does have the property that it can be used to fit measured data relatively well because of the number of parameters. The contaminated-normal density is shown mathematically in Table 2-1.

2.4 K Density

The K probability density function is based on a finite two-dimensional random walk phenomena where the electric field is expressed as the sum of contributions of N independent scatterers which are described by random variables of magnitude and phase (Jakeman). Except for the two extreme cases where N is either unity or very large, this concept is difficult to use in modeling the physical world. The K probability density is given by the expression shown in Table 2-1.

2.5 Gamma Density

The Gamma probability density function has been shown to be an approximate solution for the RCS of the sum of a finite number of random vectors and is closely related to the K density (Nakagami). The Gamma density has two parameters which are related to the mean and variance of the random variable. It can be shown that the Exponential and Chi square densities are special cases of the Gamma density. The Gamma probability density is expressed in Table 2-1.

2.6 Weibull Density

The Weibull probability density function has been used to represent both sea clutter and land clutter with some success (Fay, Boothe). There is as yet no theoretical interpretation for the usefulness of this model although it is not too different from the K density for some range of its parameters. The

TABLE 2-1 PROBABILITY DENSITY FUNCTIONS

Rayleigh (one parameter \bar{x} or σ^2 ; $x = (\text{RCS})^{1/2}$)

$$f(x) = \begin{cases} \frac{x}{\sigma^2} \exp [-x^2/2 \sigma^2] & x \geq 0 \\ 0 & \text{otherwise} \end{cases}$$

$$\bar{x} = \sqrt{\frac{\pi}{2}} \sigma^2$$

Exponential (one parameter \bar{x} or σ^2 ; $x = \text{RCS}$)

$$f(x) = \begin{cases} \lambda e^{-\lambda x} & x > 0 \\ 0 & \text{otherwise} \end{cases}$$

$$\bar{x} = \frac{1}{\lambda} \quad \sigma^2 = \frac{1}{\lambda^2}$$

Rice (two parameters: A , σ^2 ; $x = \text{RCS}$)

$$f(x) = \begin{cases} \frac{x}{\sigma^2} \exp [-(x^2 + A^2)/2\sigma^2] I_0 \left(\frac{A}{\sigma^2} x \right) & x \geq 0 \\ 0 & \text{otherwise} \end{cases}$$

A = amplitude of constant clutter return

σ^2 = variance of Rayleigh clutter

$I_0(x)$ = modified Bessel function of the first kind and order zero

Chi (one parameter n or \bar{x}_n or σ^2 ; $x = (\text{RCS})^{1/2}$)

$$f(x) = \begin{cases} \frac{2(n/2)^{n/2}}{\sigma^n \Gamma(n/2)} x^{n-1} \exp [-(n/2\sigma^2)/x^2] & x \geq 0 \\ 0 & \text{otherwise} \end{cases}$$

$$\bar{x} = n \quad \sigma^2 = 2n$$

TABLE 2-1 PROBABILITY DENSITY FUNCTIONS (Continued)

Contaminated-Normal (three parameters \bar{x} , σ_1^2 , σ_2^2 ; $x = (\text{RCS})^{1/2}$ or RCS)

$$f(x) = \frac{1}{2\sigma_1 \sqrt{2\pi}} \exp[-(x-\bar{x})^2/2\sigma_1^2] + \frac{1}{2\sigma_2 \sqrt{2\pi}} \exp[-(x-\bar{x})^2/2\sigma_2^2]$$

K-Density (two parameters k , \bar{x} ; $x = (\text{RCS})^{1/2}$)

$$f(x) = \begin{cases} k^k x^{k-1} \exp[-kx/\bar{x}] / \Gamma(x)(\bar{x})^k & \cdot x \geq 0 \\ 0 & \text{otherwise} \end{cases}$$

$$k = (\bar{x}/\sigma)^2$$

Gamma (two parameters, r , λ^2 ; $x = \text{RCS}$)

$$f(x) = \begin{cases} \frac{\lambda}{\Gamma(r)} (\lambda x)^{r-1} \exp(-\lambda x) & x \geq 0 \\ 0 & \text{otherwise} \end{cases}$$

$$\bar{x} = r/\lambda \quad \sigma^2 = r/\lambda^2$$

Weibull (two parameters α , b ; $x = \text{RCS}$)

$$f(x) = \begin{cases} \frac{1}{\alpha} b x^{b-1} \exp(-x^b/\alpha) & x \geq 0 \\ 0 & \text{otherwise} \end{cases}$$

$$\bar{x} = \alpha b \quad \sigma^2 = \alpha b^2$$

Log-Normal (two parameters μ , σ^2 ; $x = \text{RCS}$)

$$f(x) = \begin{cases} \frac{1}{x\sigma \sqrt{2\pi}} \exp[-(\ln x - \mu)^2/2\sigma^2] & x \geq 0 \\ 0 & \text{otherwise} \end{cases}$$

$$\mu = E[\ln x] \quad \sigma^2 = E\{(\ln x - \mu)^2\}$$

Weibull density parameter can be determined from the median of the observed RCS or its mean. The Weibull probability density is described by the equation shown in Table 2-1.

2.7 Log-Normal Density

The log-normal density arises from a theory of a wave experiencing multiple scattering and may be applicable to low grazing angles with this phenomena can take place. However, since this distribution can produce large mean to median ratios, it may have application to situations where clutter is dominated by large specular returns or a few large surfaces predominate the received signal.

The log-normal density has two parameters which are its mean and standard deviation. The log-normal name results from the fact that if the RCS is characterized by this density, then the natural log of the RCS has a Gaussian distribution. The log-normal probability density function is defined in Table 2-1.

2.8 General Comments Regarding These Density Functions

The density functions listed in this paper represent only a small sample of possible densities that attempts to fit measured data to that might be tried. However, they do represent functions that previous researchers have had some success with, in particular, the Rayleigh (Exponential) for sea backscatter and the Weibull for land backscatter. These statistical models are further limited by the assumed stationarity of the density functions over the measurement period, independence of ground truth parameters, lack of polarization sensitivity, and so on. However, exploring their applicability is still worthwhile since they lead to relatively simple mathematical formulations that can be easily embedded in sophisticated system performance models. Furthermore, they can be used to bound the accuracy with which a measurement radar must achieve to provide reliable clutter statistical data.

3.0 RADAR MEASUREMENT ACCURACY CONSIDERATIONS

Table 2-1 indicates that if the clutter RCS (or amplitude) obeyed any of the probability laws shown, the measurement radar would be required at most to measure the mean and variance of the clutter return. Additional analyses

(Foster) show that in order to bound the error in the assumed density function by 10%, the radar measurements must lead to an estimate of the mean with nearly the same accuracy. Thus, imposing a design goal for RCS clutter measurement accuracy of 5% is justified based on a priori clutter statistic assumptions.

3.1 Goodness of Fit Comments

Many techniques are available to test the goodness of fit between a hypothesized density function and an empirical density function (Hogg). These include the Kolmogorov-Smirnov and Chi-square goodness of fit tests. The Kolmogorov-Smirnov test is dependent on the largest deviation from the hypothetical cumulative distribution exhibited by the experimentally derived distribution. The Chi-square test is similar but tends to use an average of the deviations in its test. Since the latter approach tends to smooth "wild" data points, the Chi-square test is probably more suitable to this experiment than the Kolmogorov test even though it is more difficult to implement.

3.2 Comments on the Quantity of Experimental Data Required

The Chi-square test assumes accurate independent samples of the random variable are available with more samples yielding higher confidence in the results of the hypothesis test and the ability to differentiate between several postulated densities. A technique to determine the number of independent samples required to estimate the standard deviation within a given accuracy and confidence interval is given by Currie (Currie) assuming a normal density function for the clutter signal out of a log detector (i.e., the samples are log normal). For the situation where the standard deviation of the logarithmic clutter return is 7 dB and it is desired that the estimated standard deviation be within 2 dB 95% of the time, it is shown that 133 independent samples are required. The number of samples is proportional to the square of the assumed standard deviation.

The time required between samples to ensure independence is a function of the clutter decorrelation time which in turn is dependent on its doppler bandwidth. Transmitting on different frequencies on a pulse-by-pulse basis can potentially decorrelate the samples in a controlled manner. More analysis

will have to be done to determine the best PRF to achieve the required number of independent samples.

4.0 CONCLUSIONS AND GENERAL GUIDELINES

This report has provided an introductory discussion of simple probabilistic clutter models and other topics related to the specification of system level requirements for the HBR clutter measurement radar. Preliminary conclusions based on the assumption that the clutter will behave according to the laws of the density functions are that the radar must be calibrated to within 5% of the expected mean clutter RCS and that approximately 133 independent clutter samples would be needed to provide an estimate of the density function (based on an empirical calculation of the measured data's standard deviation) within 2 dB with a confidence interval of 95%. Clearly, these requirements need further study and are provided merely to familiarize the reader with a feeling for the inferences that can be made about radar system performance using simple models.

REFERENCES

Booth, R., "The Weibull Distribution Applied to the Ground Clutter Backscatter Coefficient", Report No. RE-TR-69-15, U.S. Army Missile Command, Alabama, June 1969.

Parzen, E., Modern Probability Theory and Its Applications, John Wiley and Sons, Inc., New York, 1960.

Thomas, J., Statistical Communication Theory, John Wiley and Sons, Inc., New York, 1969.

Trunk, G., "Radar Properties of Non-Rayleigh Sea Clutter", IEEE Trans., Vol. AES-8, pp. 196-204, March 1972.

Jakeman, E., "A Model for Non-Rayleigh Sea Echo", IEEE Trans., Vol. AP-24, No. 6, November 1976.

Nakagami, M., "The m Distribution - A General Formula of Intensity Distribution of Rapid Fading", Statistical Methods in Radio Wave Propagation, Pergamon Press, New York, 1960.

Fay, F., "Weibull Distribution Applied to Sea Clutter", International Radar Conference, pp. 101-104, 1977.

Foster, C., Hightower, C., SRS Technologies, In progress.

Hogg, R., Probability and Statistical Inference, MacMillan Publishing Co., Inc., New York, 1977.

TECHNICAL MEMORANDUM

TO: C. HIGHTOWER

DATE: 21 APRIL 1987

FROM: C. FOSTER

REF: TM87-009

SUBJECT: HYBRID BISTATIC RADAR (HBR) PROJECT -
SRS CLUTTER WORKSTATION USER'S MANUAL

REFERENCE 1 - DAVID MAESCHEN, "RDMAP", (FORTRAN PROGRAM)

REFERENCE 2 - CATHERINE SANDERS-FOSTER, "RDMENU", (FORTRAN PROGRAM)

REFERENCE 3 - SRS CLUTTER WORKSTATION MEMO TM87-005

The program in Reference 1 contains the driver and clutter models used in the Hybrid Bistatic Radar (HBR) project. The program in Reference 2 is a user friendly program that generates a command file with all the necessary inputs to run the driver program in Reference 1, the EXEC program which generates the data files for plotting and the DISPOPN program which actually produces the plots. A data file is also generated which is necessary to run the EXEC program. Several options are offered for varied output:

This memo will outline all the requests for input made of the operator and the various options available. To invoke this program, at the VAX system prompt (\$) input: \$ @RDMENU. This message and request for input will appear on the screen:

SRS CLUTTER MEASUREMENT TOOL

SELECT TYPE OF INPUT:

- 1) AUTOMATIC
- 2) MANUAL

If the automatic mode is selected the following inputs are requested:

SELECT CLUTTER MODEL:

- 1) BEAM PATTERN ONLY
- 2) COMPREHENSIVE MODEL-SPATIAL DOMAIN
- 3) COMPREHENSIVE MODEL-ELEVATED TERRAINS
- 4) COMPREHENSIVE MODEL-TIME DOMAIN
- 5) COMPREHENSIVE MODEL-CONTOUR PLOTS W/DOPPLER
- 6) PERTURBATION MODEL-SPATIAL DOMAIN
- 7) GREEN'S MODEL-SPATIAL DOMAIN

Clutter Model #1 produces only one plot, the range/gain contours or beam pattern. Clutter model #2 produces thirteen different plots in the spatial domain. These plots include: bistatic range, doppler frequencies, bistatic angle, very rough terrain shadowing, slightly rough terrain (HH, VH, HV and VV) polarizations, very rough terrain (HH, VH, HV and VV) polarizations and the beam pattern. Clutter model #3 produces the same thirteen plots. But an elevated terrain is used for the calculations. Clutter model #4 produces eleven different plots. They include: the area, the beam pattern, very rough terrain shadowing, slightly rough terrain (HH, VH, HV, VV) polarizations and very rough terrain (HH, VH, HV, VV) polarizations. However, these plots are transformed to the time domain, with the vertical axis representing Bistatic Range and the horizontal axis representing Doppler frequency. These plots consist of a single line plot corresponding to the summation of doppler frequencies across the area of interest. Clutter model #5 produces five different plots in the time domain. They include: the beam pattern, slightly rough terrain HH and VV polarizations, and very rough terrain HH and VV polarizations. These plots are contour plots and differ from those in clutter model #4 by presenting a mesh of doppler frequencies over a specified bistatic range. The plots from clutter models #4 and #5 are calculated using doppler processing. Clutter model #6 produces four different plots in the spatial

domain. They include: very rough terrain (HH, VH, HV and VV) polarizations. The calculations for this model involve the use of very rough terrain found in the perturbation theory. Clutter model #7 produces four different plots in the spatial domain. These plots include: slightly rough terrain (HH, VH, HV and VV) polarizations. The calculations for this model involve the use of slightly rough terrain used in Green's theorem. Depending on operator input a certain preexisting command file is selected.

The next input required specifies a certain geometry. The input message is:

TSR/RSR = TRANSMITTER/RECEIVER SLANT RANGE (FT)
TGA/RGA = TRANSMITTER/RECEIVER GRAZING ANGLE (DEG)
OPA = RECEIVER OUT-OF-PLANE ANGLE (DEG)

ENTER GEOMETRIC SCENARIO IN CHARACTER FORMAT (I.E. '1')

- 1) TSR=RSR=25,000, TGA=RGA=10, OPA=0
- 2) TSR=RSR=25,000, TGA=RGA=10, OPA=34.8
- 3) TSR=RSR=25,000, TGA=10, RGA=1, OPA=0
- 4) TSR=RSR=25,000, TGA=10, RGA=3, OPA=0

The last two inputs required in the automatic mode concern the scale in which the plots are to be generated, and whether the operator wishes to make any changes. The input requests are:

SELECT DESIRED SCALE:

- 1) LARGE SCALE (NOT USED W/TIME DOMAIN)(enlarged plots)
- 2) SMALL SCALE (standard plots)

DO YOU WISH TO CHANGE ANYTHING (1=YES, 2=NO)

If the answer to the last question is no, then depending on the three prior inputs, an appropriate command is written to "rdmap.com". Otherwise the program starts from the beginning, allowing the operator to change any of his previous inputs. A message is then written to the screen informing the operator how to execute the command file he has just written. The message states:

To execute driver program, enter at VAX system prompt: \$ @RDMAP
Scale selection is the only plot option available in the automatic mode.

If the manual mode is selected, the following inputs are required, starting with:

CREATE COMMAND FILE:
IF YOU WISH TO DEFAULT TO SYSTEM VALUES FOR ANY
VARIABLE, ENTER A SLASH (/).

DEFINE GROUND PLANE (M)
ENTER XO, X1, DX, YO, Y1, DY

DEFINE TERRAIN
ENTER IT, NL, IC, HS, PSS, PSL, DL, ER, RM

The inputs requested above and their default values are:

Ground Plane (plane of interest)
XO: left boundary in X direction (M) (-10000)
X1: right boundary in X direction (M) (10000)
DX: stepsize in X direction (M) (200)
YO: lower boundary in Y direction (M) (-10000)
Y1: upper boundary in Y direction (M) (10000)
DY: stepsize in Y direction (M) (200)
Terrain characteristics:
IT: Terrain Type (1) (homogeneous terrain)
NL: Number of layers (0)
IC: Terrain correlation function (1=exponential,2=gaussian) (2)
HS: Short scale Height (M) (0.03978)
PSS: Small scale RMS slope angles (DEG) (35)
PSL: Large scale RMS slope angles (DEG) (35)
DL: Layer depth (M) (0)
ER: Relative permittivity (15.0, 0.0)
RM: Permeability (1.0, 0.0)

If a slash (/) is entered at any point in a line of input, the remainder of variables in that line default to system values. If you wish to enter only one value in a line of variables, enter the number of commas equal to the number of variables in that line prior to the variable you wish to change, then the value you wish to input. If you wish the rest of the variables in that line to default to system values, input a slash (/), or more commas and

other values if there are more variables you wish to change in that line.

Example:

```
Enter IT, NL, IC, HS, PSS, PSL, (DL(I), ER(I), RM(I), I=1,NL+1)
INPUT:  , , 1 , , 25.0 /
```

IC becomes 1, PSL equals 25.0 and the remaining variables equal system values.

The next input required asks the operator to decide whether the transmitter position will be entered absolutely or relatively. The system default values will follow each input request.

```
DEFINE TRANSMITTER POSITION
SELECT ABSOLUTE COORDINATES OR RELATIVE POSITION
(1=ABSOLUTE, 2=RELATIVE) (2)
```

If the absolute method is chosen, the following input request is made:

```
ENTER POSITION (M), VELOCITY (M/S)
(0.0, 1524.0, 1524.0), (113.0, 0.0, 0.0)
```

Three components must be entered for each variable, the x, y and z coordinates for the position and the x, y and z components for the velocity.

If the relative method is chosen, the following inputs are required:

```
USING KNOWN ALTITUDE OR KNOWN SLANT RANGE?
(1=ALTITUDE, 2=SLANT RANGE) (1)
ENTER GRAZING ANGLE (DEG) (20.0)
```

```
ENTER OUT-OF-PLANE ANGLE (DEG) (0.0)
```

```
ENTER VELOCITY (M) (X, Y AND Z COMPONENTS)
(113.0, 0.0, 0.0)
```

If the known altitude method is chosen, the following input request is made:

```
ENTER ALTITUDE (M) (3657.607)
```

Otherwise, the request for slant range is made:

```
ENTER SLANT RANGE (M) (7620.015)
```

The absolute coordinates are then calculated from the information entered.

The next line of input required is:

```
ENTER BEAM SHAPE, SIZE, CENTER (M), ANGLE (DEG)
IB1, AA1, AB1, C1, A1
```

These parameters and their system default values are defined as:

```
IB1: beam shape: 0=omnidirectional
                  1=rectangular diffraction
                  2=elliptical diffraction (not implemented)
                  3=realistic (1)
AA1: transmitting aperture height (M) (0.3048006)
AB1: transmitting aperture length (M) (1.5240031)
C1: beam center (M) (X, Y and Z) (0.0, 0.0, 0.0)
A1: Angle of orientation (DEG) (0.0)
```

The same sequence of inputs is repeated for the receiver. When entering relative positional information for the transmitter, if the grazing angle, out-of-plane angle or slant range are changed, the values entered will become the new default values. These values will be printed with the input requests, should the operator also choose the relative method for the receiver position entry. After receiver input is completed, the next input request is:

```
DEFINE PULSE
WAVELENGTH, PULSESHAPE, PULSE LENGTH (M)
AND TIME SEQUENCE (S)
RL, PS, PL, TO
```

These parameters and their system default values are defined as:

```
RL: wavelength (M) (0.25)
PS: pulse shape (1)
PL: pulse length (M) (37.5)
TO: time sequence: initial (0), final (0), delta (1) (S)
```

There are two pulse shapes available (1=rectangular, 2=sinusoidal).

The next inputs required are:

```
SELECT BEAM CENTERS USED FOR CALCULATIONS
AND TRANSFORM IF DESIRED.
BOTH/TRANSMITTER/RECEIVER ? (0/1/2) OR CNR (3/4/5)
TRANSFORM ? (0-3)
ISS, ITR
```

ISS is the flag which indicates which beam centers will be used for calculations (0=both beam centers, 1=transmitter's beam center, 2=receiver's beam center, 3=both beam centers, CNR plots, 4=transmitter's beam center, CNR plots, 5=receiver's beam center, CNR plots). ITR indicates whether or not the operator wants the plots transformed from the spatial domain to the time domain (0=spatial domain w/o shadow weighted reflectivities, 1=spatial domain w/ shadow weighted reflectivities, 2=time domain (w/o shadow weighting), 3=time domain (w/ shadow weighting)). ISS and ITR both default to 0. If a transform is requested, additional input is required:

```
DEFINE RANGE DOPPLER (M, HZ)
ENTER RMIN, RMAX, DELTAR, DMIN, DMAX, DELTAD
```

These parameters and their system defaults are:

```
RMIN: lower boundary (range gates) (-10)
RMAX: upper boundary (range gates) (10)
DELTAR: size of range gate (M) (37.5)
DMIN: minimum doppler frequency (0)
DMAX: maximum doppler frequency (0)
DELTAD: Type of processing (10=doppler processing,
1000=no doppler processing) (1000)
```

The doppler frequency range can extend from -500 to +500 Hz relative to the aimpoint frequency. But the region of interest generally lies within the -250 to +250 Hz range of the aimpoint frequency. If DMIN and DMAX are left at 0, a single line plot will be produced, corresponding to the summation of doppler frequencies for a single cut over the region of interest. If other values than 0 are used, a contour plot of doppler frequencies over the entire range-doppler mesh will be produced. A DELTAD of 10 Hz will produce doppler processed results. Whereas, a DELTAD of 1000 Hz will eliminate doppler processing.

The next inputs required are the clutter models to be executed. The operator must enter the number of models selected and what those models are. There are no defaults for these inputs. The input request message is:

ENTER NUMBER OF VARIABLES, AND VARIABLES

1 RANGE	6 BEAM	11 SRTSH	16 VRTSH
2 DOPPLER	7 COHHH	12 SRTTH	17 VRTHH
3 BISTATI	8 COHVV	13 SRTVH	18 VRTVH
4 AREA	9 COHHV	14 SRTHV	19 VRTHV
5	10 COHVV	15 SRTVV	20 VRTVV

The models available are:

- 1) Bistatic Range
- 2) Doppler Frequency
- 3) Bistatic Angle
- 4) Pulse Area
- 5) (not implemented)
- 6) Beam Pattern
- 7) Coherent Reflectivities, HH polarization
- 8) Coherent Reflectivities, VH polarization
- 9) Coherent Reflectivities, HV polarization
- 10) Coherent Reflectivities, VV polarization
- 11) Slightly Rough Terrain Shadowing
- 12) Slightly Rough Terrain HH polarization
- 13) Slightly Rough Terrain VH polarization
- 14) Slightly Rough Terrain HV polarization
- 15) Slightly Rough Terrain VV polarization
- 16) Very Rough Terrain Shadowing
- 17) Very Rough Terrain HH polarization
- 18) Very Rough Terrain VH polarization
- 19) Very Rough Terrain HV polarization
- 20) Very Rough Terrain VV polarization

Only two more inputs are required to complete the command file. They are:

SELECT DESIRE SCALE: (2)

- 1) LARGE SCALE (NOT USED W/TIME DOMAIN)
- 2) SMALL SCALE

DO YOU WISH TO CHANGE ANYTHING? (1=YES, 2=NO)

The scale system default value is 2. If no change requests are made, previous inputs are written to the command file and the audit trail. Otherwise, the input sequence starts over again.

The remaining inputs are required for generation of the data file necessary to run the EXEC program, which generates the data files for plotting. There are no defaults for these inputs. These inputs are:

DO YOU WISH TO INPUT WINDOW SIZE? (1=YES, 2=NO)

If the operator requests manual input of window size, the following parameters must be input:

ENTER XMIN, XMAX, YMIN, YMAX (KFT):

XMIN and XMAX are the left and right window boundaries in the X direction in kilofeet. YMIN and YMAX are the lower and upper window boundaries in the Y direction in kilofeet. Although the inputs for the command file involving distance were in meters, the window size inputs are in kilofeet in order to produce plots consistent with those plots produced by ERIM, thus allowing comparison of results. The next input required concerns the axes lengths and rotations on the plots. The following input request is made:

DO YOU WISH TO SELECT AXES LENGTHS & ROTATIONS?
(1=YES, 2=NO)

If the option to enter these parameters is chosen, the following input requests are made:

ENTER VERT., HORIZ., AND Z AXES LENGTHS (IN):

ENTER ROTATION ANGLES ABOUT THE X AXIS,
Y AXIS AND Z AXIS (DEG):

The vertical and horizontal axes can be either the X or Y axis depending on the angles of rotation. The rotation angle variables are self-explanatory. The axes lengths are entered in inches, bound only by the page size and restrictions of the plotter. The axes rotations are entered in degrees.

If the window size is manually entered, the contour level range and increment

must be manually entered. The following input request is made for each variable selected:

ENTER CONTOUR LEVEL MIN, MAX AND DELTA FOR:
(Variable name) (SEE USER'S MANUAL)

MIN and MAX are the lower and upper bounds of the contour level range for each variable. DELTA is the increment between contours. Although the window size, contour level range and increment can be set manually when plotting in the time domain or on large scale plots, it is easier to allow these parameters to be set to system default values which have been determined to best suit these conditions. This is done by not selecting manual input of window dimensions. Otherwise, input of the contour level range and increment is required. The acceptable variations of contour level range and increment for each variable follows:

<u>VARIABLE</u>	<u>CONTOUR LEVEL RANGE</u>	<u>INCREMENT</u>
Bistatic Range(enlarged)	BR-4.92 to BR+4.92 (kft)	0.123 kft
(standard)	BR-40 to BR+40 (kft)	1.0 kft
Doppler	-1000 to 1000 (Hz)	20.0 Hz
Bistatic Angle	0.0 to 180.0 (deg)	10.0 deg
Area	0.0 to 100.0 (dB)	5.0 dB
Beam Pattern	-21.0 to 0.0 (dB)	3.0 dB
Remaining Variable	-60.0 to 10.0 (dB)	5.0 dB

The increment size may be changed to suit the operator's current needs. But the contour level range should remain within the bounds listed above.

The final input concerns color-filled contour plots. This option is only available for the geometric plots. The input request is:

DO YOU DESIRE FILLED CONTOURS FOR
VARIABLE # __? (1=YES, 2=NO)

A simple 1 or 2 for yes or no is all that is required. This completes

creation of the data file. Again, a message is printed on the screen instructing the operator how to run the command file he just created. He is instructed to enter at the VAX system prompt: \$ @RDMAP. Execution of this program can be interrupted by entering a control C. Additional capabilities include an Audit trail contained in the file Rdmnu.dat, and analytical tools, with results contained in EXSC.dat. Data files for both the audit trail and analysis are printed out on each run. The plots generated are first displayed on the RAMTEK. Then a hard copy of the RAMTEK screen is sent to, and then produced on the DSCAN. Examples of the plots generated and the information they contain can be found in Reference 3.

DESIGN PLAN

ACTIVE RADAR CALIBRATOR (ARC) SPECIFICATION - REVISION 1

ELIN A003

CONTRACT TITLE: BISTATIC CLUTTER PHENOMENOLOGICAL
MEASUREMENT/MODEL DEVELOPMENT

CONTRACT NUMBER: F30602-86-C-0045

CONTRACT PERIOD: 1 APRIL 1986 TO 31 SEPTEMBER 1987

PREPARED BY: CHARLES H. HIGHTOWER

DATE: 7 JANUARY 1987

Prepared For:
ROME AIR DEVELOPMENT CENTER
GRIFFISS AIR FORCE BASE
NEW YORK 13441-5700

1.0 INTRODUCTION

This document describes requirements for an Active Radar Calibrator (ARC) that will support the Rome Air Development Center (RADC) Clutter Measurements Program (CMP). The ARC will be used to provide absolute calibration of an airborne bistatic and monostatic clutter measurements system operating at L-band developed by the Environmental Research Institute of Michigan (ERIM). The ERIM measurement system is unique in that the bistatic illuminator aircraft does not contain the monostatic radar. A second aircraft contains the bistatic receiver and the monostatic radar transmitter. The bistatic receiver is time multiplexed to act as the monostatic radar receiver. This configuration imposes unusual requirements on the ARC since the distance to the ARC from the two transmitters will not, in general, be the same.

Section 2.0 describes the functional requirements of the CMP ARC with detailed requirements summarized in Sections 3.0 and 4.0.

2.0 ARC FUNCTIONAL REQUIREMENTS

The ARC will be used to provide an absolute radar cross section (RCS) reference for the CMP measurements program. Because of measurement system design and required test geometries, the linear ARC output signal will compete with extremely high levels of clutter RCS for both monostatic and bistatic operation. Because of this, the ARC will require both time delay and Doppler offset of the received radar signal prior to transmission. The reception and transmission of linear polarizations is needed. Since low grazing angle operation will be required, the ARC shall be provided with a mounting fixture to elevate the device above the ground and also provide elevation and azimuth adjustment of the ARC antennas. The ARC shall also be reasonably portable and operate on battery power.

3.0 DETAILED ARC REQUIREMENTS

The ARC shall meet the specific requirements defined in the following paragraphs.

3.1 Accuracy

The ARC shall be calibrated to provide its design RCS within ± 0.5 dB. Calibration curves shall be provided to allow the ARC's RCS to be adjusted for elevation and azimuth boresight angle offsets, temperature variations, and radar frequency changes while maintaining 0.5 dB accuracy. The orientation of the receive antenna and transmit antenna electric fields shall be clearly marked as shall the electrical boresight of each ARC antenna.

3.2 Power Requirements

The ARC shall be sized to provide an adequate Signal-to-Noise Ratio (SNR) for both monostatic and bistatic operation. The following information is provided to aid in this design process.

3.2.1 CMP Experiment Geometries

For ARC design purposes, two CMP experiment geometries shall be considered.

The first represents a very low grazing angle for the bistatic receiver/monostatic radar and represents the maximum range between the ARC and the monostatic system. The second geometry represents the minimum ranges between the ARC and the bistatic transmitter and the ARC and the bistatic receiver/monostatic radar. The parameters associated with these geometries are provided in Table 3-1.

Table 3-1 ARC Design Geometries Definition

GEOMETRY 1 - MAXIMUM RANGE GEOMETRY AND LOW RECEIVER GRAZING ANGLE

Receiver Grazing Angle (degrees)	0.5
Receiver Altitude (feet)	1,300
Receiver Range to ARC (feet)	148,971
Monostatic Transmitter Range to ARC (feet)	148,971
Bistatic Transmitter Grazing Angle (degrees)	20
Bistatic Transmitter Altitude (feet)	12,000
Bistatic Transmitter Range to ARC (feet)	35,086

GEOMETRY 2 - MINIMUM RANGE GEOMETRY AND MEDIUM RECEIVER GRAZING ANGLE

Receiver Grazing Angle (degrees)	4.0
Receiver Altitude (feet)	1,300
Receiver Range to ARC (feet)	18,636
Monostatic Transmitter Range to ARC (feet)	18,636
Bistatic Transmitter Grazing Angle (degrees)	35
Bistatic Transmitter Altitude (feet)	12,000
Bistatic Transmitter Range to ARC (feet)	20,921

3.2.2 ERIM Measurement System Radar Parameters

Parameters of the ERIM monostatic and bistatic radar systems are presented in Table 3-2 and shall be used to determine the ARC design.

Table 3-2 ERIM Measurement System Description

Monostatic Radar System Parameters

Transmitter Power (Watts)	5,000
Transmit Antenna Gain on Boresight (dB)	16.5
Transmitter System Losses (dB)	2
Receive Antenna Gain on Boresight (dB)	16.5
Receive System Losses (dB)	5
Receiver Noise Figure	3
Center Frequency (GHz)	1.25
Pulse Length (nanoseconds)	4,000

Bistatic Radar System Parameters

Transmitter Power (Watts)	5,000
Transmit Antenna Gain on Boresight (dB)	16.5
Transmitter System Losses (dB)	2
Receive Antenna Gain on Boresight (dB)	16.5
Receive System Losses (dB)	5
Receiver Noise Figure (dB)	3
Center Frequency (GHz)	1.25
Pulse Length (nanoseconds)	125

3.2.3 Monostatic and Bistatic Clutter Levels

Expected levels of monostatic and bistatic clutter RCS for the CMP measurements are difficult to estimate precisely. However, the following guidelines are provided. It is estimated that the monostatic clutter level in a range cell of interest for both geometries defined above will lie below 60 dBsm. Similarly, for bistatic clutter, the clutter in a range cell of interest will probably not exceed 65 dBsm. In order to ensure that the equivalent ARC RCS shall exceed these clutter levels, the linearly amplified ARC signal shall be time delayed up to 400 nanoseconds. It can be assumed that the corresponding interfering clutter will have decayed by at least 10 dB during this time period. Furthermore, a Doppler processing gain of 20 dB can be assumed provided the ARC offsets the amplified signal into a Doppler region where no clutter energy exists. This frequency range lies between +200 Hz of the center frequency of the radar. The ARC calibration signal shall exceed the residual clutter levels after time delay and Doppler processing gains have been taken into account by at least 20 dB. That is, the ARC shall have a minimum monostatic RCS of 50 dBsm and a minimum bistatic RCS of 55 dBsm.

3.3 Other Requirements

The ARC shall provide a fixed loop time delay of TBD nanoseconds with an accuracy of +TBD nanoseconds. The Doppler offset should be manually selectable in 50 Hz steps over its +250 Hz interval. A manually controllable attenuator shall also be included in the ARC so that the output signal level can be controlled to prevent ERIM measurement receiver saturation in the event the ARC is used at closer ranges. An attenuator range of 0 to 60 dB or greater is required.

The ARC shall be portable and capable of continuous operation for at least four (4) hours without battery replacement or recharging. The ARC's weight shall not exceed 30 pounds. The ARC shall include a temperature sensor for manual recording and be provided with a carrying case that will protect the unit during shipment and field operations. The unit shall be packaged for use in a broad range of environments including desert and arctic regions.

4.0 DOCUMENTATION REQUIREMENTS

Each ARC shall be delivered with documentation that provides a general description of its operation and design. This documentation shall also contain performance specifications for the unit as delivered including as a minimum: equivalent RCS; receiver sensitivity (microvolts); design frequency;

bandwidth; antenna type and gain; antenna response of ARC; maximum effective radiated power (milliwatts); size; weight; power; and option definitions.

The documentation shall also include recommendations for ARC deployment including assembly, testing, positioning, and checkout. Lastly, calibration curves and calculations for the unit shall be included.

DESIGN PLAN
HYBRID BISTATIC RADAR (HBR)
CLUTTER MEASUREMENTS PROGRAM (CMP)
ELIN A003

CONTRACT TITLE: BISTATIC CLUTTER PHENOMENOLOGICAL
MEASUREMENT/MODEL DEVELOPMENT

CONTRACT NUMBER: F30602-86-C-0045

CONTRACT PERIOD: 1 APRIL 1986 - 30 SEPTEMBER 1987

PREPARED BY: CHARLES H. HIGHTOWER

DATE: 20 MARCH 1987

Prepared for:
ROME AIR DEVELOPMENT CENTER
GRIFFISS AIR FORCE BASE
NEW YORK 13441-5700

SRS

TECHNOLOGIES

ADVANCED TECHNOLOGY DIVISION
17252 ARMSTRONG AVENUE
IRVINE, CALIFORNIA 92714
(714) 250-4206

TABLE OF CONTENTS

<u>PARAGRAPH</u>	<u>TITLE</u>	<u>PAGE</u>
1.0	INTRODUCTION.....	
2.0	CLUTTER MEASUREMENTS TEST MATRIX AND HBR GEOGRAPHICAL CONSIDERATIONS..	
2.1	HBR Test Matrix Geometries.....	
2.2	HBR Operational Coverage.....	
2.3	Site Selection.....	
3.0	INTRODUCTION TO SCATTERING MODELS.....	
3.1	Candidate Clutter Reflectivity Models.....	
3.1.1	Perfectly Rough Surface Model.....	
3.1.2	Barton's Scattering Model.....	
3.1.3	Kirchhoff or Physical Optics Model.....	
3.1.4	Perturbation Theory Models.....	
3.1.5	Composite Model With Shadowing.....	
3.1.6	Variations of the Composite Model.....	
3.2	Statistical Clutter Scattering Model Candidates.....	
3.2.1	Rayleigh Fluctuation Model.....	
3.2.2	General Statistical Fluctuation Model.....	
3.2.3	Monte Carlo Statistical Fluctuation Model.....	
3.2.4	General Monte Carlo Statistical Fluctuation Model.....	
3.2.5	Other Statistical Models.....	
4.0	GROUND TRUTH MEASUREMENT REQUIREMENTS.....	
4.1	Surface Physical Characteristics	
4.2	Surface Electrical Characteristics.....	
4.2.1	HBR Terrain Electrical Characteristics.....	
4.2.1.1	Water and Ice.....	
4.2.1.2	Frozen and Semi-frozen Tundra.....	
4.2.1.3	Soil and Rocks.....	
4.3	Ground Truth Measurements Definition.....	
5.0	TEST PLANNING.....	
5.1	Test Planning Procedure.....	
5.1.1	Calibration.....	
5.1.2	Flight Tests.....	
5.1.2.1	Flight Calibration.....	
5.1.3	Platform Position Determination Systems.....	
5.1.4	Radar Data Collection.....	
5.1.5	Data Recording.....	
5.1.6	Ground Truth Instrumentation.....	
5.2	Test Plan Implementation.....	

LIST OF FIGURES

<u>Number</u>	<u>Title</u>	<u>Page</u>
1-1	CMP Data Collection Geometry.....	
2-1	HBR CONUS Defense Coverage.....	
2-2	HBR Fleet Defense Coverage.....	

LIST OF TABLES

<u>Number</u>	<u>Title</u>	<u>PAGE</u>
2-1	CMP Test Matrix.....	
2-2	HBR Operational Area Geography, Terrain Types, and Characteristics...	
2-3	CMP Measurement Site Selection Matix.....	
3-1	Ad Hoc Clutter Statistical Flucuation Models.....	
4-1	Typical Dielectric Constants of HBR Operational Areas.....	
4-2	Ground Truth Measurements Requirements.....	

1.0 INTRODUCTION

The Hybrid Bistatic Radar (HBR) concept is being considered as a candidate surveillance sensor against the low observable cruise missile penetration threat. The motivation for the HBR system, among other features, is the potential increase in target Radar Cross Section (RCS) at very large bistatic angles and the reduction in the magnitude of associated terrain and sea clutter. Validation of both of these features, high target RCS and low clutter, and the establishment of bistatic clutter statistics is necessary prior to proceeding with HBR full-scale development.

The objectives of this design plan are to describe the measurements needed to adequately describe the behavior of bistatic clutter so that the full potential of the HBR concept can be investigated. The Clutter Measurements Program (CMP) conducted by the Environmental Research Institute of Michigan (ERIM) will by necessity be limited to a restricted sampling of HBR geometries. Consequently, it is important to design the measurement program so that data is collected which most nearly represents the majority of HBR operational scenarios.

The contents of this design plan form the basis for the detailed test planning that will be conducted later in the CMP program. It also provides the motivation for the ERIM measurement system and SRS ground truth measurements. The basic objective of the HBR CMP is to acquire calibrated bistatic and monostatic clutter data and associated ground truth measurements to form a comprehensive data base. This data base shall be adequate to:

1. Represent bistatic and monostatic clutter behavior for the HBR geometry and radar parameters
2. Allow validation of scattering models, clutter statistics, and distributions
3. Permit clutter behavior and statistics to be correlated with both physical and electrical properties of different terrain types
4. Provide a reasonable basis for comparison of bistatic and monostatic clutter behavior.

Section 2.0 describes the test matrix proposed for CMP measurements which represents the majority of HBR geometries and is suitable for clutter model validation. Also described in this section are geographical areas of importance to an operational HBR system. A number of candidate clutter models are presented in Section 3.0 that describe the mean clutter reflectivity coefficient. Models for clutter fluctuation statistical behavior are also presented. Ground truth measurements required for model validation are described in Section 4.0. Finally, CMP test planning requirements are presented in Section 5.0.

2.0 CLUTTER MEASUREMENTS TEST MATRIX AND HBR GEOGRAPHICAL CONSIDERATIONS

In order to provide clutter data representative of actual HBR operation, the location of the ERIM bistatic illuminator aircraft, bistatic receiver and monostatic radar aircraft, and clutter region for examination must be defined. Furthermore, this geometrical information must be considered in the context of HBR operation as well as its value to clutter model validation.

Figure 1-1 illustrates a typical CMP data collection geometry. The aircraft at the higher altitude is the bistatic illuminator. The lower aircraft contains a monostatic radar whose receiver is multiplexed to receive echos from its transmissions plus those echos from the bistatic illuminator.

2.1 HBR Test Matrix Geometries

In support of the HBR Executive Review Committee Special Assessment Study Meetings, Decision Science Applications (DSA) examined HBR engagement geometries and identified 96 combinations of illuminator grazing angle, receiver grazing angle, and out-of-plane angle as representative of system operation. These 96 combinations were further refined during the Assessment Study period and reduced to 16 proposed measurement scenarios. This number was chosen for compatibility with ERIM aircraft flight duration while still representing those HBR geometries of most frequent occurrence. The proposed test matrix is given in Table 2-1. The altitudes, angles, and ranges are defined in Figure 1-1.

Note that a sampling of out-of-plane angles is obtained in the matrix. This variation will be important in the validation of the candidate clutter models. In addition, shadowing information will be provided as receiver grazing angle varies.

2.2 HBR Operational Coverage

The initial General Dynamics feasibility study explored the HBR concept for defense of the Continental United States (CONUS) from bomber and cruise missile threats, and detection of airborne and ship targets for Fleet defense. The geographical regions associated with these defenses are shown in Figures 2-1 and 2-2. The CONUS defense ring shown in Figure 2-1 is approximately 200 Nmi wide. Approximately half of the ring lies along the coastal regions of the United States. The remaining half curves over Canada spanning the Canadian Rockies, the arctic islands, and into the maritime provinces on the east coast. Fleet defense areas shown in Figure 2-2 were chosen by General Dynamics to represent typical Battle Group Centers and generally lie in the northern hemisphere between the equator and about 60 degrees latitude.

Based on the proposed HBR operational areas discussed in the previous paragraph, some generalizations regarding the expected terrain types and characteristics can be made. It should be noted that clutter behavior outside the defensive areas is also of interest since they will be illuminated by the antenna sidelobes. These observations are summarized in Table 2-2.

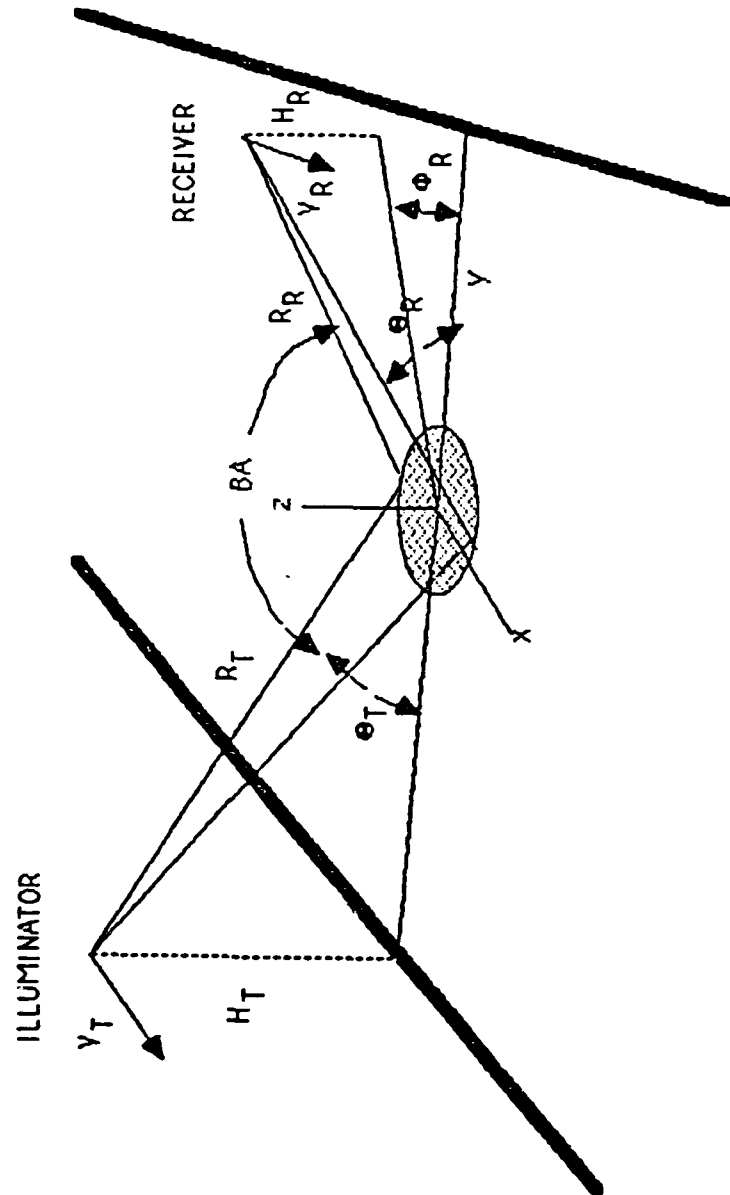


Fig. 1-1 CMP Data Collection Geometry

TRANSMITTER GRAZING ANGLE = 20 DEGREES		
RCVR GRAZING ANGLE (DEGREES)	OUT-OF-PLANE ANGLE (DEGREES)	
	0	5 10 20 35
10	A-1	A-2
4	A-3	A-4 A-5
2	A-6	A-7 A-8 A-9 A-10
0.5	A-11	A-12
TRANSMITTER GRAZING ANGLE = 35 DEGREES		
RCVR GRAZING ANGLE (DEGREES)	OUT-OF-PLANE ANGLE (DEGREES)	
	0	5 10 20 35
10	B-1	B-2
4	B-3	B-4 B-5
2	B-6	B-7 B-8 B-9 B-10
0.5	B-11	B-12

TRANSMITTER ALTITUDE = 12,000 FEET IN ALL CASES
 RECEIVER ALTITUDE = 1,300 FEET FOR ALL CASES EXCEPT 10 DEGREE GRAZING ANGLE
 WHERE IT IS 4,341 FEET

Table 2-1 CMP Test Matrix

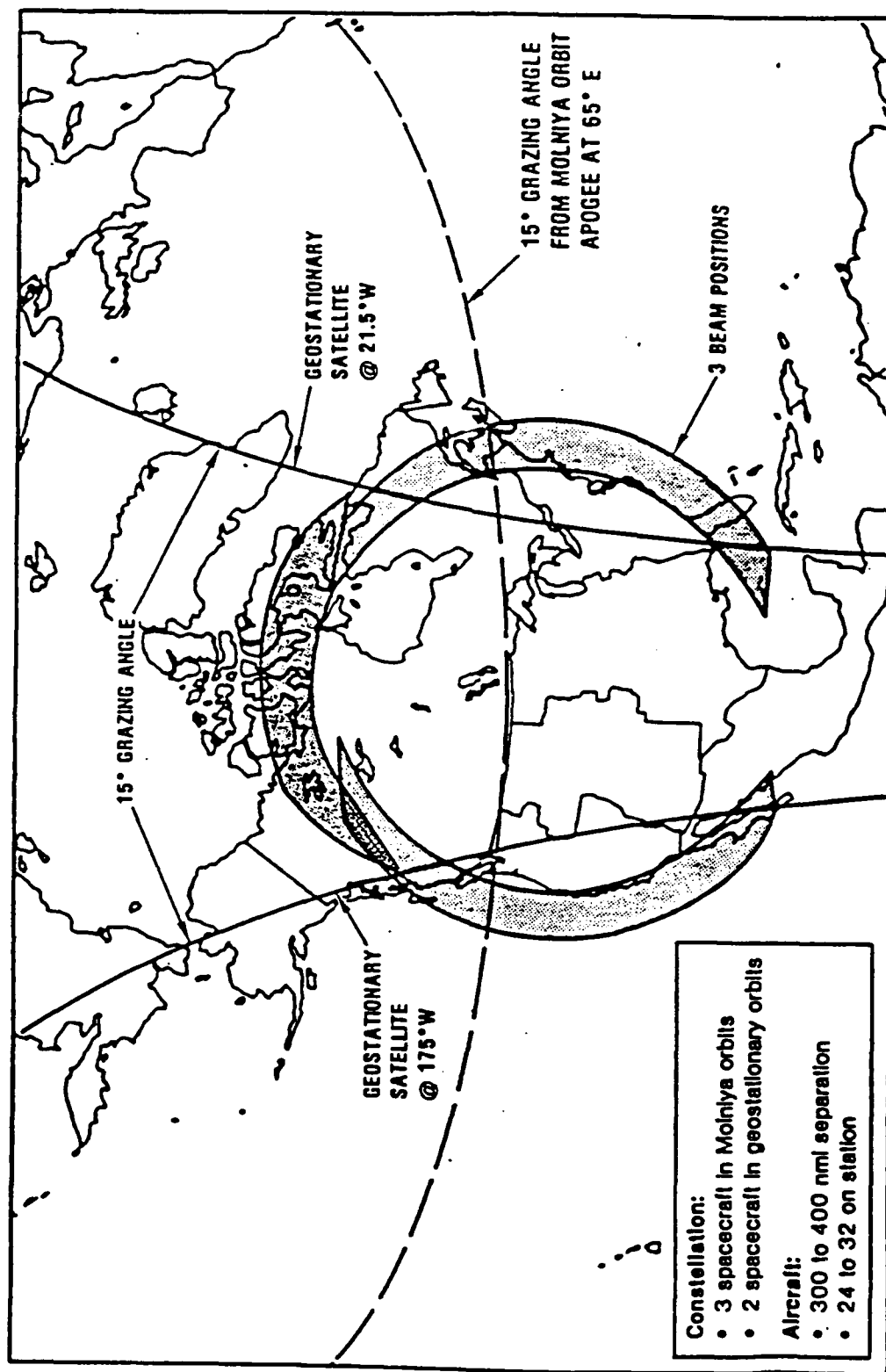
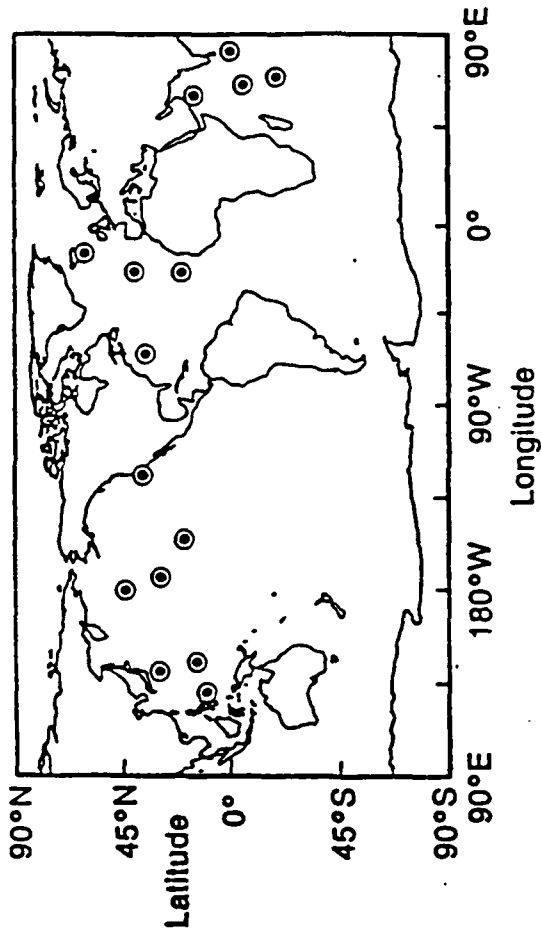


Fig. 2-1 HBR CONUS Defense Coverage

Fleet Defense Evaluation Scenario



⊙ Ship position

Fig. 2-2 HBR Fleet Defense Coverage

Table 2-2 HBR Operational Area Geography, Terrain Types, and Characteristics

<u>Operational Area</u>	<u>Terrain Type</u>	<u>Characteristics</u>
US West Coast	Ocean	23 Degrees N to 48 Degrees N Latitude
US East Coast	Ocean	23 Degrees N to 48 Degrees N Latitude
Western Canada	Mountainous	Boreal Forests, Desert Valleys, Jagged Mountains, Lakes, Streams, Snow, Ice
Northwest Territories	Rocky Plateau, Island Fragments, Numerous Arctic Straits and Bays	Treeless Trunda, Wooded Plains, Rivers, Snow, Ice
Eastern Canada	Rocky Plateau, Mountains, Islands	Boreal Forests, Rugged Mountains, Lakes, Rivers, Snow, Ice

Other factors to consider in measurement site selection are seasonal variations of the terrain listed in Table 2-2. For example, arctic tundra varies from a mucky, moss-covered surface in the summer to an almost impenetrable frozen substance in the winter. Similarly, Arctic ocean areas become choked with frozen sea ice in the winter. It is also necessary to consider seasonal variations of the weather and the effect on sea states for the ocean areas described.

2.3 Site Selection

Based on the HBR operational areas described above, it appears that CMP test matrix geometries should encompass nearly equal amounts of ocean and land. Ocean areas within 200 Nmi of both coasts for various sea states should be examined. Clutter data from the Canadian Arctic regions is also required.

Site selection for ocean clutter measurements is straight-forward and actual HBR operation areas off either coast of the United States can be selected. However, since a cost effective measurements program is a desirable goal, a major obstacle to CMP test planning becomes the location of readily accessible terrain within the Continental United States that is similar to that of the Canadian Arctic.

A potential solution to this problem is discussed in Section 4.0. It is shown there that the electrical properties of ice and frozen soil commonly used in surface scattering models are nearly identical to those of very dry soil. Hence, a reasonable insight to the behavior of electromagnetic scattering from Arctic regions (ice, frozen trundra, etc.) made be obtained by clutter

measurements from sites selected in the arid deserts of the western United States.

This is especially fortuitous since the Western United States has both ocean and desert areas in close geographic proximity. Consequently, collection of clutter data representing the majority of HBR operational scenario terrain types could be made from one area which should lead to a cost-effective measurements program.

A site selection matrix is presented in Table 2-3 which will provide clutter data representative of HBR operation. CMP instrumentation aircraft can be based at either Point Mugu Naval Air Station or at Edwards Air Force Base in California. Point Mugu would be the best location for ocean measurements since it lies along the Pacific Coast and there are many islands and off-shore oil platforms for calibration repeater and position beacon location nearby. Edwards Air Force Base is suitable for flights over arid desert terrain simulating scattering from frozen tundra and ice. In addition, Edwards Air Force Base is close to the Sierra Nevada Mountains and several lesser ranges.

Table 2-3 CMP Measurement Site Selection Matrix

<u>Base</u>	<u>Coordinates</u>	<u>Terrain Type</u>
Point Mugu NAS	34.15 N 119.10 W	Sea States from Calm to Aircraft Limits
Edwards AFB	34.88 N 117.90 W	Very Dry to Very Wet Desert
Edwards AFB	34.88 N 117.90 W	Snow Covered Mountains

Specific areas for clutter measurement near the regions sited in Table 2-3 will be identified in the CMP Test Plan and Procedures as detailed examination of the proposed sites is completed.

3.0 INTRODUCTION TO SCATTERING MODELS

The solution to the problem of modeling reflection of a plane wave at the boundary of an irregular and inhomogeneous surface has been attempted by many researchers over the past several decades. These solutions are important since they allow the performance of radar systems in a real clutter environment to be predicted. Such models range from simple curve fitting of measured data to elegant mathematical solutions of Maxwell's equations. Models for sea, land, ice and vegetation covered terrain have been proposed and compared to available radar data with limited success. In order to bound the problem of model validation and selection for the CMP effort, several models have been selected from this large body of knowledge which appear to have gained acceptance through comparison with limited monostatic and bistatic measurements. The models presented are not exclusive and should be considered only as a reasonable sampling of those available for investigation during the HBR Clutter Measurements Program.

3.1 Candidate Clutter Reflectivity Models

3.1.1 Perfectly Rough Surface Model

Rough surface scattering is often represented by a reflectivity coefficient that obeys Lambert's law. For the bistatic case, an ideal lambertian surface is characterized by the following model

$$\sigma^{\circ}(\theta_0, \phi_0; \theta_s, \phi_s; p_0, p_s) + \sigma^{\circ}(\theta_0, \phi_0; \theta_s, \phi_s; p_0, p_s) = \sigma_0^{\circ} \cos \theta_0 \cos \theta_s,$$

where,

σ_0° = constant related to the dielectric properties of the scattering surface

θ_0 = angle of incidence

θ_s = angle of reflection.

3.1.2 Barton's Scattering Model

This model is of interest since it was used to represent clutter in the original HBR feasibility study. The mathematical formulation is given by the following equations.

$$\sigma_G^{\circ} = \frac{e_a F_d^2 Z}{\beta_0^2} \exp [-(\beta/\beta_0)^2]$$

3.1.3 Kirchhoff or Physical Optics Models

Models derived from the Kirchhoff intergral representation for a scattered plane wave from a random surface have been shown to agree fairly well with measured backscatter (monostatic) data and in the bistatic case for certain experimental surfaces (e.g., flat conducting plates with a Gaussian surface height correlation functions). Consequently, these models are good candidates for comparison with CMP data. This is especially true when the terrain has been selected to have homogeneous physical and electrical characteristics.

Two formulations for these models depend on the assumption of the nature of the surface correlation function. For terrain where the RMS surface height is much larger than the wavelength of interest, analytical formulations for the relectivity coefficient are as follows

$$V_{jk}^S = \frac{4}{\pi} k_0^4 h^2 \cos^2 \theta_i \cos^2 \theta_s |\alpha_{jk}|^2 I$$

3.1.4 Perturbation Theory Models

Another class of model exists for the condition where the surface height standard deviation and correlation length are smaller than a wavelength. These models are based on the assumption that the surface can be described by a random surface which is Fourier-transformable. Typical formulations for these models are given below again depending on the assumption for the surface correlation function.

$$V_{jk}^V = |\beta_{jk}|^2 \frac{4}{\xi_z^2 \omega^2} \exp \left(- \frac{(\xi_x^2 + \xi_y^2)}{\omega^2} \right)$$

3.1.5 Composite Model With Shadowing

The Physical Optics and Perturbation models represent scattering from two classes of surfaces. Namely, those that are rough compared to a wavelength and those that are fairly smooth in relation to a wavelength. In addition, the derivations for both these models neglect the effect of incident and reflected wave blockage by undulations of the surface (i.e., shadowing). Furthermore, naturally occuring surfaces may include both types of surfaces in various proportions. Thus, it is natural to formulate a model which is the weighted sum of the two models with each component weighted by an appropriate shadow function. Such a formulation is provided below.

$$\bar{\sigma}_{jk}^0 = a \cdot S_1(\theta_i, \theta_s, \phi_s, w_s) V_{jk}^S(\theta_i, \theta_s, \phi_s, k_0, h, w_s, \epsilon_r, \mu_r) \\ + b \cdot S_2(\theta_i, \theta_s, \phi_s, w_L | p_0, q_0) \cdot V_{jk}^L(\theta_i, \theta_s, \phi_s, w_L, \epsilon_r, \mu_r)$$

3.1.6 Variations of the Composite Model

In the Composite Model of paragraph 3.1.5, the fact that the small-scale roughness is tilted by the large scale surface upon which it rests is ignored.

It is relatively straight forward to modify the expression for the slightly rough component in the composite model to take this effect into consideration through a "local incident angle."

3.2 Statistical Clutter Scattering Model Candidates

The models described in the previous paragraphs are all limited to determination of the mean clutter reflectivity coefficient and do not provide any information on the statistical nature of reflectivity coefficient. In the following paragraphs, a number of elementary models providing the statistical behavior are discussed for comparison with CMP data.

3.2.1 Rayleigh Fluctuation Model

The total field scattered by a rough surface can be thought of as the sum of a large number of elementary plane waves in mutual phase interference. Thus, the resulting field at a given point in a given direction can be represented by a vector sum in the complex plane. If the amplitudes of the waves are all equal and the phases are uniformly distributed between -180 degrees and +180 degrees, then the amplitude fluctuations are described by the Rayleigh probability density function. The resulting power fluctuations corresponding to the reflectivity coefficient are then exponentially distributed. The corresponding density functions for the reflection coefficient are then

$$f(x) = \begin{cases} \lambda e^{-\lambda x} \\ 0 \end{cases}$$

$$\bar{x} = \frac{1}{\lambda}$$

3.2.2 General Statistical Fluctuation Model

Beckmann addresses the problem for the case where not all the wave amplitudes are equal nor are the phases uniformly distributed over -180 degrees to +180 degrees. Such a situation is likely to occur for slightly rough surfaces and low grazing angles characteristic of the HBR geometry. The resulting expression for the amplitude density function is given below and involves an integration best accomplished with a computer.

$$p(r) = \frac{r}{2\pi \sqrt{s_1 s_2}} \int_0^{2\pi} \exp \left[-\frac{(r \cos \psi - \alpha)^2}{2s_1} - \frac{(r \sin \psi - \beta)^2}{2s_2} \right] d\psi$$

This expression is also valid for the case where the wave amplitudes are not independent with some additional calculations.

3.2.3 Monte Carlo Statistical Fluctuation Model

A more complex approach for determination of reflection coefficient fluctuation characteristics begins with evaluation of the mathematical expression for the scattering coefficient based on the Helmholtz integral given by

$$\rho = \frac{F_2}{\lambda} \iint_A e^{i\mathbf{r} \cdot \mathbf{r}'} dx dy$$

This approach is desirable since characteristics of the radar system can be incorporated into the integral's evaluation and the variation of the actual received signal computed. This is accomplished by creating a random surface with desired electrical and surface height characteristics and restricting the evaluation of the integral to the area illuminated by the system as determined from the antenna pattern(s) and pulse width. In order to reduce the associated computational load created by the requirement to accurately represent the variation in the dot product in the exponential over each incremental area, the total area can be further restricted by considering Doppler processing resolution cell constraints.

3.2.4 General Monte Carlo Statistical Fluctuation Model

The Helmholtz integral used in the previous paragraph provides only a scalar representation the reflectivity coefficient. Consequently, it does not provide an indication of how polarization affects the statistical fluctuations. In order to overcome this limitation, a more complex integral for the scattered field based on the vector second Green's Theorem as formulated by Stratton and Chu and modified by Silver can be used. This expression is given below.

$$E' = K \hat{n}_s \times \int [(\hat{n} \times E - \eta_s \hat{n}_s \times (\hat{n} \times H))] e^{jk_s \cdot \hat{n}_s} dS,$$

3.2.5 Other Statistical Models

In addition to the Rayleigh density function, other density functions have been shown to describe clutter fluctuations under various conditions. Table 3-1 summarizes a number of these functions. During data analysis, these statistical distributions can be tested for fit to the experimental data by various statistical hypothesis tests.

Table 3-1 Ad Hoc Clutter Statistical Flucuation Models

<u>PROBABILITY DENSITY FUNCTION</u>	<u>COMMENTS</u>
Rice-Nakagami	Approximates Chi Density - Two Parameters Single Dominant Scatterer of Many
Contaminated Normal	Three Parameters No Physical Interpretation
K-Distribution	Two Parameters N-independent Scatterers with Random Phase and Amplitude
Gamma	Two Parameters Finite Number of Random Scatterers
Weibull	One Parameter No Physical Interpretation
Log-normal	Two Parameters Represents Multiple Scattering

4.0 GROUND TRUTH MEASUREMENT REQUIREMENTS

Examination of the more complex clutter models based on electromagnetic theory defined in the foregoing section shows that scattering is typically characterized by physical and electrical properties of the underlying terrain. Physical characteristics describe the roughness of the surfaces involved and how they vary over the region of interest. Sufficient ground truth information is required to estimate the surface height and surface slope probability density functions. Electrical properties of interest include the complex dielectric constant (sometimes called complex permittivity) of the surface and any underlying layers of material. These measurements fall into the category of "Ground Truth" and must be made in conjunction with CMP flight measurements.

4.1 Surface Physical Characteristics

Surface height measurements in two-dimensions are required to estimate the surface height and slope density functions. Whether or not the surface can be represented as a composite of different roughness scales is also important. If this is the case, measurement of surface height variations on the order of 0.1 wavelength or less are desirable for prediction of small-scale scattering behavior. In addition, these measurements should be taken at intervals of about 0.5 wavelength. This is best achieved by field measurements using appropriate instrumentation. Larger scale surface height variations can be determined from topographical map data. In addition, knowledge of these characteristics for material lying beneath the surface is needed if signal penetration depth is significant.

4.2 Surface Electrical Characteristics

The microwave scattering behavior from surfaces is strongly influenced by its dielectric constant, which, in turn, is largely a function of moisture content. The complex dielectric constant of a surface relative to free space is defined as

$$\epsilon_c = \left(\epsilon - j \frac{\sigma}{\omega \epsilon_0} \right) \epsilon_0$$

where,

ϵ_c = complex dielectric constant relative to free-space

ϵ = surface permittivity

σ = surface conductivity

ω = $2\pi f$ = radar frequency

ϵ_0 = dielectric constant of free space.

4.2.1 HBR Terrain Electrical Characteristics

An important objective of CMP measurement site selection is data collection from terrain exhibiting electrical properties similar to those expected for an

operational HBR system. Complex dielectric constant values (relative to free space) at L-band for surfaces similar to those expected for HBR operational areas are given in Table 4-1.

Table 4-1 Typical Dielectric Constants of HBR Operational Areas

<u>Surface Material</u>	<u>Dielectric Constant</u>
Fresh Water (20 degrees C)	80.0 - j5.5
Sea Water (20 degrees C)	70.0 - j66.0
Fresh Ice	3.15 - j0.001
Sea Ice	(3.3 - j0.25) to (3.0 - j0.03)
Soil	(2.0 - j0.0) to (25.0 - j5.0)
Rock	(2.0 - j0.0) to (10.0 - j0.0)
Vegetation	(2.5 - j0.0) to (80.5 - j5.5)

4.2.1.1 Water and Ice

As can be seen from Table 4-1, the major difference between fresh water and sea water is the imaginary part of the dielectric constant which is proportional to conductivity (or motion of electrons in the substance). In contrast, the real part of the dielectric constant relates to the so-called "displacement" current of Maxwell's equations. As a consequence, the penetration depth of an L-band signal into sea water will be much less than into fresh water. However, even for fresh water the penetration depth is only about 0.3 foot.

Fresh ice and sea ice are also very nearly equivalent electrically. The low values of the real part of the complex dielectric constant (i.e., relative permittivity) are the result of water molecules being relatively immobile in the frozen state. The presence of entrapped liquid water can vary these values slightly. Because of the low dielectric constant, ice is relatively transparent compared to water. The major difference in scattering between these ices is the entrapment of air and other materials.

4.2.1.2 Frozen and Semi-frozen Tundra

Table 4-1 indicates that freezing sea and fresh water significantly reduces the complex dielectric constant. The dielectric constant of the frozen state for both types of ice is very close to the lower range of soil. Soil with such low dielectric constant values is typically very dry. Thus, the effect of dielectric constant on scattering from frozen tundra and very dry soil should be identical. This suggests that scattering from tundra-like terrain (when it is frozen) may be simulated by scattering from very dry soil; provided the soil has similar surface height characteristics. Likewise, scattering from the melted top layer of tundra may be represented by scattering from soil with a high water content; provided, of course, the soil has similar physical characteristics. Thus, scattering from tundra may be approximated by

measurements made over extremely dry or extremely wet desert regions with suitable physical characteristics.

4.2.1.3 Soil and Rocks

The dielectric constant for soil and rocks can vary significantly as shown by the range in Table 4-1. Prediction of the dielectric constant for soil-water mixtures is very difficult and has been investigated by many researchers. Prediction is difficult because of the many variables involved. These include soil texture, composition, particle sizes, amount of bound water, and amount of free water. Bound water refers to water molecules held tightly to soil particles by matric and osmotic forces.

Because of inconsistencies reported in the literature regarding soil dielectric models and their relationship to soil moisture, composition, etc., it is apparent that the CMP ground truth effort should measure the complex dielectric constant directly and not rely on analytical models relating measurements of soil moisture content, et. al. to dielectric constant. However, limited soil moisture and composition measurements should be made to validate the dielectric constant values obtained by direct means.

4.3 Ground Truth Measurements Definition

Based on the above discussion, it is clear that ground truth data describing physical and electrical characteristics of selected measurement sites is required. A summary of these measurements and other pertinent information is given in Table 4-2.

Table 4-2 Ground Truth Measurement Requirements

<u>Measurement Type</u>	<u>Resolution/Range</u>	<u>Comment</u>
Small-scale Height	2 - 3 cm	0.1 Wavelength
Large-scale Height	1 - 10 m	4 - 40 Wavelengths
Small-scale Grid Interval	10 - 15 cm	1/2 Wavelength
Large-scale Grid Interval	10 - 100 m	Survey Map Limited
Complex Dielectric Constant		
Real Part	1.0 to 80.0	
Imaginary Part	0.01 to 20	
Depth	Surface and 10 cm Below surface	

5.0 TEST PLANNING

This section addresses specific constraints levied on the measurement system in order to achieve the objectives of the Clutter Measurements Program.

5.1. TEST PLANNING PROCEDURE

Instrumented aircraft for this program will be operated and maintained by the Environmental Research Institute of Michigan (ERIM). Two aircraft will be utilized. One will act as a bistatic illuminator and the other will receive the bistatic transmissions. The receiver on the latter aircraft will also be used to receive pulses transmitted from a collocated transmitter (i.e., the monostatic transmitter). Specific requirements for the measurement programs are:

- a. Employ a Navy P-3 aircraft as the bistatic receiver, monostatic radar, and data recording system
- b. Employ a suitable aircraft to house the bistatic illuminator
- c. The aircraft shall fly prescribed paths as described in test procedures documentation
- d. The transmitted frequency shall be 1.25 GHz
- e. Pulse peak power shall be 5 KW
- f. The bistatic pulse shall be 125 ns in duration
- g. The monostatic pulse shall be 4 microseconds in duration
- h. Bistatic and monostatic pulses shall be interleaved to achieve unambiguous clutter Doppler returns
- i. The aircraft flight paths shall replicate the geometries described in Table 2-1

5.1.1 CALIBRATION

Calibration of measurement instrumentation shall be performed to meet the following requirements:

- a. All calibration shall be traceable to the National Bureau of Standards
- b. All flight equipment shall be bench-calibrated, reinstalled in the aircraft and rechecked
- c. Aircraft test flights shall be performed to determine INS platform drifts
- d. Each calibration procedure will have a ground procedure and flight equivalent

- e. The transmitter antenna shall maintain a pointing accuracy of 0.5 degrees
- f. The receiver antenna shall maintain a pointing accuracy of 0.5 degrees
- g. Active radar repeaters shall be used to verify transmitter and receiver antenna pointing accuracies
- h. Calibration tests will be carefully documented
- i. Pre-flight and postflight calibration shall be accomplished.
- j. Internal RF calibration shall be accurate to 1 dB for both the bistatic and monostatic radar systems. Errors due to data processing, platform position errors, geometry effects, and antenna patterns are not included in this figure
- k. Antenna patterns shall be measured to within 1 dB over the angular region specified in the test procedures

5.1.2 FLIGHT TESTS

5.1.2.1 Flight Calibration

In-flight calibration shall be performed prior to a measurement pass and immediately after a pass. This calibration will be performed to provide data that is directly relatable to the ground and airborne calibration tests described in paragraph 5.2.

5.1.3 Platform Position Determination Systems

Each aircraft shall contain a position and attitude determination system. Position, velocity, acceleration, heading, pitch, roll, and yaw shall be supplied at intervals of 0.1 seconds or less to the recording system. The use of an external positioning system to augment on-board systems is recommended. In addition, active radar repeaters shall be placed in the test areas to provide further position accuracy. This information shall be used to maintain the aircraft in the proper relative positions and the antennas pointed at the desired aim points.

5.1.4 Radar Data Collection

Coherent bistatic and monostatic clutter returns of specified polarization combinations shall be sampled and stored digitally. Atomic clocks on both aircraft shall be used to synchronize transmission and reception of the radar signals. Alternate means of time tagging platform metric data may be employed. Maximum receiver dynamic range shall be obtained by attenuation control on a pulse-by-pulse basis during the measurement pass as determined by the operator. Maximum use of on-board signal diagnostic equipment to validate recorded data is mandatory to prevent loss of data.

5.1.5 Data Recording

Data shall be recorded in real-time in digital format. This data shall include aircraft state information (i.e., auxiliary data) and radar signal samples. This data shall be recorded in a high density mode. The flight data tapes will be ground processed and converted to a computer compatible format as defined in the test procedure documentation.

5.1.6 Ground Truth Determination

A video camera shall be mounted on or near the antennas of both aircraft to provide visual information regarding the clutter terrain under measurement. Flight measurements shall be coordinated with the parallel ground truth measurements effort conducted by SRS Technologies.

5.2 TEST PLAN IMPLEMENTATION

Test plan implementation information will be found in the ERIM Design Plan and Test Plan documents referenced below:

"Test Plan for Hybrid Bistatic Radar Clutter Measurements Program, Contract F30602-86-C-0055, CDRL A002, January 1987;"

"Design Plan for Hybrid Bistatic Radar Clutter Measurements Program, Contract F30602-86-C-0055, CDRL A003, January 1987."

TEST PLAN/PROCEDURES
PHASE 1 DATA COLLECTION
ELIN A002

CONTRACT: BISTATIC CLUTTER PHENOMENOLOGICAL
MEASUREMENT/MODEL DEVELOPMENT

CONTRACT NUMBER: F30602-86-C-0045

CONTRACT PERIOD: 1 APRIL 1986 TO 31 SEPTEMBER 1987

PREPARED BY: CHARLES H. HIGHTOWER

DATE: 4 JUNE 1987

Prepared For:
ROME AIR DEVELOPMENT CENTER
GRIFFISS AIR FORCE BASE
NEW YORK 13441-5700

SRS
TECHNOLOGIES

CORPORATE HEADQUARTERS
1500 QUAIL STREET, SUITE 350
P.O. BOX 9219
NEWPORT BEACH, CALIFORNIA 92660
(714) 833-9088

TABLE OF CONTENTS

SECTION	TITLE
1.0	INTRODUCTION
2.0	DATA COLLECTION OBJECTIVES
3.0	PARTICIPANTS
4.0	PHASE 1 MISSION PLAN
4.1	CLUTTER DATA COLLECTION TEST CASE DESCRIPTION
4.2	COLLECTION PROCEDURES
4.3	MISSION SITE DEFINITION
5.0	COMMUNICATIONS PLAN
6.0	GROUND SUPPORT ACTIVITIES
6.1	ARC BEACON POSITIONING
6.2	UHF POSITIONING BEACON INSTALLATION
6.3	GROUND TRUTH DATA COLLECTION
6.3.1	SURFACE ROUGHNESS DATA
6.3.2	SURFACE SLOPES
6.3.3	TERRAIN GEOLOGICAL CHARACTERISTICS
6.3.4	TERRAIN ELECTRICAL PROPERTIES
6.4	VIDEO RECORDING
7.0	MISSION DESCRIPTION
7.1	DATA GOALS
7.2	MISSION PLAN
8.0	WAYPOINT DESCRIPTIONS
9.0	CONTINGENCY PLANNING
APPENDIX A	PHASE 1 GEOMETRY TEST PLANNING ANALYSIS

LIST OF FIGURES

NUMBER	TITLE
4-1	PHASE 1 DATA COLLECTION SCHEDULE
4-2	PHASE 1 DATA COLLECTION PASS DEFINITION
7-1	PHASE 1 FLIGHT PATH ILLUSTRATION

LIST OF TABLES

NUMBER	TITLE
3-1	PHASE 1 PARTICIPANTS AND RESPONSIBILITIES
4-1	LIMITED CALIBRATED CLUTTER DATA COLLECTION GEOMETRY

1.0 INTRODUCTION

This document has been prepared as part of Contract No. F30602-86-C-0045 entitled, *Bistatic Clutter Phenomenological Measurement/Model Development* funded by Rome Air Development Center (RADC). Its objective is to provide detailed planning of experiments and associated flight tests for the *Clutter Measurements Program* (CMP) being conducted by the Environmental Research Institute of Michigan (ERIM) for RADC and the Defense Advanced Research Projects Administration (DARPA). The following Test Plan/Procedures deals specifically with Phase 1 of ERIM's CMP clutter data collection.

This document assumes the reader is familiar with the following CMP reports:

1. Design Plan, Hybrid Bistatic Radar (HBR) Clutter Measurements Program (CMP), ELIN A003, SRS Technologies, UR87-060, 20 March 1987 (U)
2. Design Plan for Hybrid Bistatic Radar Clutter Measurements Program, Contract F30602-86-C-0055, ERIM, January 1987 (U).

Phase 1 CMP clutter data collection flights will take place sometime in the June - July 1988 period in the vicinity of Ann Arbor, Michigan. The objective of these flights is pilot and radar operator training, measurement and data recording system validation, and collection of limited clutter data. This Test Plan/Procedures document describes events associated only with the calibration and clutter data collection portion of these flights. It is assumed that ERIM will perform similar planning for crew training and measurement system validation and that the system has satisfactorily passed these tests prior to clutter data collection.

Approximately 12 hours of flight time are available for Phase 1. Collection of limited clutter data will utilize about three (3) hours of this time.

Test Plans/Procedures for the more extensive Phase 2 clutter data collection flights scheduled for late 1988 and early 1989 will be prepared at a future date when lessons learned from the Phase 1

measurements can be included.

2.0 DATA COLLECTION OBJECTIVES

The objectives of Phase 1 CMP clutter data collection are:

1. Demonstrate Active Radar Calibrator (ARC) signal acquisition in a realistic clutter environment
2. Collect near-simultaneous monostatic and bistatic clutter data characteristic of relatively well-behaved terrain.

The first objective is a result of concern with multipath effects on ARC calibration as well as the detectability of the ARC signal in the presence of strong clutter returns. The second objective will provide limited clutter data for validation of processing and analysis software. It should be noted that terrain for Phase 1 clutter data collection has been chosen to support the overall objective of system validation and not necessarily for HBR relevance.

3.0 PARTICIPANTS

Participants and responsibilities during Phase 1 CMP data collection efforts are shown in Table 3-1.

Table 3-1 Phase 1 Participants and Responsibilities

ORGANIZATION	RESPONSIBILITY
ERIM	CV-580 flight crew and radar operator
	P-3 radar operator
	UHF beacon positioning team
	ARC positioning team
SRS TECHNOLOGIES	Ground truth collection team
	Flight test support personnel
US NAVY	P-3 Flight crew
RADC/DARPA	Experiment Support

4.0 PHASE 1 MISSION PLAN

The purpose of this section is to provide specific functional requirements for the limited clutter data collection of the Phase 1 flights. Approximately three (3) hours out of a total of 12 hours are available to accomplish the objectives stated in the previous section. As stated previously, the following test procedures are contingent on the successful achievement of ERIM pilot and crew training and system validation tests.

Figure 4-1 shows a schedule of events necessary for collection of clutter data. These events include (1) survey of UHF beacon sites and ARC sites, (2) ERIM's system validation flights for crew training and system checkout, (3) limited calibrated clutter data collection, and (4) contingency time. Also shown are Ground Truth measurement events including (5) surface height and slope measurements (6) terrain geological characteristics determination, and (7) terrain electrical properties measurement.

4.1 CLUTTER DATA COLLECTION TEST CASE DESCRIPTION

The clutter data collection geometry selected for Phase 1 is defined in Table 4-1. This geometry does not correspond to any of the 16 Hybrid Bistatic Radar (HBR) scenarios proposed earlier in the program. Instead, it was chosen to eliminate multipath degradation on ARC calibration signals which would otherwise complicate validation of data processing and analysis software. In addition, the large grazing angles virtually eliminate antenna sidelobe problems. The transmitter aircraft has been lowered from 12,000 feet to 10,000 feet so its crew will not require oxygen. The receiver aircraft's altitude has been raised from 1,300 feet to 4,000 feet to reduce turbulence and hazards associated with low altitude flight.

In addition, only one side of the "race track" pattern for each aircraft will be used for data collection. This will reduce the amount of time available for data acquisition, but the resulting reduction of pilot workload and simplification of air and ground test procedures justifies this decision. Thus, the pilot's will only have to accurately enter and fly one side of the race track.

As the two aircraft proceed in parallel directions along their respective race tracks, the pilots can imagine that they are dragging (skimming) a board along the ground between them that is equal in length to their lateral separation distance (26,000 feet) and about 1500 feet wide. This board is the region

TASK \ DAY	1	2	3	4	5	6	7	8	9	10	11	12
SURVEY UHF BEACON SITES	█											
SURVEY ARC SITES		█										
SETUP UHF BEACONS AND ARCS				█								
SYSTEM VALIDATION FLIGHTS					█							
LIMITED DATA COLLECTION FLIGHTS									█			
CONTINGENCY OPERATIONS										█		
GROUND TRUTH SURFACE HEIGHT MEASUREMENTS	█											
TERRAIN GEOLOGICAL CHARACTERISTICS RECORDING				█								
TERRAIN ELECTRICAL PROPERTIES MEAS.										█		

Figure 4-1 Phase 1 Data Collection Schedule

Table 4-1 Limited Calibrated Clutter Data Collection Geometry

PARAMETER	DESCRIPTION
Transmitter Grazing Angle	30 degrees
Receiver Grazing Angle	25 degrees
Bistatic angle	125 degrees
Out-of-Plane Angle	0 degrees
Aircraft lateral separation during pass	25,898 ft
Aircraft speed	220 Knots
Flight Path	Half Race track
P-3 (transmitter) altitude	10,000 feet
CV-580 (receiver) altitude	4,000 feet

over which the system is measuring ground clutter at any instant in time.

4.2 COLLECTION PROCEDURES

According to ERIM convention, a single aircraft flight is called a mission. Within each mission are individual data collection passes. The aircraft paths are determined by four waypoints for each aircraft pass. The first waypoint is the FROM waypoint. The FROM waypoints are selected far from the start of the data collection to aid in coordination of P-3 and CV-580 flight paths and timing. Each aircraft will try to arrive at the FROM waypoint at the same time and on the proper heading but this is not critical. The next waypoint or LINEUP waypoint is the first point where exact synchronization is attempted. During the next 12 NMi, the aircraft are stabilized on the desired flight paths and relative positions achieved so that data collection can begin. Data collection is initiated at the START DATA COLLECTION waypoints. Data is collected for 5 minutes (about 18 NMi) until the aircraft pass over the END DATA COLLECTION

waypoints. After data collection for this pass has been completed, the aircraft return to the FROM waypoints and repeat the process. The data collection passes are continued until available time is exhausted. Each pass (i.e., a full circuit of the race track) will take about 25 minutes. The number of data collection passes will be limited by the time available for data collection and will have to be determined during the data collection period. A minimum of two (2) passes is recommended. The Phase 1 data collection pass definition is illustrated in Figure 4-2.

4.3 MISSION SITE DEFINITION

Preliminary site studies indicate that a region to the northwest of Ann Arbor, Michigan would be suitable for Phase 1 data collection. The SYSTEM REFERENCE POINT of Figure 4-2 is located at 84 deg. 12 min. West longitude and 42 deg. 25 min. North latitude. The data collection ground tracks are due North of this point. It appears that this area is relatively uninhabited and fairly flat.

Topographic quadrangle maps are available from the Department of the Interior, U.S. Geological Survey National Cartographic Information Center (NCIC). Maps in 7.5 x 7.5 minute blocks (1 inch = 2000 feet) surrounding this area are DANSVILLE, MILLVILLE, PARKERS CORNERS, PLEASANT LAKE, STOCKBRIDGE, GREGORY, GILLITTE, GRASS LAKE, AND CHELSEA. Based on information received from NCIC dated 1 July 1986, Digital Elevation Model (DEM) data for these quadrangles is not available. However, by the time Phase 1 starts, digital data may be available.

Accuracy of the topographical maps is based on a standard that no more than 10 percent of well-defined test points are more than 40 feet in error. Similarly, vertical accuracy standards require that no more than 10 percent of the elevations of test points interpolated from contours shall be in error by more than half the contour interval.

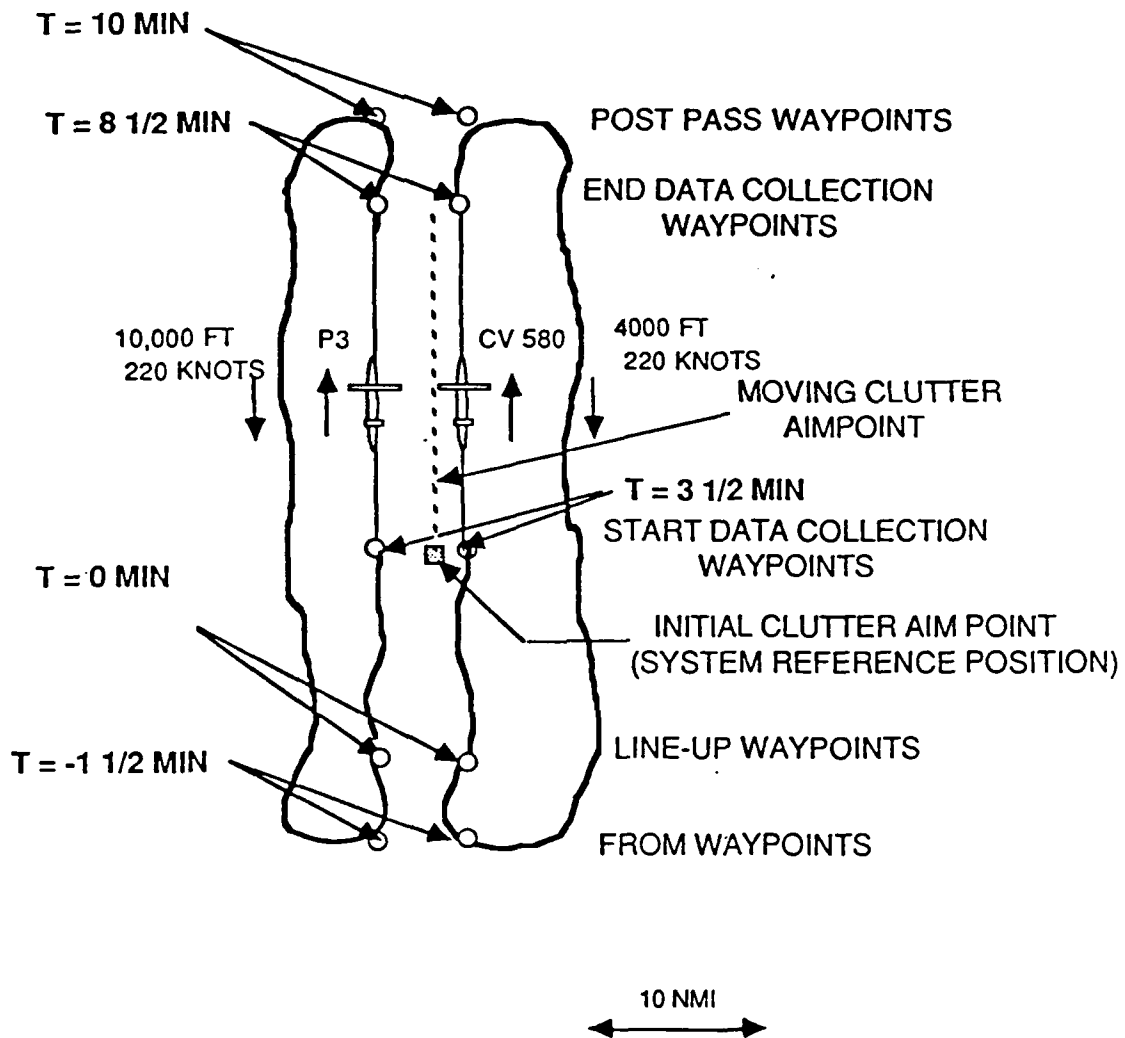


Figure 4-2 Phase 1 Data Collection Pass Definition

5.0 COMMUNICATIONS PLAN

Each aircraft should be in contact with Air Traffic Control (ATC) during this mission and receiving radar advisories. The data collection area is within 20 Nmi of Jackson and Lansing airports. It is about 40 Nmi from Detroit Metro airport.

The P-3 and CV 580 pilots will be in radio contact at a suitable VHF/UHF frequency. Minimal use of this communications link is suggested to prevent interference with data collected. In addition, a digital RF data link between the two aircraft can be used to relay messages. The latter link is used to relay CV-580 data to the P-3 data recording system.

6.0 GROUND SUPPORT ACTIVITIES

Ground support activities are a vital element of the Phase 1 data collection effort. Ground support includes ARC beacon positioning, UHF position beacon location, and ground truth measurements. ERIM will perform the first two activities and SRS the latter.

6.1 ARC BEACON POSITIONING

Active Radar Calibrators (ARC's) are necessary for calibration of received clutter data and to provide calibration compensation during data reduction for aircraft position uncertainty induced effects. Five ARC's shall be placed on the dashed line shown in Figure 4-1 (the ground trace of the antenna aim points) at approximately 4.5 NMI intervals (Actual ARC spacing will be dependent on the number of ARCs available and must be determined during the experiment). The position of each ARC shall be determined with respect to the SYSTEM REFERENCE POSITION within 10 feet.

The receive antenna of each bistatic ARC shall be oriented 30 degrees above the horizontal. The bistatic ARC transmit antenna shall be oriented 25 degrees above the horizontal. The ARC bistatic receive antenna shall be pointed in azimuth so that it will be illuminated by the CV 580. The ARC bistatic transmit antenna shall be oriented in azimuth so it will illuminate the P-3 as it passes by.

The monostatic ARC transmit and receive antennas shall be oriented broadside to the P-3 at its point of closest approach at elevation angles of 25 degrees.

6.2 UHF POSITIONING BEACON INSTALLATION

ERIM shall be responsible for locating the UHF beacons within the data collection area to provide optimum aircraft location data.

6.3 GROUND TRUTH DATA COLLECTION

There are three types of ground truth data for collection by SRS Technologies personnel. These are terrain (1) surface roughness and slope data, (2) geological characteristics, and (3) electrical characteristics. Items 1 and 2 can be obtained prior to the flight tests when convenient since they are not expected

to change within the short duration of the Phase 1 measurements. However, since item 3 can be seriously affected by the moisture content of the ground, these measurements shall be made shortly before or after the data collection passes.

6.3.1 Surface Roughness Data

Surface height data along the terrain "swept" by the two aircraft is required for model validation. This shall be accomplished by an acoustic sensor mounted on a horizontal track. The data from this sensor shall be converted to digital words and stored on magnetic media for later analysis. Logistical considerations limit the amount of terrain which can be measured in this manner. However, it is recommended that surface height data be measured along two orthogonal axes; the first in the north-south direction and the second in the east-west direction. The length of the data collection area is about 18 NMI. The orthogonal measurements should be made at the beginning, middle and end of the data collection aimpoint ground track (i.e., about 9 NMI apart). The length of each axis should be on the order of 30 feet and the altitude and position of the grid accurately determined and recorded.

This data can be augmented by limited surface height measurements with a contour gauge marketed under various trade names such as "Formit." This tool consists of a row of wires held in place by friction by two plates. When the row ends are pressed against an irregular surface, the individual wires will adjust to reproduce the irregular contour form. The surface roughness can be transferred by tracing the contour with a pencil on a piece of paper.

6.3.2 Surface Slopes

Surface slope data can be extracted from the surface height data described in paragraph 6.3.1 but is limited by the length of the grid axes. Thus, visual estimates (magnitudes, directions and gradients) in the field will be needed. This data will be supplemented by topographical map information during data processing.

6.3.3 Terrain Geological Characteristics

6.3.3.1 Layering

At L-band frequencies, penetration of the surface can occur up to several wavelengths depending on the moisture content and composition of the soil. Thus, a systematic measurement of layering is needed to determine this factor's importance to scattering. Foilage type and density above the soil should be noted at each of the surface roughness measurement sites. Similarly, ice or snow covering should be described. A tubular soil sampler (e.g., Lord Model 225) can be inserted into the ground and visual determination of soil profiles made. The presence of significant layering and interface roughness estimates should be made.

6.3.4 Terrain Electrical Properties

The most important electrical parameter affecting terrain scattering is the complex dielectric constant (permittivity) which is largely a function of soil moisture. To avoid the use of soil mixture models and water content measurements, direct measurement of the local surface (and subsurface) complex permittivity will be made. This will be accomplished at the surface roughness measurement sites and shall be done at the surface and beneath the surface. A permittivity measurement device available from Applied Microwave Corporation (AMC) is recommended for this task. The sensor head is simply pressed against the surface to be measured and the real and imaginary parts of the dielectric constant recorded. Subsurface measurements are made in the same manner except that the head is lowered into holes drilled by the soil sampler at various depths. Samples at one foot inch intervals down to 3 feet should be adequate.

Since this device is portable and surface measurements easily performed, additional sites should be examined as time permits.

6.4 Video Recording

A VHS video recording of the test area should be made within two hours of the data collection flights. This recording should include the clutter aim point and areas approximately 0.5 Nmi to either side. Any unusual geological features, surface cover, topology, or man-made features should be recorded and their locations accurately measured.

7.0 MISSION DESCRIPTION

The Phase 1 mission is primarily designed to train pilots and radar operators, validate data collection system performance, and collect limited clutter data. The following paragraphs describe the latter objective of Phase 1, namely, limited data collection. The Phase 1 data collection activity will require close coordination of the flight paths of the Navy P-3 and ERIM CV 580 aircraft. As mentioned previously, the mission will be conducted northwest of Ann Arbor, Michigan.

In addition to these aircraft, positioning beacons, radar calibration repeaters, ground truth instrumentation, and supporting personnel will be required on the ground.

7.1 DATA GOALS

Near simultaneous collection of calibrated bistatic and monostatic ground clutter data at L-band frequencies over a limited geographical area is desired. The ERIM CV-580 acts as the transmitter for the bistatic system while the Navy P-3 acts as the bistatic receiver. The Navy P-3 also interleaves transmitted pulses between the bistatic radar transmissions and receives their echos to act as the monostatic radar.

The geometry of the mission has been selected so that Active Radar Calibrators (ARC's) along the mission aim point ground path will be in the field-of-view of each radar system and provide accurate calibration information. Also located in the data collection area are UHF beacons which are used by processors on board each aircraft to determine relative position and provide this information visually to the pilots.

7.2 MISSION PLAN

The flight profile for Phase 1 clutter data acquisition is shown in Figure 7-1 superimposed over the desired test area. It is anticipated that the ERIM CV-580 and Navy P-3 will take off from the Ann Arbor airport at approximately the same time and rendezvous in the vicinity of the FROM waypoints. Since video recording of terrain examined is desired, this mission shall be conducted when Visual Flight Rules (VFR) are in effect over the test area. Radar systems on board each aircraft will be turned on and checked out during this time. Flight time from Ann Arbor to the FROM waypoints will be about 15 minutes. Communication

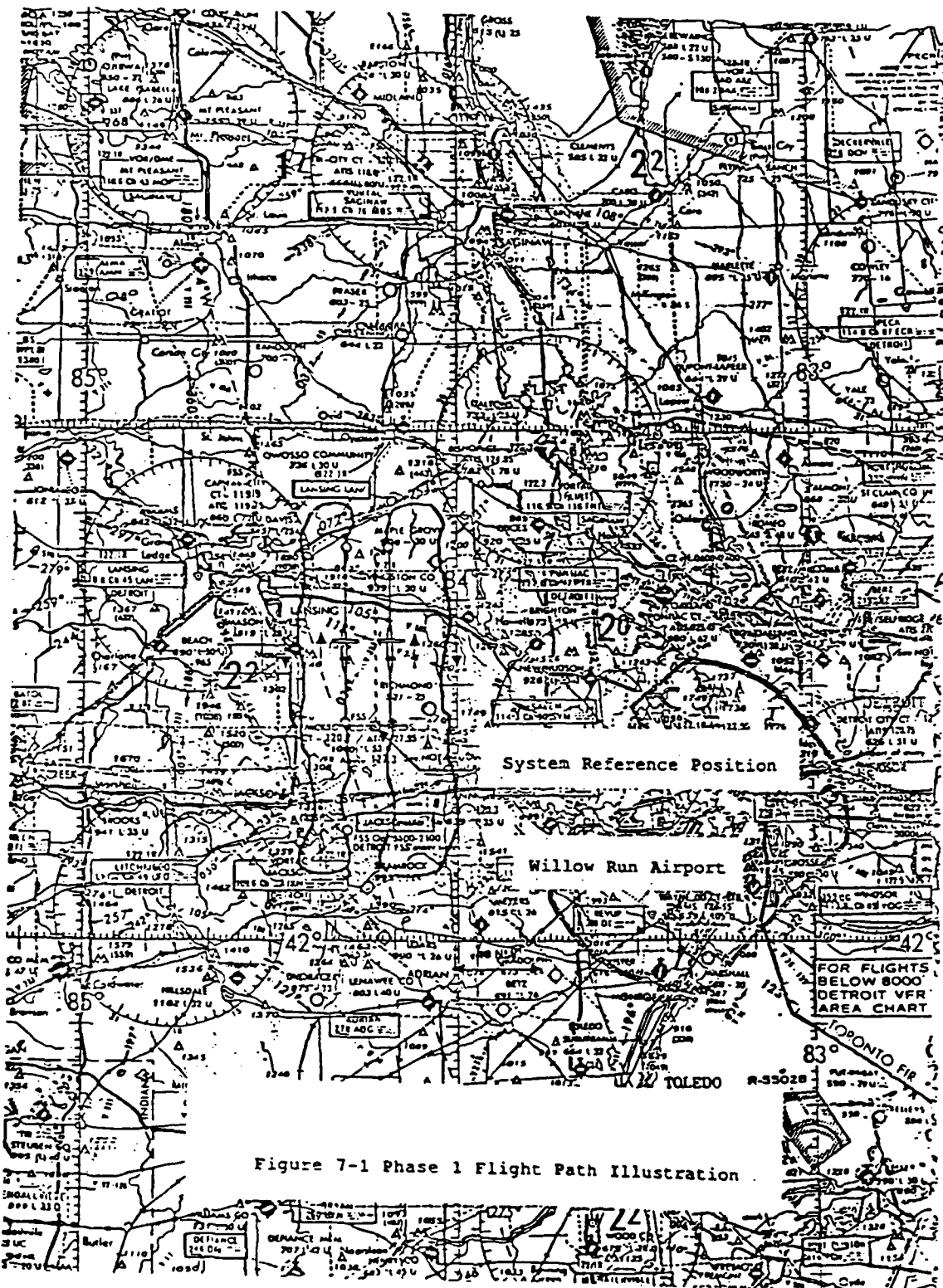


Figure 7-1 Phase 1 Flight Path Illustration

with Air Traffic Control (ATC) by both aircraft will be made requesting radar advisory service for safety purposes. Aircraft will squawk Mode C (altitude encoding) unless these transmissions interfere with data collection.

The two aircraft will then fly the pass as described in Section 4.2 and collect calibrated clutter data.

8.0 WAYPOINT DESCRIPTIONS

Waypoint information will be computed by the on-board computer prior to the pass and provided to the pilots by the radar operator.

9.0 CONTINGENCY PLANNING

The primary concern during this mission is weather effects on flight safety and data collection. Flight safety is the most important priority with collection of clutter data secondary. Consequently, this mission should be undertaken only during good weather conditions. This means VFR conditions shall prevail in the general test area. Wind and turbulence effects on aircraft performance at altitude shall be minimal. A successful mission requires both aircraft to be operating properly.

9.1 BAD WEATHER ALOFT

Bad weather in the test area is sufficient reason to cancel the data collection flight. The only available contingency in this event is to postpone the flight until weather improves.

9.2 AIRCRAFT INOPERATIVE

In the event the CV-580 aircraft or the bistatic transmitter equipment is inoperative, two contingency events are possible. First, the mission can be postponed until the problems are resolved. Secondly, should the former be impossible, The P-3 will fly as planned and only monostatic radar clutter data collected.

If the P-3 aircraft or on-board data collection equipment is inoperative, the mission must be postponed until it is repaired.

point of ground contact is near -2 range gates. The bistatic range at the aimpoint is 14.73 kft, thus requiring a signal travel time of approximately 14,968 ns. The maximum clutter power is approximately +55 dBsm near 0 range gates. The system noise threshold lies at -22.3 dBsm with doppler processing and -5.32 dBsm without doppler processing. Of the subsequent plots, the VRTVV and the SRTVV model show the smallest increase in expected signal compared to the physical area, with a maximum clutter power of +61 dBsm at 0 range gates for both models. The Active Radar Calibrator (ARC) signal level is at +55 dBsm, which lies at the same level as the beam area signal level and 6 dB below the next best case clutter level.

The expected signal levels for the VRTVV and the SRTVV models are lower when using a large and small scale RMS slope angle of 25 degrees. The maximum clutter powers are +50 dBsm near 0 range gates for both models. This places the ARC signal level 5 dB above the VRTVV and SRTVV model signal levels.

The clutter-to-noise (CNR) ratio plots indicate that a regime of good measurement lies between -1 to +3 range gates for accurate clutter measurements.

The aimpoint elevation angles for the transmitter and receiver are as follows:

Transmitter: $\Theta_{1} = 4.87$ degrees; $\Theta_{2} = -4.01$ degrees

Receiver: $\Theta_{1} = -16.14$ degrees; $\Theta_{2} = 5.15$ degrees

The aimpoint arrival relative to direct path is 23.4 range gates. This geometry creates negligible multipath scattering contamination, as indicated by the attached simulation results. The effect of multipath on the

transmitter's signal (30 degree grazing angle, 10,000 ft altitude) is a maximum of .26 dB for positive or negative multipath error contribution to recorded power gains. The effect of multipath on the receiver's signal (25 degree grazing angle, 4,000 ft altitude) is a maximum of .79 dB for positive multipath error contribution or .87 dB for negative multipath error contribution to recorded power gains. These figures assume a 40 degree ARC beamwidth.

TML Pascal

THE TRANSMITTER COORDINATES ARE(M):

(0.0000, -5279.3013, 3048.0060)

THE GRAZING ANGLE = 30.0

THE OUT-OF-PLANE ANGLE = 0.0 DEGREES

THE ARC HEIGHT IS(M): 5.0000

THE APERTURE DIMENSIONS ARE: 0.311 X 0.311 (M X M)

THE SPECULAR REFLECTION POINT IS (M):

(0.0000, -8.7503, 0.0000)

EDF = 0.999999

RACF = 0.030019

THE PATH DIFFERENCE(M) = 5.000163

THE DIRECT PATH POWER GAIN(dB) = -0.000009

THE MULTIPATH POWER GAIN(dB) = -30.459123

THE TOTAL POWER GAIN(dB) = 0.256628

MAXIMUM POSITIVE MULTIPATH ERROR(dB): 0.256628

MAXIMUM NEGATIVE MULTIPATH ERROR(dB): -0.264516

DO YOU WISH TO CHANGE THE ARC BEAMWIDTH?

1=YES,2=NO

TML Pascal

THE RECEIVER COORDINATES ARE(M):

(0.0000, 2614.5871, 1219.2020)

THE GRAZING ANGLE = 25.0

THE OUT-OF-PLANE ANGLE = 0.0 DEGREES

THE ARC HEIGHT IS(M): 5.0000

THE APERTURE DIMENSIONS ARE 0.311 X 0.311 (M X M)

THE SPECULAR REFLECTION POINT IS (M):

(0.0000, 10.7450, 0.0000)

EDF = 0.999999

RACF = 0.096298

THE PATH DIFFERENCE(M) = 4.226211

THE DIRECT PATH POWER GAIN(dB) = -0.000043

THE MULTIPATH POWER GAIN(dB) = -20.940407

THE TOTAL POWER GAIN(dB) = 0.675127

MAXIMUM POSITIVE MULTIPATH ERROR(dB): 0.797457

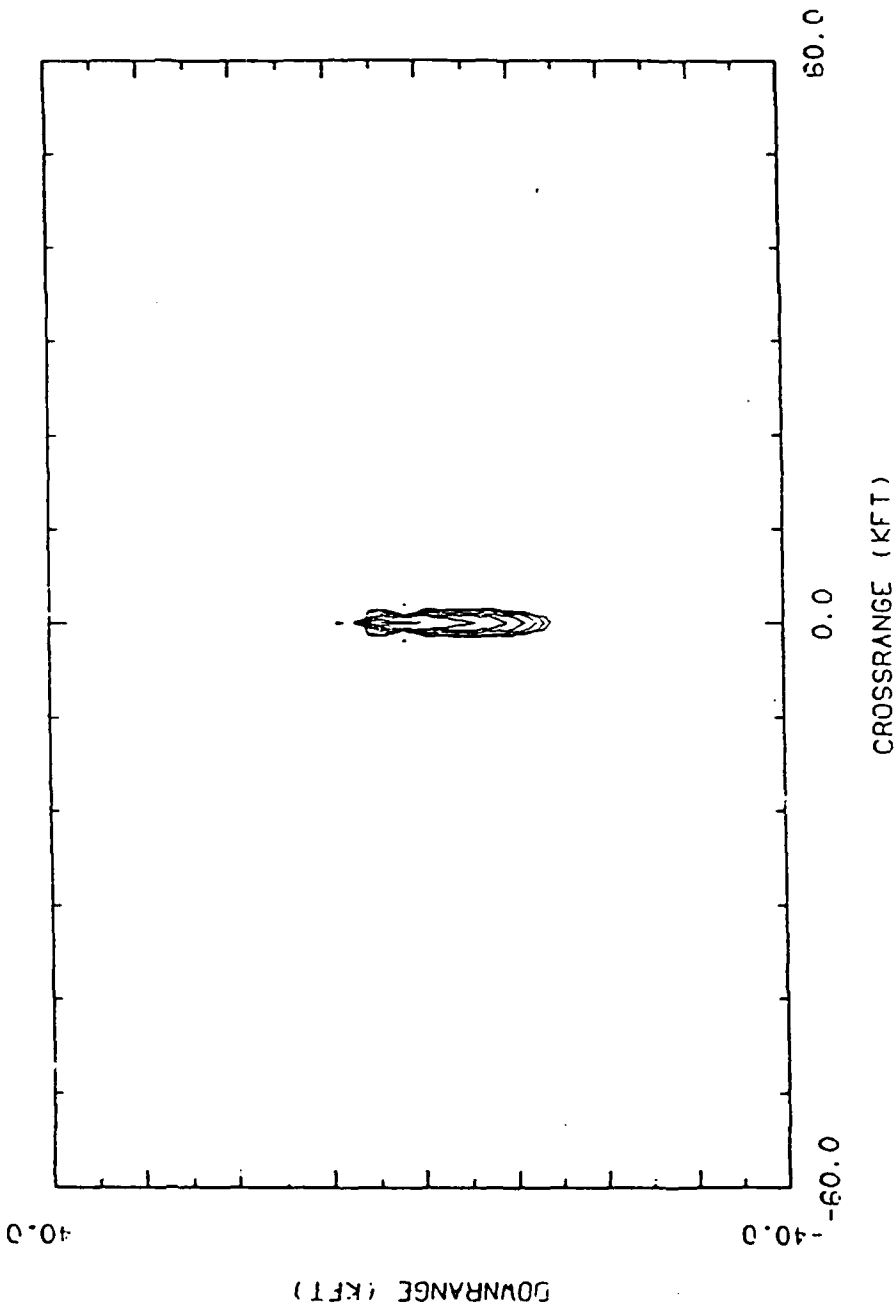
MAXIMUM NEGATIVE MULTIPATH ERROR(dB): -0.278142

DO YOU WISH TO CHANGE THE ARC BEAMWIDTH?

1=YES,2=NO

Bistatic Geometry

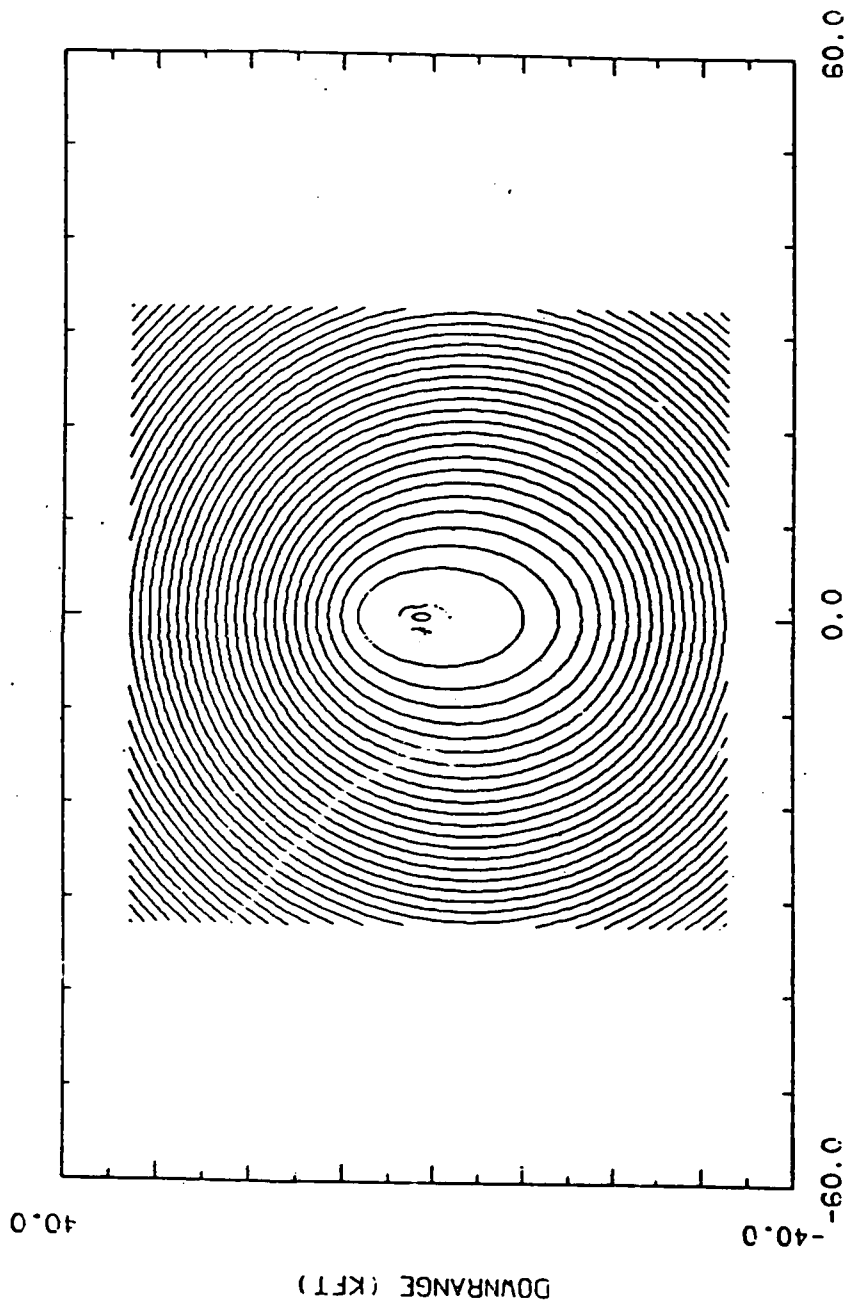
BEAM PATTERN



13:39:45 27-MAY-07

TGA=90.0. T.OPA=0. RGA=25.0. R.OPA= 0.0

BISTATIC RANGE

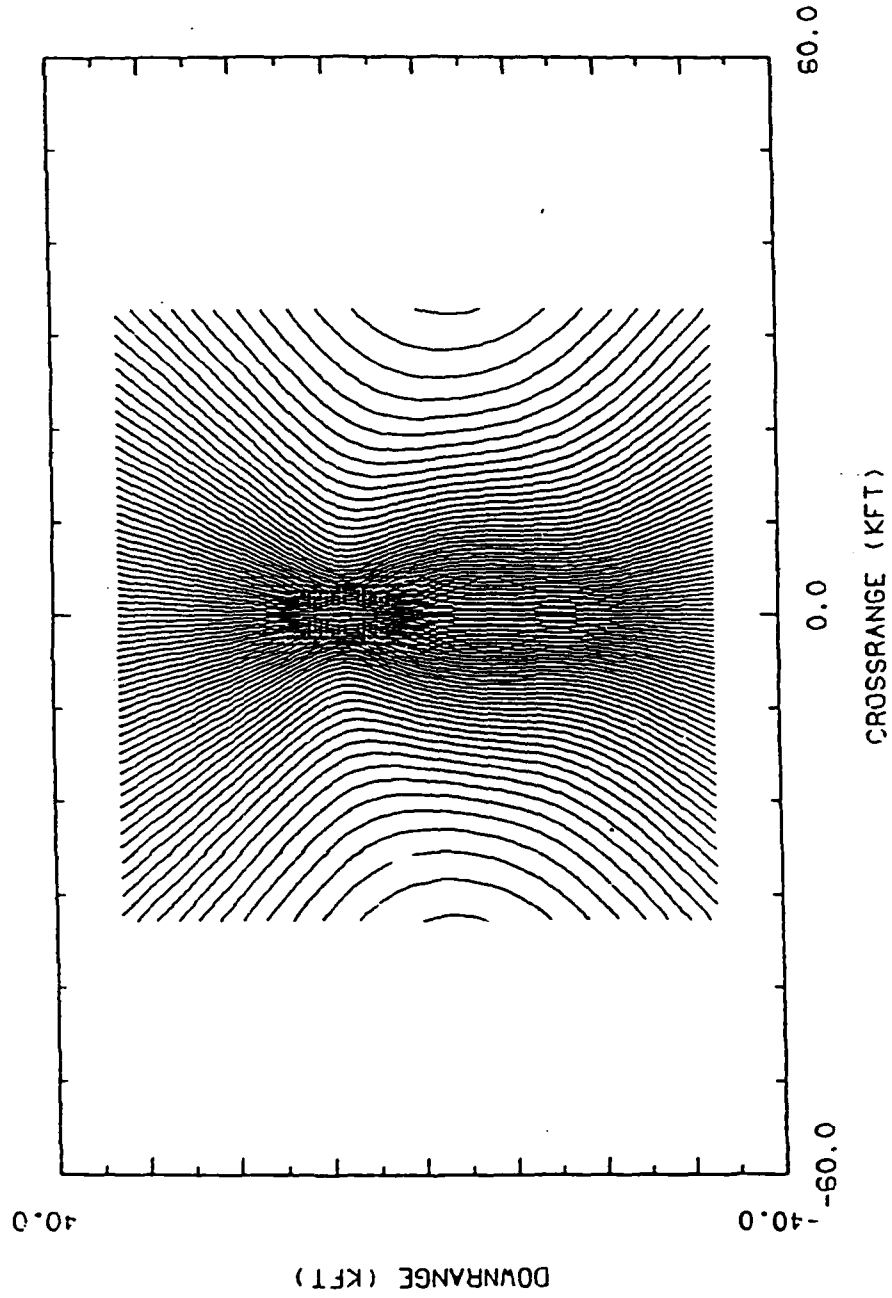


CROSSRANGE (KFT)

TGA=30.0, T.OPA=0, RGA=25.0, R.OPA= 0.0

13:13:50 27-MAY-07

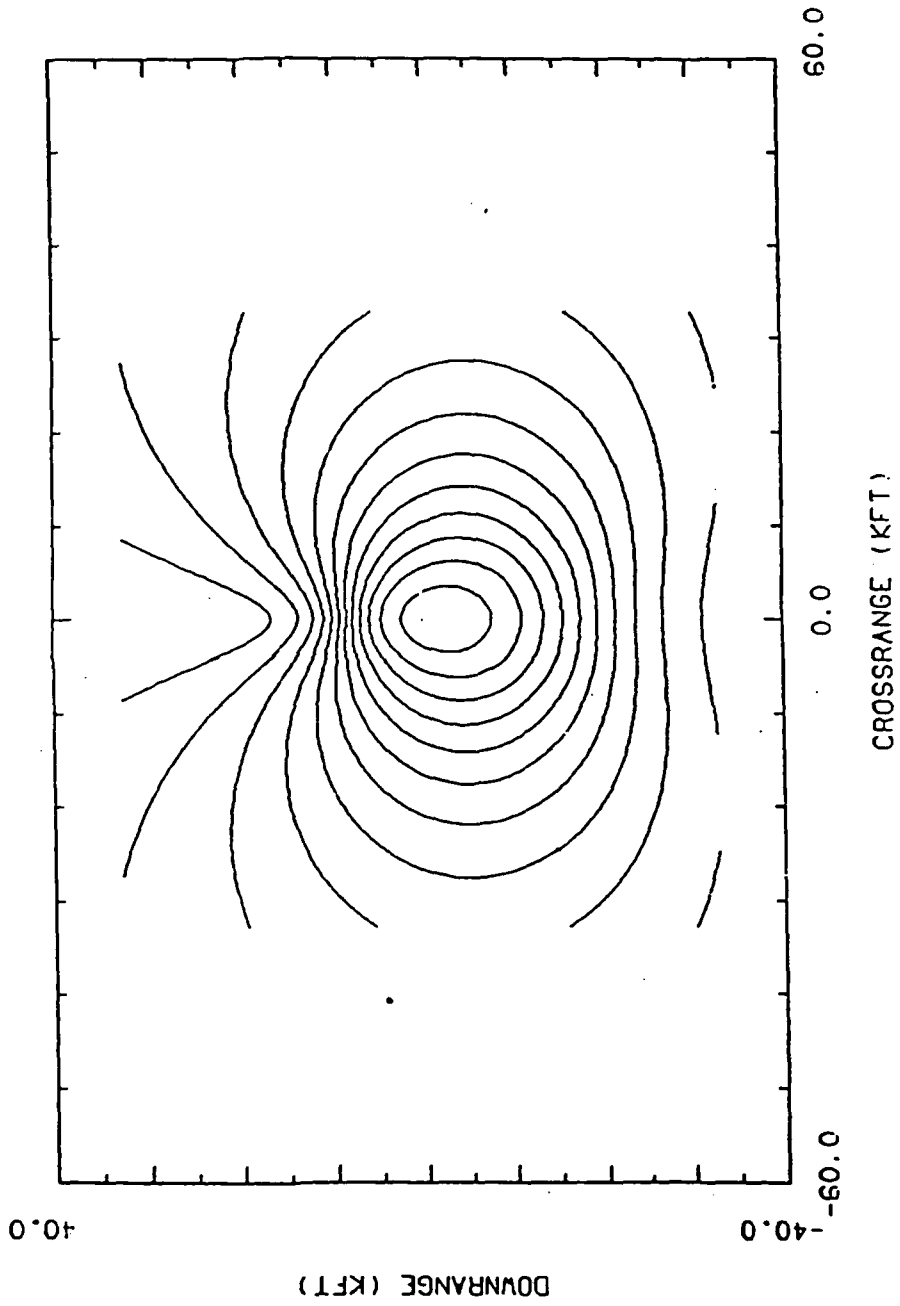
DOPPLER



13:19:15 27-MAY-87

TGA=30.0. T.DPA=0. RGA=25.0. R.DPA= 0.0

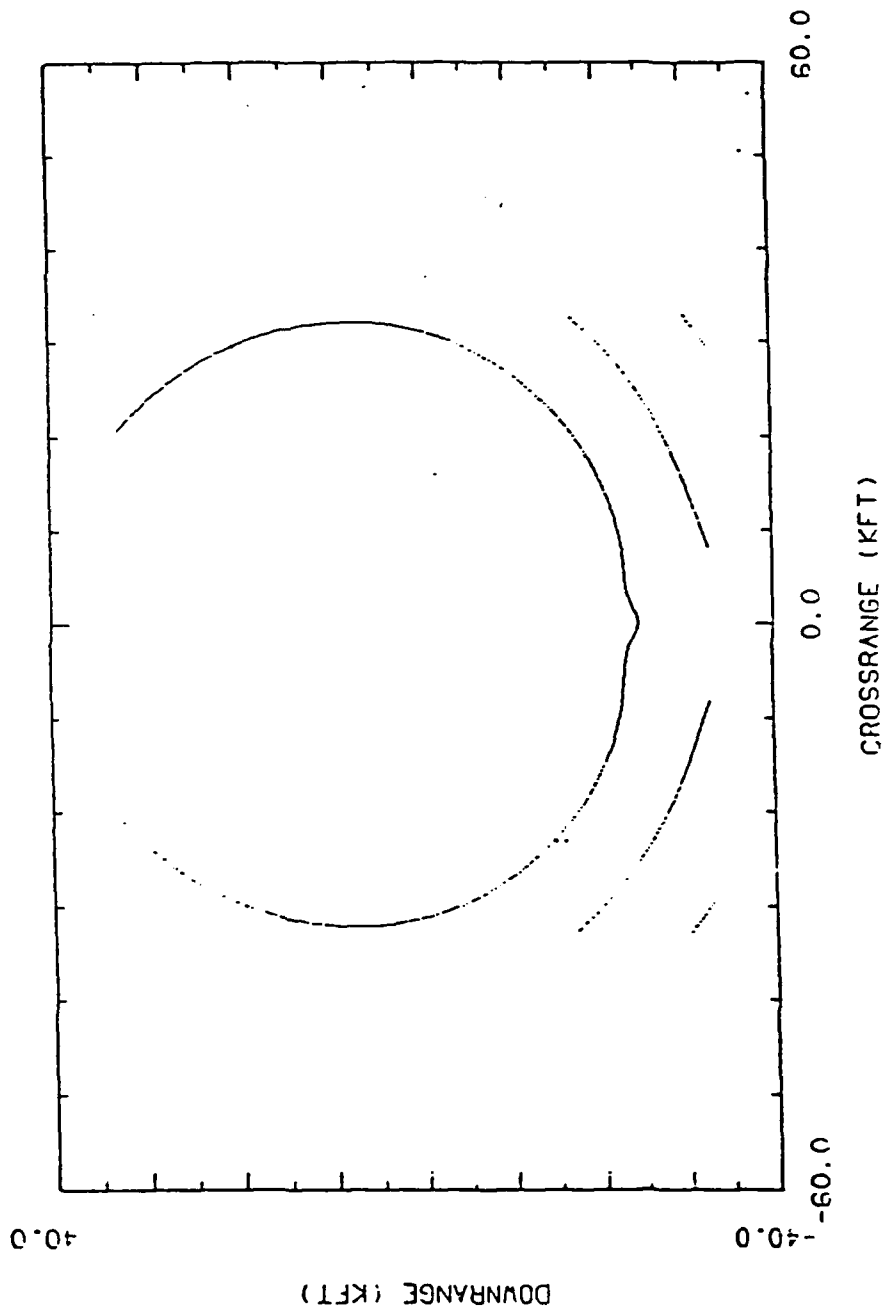
BISTATIC ANGLE



13:29:39 27-MAY-07

TGA=30.0. T.OPA=0. RGA=25.0. R.OPA= 0.0

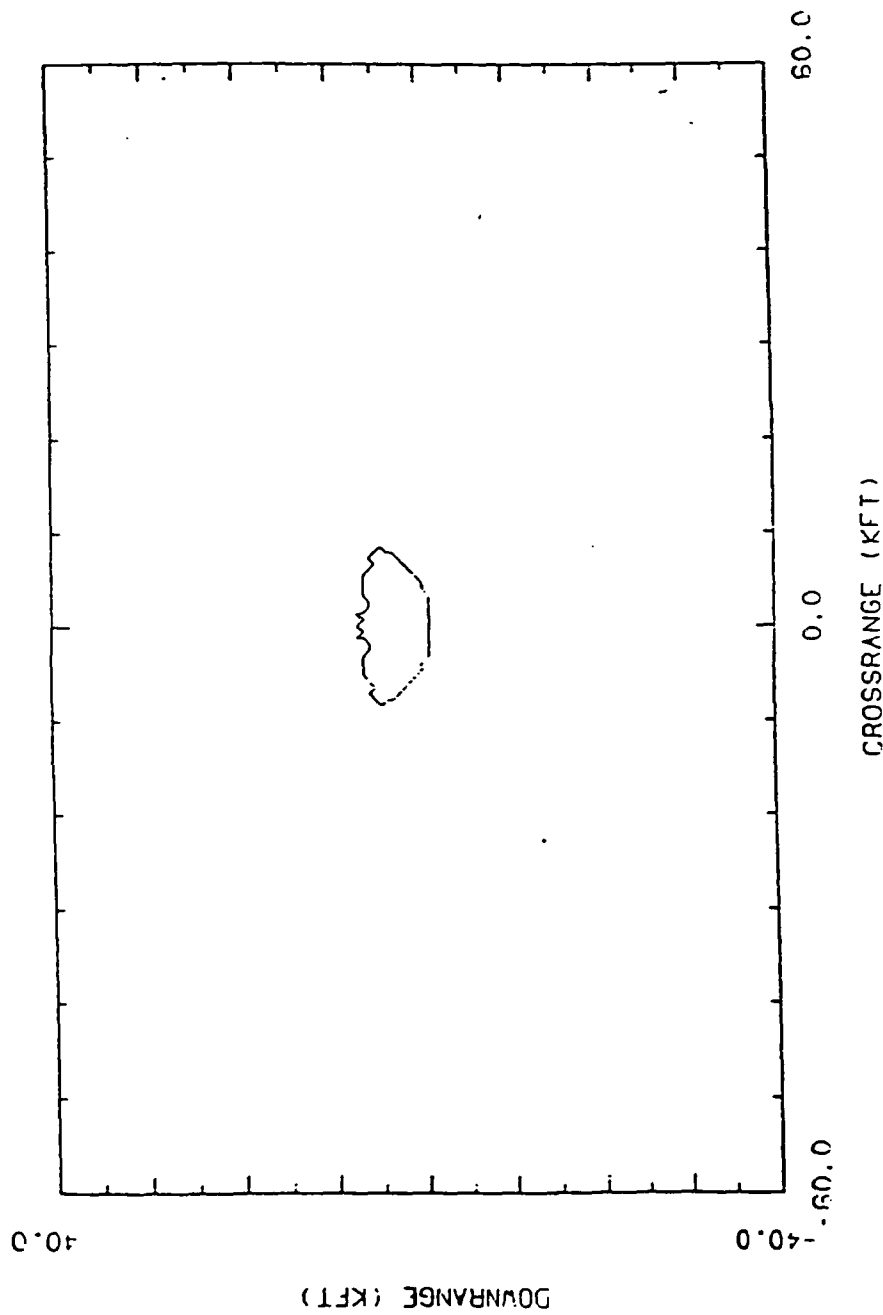
SLIGHTLY ROUGH TERRAIN SHADOWING



14:40:10 27-MAY-87

TCA=30.0. T.OPA=0. MCA=25.0. R.OPA= 0.0

VERY ROUGH TERRAIN SHADOWING

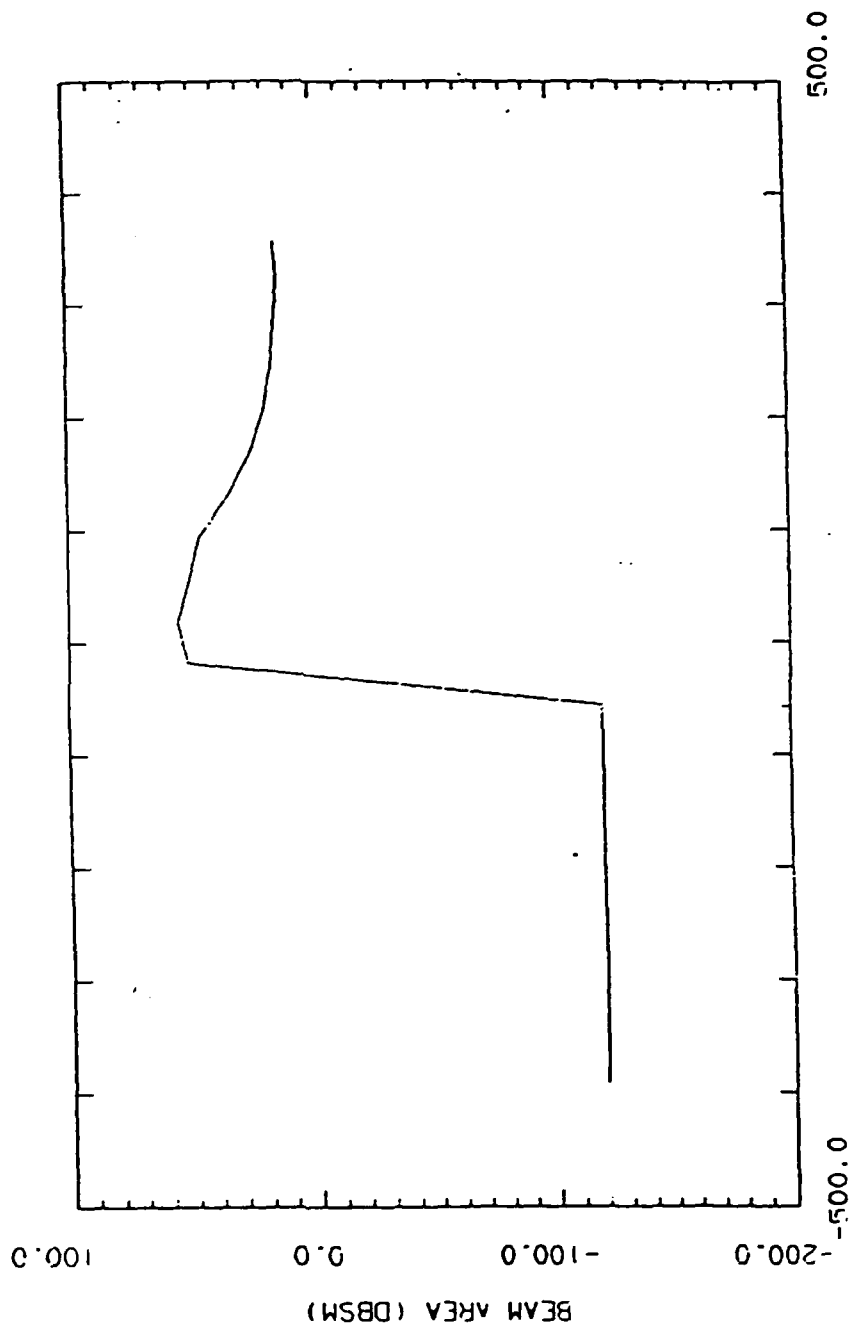


1414105 27-MAY-07

TCA=30.0. T.OPA=0. MGA=25.0. R.OPA= 0.0

THIS PAGE INTENTIONALLY LEFT BLANK.

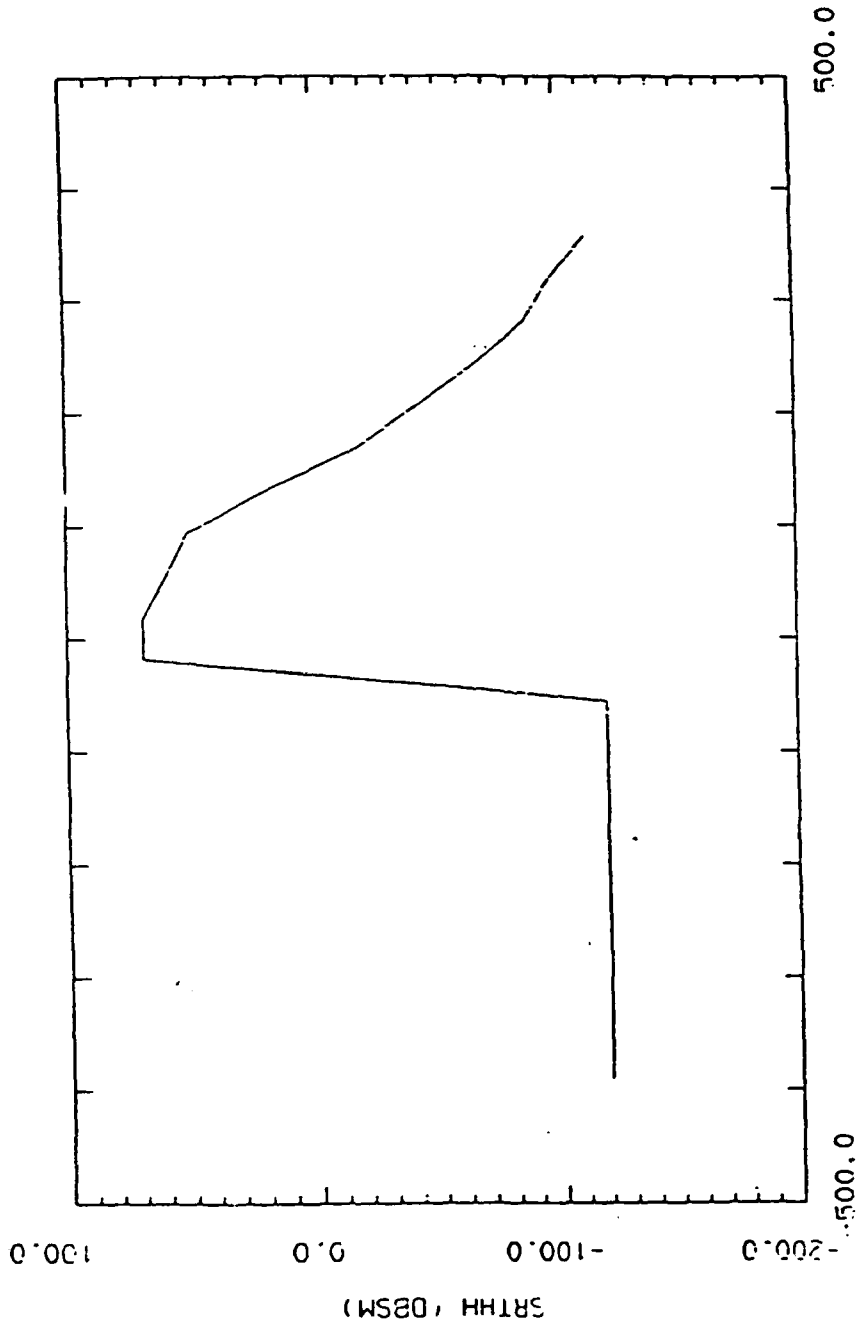
Phenomenology Predictions



BISTATIC RANGE (M)

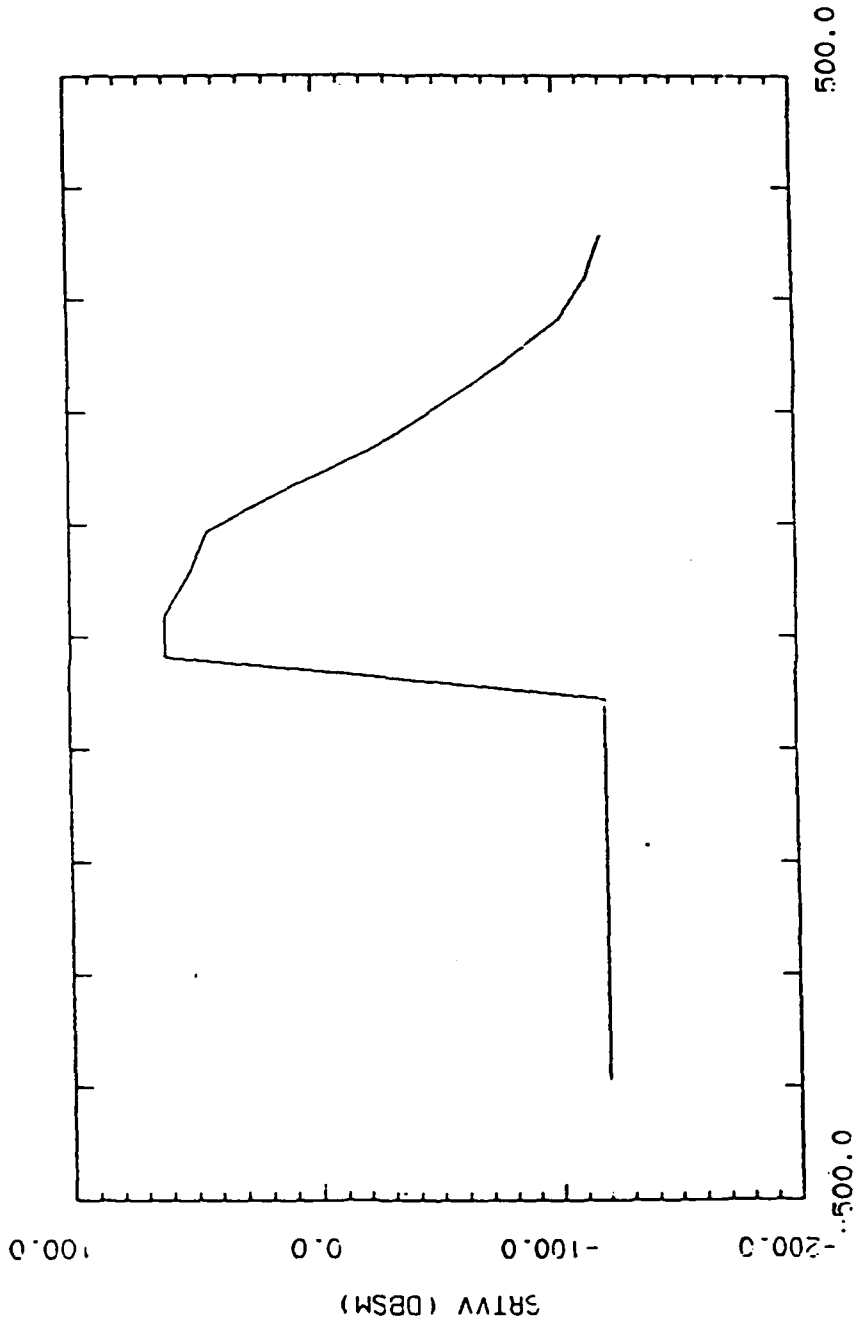
20:34:43 27-MAY-87

TCA=30.0. T.OPA=0. MCA=25.0. R.OPA= 0.0



23:34:50 27-MAY-07

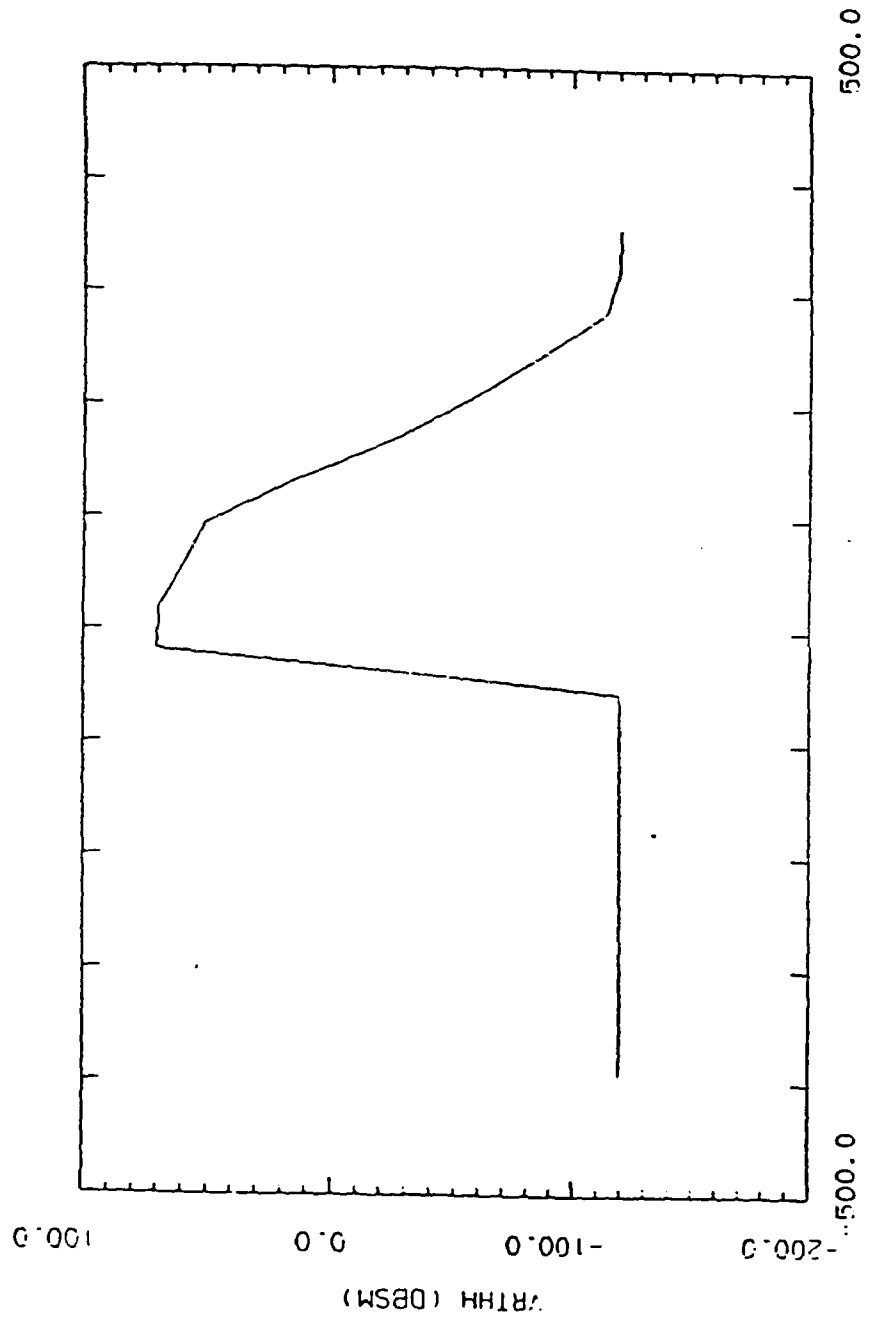
TCR=30.0. I.C.P.A=0. I.R.A=25.0. II.C.P.A= 0.0



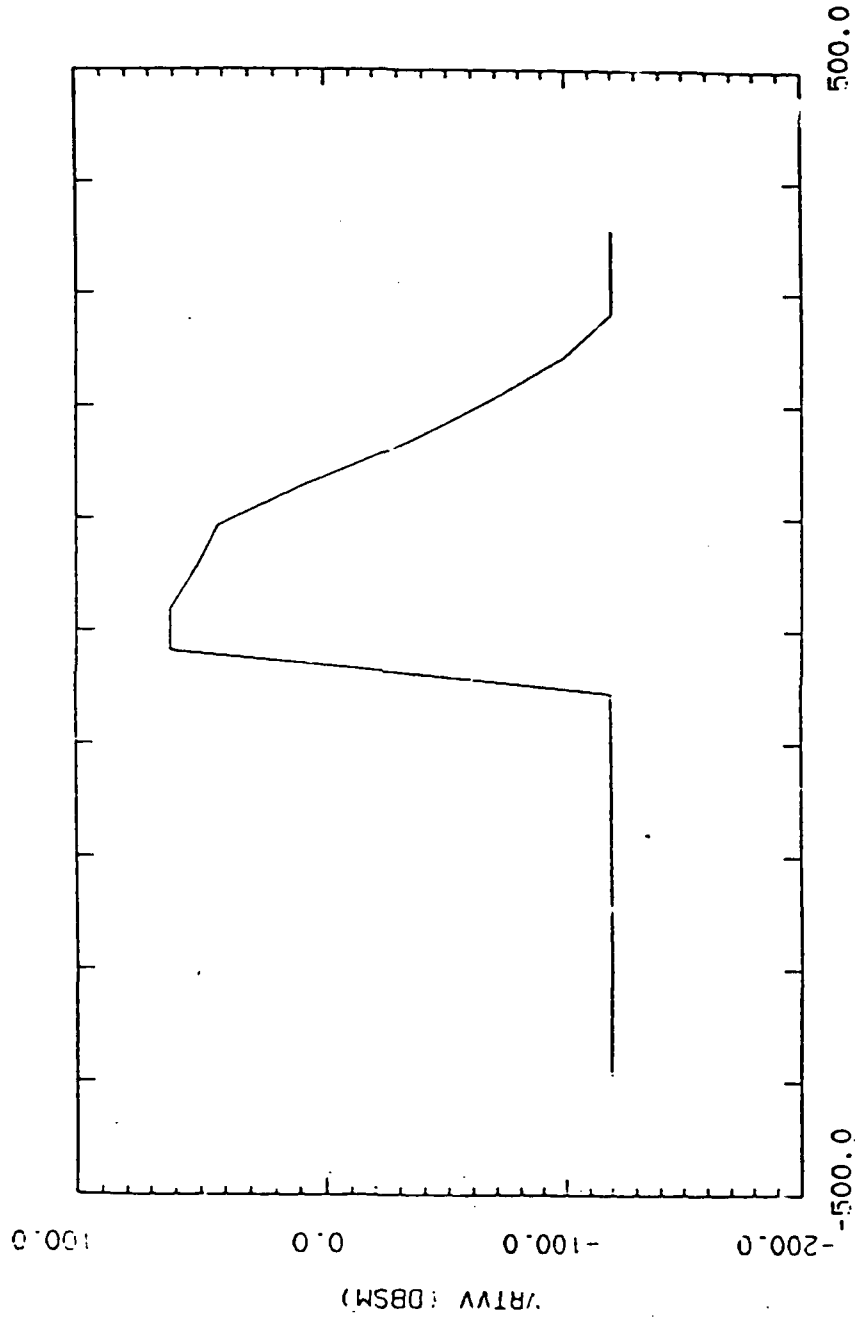
BISTATIC RANGE (M)

20:35:13 27-MAY-87

TCA=30.0, F.OPA=0, RGA=25.0, R.OPA= 0.0



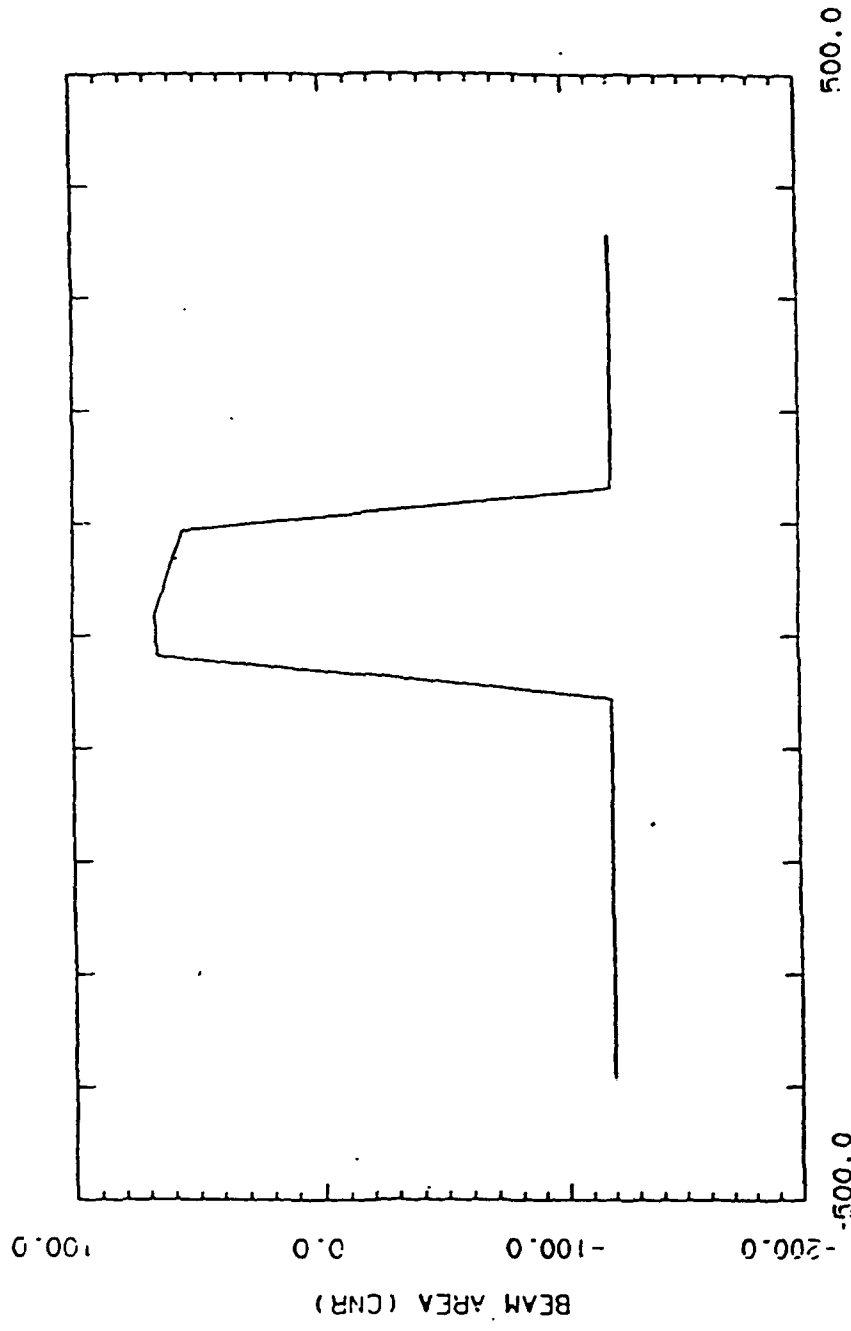
TGA=30.0, T.OPA=0, RGA=25.0, II.OPA= 0.0 23:35:27 27-MAY-07



BISTATIC RANGE (M)

23:35:42 27-MAY-07

TCR=30.0. T.OPA=0. RCR=25.0. R.OPA= 0.0



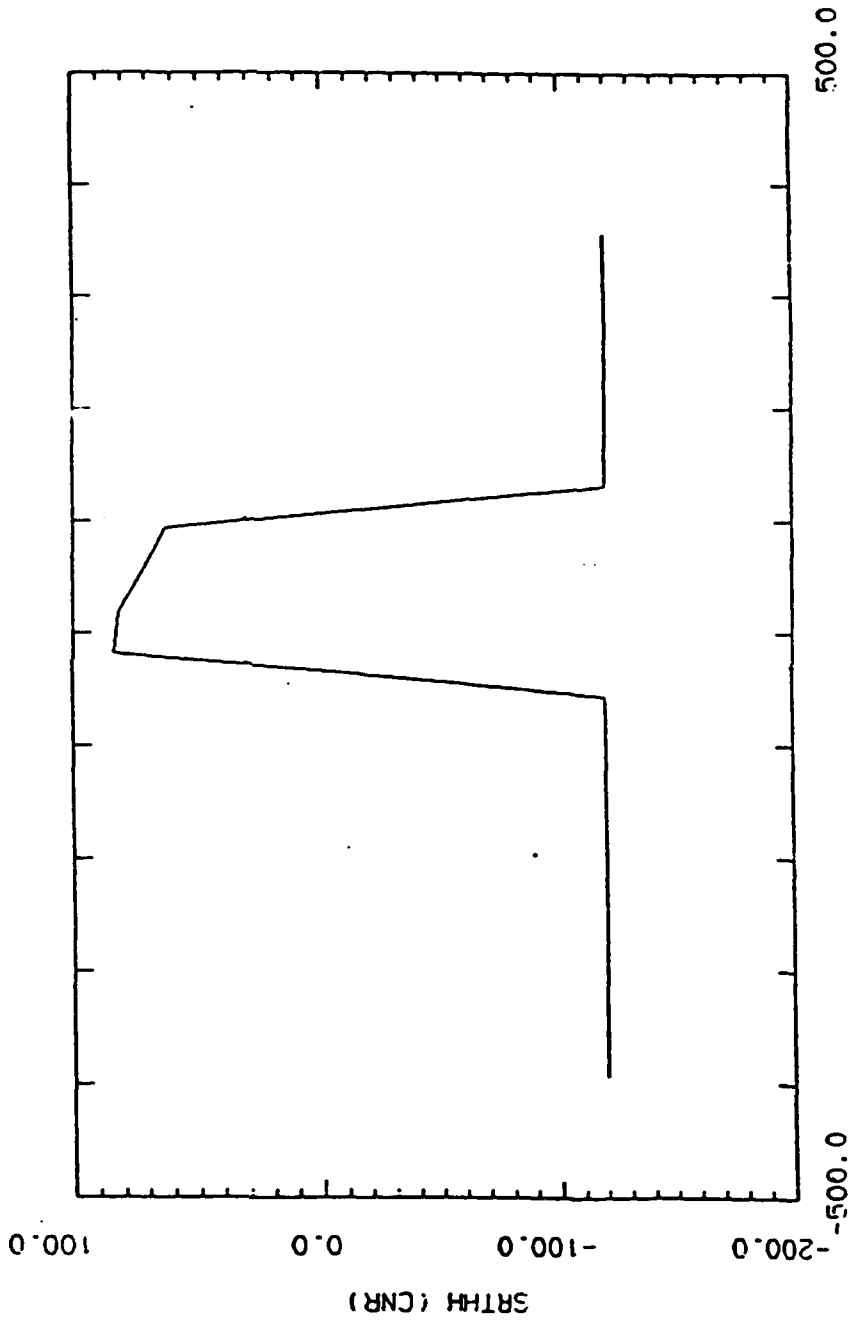
BISTATIC RANGE (M)

23:44:06 27-MAY-07

TGA=00.0. T.CNPA=0. RGA=25.0. R.CNPA= 0.0

Small Scale RMS Slope Angle = 25°

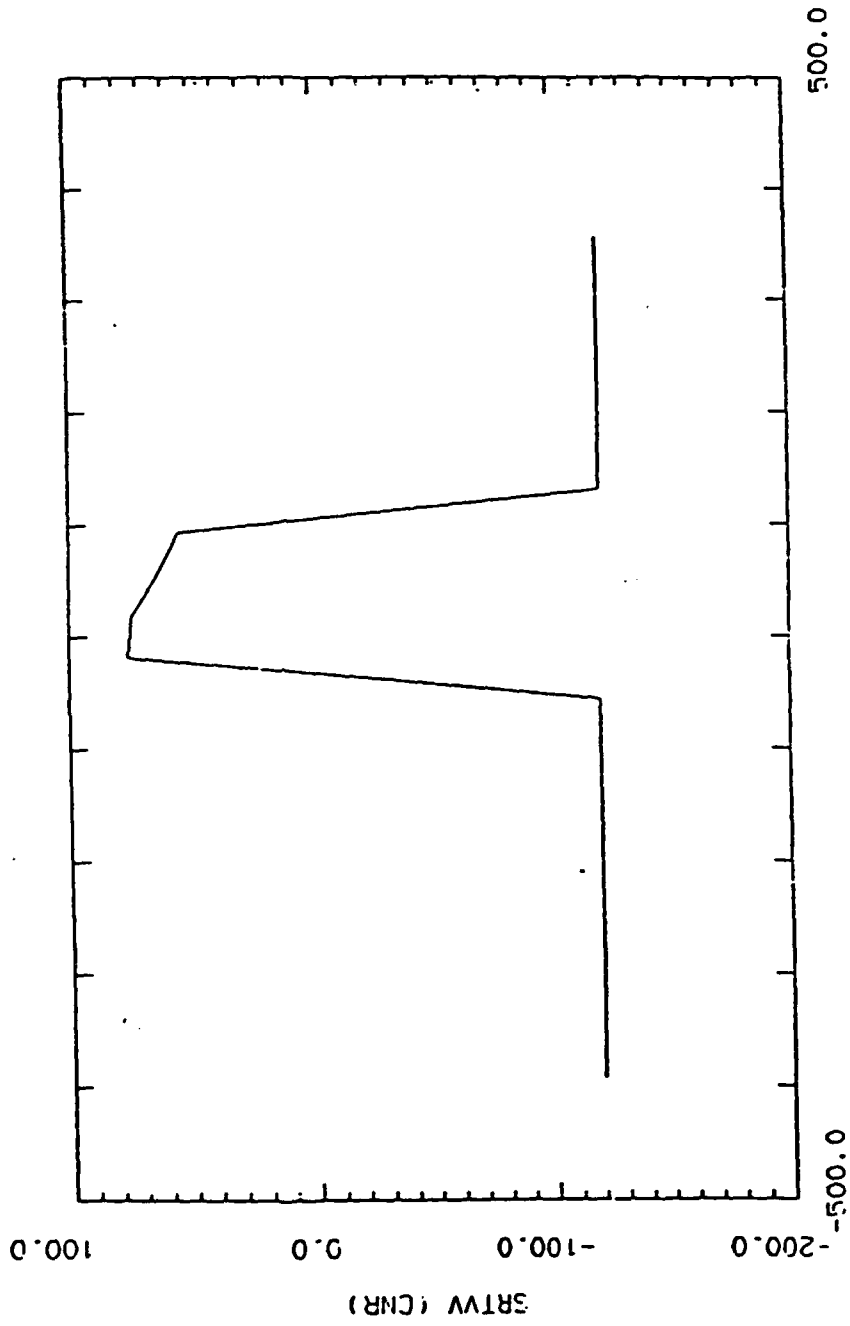
Large Scale RMS Slope Angle = 25°



BISTATIC RANGE (M)

2014121 27-MAY-07

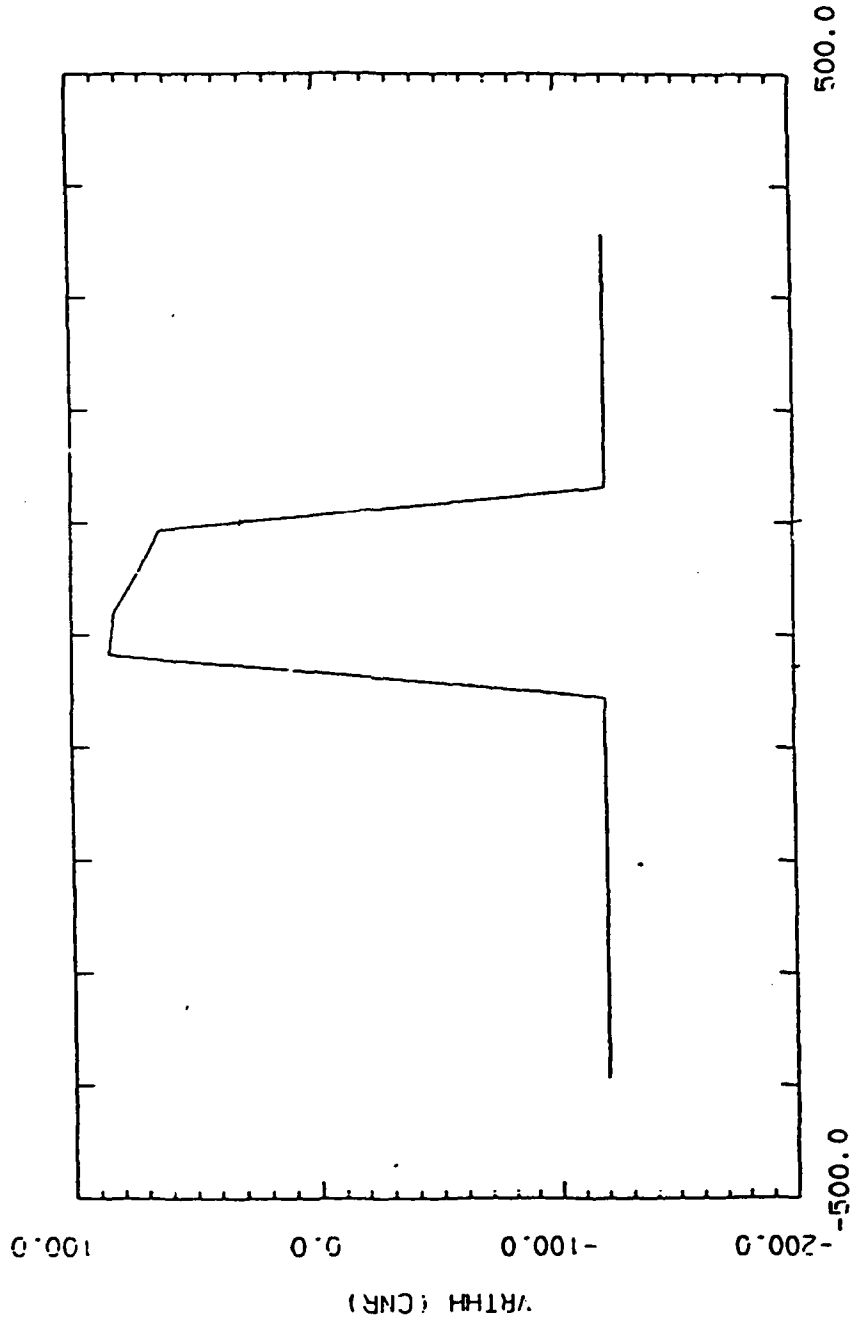
TCA=30.0, T.CPA=0, MCA=25.0, R.CPA= 0.0



BISTATIC RANGE (M)

23:44:06 27-MAY-07

TGA=00.0, T.OPA=0, RGA=25.0, P.(PA)= 0.0

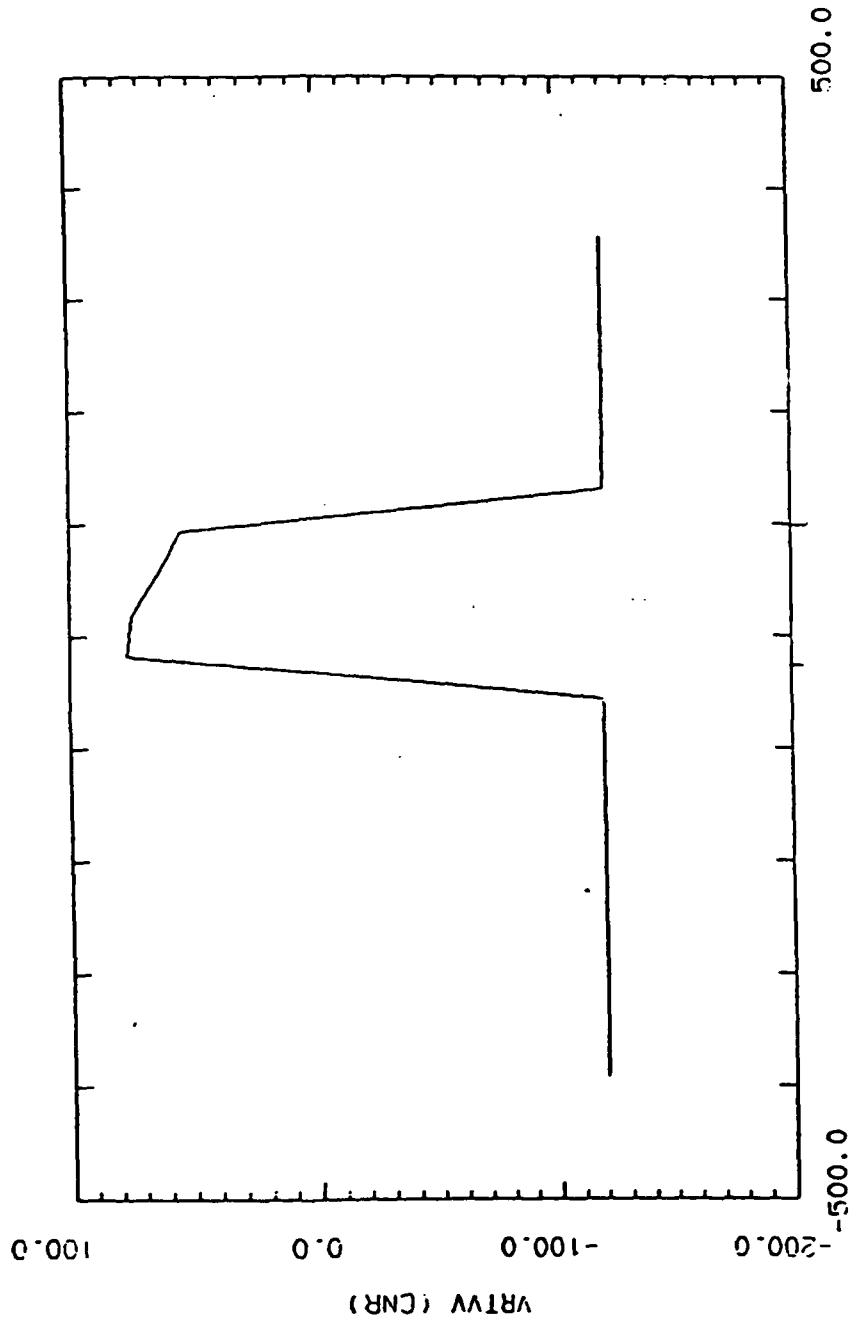


23:44:51 27-MAY-87

TCA=30.0. T.OPA=0. RGA=25.0. R.OPA= 0.0

BISTATIC RANGE (M)

V(RTHH) (CMR)



BISTATIC RANGE (M)

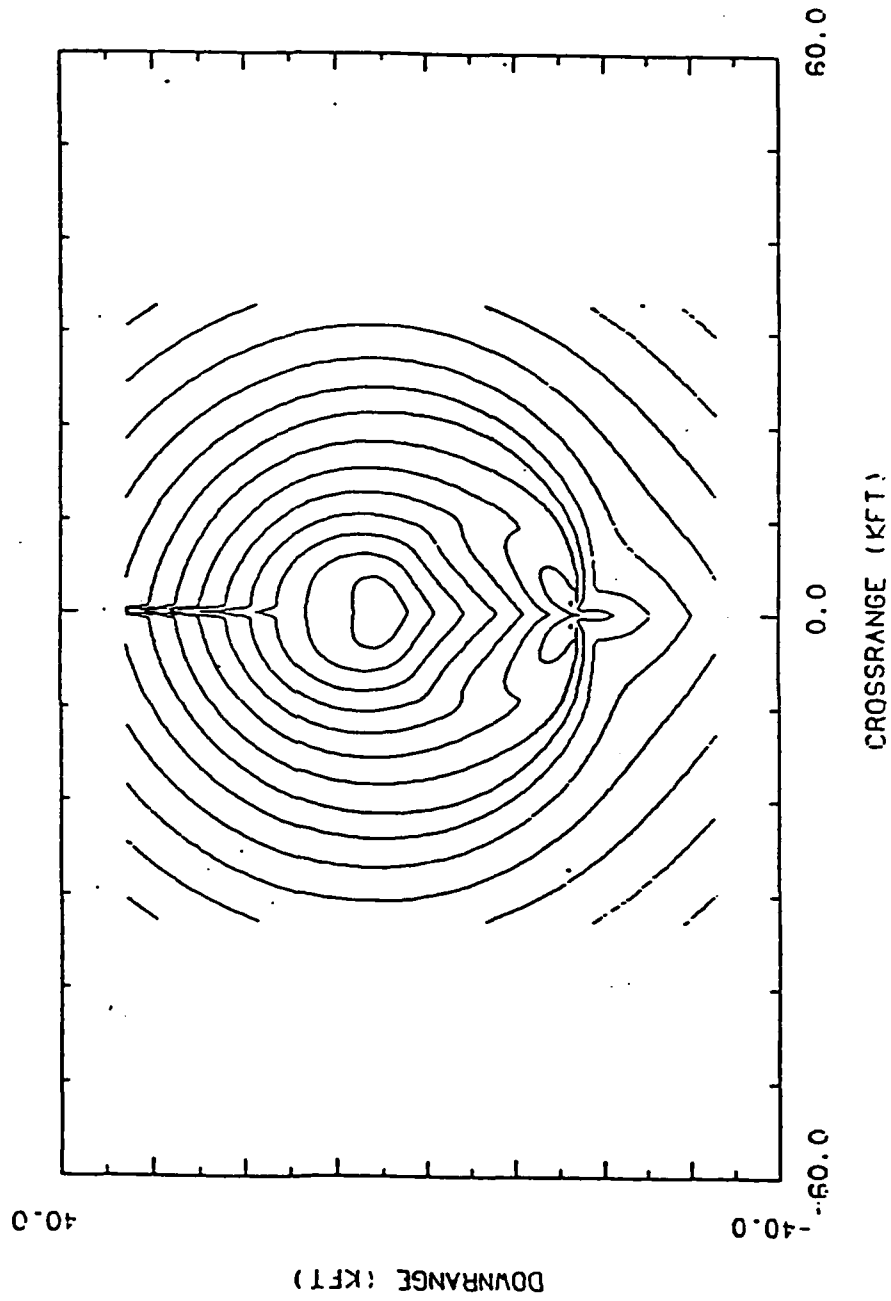
23:45:06 27-MAY-07

TGA=30.0, T.OPA=0, RGA=25.0, R.OPA= 0.0

Small Scale RMS Slope Angle = 25°

Large Scale RMS Slope Angle = 25°

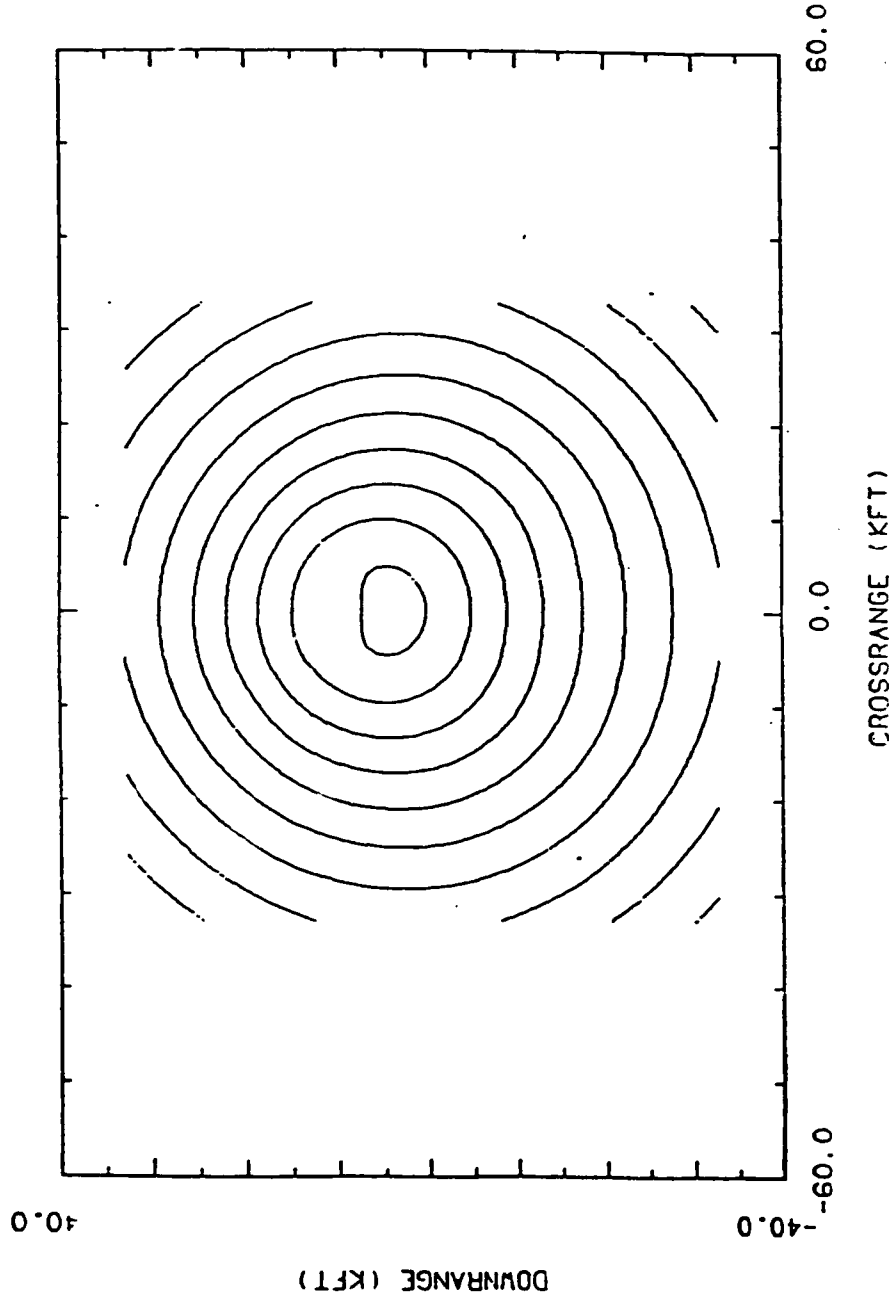
SLIGHTLY ROUGH TERRAIN SHADOWING



20122114 27-MAY-07

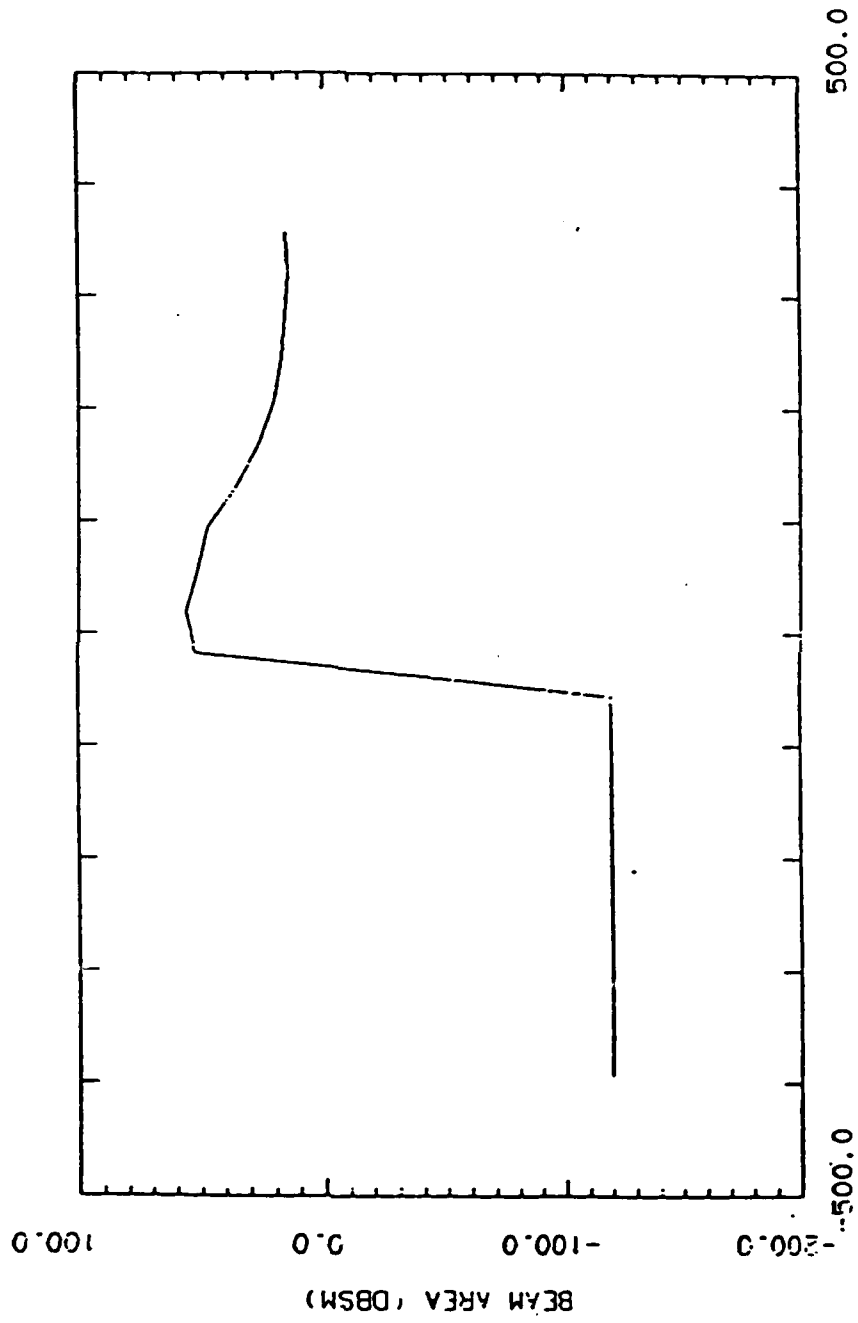
TGA=30.0. T.OPA=0. RGA=25.0. R.OPA= 0.0

VERY ROUGH TERRAIN SHADOWING



TGA=30.0, T.OPA=0, RGA=25.0, R.OPA= 0.0

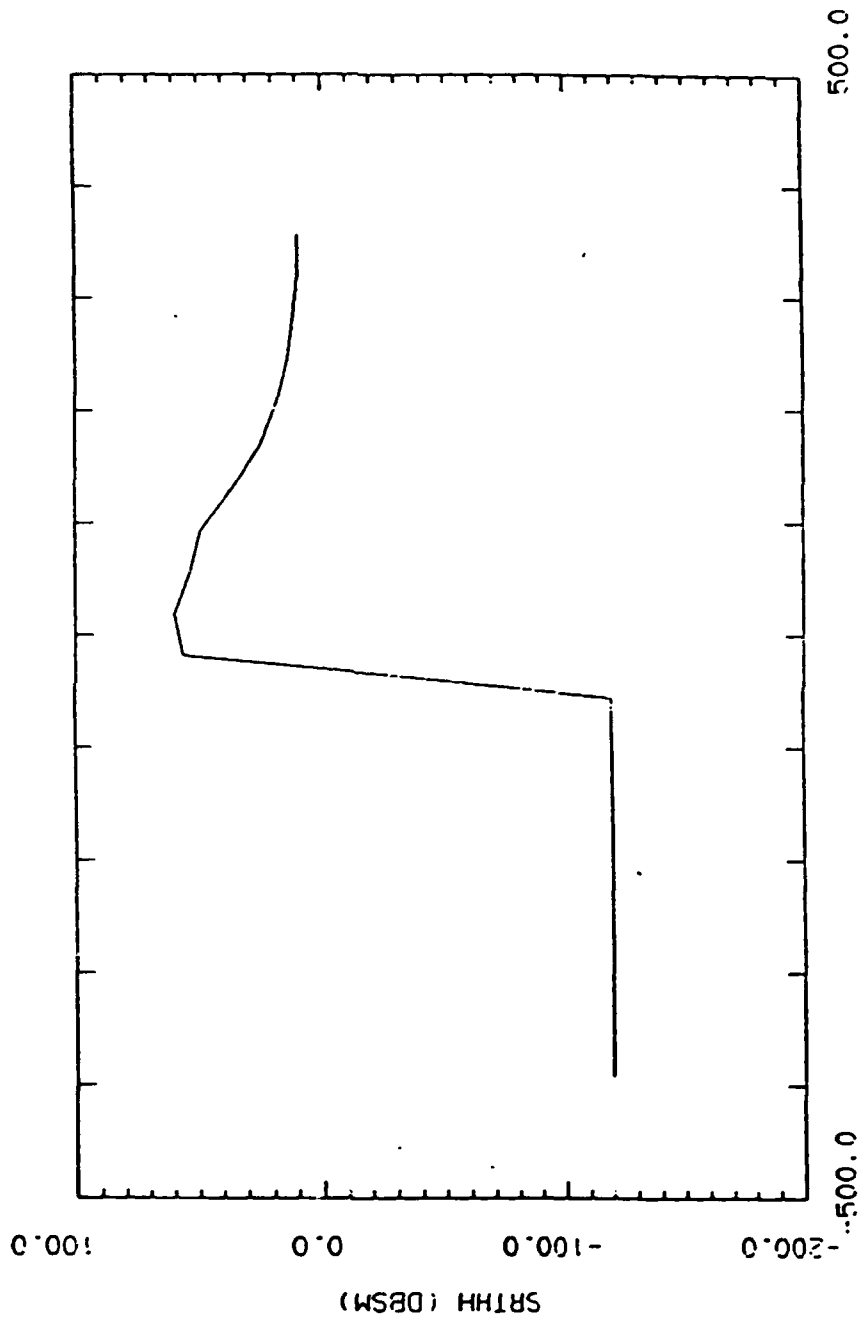
20:23:45 27-MAY-07



BISTATIC RANGE (M)

23:59:32 27-MAY-07

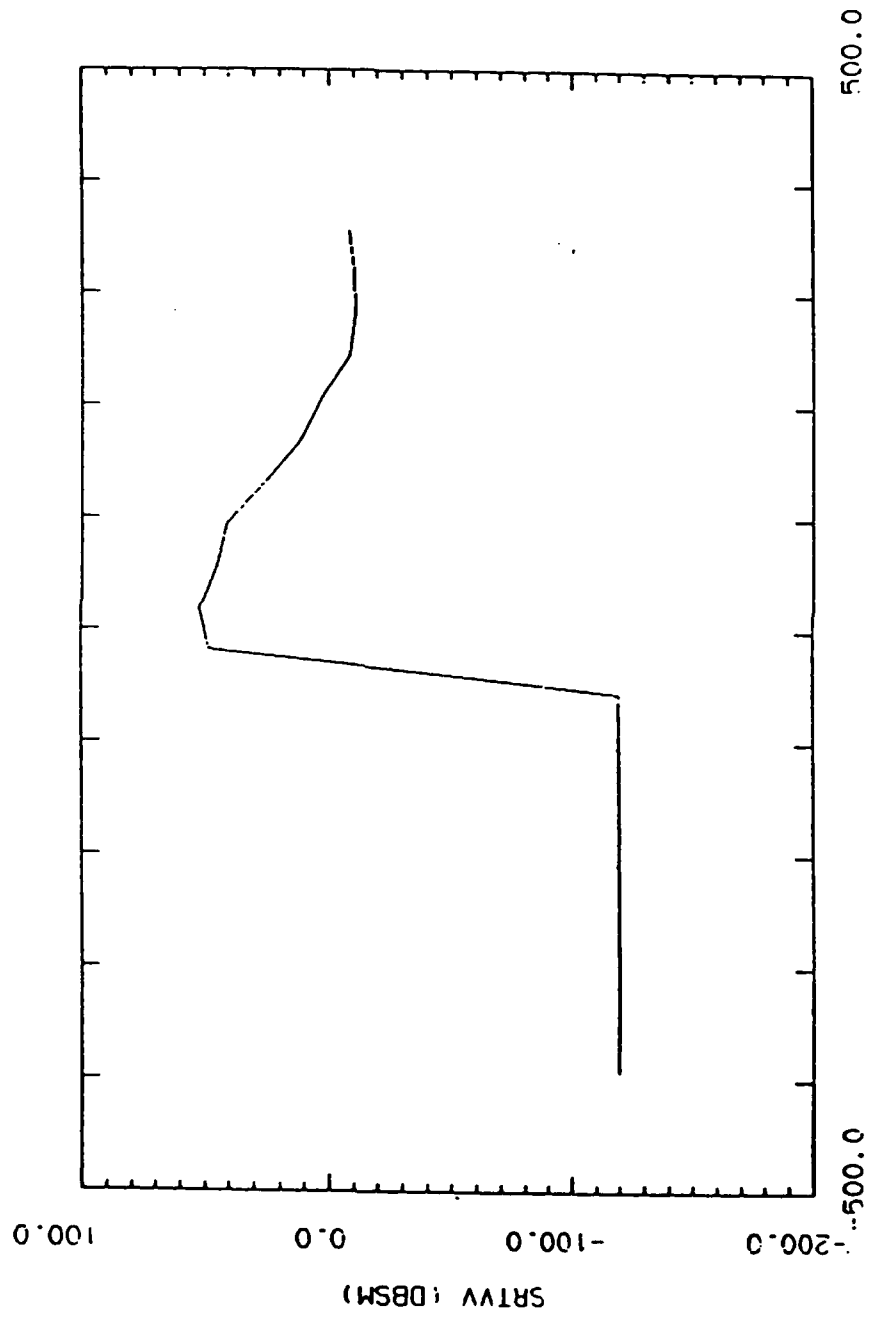
TGA=30.0, T.OPA=0, RGA=25.0, R.OPA= 0.0



BISTATIC RANGE (M)

20169149 27-MAY-07

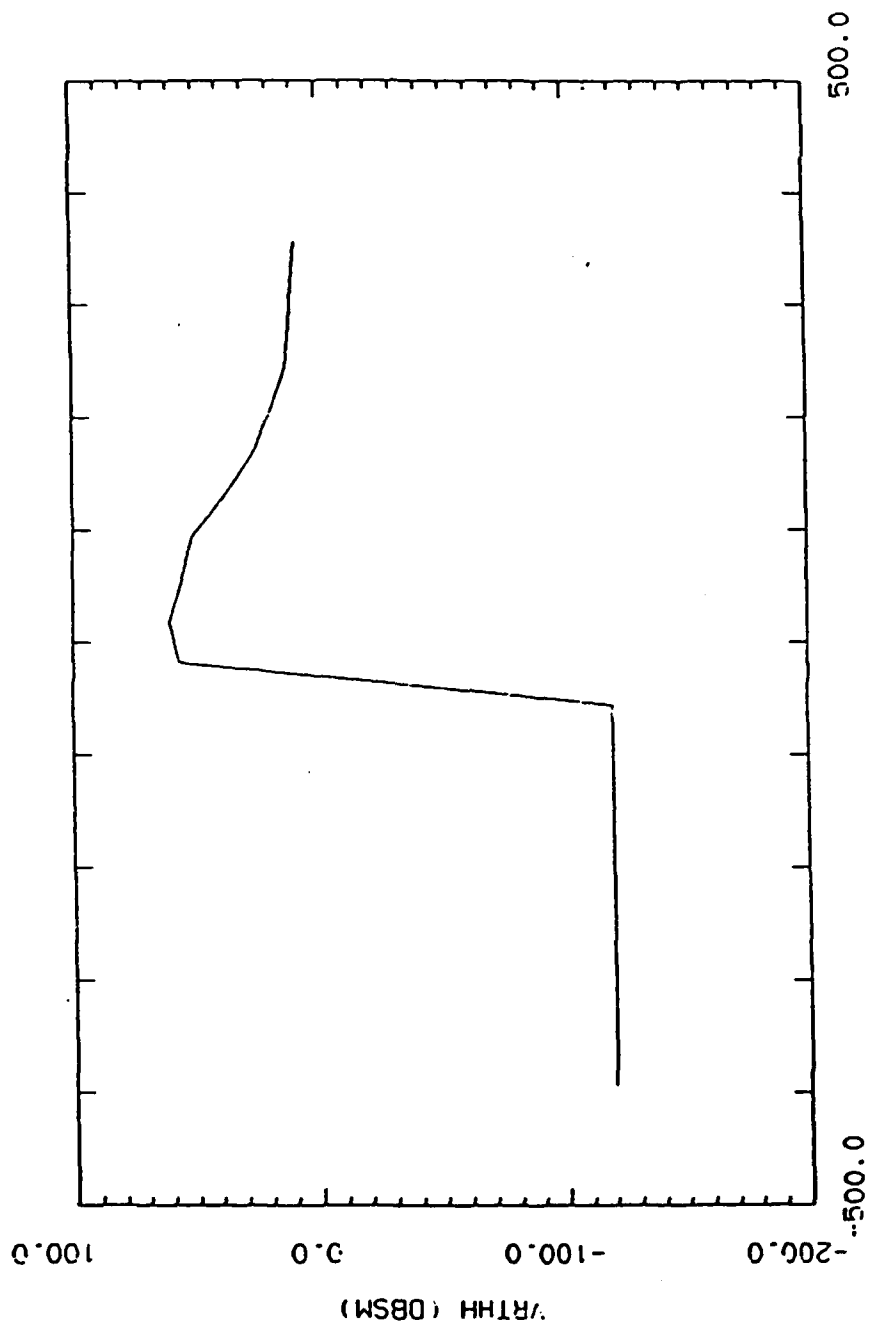
TCA=30.0, T.OPA=0, RGA=25.0, R.OPA= 0.0



BISTATIC RANGE (M)

00:00:07 28-MAY-87

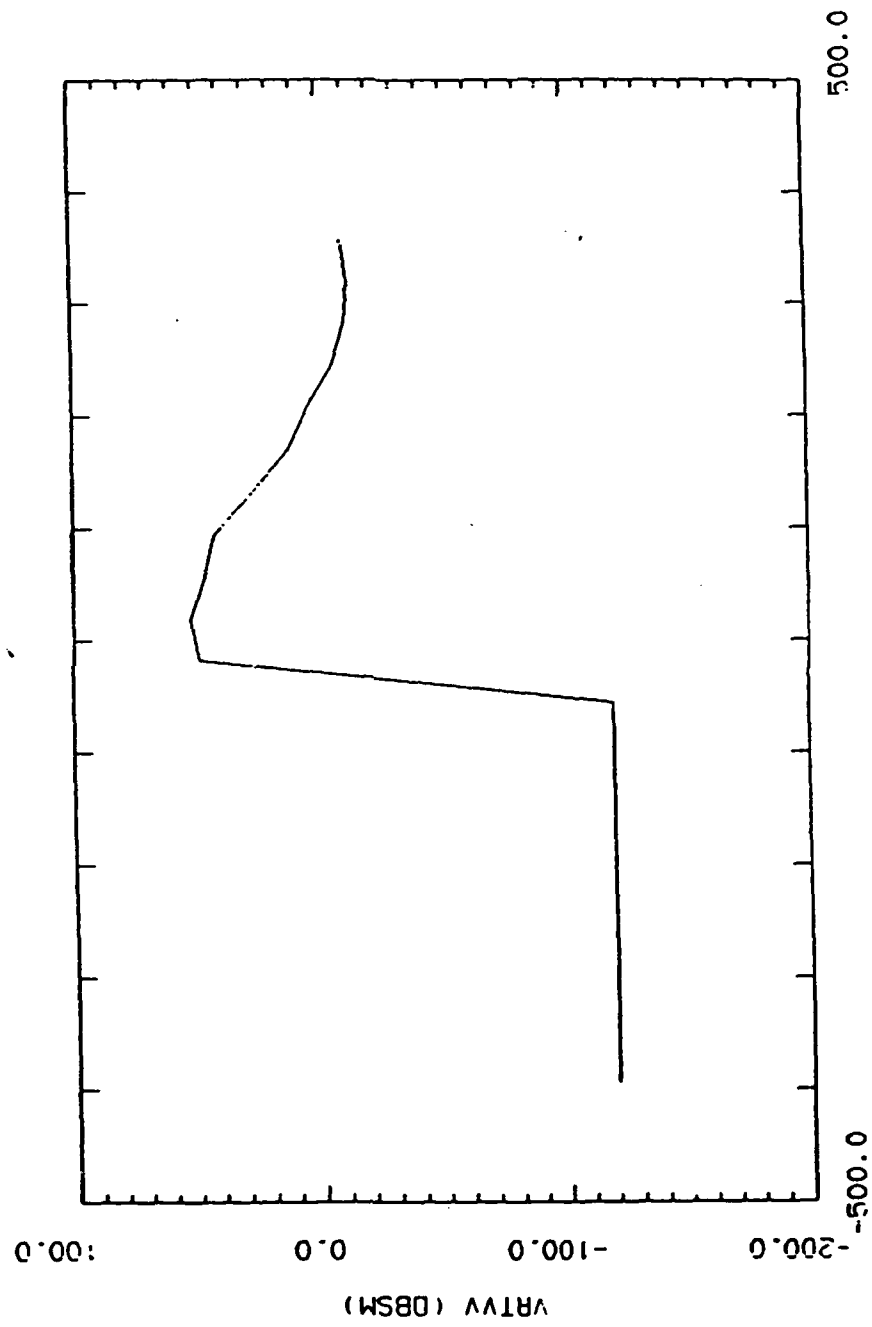
TGA=30.0. T.OPA=0. RGA=25.0. R.OPA= 0.0



BISTATIC RANGE (M)

00:00:23 20-MAY-87

TCA=30.0. T.OPA=0. RGA=25.0. R.OPA= 0.0

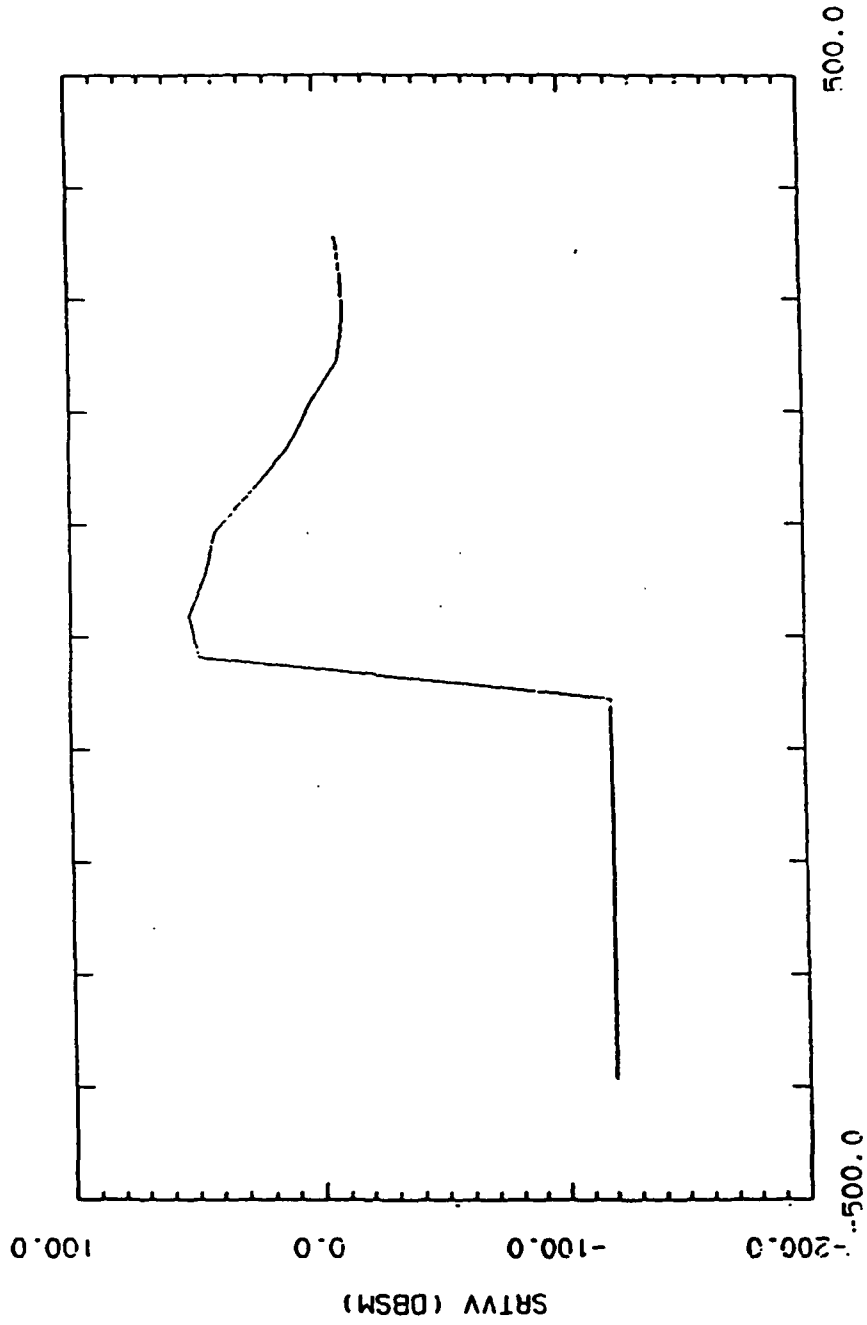


00:00:39 20-MAY-87

TGA=30.0, T.OPA=0, RGA=23.0, R.OPA= 0.0

R'STATIC RANGE (M)

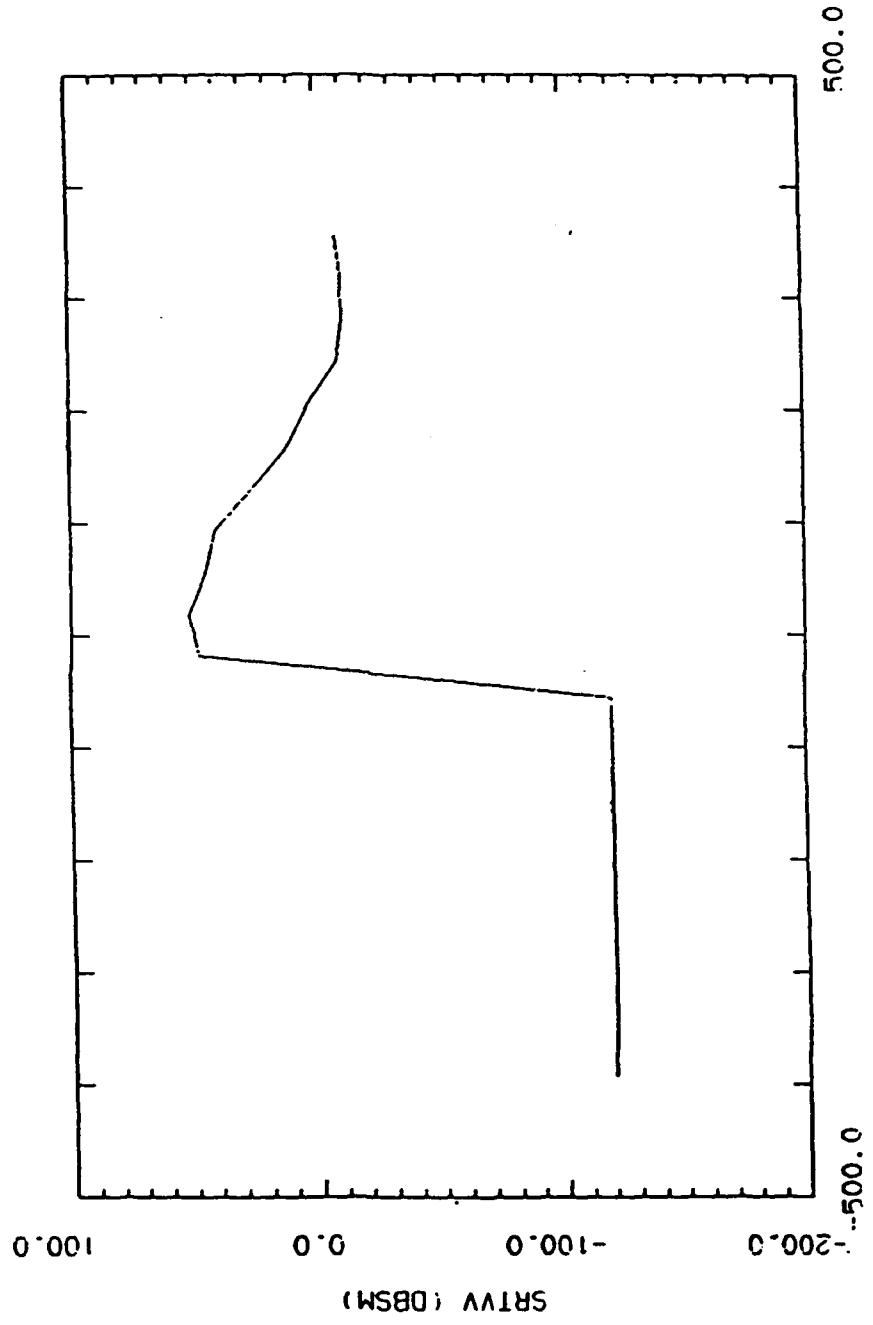
VRTV (DBSM)



BISTATIC RANGE (M)

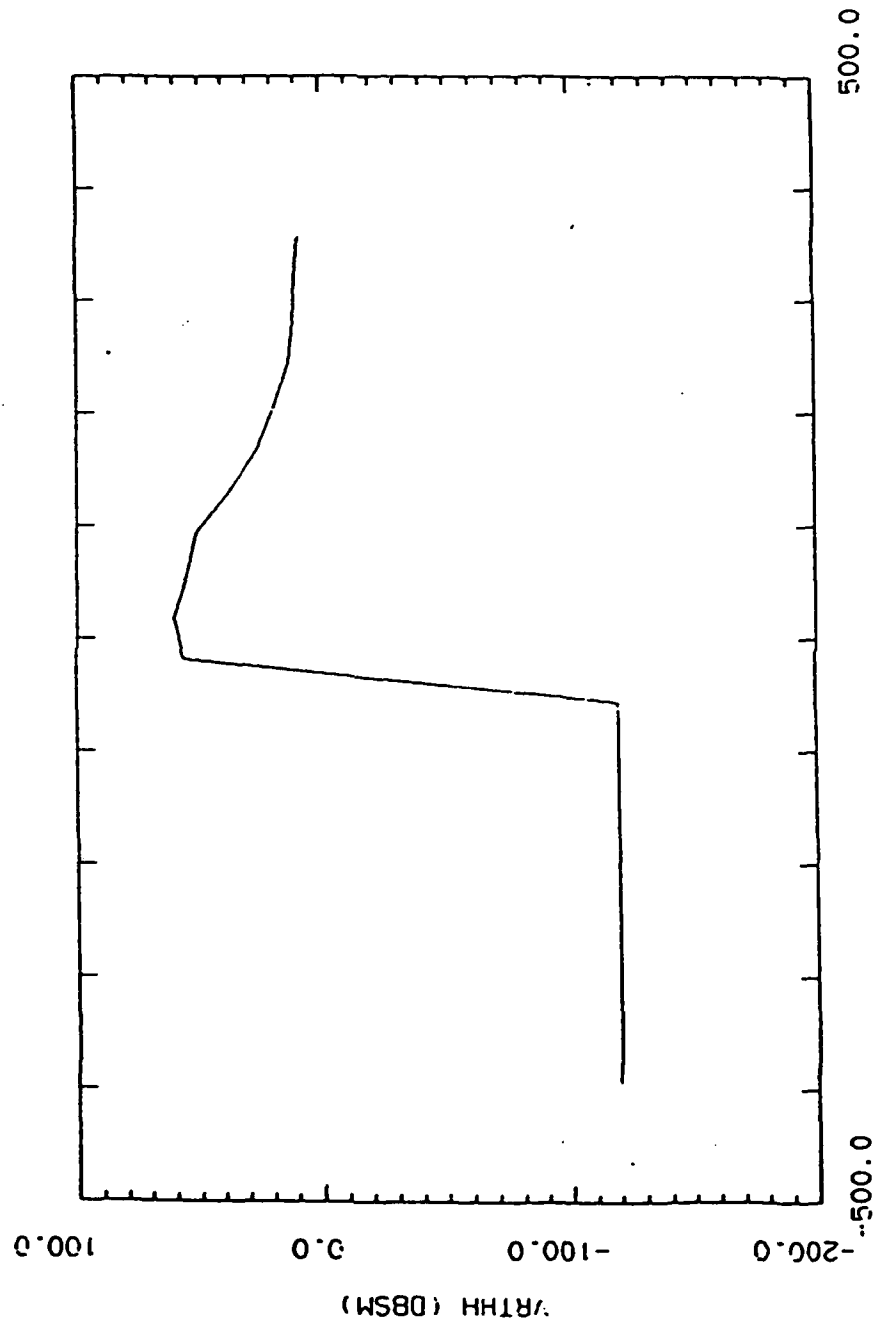
00:00:07 20-MAY-07

TEA=30.0. T.OPA=0. REA=25.0. R.OPA= 0.0



00:00:07 20-MAY-07

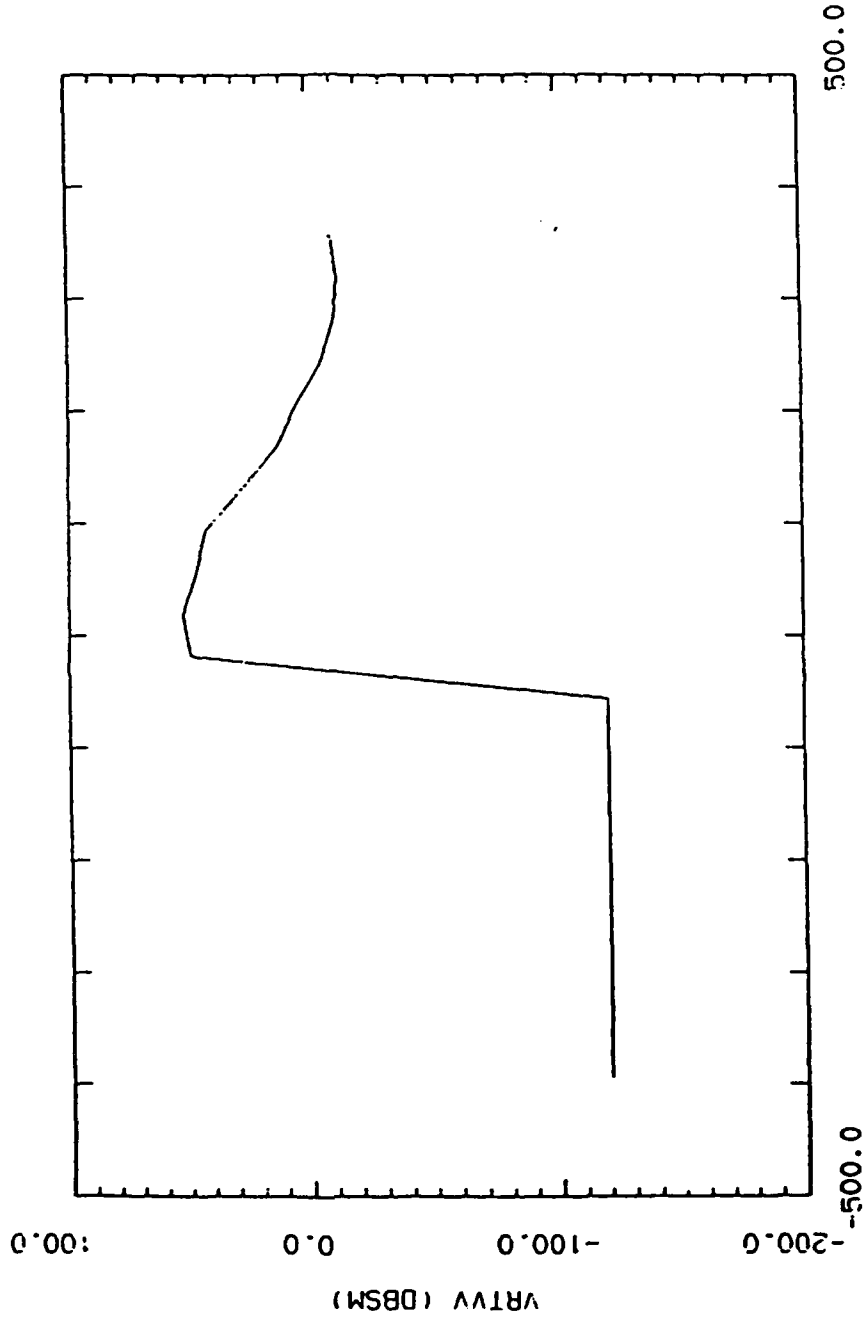
TGA=30.0. T.OPA=0. RGA=25.0. R.OPA= 0.0



BISTATIC RANGE (M)

00:00:23 20-MAY-87

TGA=30.0. T.DPA=0. RGA=25.0. R.DPA= 0.0



BISTATIC RANGE (M)

00:00:39 20-MAY-07

TGA=30.0, I.OPA=0, RGA=25.0, R.OPA= 0.0

PRELIMINARY

SRS UR87-045

DESIGN PLAN
COMPLEX PERMITTIVITY MEASUREMENT DEVICE SPECIFICATION
ELIN A003

CONTRACT TITLE: BISTATIC CLUTTER PHENOMENOLOGICAL
MEASUREMENT/MODEL DEVELOPMENT

CONTRACT NUMBER: F30602-86-C-0045

CONTRACT PERIOD: 1 APRIL 1986 TO 31 SEPTEMBER 1987

PREPARED BY: CHARLES H. HIGHTOWER

DATE: 9 DECEMBER 1986

Prepared For:
ROME AIR DEVELOPMENT CENTER
GRIFFISS AIR FORCE BASE
NEW YORK 13441-5700

PRELIMINARY

1.0 INTRODUCTION

This specification describes the functional and detailed requirements for a portable device that accurately measures the complex permittivity (i.e., dielectric constant) of various materials in the field. This tool will be used by SRS Technologies as part of the ground truth measurements task in support of the Rome Air Development Center (RADC) Clutter Measurements Program (CMP). The real part of the complex permittivity represents displacement current and the imaginary part represents conduction current of the material examined at the frequency of interest. These two parameters (along with terrain physical characteristics) are key elements of the electromagnetic scattering clutter models that will be validated by CMP measurements.

2.0 FUNCTIONAL REQUIREMENTS

The device will be used to measure the complex dielectric (permittivity) of various materials in the field. The frequency of interest is L-band (1.25 GHz). Typical materials include soil, water, vegetation, rocks and so on. It shall be hand-held, portable and contain its own power supply. The device shall be capable of withstanding rough handling and rugged environments. The device shall provide a read-out of the complex permittivity components to the operator and also store the measurements along with a sample identification code on magnetic media for uploading to a small field computer. The capability to automatically average a number of measurements shall be included as an operator selectable input.

3.0 SPECIFIC REQUIREMENTS

The following specific requirements have been identified for the permittivity measurement device.

3.1 Accuracy

The device shall measure the real part of the complex dielectric coefficient over a range of 1 to 80 (relative to free space) within 5% of the true value. The imaginary part shall be measured over a range from 0.01 to 20 (relative to free space) with an accuracy of 5% for values greater than 0.1 and within 20% of the true value for values less than 0.1.

3.2 Other Requirements

The unit shall be designed to be easily operated and calibrated in the field. The unit shall interface to the field computer over a standard serial interface bus such as IEEE 488 or RS 232C. It should also be designed so that it can be easily used to measure samples in a laboratory environment as well. Sufficient battery power for up to five (5) hours of continuous use prior to battery replacement or recharging is required. The device shall weigh less than 10 pounds including power supply. The device shall be supplied with various test materials for performance verification and calibration in the field.

4.0 DOCUMENTATION

The device shall be delivered with a description of its design, setup, operating, and calibration instructions.

SRS UR87-059

DESIGN PLAN

SRS CLUTTER MEASUREMENTS PROGRAM (CMP)

COMPARISON OF BISTATIC AND MONOSTATIC NORMALIZED SCATTERING COEFFICIENT

ELIN A003

CONTRACT TITLE: BISTATIC CLUTTER PHENOMENOLOGICAL
MEASUREMENT/MODEL DEVELOPMENT

CONTRACT NUMBER: F30602-86-C-0045

CONTRACT PERIOD: 1 APRIL 1986 - 30 SEPTEMBER 1987

PREPARED BY: CHARLES H. HIGHTOWER

DATE: 16 MARCH 1987

Prepared for:
ROME AIR DEVELOPMENT CENTER
GRIFFISS AIR FORCE BASE
NEW YORK 13441-5700

1.0 INTRODUCTION

The purpose of this technical memorandum is to present SRS Technologies Radar Clutter Workstation contours of normalized scattering coefficient and shadowing for comparison with results generated by RADC personnel at Hanscom Air Force Base. Two system geometries were utilized based on information provided by RADC. The first system represents a space based bistatic system with an illuminator located at a sufficient distance to yield a nearly constant 20 degree grazing angle over the desired surveillance area. The corresponding airborne receiver platform is located at an altitude of 60,000 feet and 200 Nmi from the center of the surveillance region (this results in a 2.8 degree grazing angle at the center of the region for the receiver). The surveillance region has a cross-range dimension of 400 Nmi and a downrange dimension of 200 Nmi. The second system considered is a monostatic radar located at the same location as the bistatic receiver. An illustration of these geometries is shown in Figure 1-1.

2.0 BISTATIC SCATTERING COEFFICIENT CONTOURS

The SRS Technologies Radar Clutter Workstation was utilized to predict the normalized scattering coefficient over the region mentioned above. In order to provide greater insight into the results, individual contour plots of large-scale, small-scale, and shadowing models were computed for HH and VV polarizations. Mr. John Lennon of RADC provided the surface height statistical parameters and electrical characteristics shown in Table 2-1.

Table 2-2 Terrain Physical and Electrical Parameters

<u>Scale</u>	<u>Scale Height (m)</u>	<u>Correlation Distance (m)</u>
Large	1.2247	6
Small	0.007071	0.1
<u>Dielectric Constant</u>	<u>Real Part</u>	<u>Imaginary Part</u>
	80	50

The wavelength utilized was 0.24 m which corresponds to L-band. The complex dielectric constant is typical of sea water and the two surface height scales are representative of a sea state of 2 to 3.

2.1 BISTATIC HH POLARIZATION CONTOURS

Clutter Workstation contours of the normalized HH scattering coefficient for the large-scale model and bistatic geometry are shown in Figure 2-1. The receiver views this region from the bottom of the figure. Note that the scattering coefficient has a value of +5 dB in a trapezoidal region along the bistatic plane (defined by the transmitter, receiver, and surveillance region center) and the intersection of the earth. The trapezoid is about 22 Nmi wide toward the receiver and 60 Nmi toward the transmitter. The coefficient drops off quite rapidly in cross-range dimension. The effects of shadowing are not included in this plot and are discussed in Section 4.0 (it is shown there that shadowing will reduce these values by about 4 dB to 8 dB over the region).

NORMALIZED SCATTERING COEFFICIENT GEOMETRY

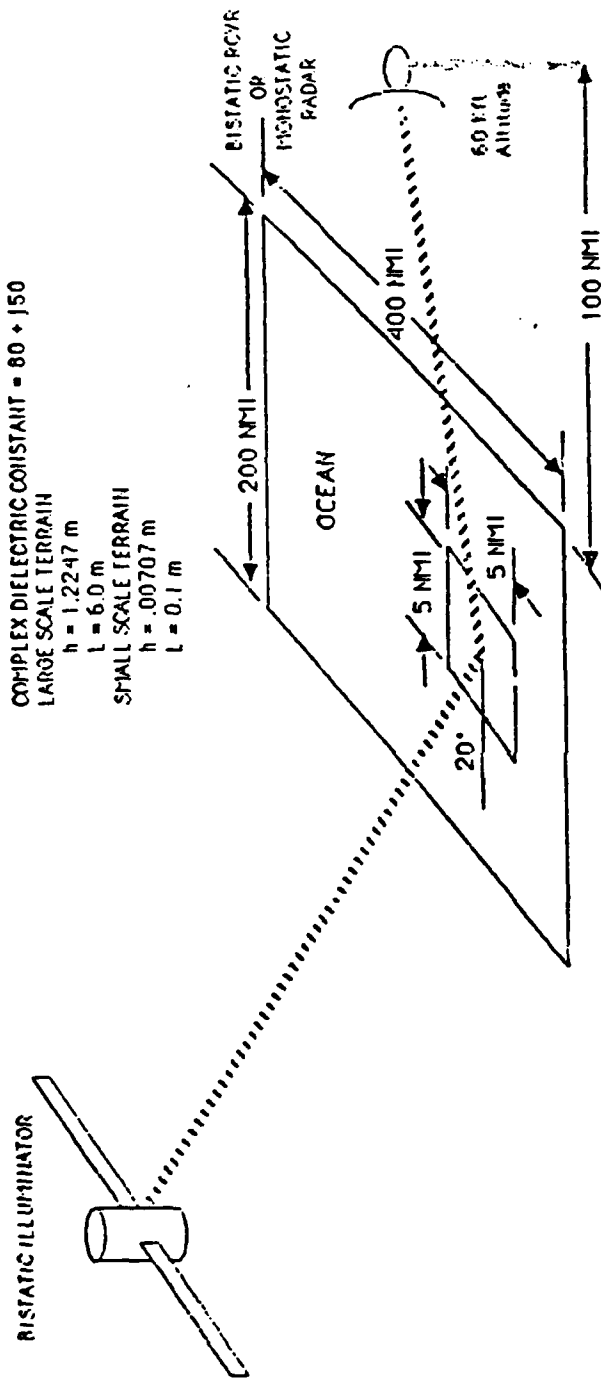


FIGURE 1-1 NORMALIZED SCATTERING COEFFICIENT GEOMETRY

VERY ROUGH TERRAIN HH POLARIZATION

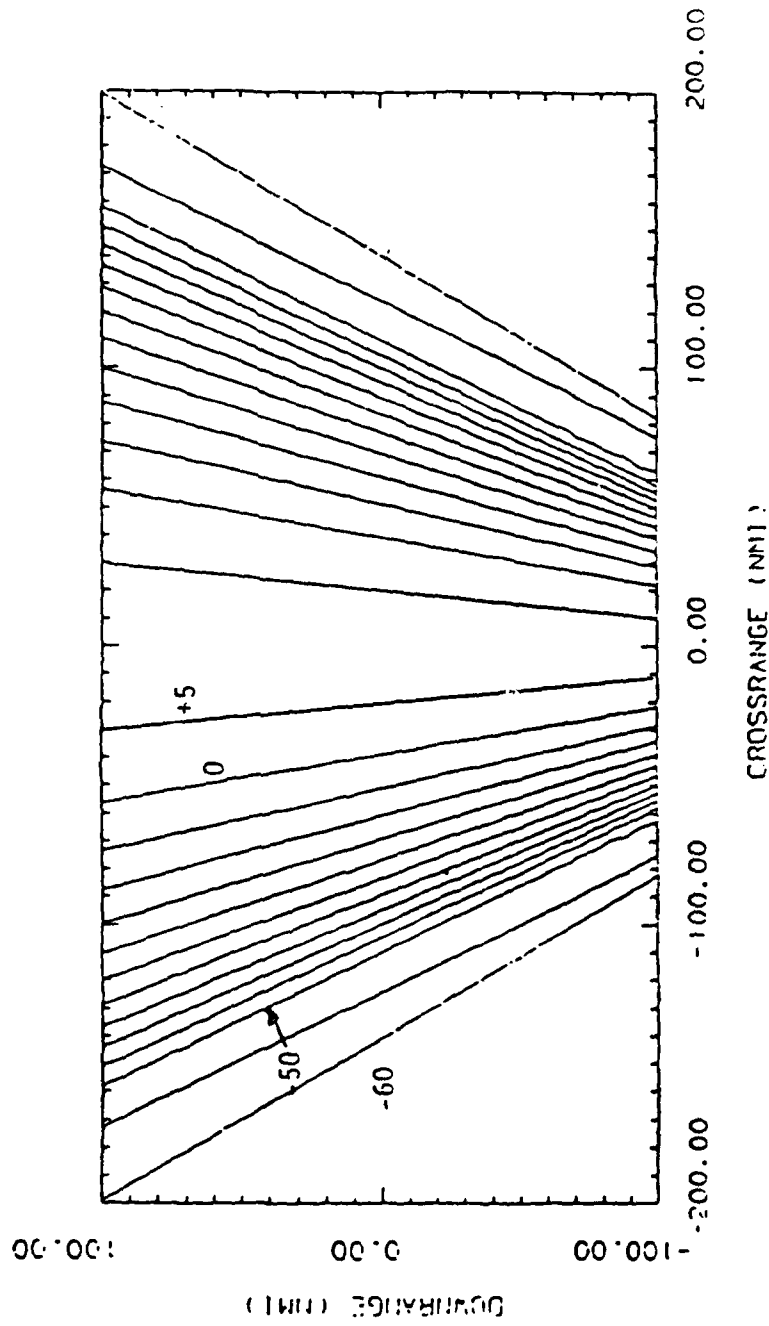


Fig. 2-1 Large - Scale HH Polarization Bistatic Scattering Coefficient

TEA=20.0, T.OPT=0, WCA=2.0, R.OPT=0.0

14:50:54 10-MAR-80

Normalized clutter coefficient contours for the small-scale model are shown in Figure 2-2. The values are significantly lower and do not exhibit the steep cross-range gradient shown by the large-scale model. It is clear that HH scattering is dominated by the large-scale model in the center of the surveillance region and by the small-scale model toward the edges. Shadowing will reduce these values by about 2.5 dB to 7 dB as discussed in Section 4.0.

2.2 BISTATIC VV POLARIZATION CONTOURS

Large-scale model contours of the normalized scattering coefficient for VV polarization are shown in Figure 2-3. The large-scale model predicts three broad "ripples" in the contours. The center ripple has a value in excess of -20 dB while the two ripples on either side are on the order of -35 dB. The coefficient decreases rapidly in the cross-range dimension outside the outer ripples. Shadowing will reduce these values as mentioned above.

The small-scale model contours are shown in Figure 2-4. The behavior is more complicated due to the presence of Brewster angle-like effects causing a deep null on either side of the center-line of the surveillance region. Again, it can be concluded that the large-scale model dominates in the center portions of the surveillance region and the edges dominated by the small-scale model. Shadowing will reduce these values (see Section 4.0).

3.0 MONOSTATIC SCATTERING COEFFICIENT CONTOURS

The monostatic normalized scattering coefficient behavior is quite different from the bistatic case. Workstation outputs indicated that there is virtually no return in either polarization considered for the large-scale model. That is, the scattering coefficient was less than -120 dB over the entire region. This result is supported by Figure 9-16 (page 724) and Figure 9-17 (page 725) provided in Volume 2 of the Radar Cross Section Handbook. The curves plotted in this reference show that when the mean-square slope (given by twice the surface height standard deviation divided by the correlation distance) is less than 30 degrees, backscattering is non-existent for incidence angles greater than 70 degrees (i.e., grazing angles less than 30 degrees). For the large-scale surface height parameters provided by RADC, the mean-square slope is 23.4 degrees so that no large-scale backscattering is to be expected from any polarization.

The situation is different for backscattering computed by the small-scale model. Figure 3-1 shows contours for HH polarization based on the small-scale model. These values range from -70 dB to -90 dB over the surveillance region. Corresponding contours for VV polarization are shown in Figure 3-2. The normalized scattering coefficient for VV range from -35 dB to -45 dB and are considerably higher than for HH polarization. Again, these results appear to be consistent with Figure 9-12 (page 710) and Figure 9-13 (page 711) of the above reference. The parameter k_1 in these figures is 2.62 for the RADC small-scale parameters and the results for k_1 equal to 1.0 and 5.0 must be visually interpolated. It is further observed that had the complex dielectric constant used by RADC for sea water been on the order of $55 + j30$, the VV backscatter would have been significantly lower.

SLIGHTLY ROUGH TERRAIN HH POLARIZATION

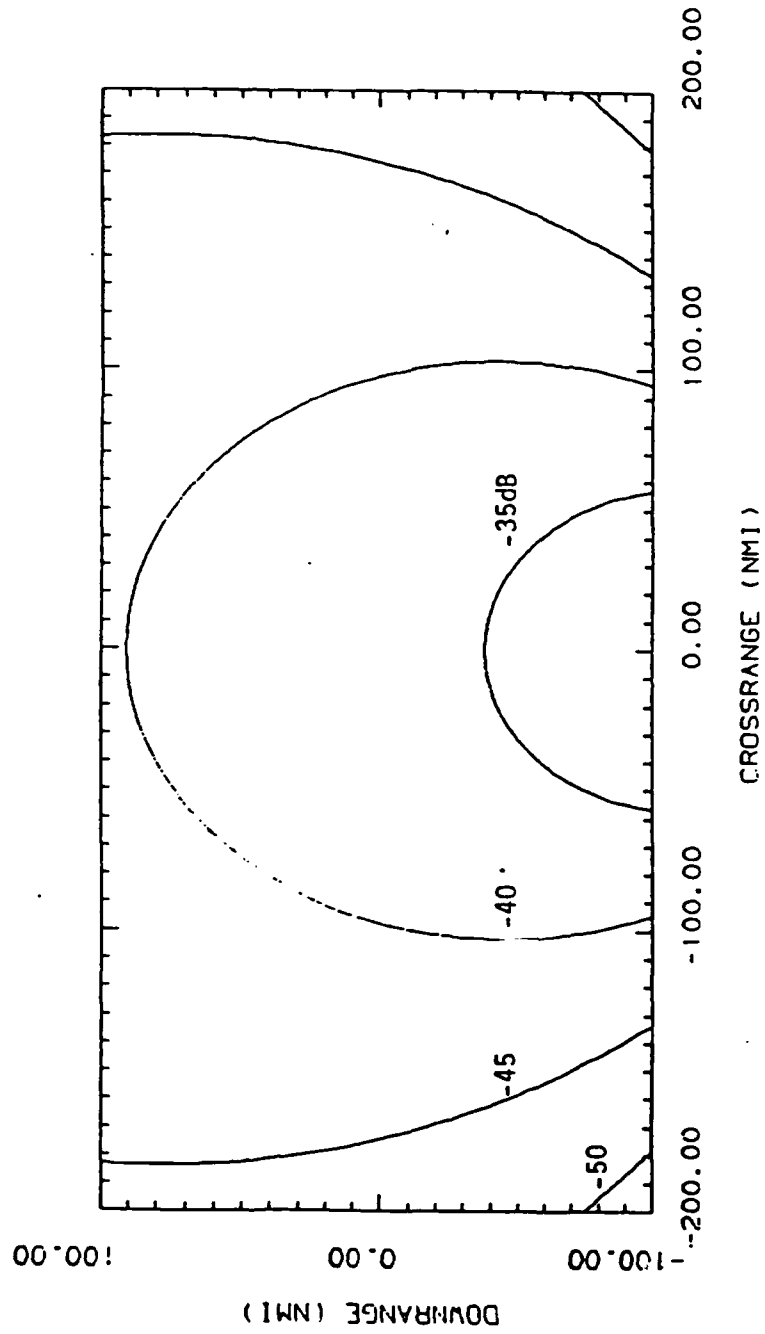


Fig. 2-2 Small - Scale HH Polarization Bistatic Scattering Coefficient

TGA=20.0. T.OPA=0. RGA= 2.0. R.OPA= 0.0

14:54:37 13-MAR-87

VERY ROUGH TERRAIN VV POLARIZATION

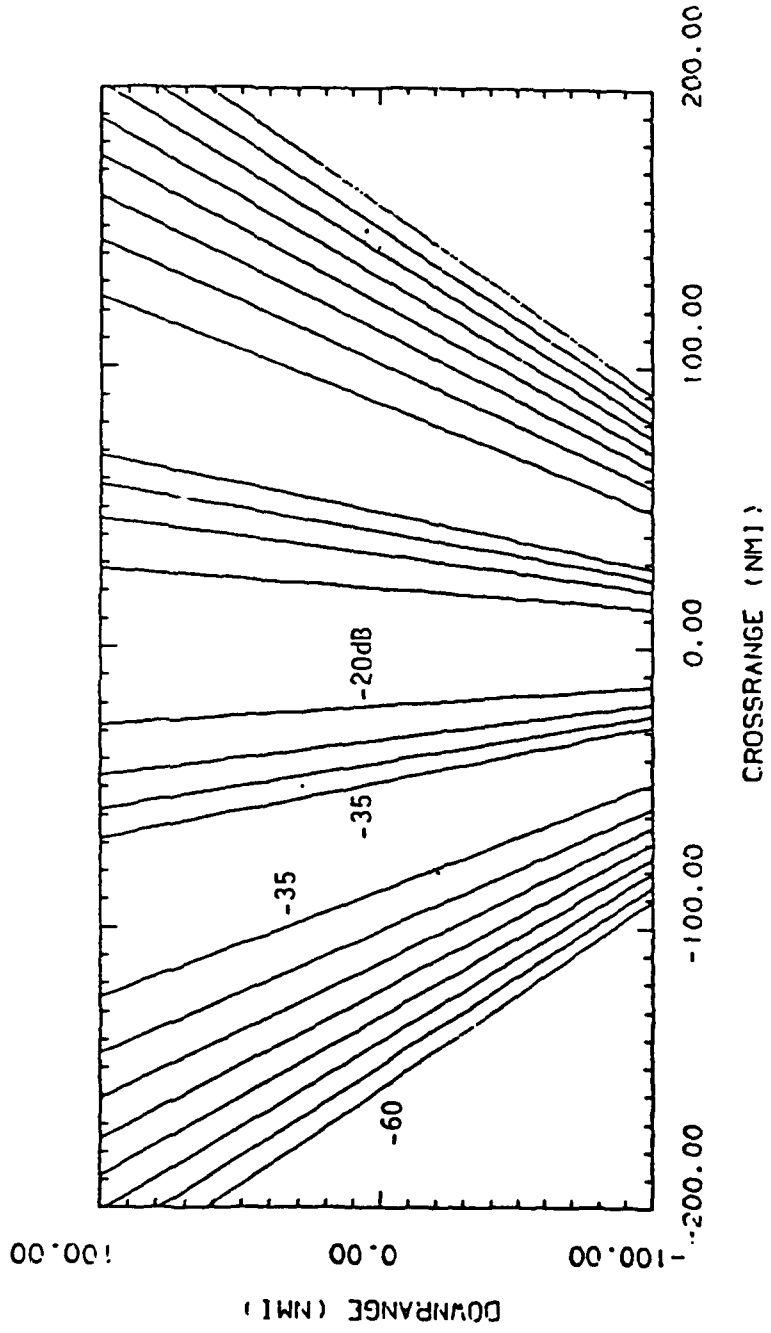


Fig. 2-3 Large - Scale VV Polarization Bistatic Scattering Coefficient

SLIGHTLY ROUGH TERRAIN VV POLARIZATION

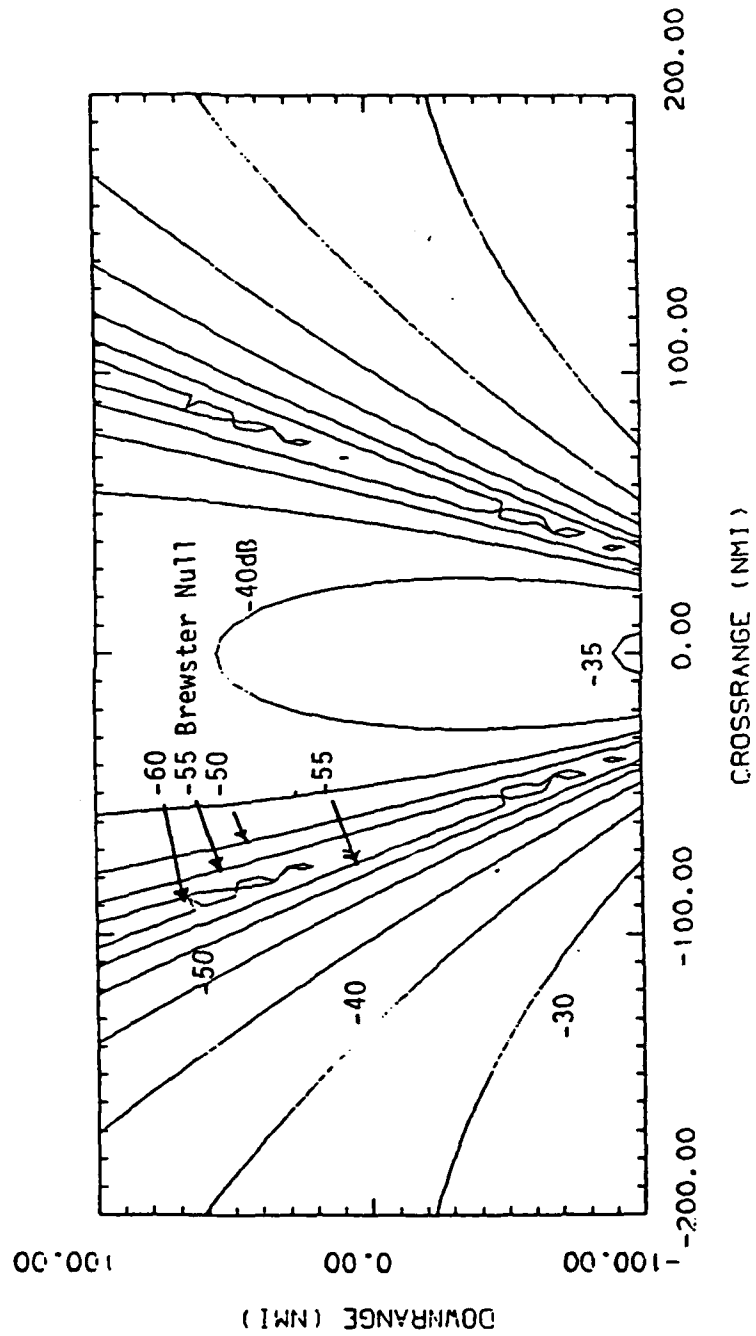


Fig. 2-4 Small - Scale VV Polarization Bistatic Scattering Coefficient

TGA=20.0. T.OPA=0. RGA= 2.0. R.OPA= 0.0

14:53:54 13-MAR-07

SLIGHTLY ROUGH TERRAIN HH POLARIZATION

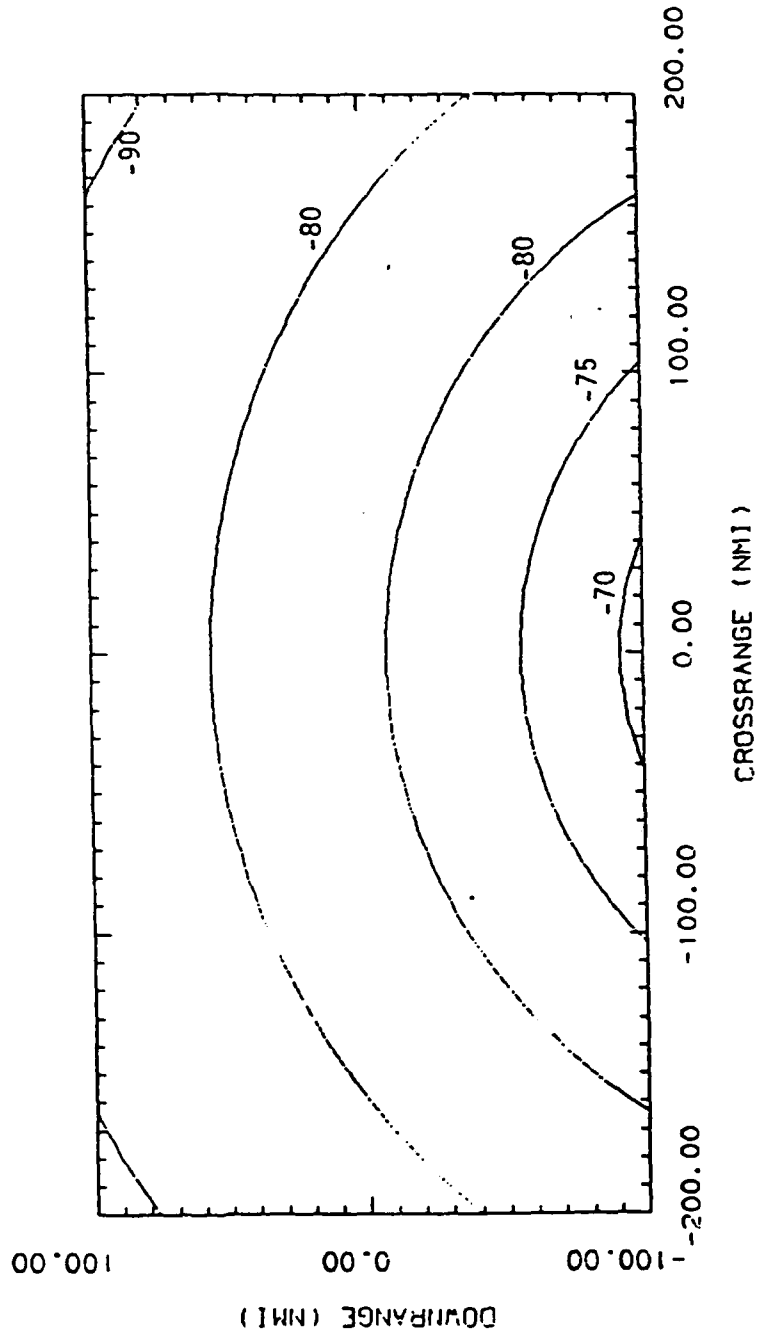


Fig. 3-1 Small - Scale HH Polarization Monostatic Scattering Coefficient

TGA= 2.0. T.OPA=0. NGA= 2.0. R.OPA= 0.0

15:50:20 13-MAR-07

SLIGHTLY ROUGH TERRAIN VV POLARIZATION

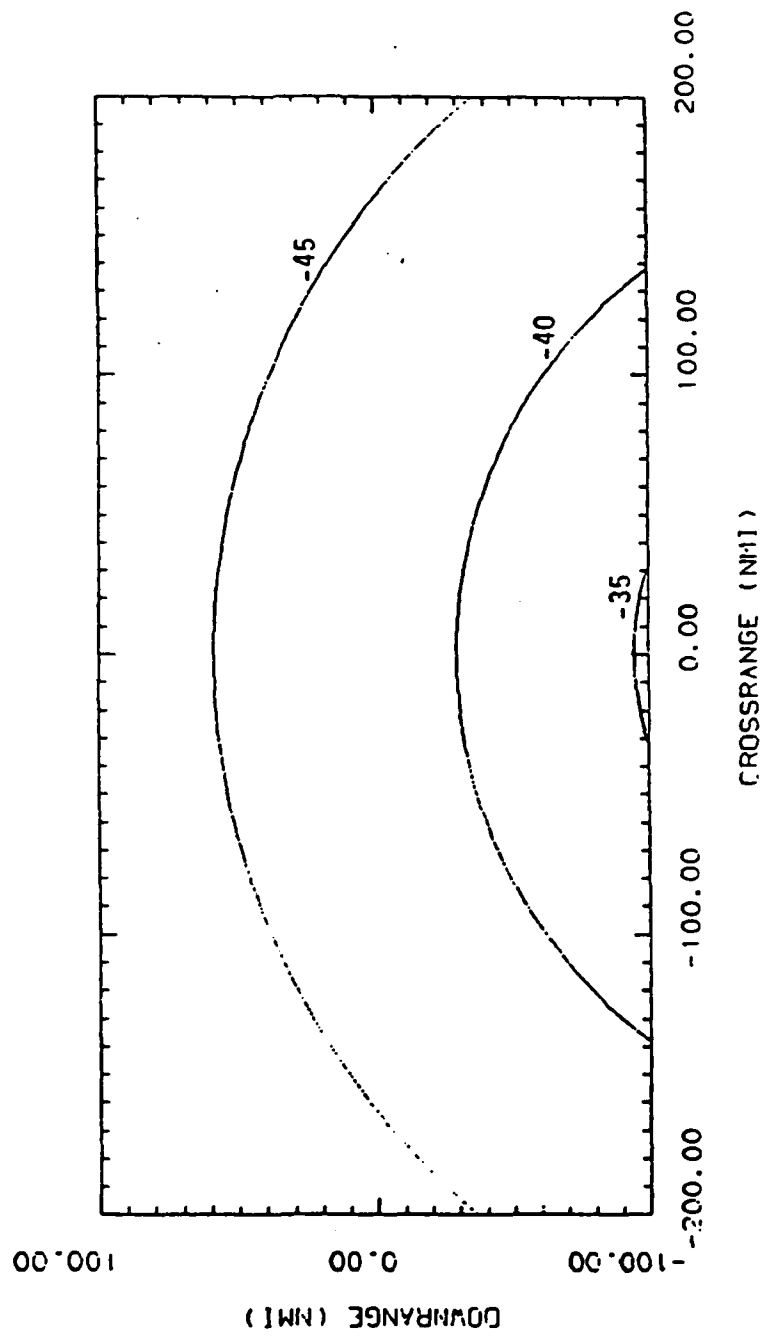


Fig. 3-2 Small - Scale VV Polarization Monostatic Scattering Coefficient

TCA= 2.0. T.WPA=0. RGA= 2.0. R.WPA= 0.0

15:41:27 13-MAR-07

4.0 SHADOWING

The SRS Technologies Radar Clutter Scattering Workstation was used to predict shadowing for both the large-scale and small-scale clutter models. Shadowing effect contours are presented in this section. The first set of shadowing contours (paragraph 4.1) represents the bistatic geometry. The second set of shadowing contours (paragraph 4.2) represents the monostatic geometry.

4.1 BISTATIC SHADOWING

4.1.1 Large-Scale Model Shadowing

Bistatic shadowing contours for the large-scale terrain scattering model appear in Figure 4-1. These contours indicate that shadowing reduces the predicted normalized clutter coefficient by 4 dB to as much as 8 dB depending on the region observed. This means that the +5 dB region shown in Figure 2-1 would be reduced to about 0 dB towards the receiver and -3 dB towards the transmitter. A similar scaling can be done for the VV contours of Figure 2-2.

4.1.2 Small-Scale Model Shadowing

Bistatic shadowing contours for the small-scale terrain are shown in Figure 4-2. These contours are slightly less for the large-scale model but have the same general form. They range from a reduction of 2.5 dB towards the receiver to 7 dB towards the transmitter. They affect the previously shown bistatic clutter coefficient contours as discussed above.

4.2 MONOSTATIC SHADOWING

4.2.1 Large-Scale Model Shadowing

Although there is virtually no backscatter predicted for the large-scale model, the corresponding monostatic shadowing contours are shown in Figure 4-3. Shadowing reduction ranges from 5.5 dB to 11 dB in the surveillance region.

4.2.2 Small-Scale Model Shadowing

The effect of shadowing on the monostatic clutter contours presented in Section 3.0 is shown in Figure 4-4. From these contours, it is expected that shadowing will cause a reduction of 2.5 dB to 7 dB in the monostatic normalized clutter coefficient over the surveillance region.

5.0 SUMMARY

Normalized clutter scattering coefficient contours have been presented for the bistatic and monostatic geometries provided by RADC. The SRS Technologies Radar Clutter Workstation utilized the physical and electrical parameters provided by RADC. In general, the contention by RADC that values for the normalized monostatic clutter coefficient are significantly lower than corresponding bistatic coefficients in the defined operation region is supported. However, it must be stressed out that this does not mean that a monostatic system will provide superior target detection performance compared to a bistatic system. The clutter contours generated are only the first step in the process of evaluating overall system performance. Effects such as

VERY ROUGH TERRAIN SHADOWING

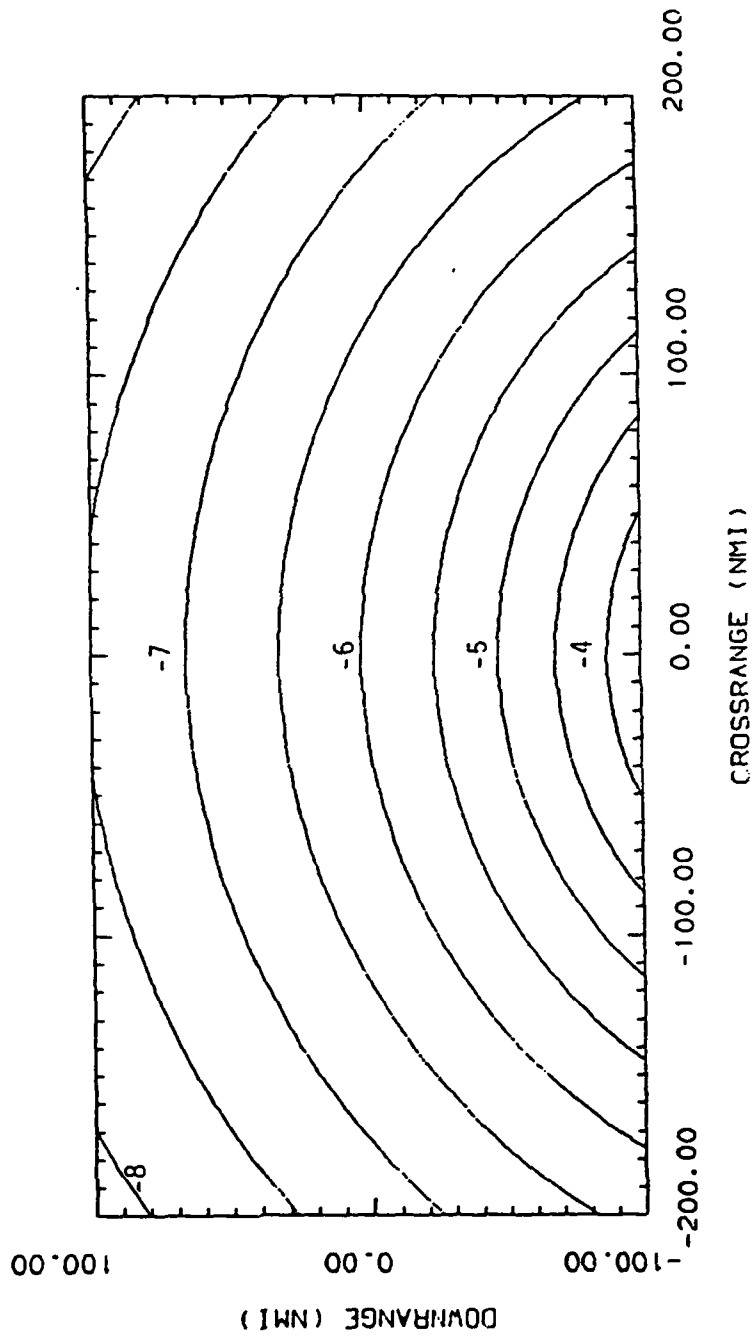
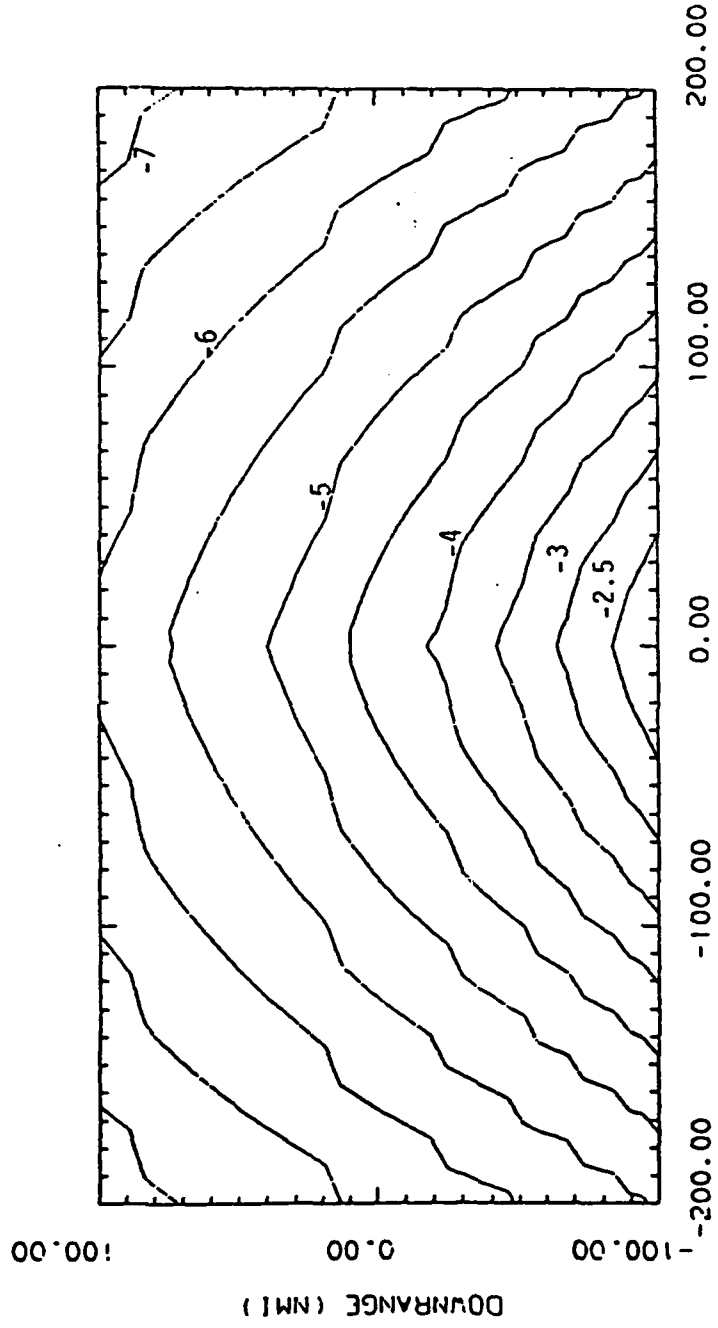


Fig. 4-1 Large - Scale Bistatic Terrain Shadowing

TGA=20.0 . T.OPA=0. RGA= 2.0. R.OPA= 0.0

17:10:58 13-MAR-87

SLIGHTLY ROUGH TERRAIN SHADOWING



CROSSRANGE (NM)

Fig. 4-2 Small - Scale Bistatic Terrain Shadowing

VERY ROUGH TERRAIN SHADOWING

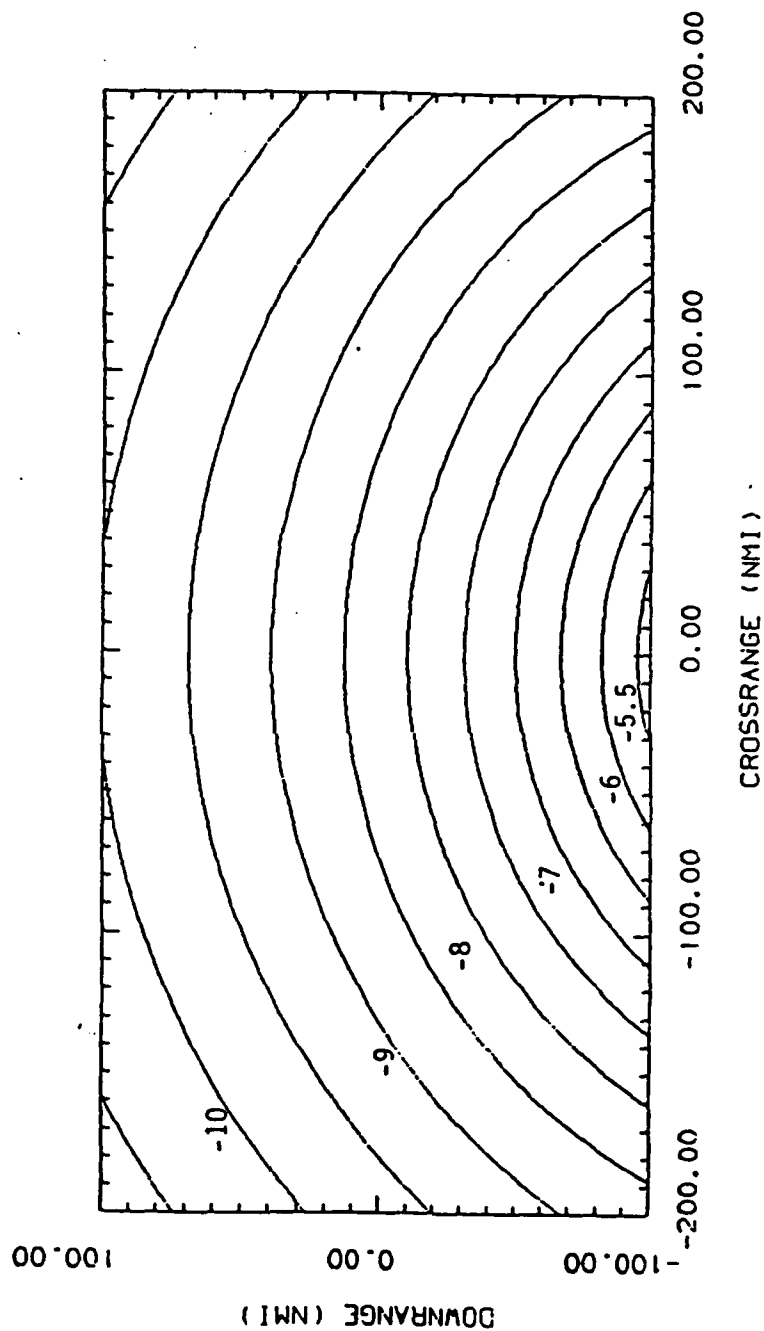


Fig. 4-3 Large - Scale Monostatic Terrain Shadowing

TGA= 2.8. T.OPA=0. RGA= 2.8. R.OPA= 0.0

16:38:34 13-MAR-87

SLIGHTLY ROUGH TERRAIN SHADOWING

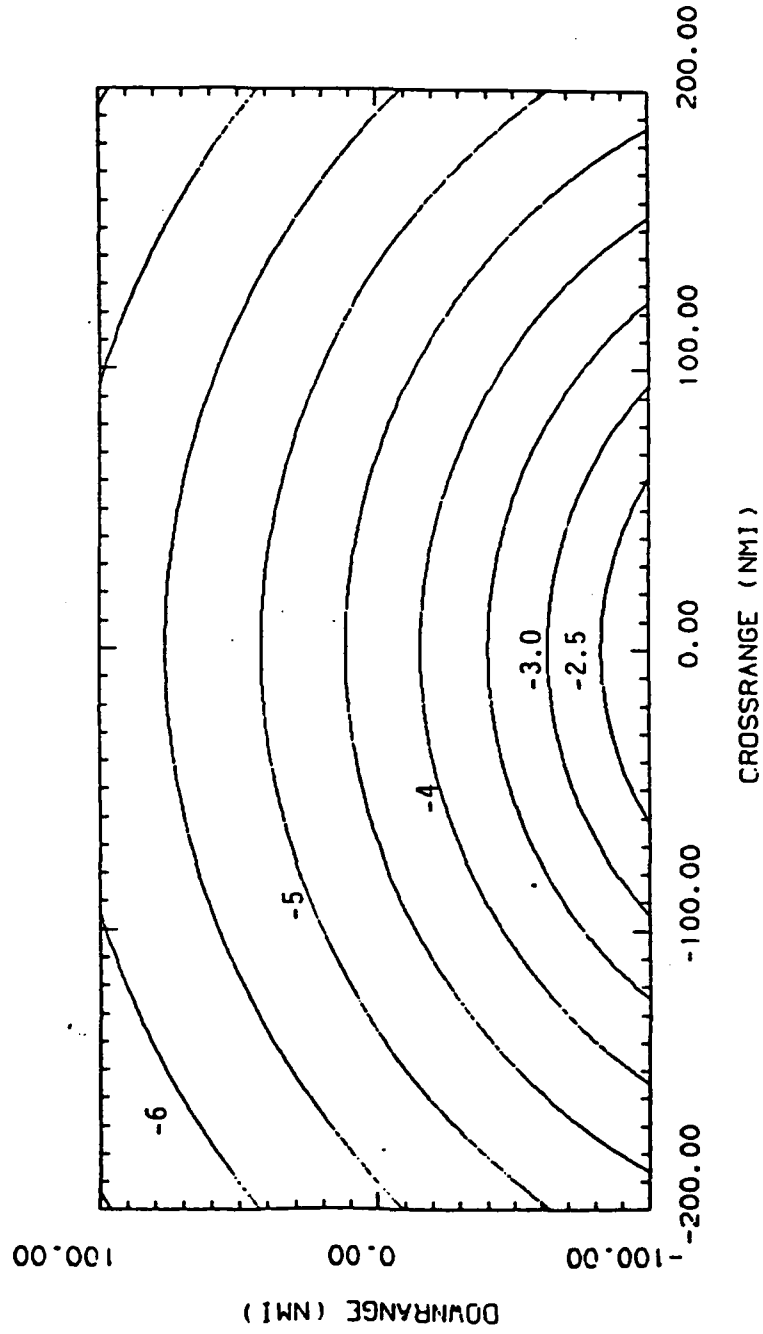


Fig. 4-4 Small - Scale Monostatic Terrain Shadowing

TGA= 2.0. T.OPA=0. RGA= 2.0. R.OPA= 0.0

16:37:39 13-MAR-07

free-space attenuation (i.e., R^2 loss) on the clutter return has been completely ignored in this process. Likewise, antenna patterns, platform velocities, waveforms, and various clutter cancellation schemes must all be considered before a final conclusion can be made.

As a final note, it should be pointed out that the SRS Radar Clutter Workstation computations differed slightly from those of RADC. RADC utilized a constant grazing angle (20 degrees) to represent the bistatic illuminator over the surveillance region. The SRS Technologies Workstation incorporated a realistic synchronous satellite altitude and range from the surveillance region so that the grazing angle varied from the nominal 20 degree value. In addition, the SRS Technologies Workstation incorporated a separate shadowing model for each terrain scale. The differences between these two shadowing models is usually on the order of a few dB's at most. Finally, we choose to separate the various factors leading to a composite normalized reflectivity coefficient to provide greater insight into the underlying physics of the problem.

DESIGN PLAN
ERIM MEASUREMENT SYSTEM CALIBRATION ACCURACY AND
MULTIPATH MITIGATION ANALYSIS SUMMARY

ELIN A003
SRS UR87-091

CONTRACT: BISTATIC CLUTTER
PHENOMENOLOGICAL
MEASUREMENT/MODEL DEVELOPMENT

CONTRACT NUMBER: F30602-86-C-0045

CONTRACT PERIOD: 1 APRIL 1986 TO 31 SEPTEMBER
1987

PREPARED BY: CHARLES H. HIGHTOWER

DATE: 17 APRIL 1987

Prepared For:
ROME AIR DEVELOPMENT CENTER
GRIFFISS AIR FORCE BASE
NEW YORK 13441-5700

SRS
TECHNOLOGIES

ADVANCED TECHNOLOGY DIVISION
17252 ARMSTRONG AVENUE
IRVINE, CALIFORNIA 92714
(714) 250-4206

1.0 INTRODUCTION

This report summarizes SRS Technologies analyses performed in support of Rome Air Development Center's (RADC's) Clutter Measurements Program (CMP) regarding (1) the Environmental Research Institute of Michigan (ERIM) system calibration error budget presented at the 15-16 January 1987 Preliminary Design Review and (2) the effect of multipath on system calibration using Active Radar Calibrators (ARC's).

The major difference between the SRS and ERIM calibration error budget analyses is an attempt to account for correlation between error sources in the SRS approach. SRS results indicate ERIM's ± 5 dB accuracy is overly conservative. SRS analyses indicate system calibration accuracy will more likely lie between 1.95 dB and 3.8 dB depending on error source correlation assumptions.

In addition, SRS Technologies analyses indicate multipath effects at the low grazing angles proposed for CMP clutter data collection could result in significant errors in clutter scattering coefficient measurement. However, a method referred to as "transfer calibration" is shown to be a potential solution to this problem.

2.0 SYSTEM CALIBRATION ERROR ANALYSIS

The following expression describes the parameters which relate transmitted power to the normalized scattering coefficient

$$\sigma_{p,q}^0 = \frac{P_{c,q}}{P_{t,p}} \frac{1}{K}$$

where,

$$K = \frac{L_r L_{A0} G_{B0} \lambda^2}{(4\pi)^2}$$

and

$$I = \int_{A_c} \frac{f_A(x,y)f_B(x,y)}{R_A^2 R_B^2} dx dy$$

The individual elements of the above expressions are defined in Reference 1. What is important regarding the expression for normalized reflectivity $\rho_{p,q}$ is that the four parameters in the first expression are clearly independent. Thus, after some elementary manipulation, the normalized error in the reflectivity coefficient can be expressed as

$$\frac{\Delta\sigma_{p,q}^0}{\sigma_{p,q}^0} = \sqrt{\left(\frac{\Delta P_{c,q}}{P_{c,q}}\right)^2 + \left(\frac{\Delta P_{t,p}}{P_{t,p}}\right)^2 + \left(\frac{\Delta K}{K}\right)^2 + \left(\frac{\Delta I}{I}\right)^2}$$

The terms on the right hand side are seen to represent normalized errors in (1) the conversion of receiver voltage to received power in the qth polarization (2) transmitted power in the pth polarization (3) system propagation losses and mainbeam gains, and (4) clutter surface area integration weighted by antenna patterns, ranges, and clutter variation.

These four normalized independent errors are mapped against the error sources identified by ERIM at the January 1987 PDR in Figure 1-1. ERIM's error analysis assumed all error sources were independent, so the resultant error was equal to the root-sum-square (RSS) of all the error components shown in Figure 1-1. In the SRS analysis, this is strictly true only for the four elements shown in the column headings. Thus, the analysis proceeded in two directions. In the first case, it was assumed that all component errors under a single heading were independent and uncorrelated. The resulting RSS values for each column are shown in the bottom row labeled UNCORRELATED VALUE. These values were again RSS'd to arrive at a total error. Since the error source labeled "cell location and pointing" was multiple valued (i.e., 0.3 dB and 1.7 dB) the overall system RSS error has two possible values. As shown at the bottom of the figure, the

↑ UNCORRELATED SOURCES ↓ ERROR SOURCES	↑ UNCORRELATED ERROR SOURCES	$\Delta P_c P_{c,q}$	$\Delta P_{1,p} P_{1,p}$	$\Delta K/K$	$\Delta I/I$
ANTENNA PATTERN, XMITT					1.15 (1.1%)
ANTENNA PATTERN, RCVR					1.05 (0.5%)
CELL LOCATION & POINTING					0.015 (0.15%)
ACTIVE RADAR CALIBRATOR					0.02 (0.2%)
TRANSMITTER POWER MEAS.			5dB (12%)		
LOSSES IN MICROWAVE COMP			1 dB (26%)		
REFLECTOR GAIN OVER MEAS		5dB (12%)			
GAINS OF RCVR TRANSFER GAIN		5dB (12%)			
REFLECTOR GAINS		5dB (12%)			
REFLECTOR CHANNEL IMBALANCE		5dB (12%)			
REFLECTOR POINTING ERRORS		5dB (12%)			
REFLECTOR POINTING NOISE		5dB (12%)			
REFLECTOR ACCURACIES LIMITED					5dB (12%)
TOTAL UNCORRELATED ERROR		1.95	1.95		1.95 (1.95%)
TOTAL CORRELATED ERROR		0.28	0.28		0.28 (0.28%)
TOTAL CORRELATED ERROR					0.28 (0.28%)

TOTAL UNCORRELATED ERROR = 5.7% TO 7.4% (1.95 DB TO 2.4 DB)
TOTAL CORRELATED ERROR = 1.0% TO 1.5% (0.18 DB TO 0.8 DB)

Figure 1-1 System Calibration Accuracy Analysis Summary

corresponding total error values are 57% and 74%, or equivalently, 1.95 dB and 2.4 dB.

Conversely, the worst case occurs when the error components under a common column add directly (i.e., are correlated) prior to the final RSS operation. In this case the resulting normalized errors are 108% and 139%, or equivalently, 3.18 dB and 3.8 dB).

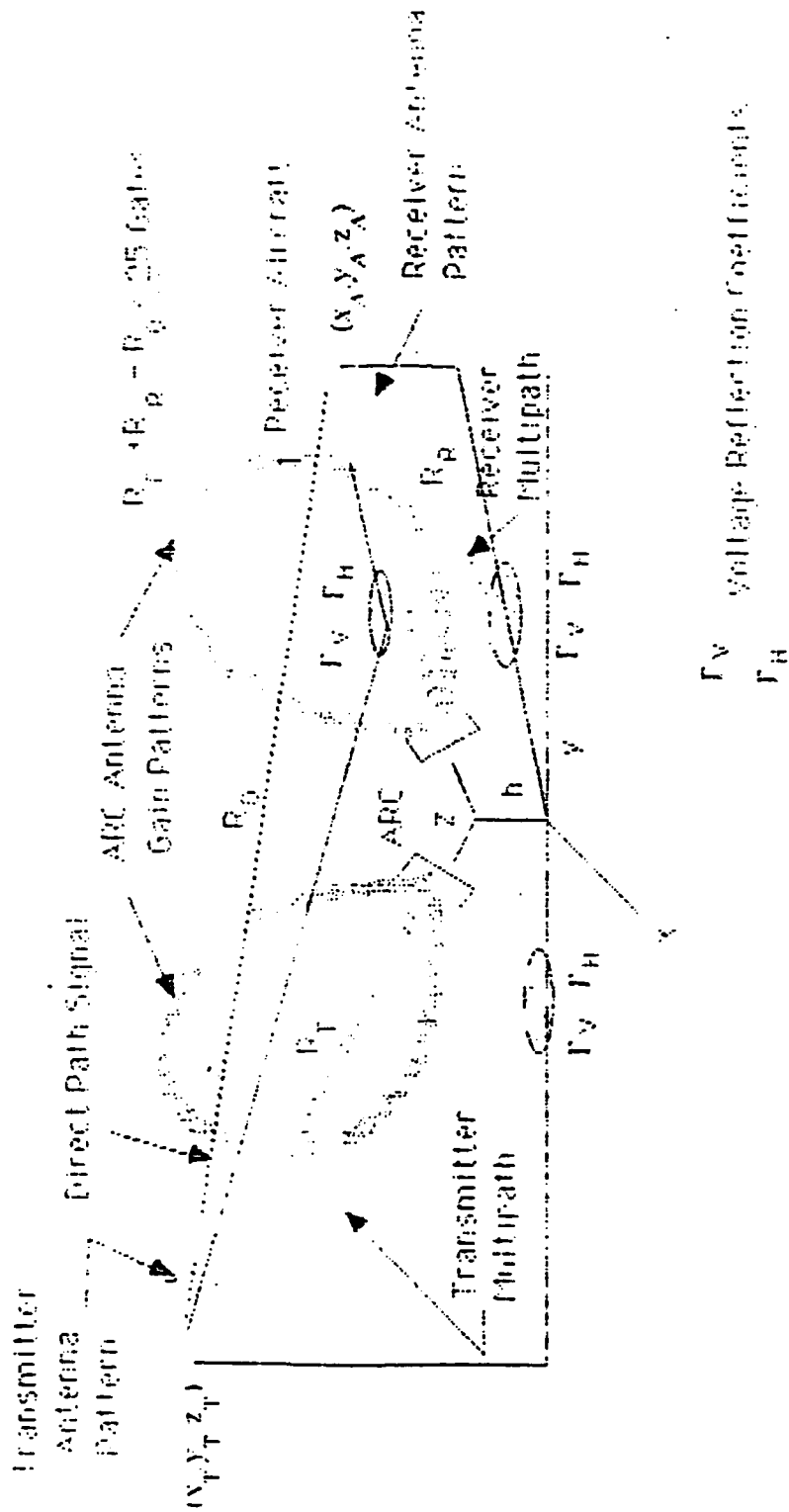
Thus, using ERIM's individual system error component estimates in a slightly different manner leads to system calibration accuracy estimates significantly better than their ± 5 dB value.

3.0 ACTIVE RADAR CALIBRATOR (ARC) MULTIPATH ANALYSIS

The potential severity of multipath on ARC calibration signals at low grazing angles was also identified at the January 1987 CMP PDR. In order to assess the magnitude of this problem for specific CMP test matrix geometries, a simulation was created which modeled the important system, geometric, and electromagnetic factors associated with this problem. Reference 2 material was used as a basis for this simulation. An illustration of the simulation is shown in Figure 3-1. Antenna pattern effects were modeled for both the aircraft and ARC. Scattering was assumed to arise from the specular point with a unity reflection coefficient (i.e., a worst case assumption) and normalized with respect to the direct path signal. Questions addressed with this simulation included (1) what is the magnitude of multipath fading for each CMP data collection geometry? (2) would a narrower ARC elevation antenna pattern reduce the problem? (3) how large must the grazing angle be to mitigate multipath?

3.1 SEVERITY OF MULTIPATH ON CANDIDATE GEOMETRIES

The magnitude of multipath fading on the proposed test matrix geometries under the above assumptions is shown in Figure 3-2. Since the phase of the multipath signal is unknown, worst case values of 0 degrees and 180 degrees were assumed. That is, in the former case, the multipath signal will add to the direct signal (Max Positive Error) and in the latter it will subtract (Max Negative Error). The results shown in Figure 3-2 indicate that an ARC signal may nearly be cancelled in some instances. In contrast, if the direct path signal and multipath signal are in phase, a positive 6 dB error may result. This is obviously an



Γ_V Voltage Reflection Coefficients
 Γ_H

Figure 3-1 ARC Multipath Simulation Illustration

Figure 3-2 Magnitude of Multipath Fading

ARC MULTIPATH SENSITIVITY ANALYSIS FOR TEST MATRIX GEOMETRIES

TEST MATRIX CASE	MAX POSITIVE ERROR (DB)	MAX NEGATIVE ERROR (DB)
20 DEGREE ILLUMINATOR (CASE 1)	2.1	-2.8
35 DEGREE ILLUMINATOR (CASE 2)	0.9	-1
RECEIVER CASES 1 AND 2 (10 DEGREE SCATTERING ANGLE)	4.75	-11.51
RECEIVER CASES 3, 4, 5 (30 DEGREE SCATTERING ANGLE)	5.8	-10.63
RECEIVER CASES 6, 7, 8, 9, 10 (20 DEGREE SCATTERING ANGLE)	5.07	-8.82
RECEIVER CASES 11 AND 12 (30 DEGREE SCATTERING ANGLE)	6.0	-6.22
45 DEGREE ILLUMINATOR (CASE 3)	3.3	-12.8
15 DEGREE ILLUMINATOR (CASE 4)	5.07	-10.5
45 DEGREE ILLUMINATOR (CASE 5, 6, 7, 8, 9, 10)	1.4	-1.69
RECEIVER CASES 13 (10 DEGREE SCATTERING ANGLE)	3.9	-10.8
RECEIVER CASES 14 (30 DEGREE SCATTERING ANGLE)	0.87	0.98

intolerable situation.

3.2 ARC ANTENNA BEAMWIDTH SENSITIVITY

It was thought that by reducing the elevation beamwidth of the ARC antenna, the specular region responsible for the multipath reflection could be placed outside its mainbeam. Using a figure of merit based on a Max Positive Error and Max Negative Error of 1 dB or less, the beamwidth and equivalent aperture size of the ARC antenna versus grazing angle was computed. The results are shown in Figure 3-3. Since the ARC must have antennas facing the receiver and transmitter, all grazing angles are considered. It is quite clear from Figure 3-3 that antenna apertures for grazing angles less than 10 degrees are impractical. As a rule-of-thumb, it appears that an ARC beamwidth should be about one-half of the grazing angle to avoid multipath (for grazing angles less than 10 degrees).

3.3 AVOIDANCE OF MULTIPATH USING TRANSFER CALIBRATION

Since a simple solution to the multipath did not appear feasible based on the previous analyses, the simulation was used to find a minimum grazing angle and other geometric constraints resulting in multipath fading effects of less than 1 dB on either leg of the bistatic geometry. Having identified such a geometry, it was felt that external system calibration could be performed in that geometry and the results would be readily transferable to the proposed data collection cases. This approach to external system calibration has been called "transfer calibration" by ERIM. Thus, the ARC signal received during a data collection pass would not be used for signal calibration. However, it is still necessary for accurate range gate position determination required during data processing.

Figure 3-4 shows a geometry which limits the extreme multipath fades to less than 1 dB. Note that the transmitter aircraft is at its proper altitude and that the receiver aircraft has only to descend to achieve its desired data collection altitude. In addition, the direct path signal will not interfere with the bistatic ARC signal.

Figure 3-3 ARC Beamwidth Versus Grazing Angle for Multipath Elimination

ARC BEAMWIDTH TO MITIGATE MULTIPATH

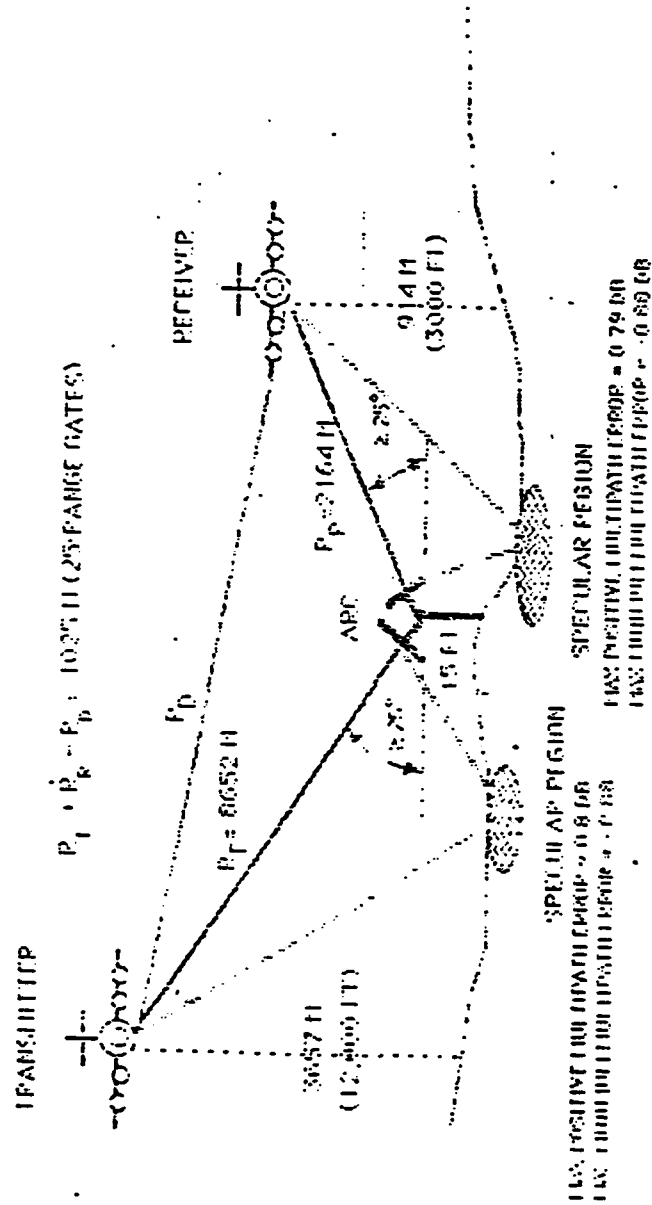
RECEIVER GRAZING ANGLE (DEGREES)	ARC ELEVATION BEAMWIDTH (DEGREES)
0.5	0.51 (26 X 26 FD)
2.0	2.15 (6.4 X 6.4 FD)
4.0	2.75 (5.0 X 5.0 FD)
10	5.54 (2.5 X 2.5 FD)
TRANSMITTER GRAZING ANGLE	
20	10.0 (0.73 X 0.73 FD)
45	22.2 (0.62 X 0.62 FD)

BASED ON POSITION OF MULTIPATH TO 1.0°

IN CURRENT ARC BEAMWIDTH IS 40 DEGREES (0.3 X 0.3 FD)

Figure 3-4 Multipath Avoidance Geometry

FLIGHT GEOMETRY RECOMMENDED FOR ARC CALIBRATION



- 1. USE ABOVE GEOMETRY FOR PARAP CALIBRATION PASSES
- 2. USE POSITIVE ORIGIN FOR SPECULAR REGION
- 3. USE POSITIVE ORIGIN FOR SPECULAR REGION
- 4. USE POSITIVE ORIGIN FOR SPECULAR REGION
- 5. USE POSITIVE ORIGIN FOR SPECULAR REGION

REFERENCES

1. Papa, R. J., Rao, K. V. N., Lennon, J. F., Coffey, J. W., "A Survey of Terrain Scattering Theory and Measurements for Air Force Systems," Rome Air Development Center, Air Force Systems Command, Griffiss Air Force Base, RADC-TR-84-78, April 1984 (Restricted Distribution).
2. Barton, D.K., "Low-Angle Radar Tracking," Proceedings of the IEEE, Vol. 62, No. 6, June 1974.

DESIGN PLAN
SIGNAL PROCESSING MODULE DEVELOPMENT SCHEDULE
ELIN A003

CONTRACT TITLE: BISTATIC CLUTTER PHENOMENOLOGICAL
MEASUREMENT/MODEL DEVELOPMENT

CONTRACT NUMBER: F30602-86-C-0045

CONTRACT PERIOD: 1 APRIL 1986 TO 30 SEPTEMBER 1987

PREPARED BY: CHARLES H. HIGHTOWER

DATE: 1 JULY 1987

Prepared for:
ROME AIR DEVELOPMENT CENTER
GRIFFISS AIR FORCE BASE
NEW YORK 13441-5700



ADVANCED TECHNOLOGY DIVISION
17252 ARMSTRONG AVENUE
IRVINE, CALIFORNIA 92714
(714) 250-4206

1.0 INTRODUCTION

The purpose of this document is to provide a plan for development of signal processing software required to support the Clutter Measurements Program (CMP) Contract No. F30602-86-C-0045. Applicable documents include:

1. Design Plan, Computer Compatible Tape Interface Specification, ELIN A003, SRS Technologies, SRS UR87-114, 12 June 1987
2. Design Plan, Flight Data Processing Software Functional Specification, ELIN A003, SRS Technologies, SRS UR87-116, 15 June 1987.

Item 1 describes the data structure of the Computer Compatible Tapes (CCT's) that will be provided by the Environmental Research Institute of Michigan (ERIM) for signal processing and data analysis. Item 2 describes signal processing functional requirements and provides the logical organization of the software modules that will be implemented by SRS Technologies in support of CMP.

As a point of clarification, signal processing is used in this document to describe operations performed in the conversion of CCT digitized clutter samples to calibrated scattering coefficient data. Signal processing enhances the accuracy and capabilities of the flight data collection system. In contrast, data analysis describes operations performed on the calibrated scattering coefficient data to validate clutter models, obtain clutter statistics, and other related analyses. This document deals only with signal processing, it does not address data analysis which will be accomplished later in the program.

2.0 HIERARCHICAL SOFTWARE ORGANIZATION

A structured approach in the development of CMP signal processing is planned. In order to initiate this process, the overall software has been functionally organized into the modules and submodules shown in Table 2-1. These modules exhibit a high level of cohesion (i.e., all activities in a module are functionally related) and a minimum of coupling between modules (particularly, pathological dependence of the internal operation of one module on the internal operations of another module). A high-level description of the modules is given in Attachment 2.

3.0 PROGRAMMING STANDARDS AND CONVENTIONS

3.1 STANDARDS

Programming design and coding will adhere to basic conventions of structured programming that emphasize the following control structures (1) SEQUENCE, (2) IF-THEN-ELSE, (3) DO-WHILE, (4) DO-UNTIL, and (5) CASE. Branching statements (GO TO's) should pass control only to a statement in the same procedure (subroutine) of a module. Backward jumps should be minimized.

Code will be written in FORTRAN 77 as implemented by Digital Equipment Corporation for use on VAX series machines. Each module shall contain internal documentation describing its (1) name and function, (2) inputs and outputs, (3) internal and external variables (types defined), (4) subroutines called, and (5) revision number, date of revision, and creator.

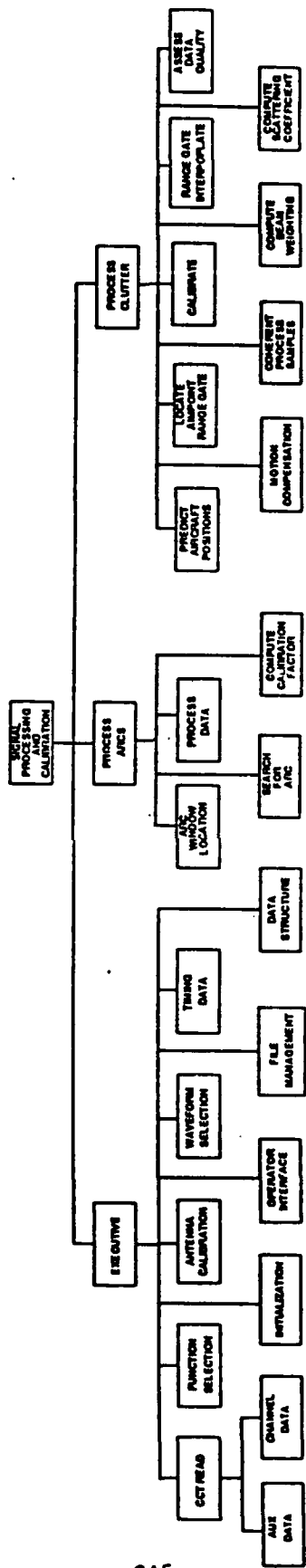


FIGURE 2-1 CMP SIGNAL PROCESSING SOFTWARE MODULE HIERARCHY

The preferred method of passing variables that are to be modified is through a parameter list rather than a common data area. However, because of the large amount of data to be processed, this may not be efficient. If this is the case, common data shall be well documented in the internal module description and design specification.

Prior to initiation of module coding, a "module mini-specification" shall be prepared and approved by the program manager, project engineer, and programmer(s). The mini-specification shall be a brief document (of one or two pages at most). A sample mini-specification is shown in Attachment 1.

Each programmer will be responsible for maintenance and backup of their own code. The project leader shall be responsible for maintaining the latest version of the individual modules and overall signal processing software including adequate backups. Changes to modules must be approved by the project leader prior to implementation in the baseline code.

3.2 CONVENTIONS

The following conventions shall be followed in the development of CMP signal processing software.

Parameters that depend on system assumptions or might be changed during the course of the CMP effort (e.g., number of data records, transmit power, number of ARC's, etc.) should be treated as symbolic parameters. In fact, such seemingly fixed parameters such as the number of receiver channels or even the speed of light should also be treated in this manner.

Naming conventions should be uniform throughout the software. Program, subprogram, module, procedure, routine and data names should be uniquely chosen to identify the applicable function performed. Naming conventions should not be cryptic and should be easy to understand and remember.

4.0 SCHEDULE

Development of the CMP signal processing software is planned to take place from 1 July 1987 to 30 September 1987. Since a real CCT tape will not be available until the following summer, testing will be accomplished using an internally generated CCT emulation. Because of the short time available for development of the signal processing software, CCT emulation will be limited to creating data of the correct type and format. Simulation of clutter and ARC signals from moving platforms will not be done.

A development schedule for the signal processing software is shown in Figure 4-1 in the form of a PERT chart. The main development paths are (1) Executive module, (2) Process Clutter, (3) and Process ARC modules. The ARC Process module utilizes much of the same software developed for the Process Clutter module so it is scheduled for development after the Process Clutter code has been completed.

Each path has been converted to a task timeline schedule and shown in Figures 4-2 (Executive Module), 4-3 (Process Clutter Module), and 4-4 (Process ARC Module).

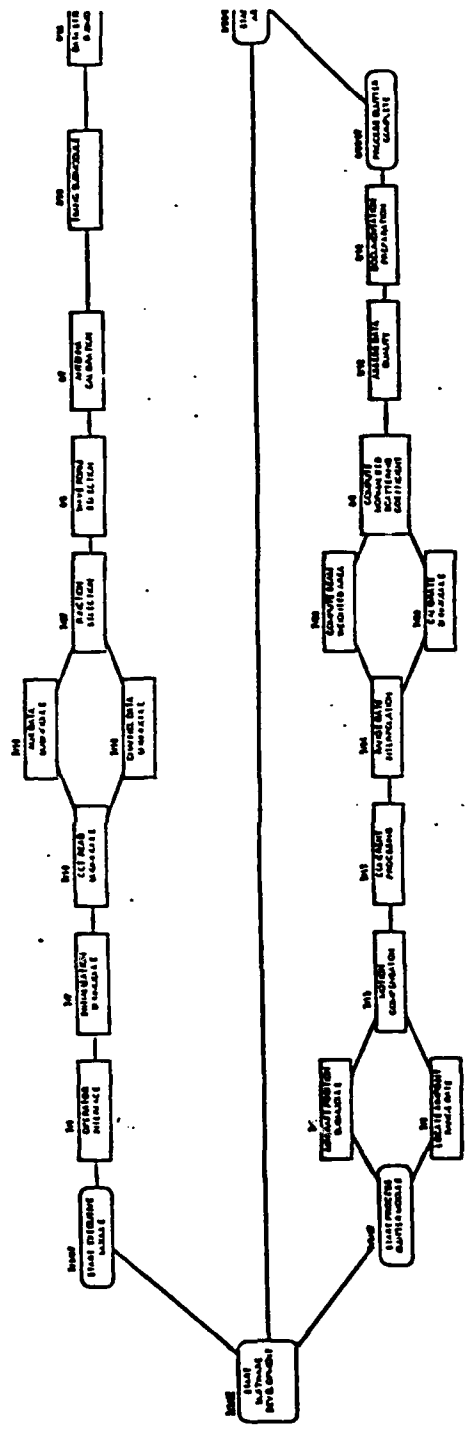


Figure 4-1 CMP Signal Processing Software Development Schedule

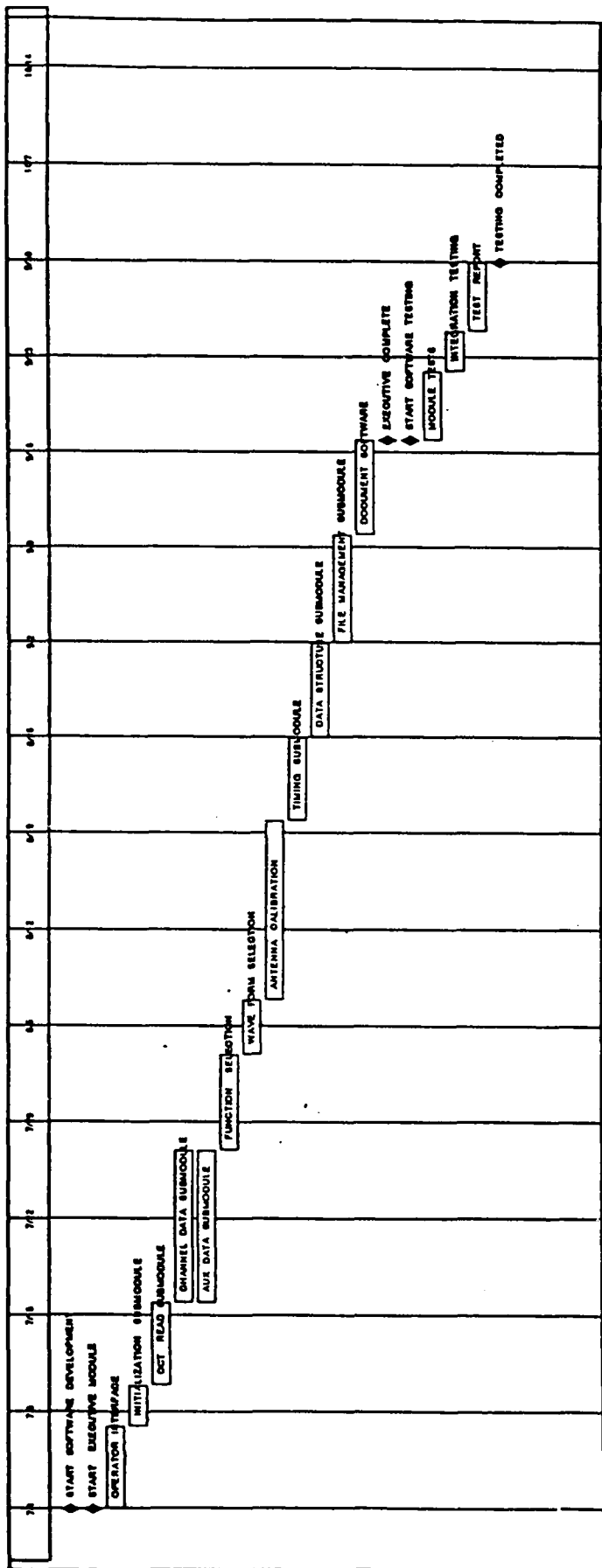


Figure 4-2 Executive Module Schedule

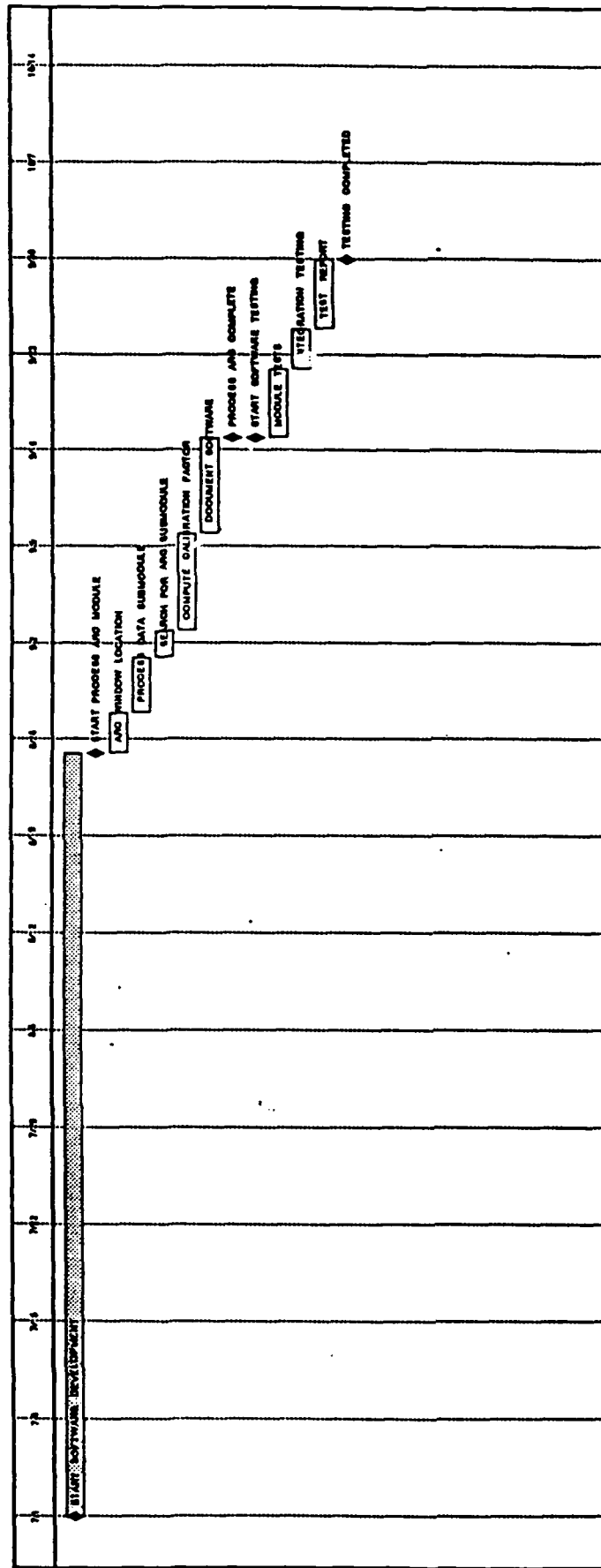


Figure 4-3 Process ARCS Module Schedule

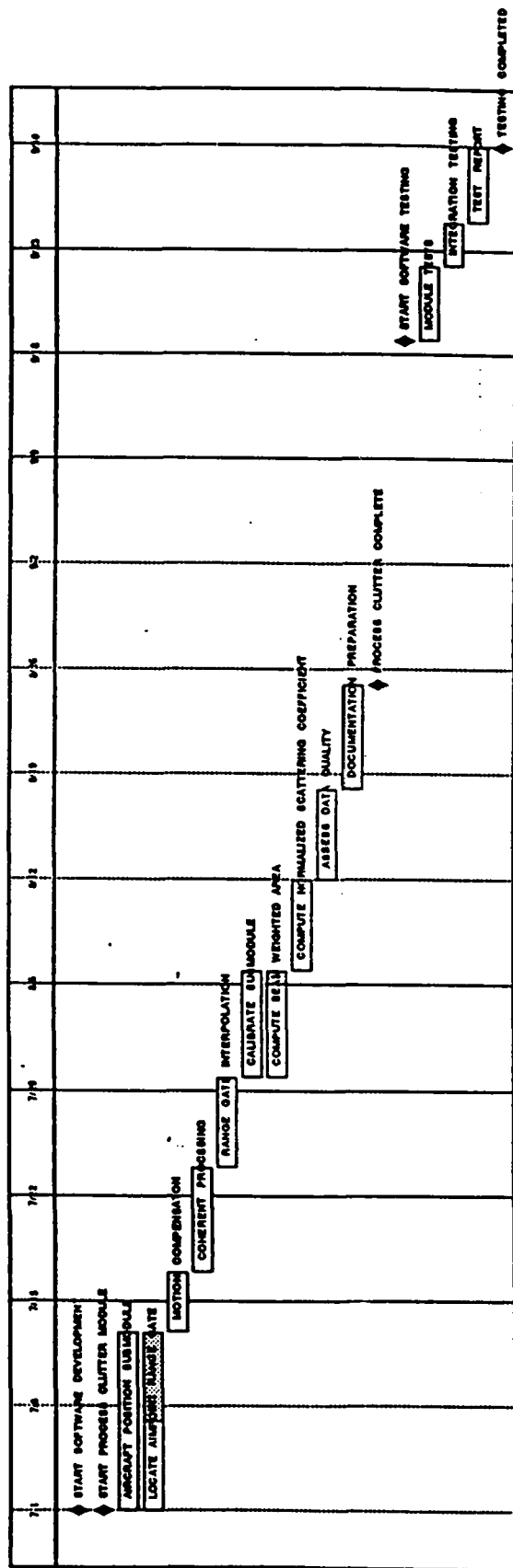


Figure 4-4 Process Clutter Module Schedule

5.0 PROJECT ORGANIZATION

The Signal Processing Software (SPS) team will be organized as shown in Figure 5-1.

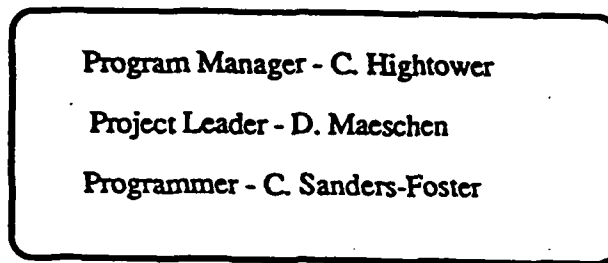


Figure 5-1 Signal Processing Software Development Team

ATTACHMENT 1 - SAMPLE MODULE MINI-SPEC FORMAT

MODULE: Clcopy

FUNCTIONAL DESCRIPTION:

The clutter copy module copies a set of CCT clutter tapes to a disk file for processing. The multivolume set of tapes should correspond to a specific mission and pass. The tapes are 2400 ft 1600 bpi track tapes. They consist of 1942 byte records, and they are copied to an unformatted sequential file for processing by the clutter processing program. The file is named MiPj.DAT where i and j are the mission and the pass numbers.

The procedure is as follows. The initial tape...

INPUT VARIABLES:

MISSION, IPASS I*4, I*4 Mission, Pass

OUTPUT VARIABLES:

INTERNAL VARIABLES:

IRECORDLENGTH	I*4	Record Length (bytes)
IRECORD(IRECORDLENGTH)	I*1	Record
IEOF	I*4	End of File Flag

SUBMODULES: None

SUPERMODULES: None

INTERMODULE DEPENDENCIES:

The output file is processed by the clutter executive module, Clxec, in the program Clproc.

NOTATIONS:

Clname indicates CLutter *NAME* of program or module.

ALGORITHMS: None

REFERENCES: None

LENGTH: 103 Lines; 2586 Bytes

CURRENT REVISION DATE:PREVIOUS REVISION DATE: 7 July 1987: None

CREATOR: David M. Maeschen

LANGUAGE: FORTRAN 77

SYSTEM: VAX 11/750 VMS 4.3

SUPPORT: Uses the tape drive MSA0

APPROVALS:

Program Manager: _____

Project Engineer: _____

Programmer: _____

ATTACHMENT 2 - MODULE DESCRIPTION

EXECUTIVE MODULE

The EXECUTIVE module controls execution of the CMP signal processing software and performs other utility functions. Submodules within the EXECUTIVE module will perform initialization (INITIALIZATION), read the CCT data from tape or disk and separate aircraft/system data (AUX DATA) from radar clutter data (CHANNEL DATA). This information will be stored (FILE MANAGEMENT) in a data structure (DATA STRUCTURE) allowing other modules access to it. Since several passes through this data are necessary prior to signal processing, a function selection (FUNCTION SELECTION) submodule will determine the desired process (e.g., aircraft state vector extraction, antenna calibration data extraction, etc.).

The operator will control the signal processing software via the OPERATOR INTERFACE submodule. Antenna calibration table creation and waveform selection will be accomplished by the ANTENNA CALIBRATION and WAVEFORM SELECTION submodules. The latter submodule identifies the waveform associated with each of the possible eight channels and determines if stepped gain is being used. The number of samples in a given channel for coherent processing is also controlled by this submodule. Any timing information needed by the remaining processing modules or submodules will be handled by the TIMING DATA submodule.

There are eleven submodules in the EXECUTIVE module.

PROCESS ARCS MODULE

This module processes CCT pass data to create a calibration table between 6-bit A/D samples and normalized RCS for each data channel. In order to accomplish this, portions of the data containing ARC signals must be identified and ARC signal detection performed. The submodules ARC WINDOW LOCATION, SEARCH FOR ARC and PROCESS DATA perform these functions. PROCESS DATA includes coherent processing, range gate interpolation, and aircraft position error compensation.

The ARC data will provide a known normalized RCS value for a particular set of I & Q A/D samples that will be computed by the COMPUTE CALIBRATION FACTOR submodule. This submodule will also utilize the internal calibration data recorded before and after each pass to establish a receiver transfer function curve about the ARC reference point. If differences exist between the pre and post pass internal calibration data, this information will be sent to the ASSESS DATA QUALITY submodule which is discussed in the PROCESS CLUTTER MODULE section.

This process will be performed for both monostatic and bistatic ARC and internal calibration data. The PROCESS ARCS MODULE contains four submodules.

PROCESS CLUTTER MODULE

Processing performed by this module will result in a time series of calibrated normalized surface scattering coefficients for later data analysis. In order to accomplish this, the position of each aircraft will be determined by the PREDICT AIRCRAFT POSITIONS submodule. The aimpoint range gate will be accurately calculated by the LOCATE AIM POINT RANGE GATE submodule. If necessary, the I & Q data will be motion compensated using INS acceleration information recorded on the AUX data record by the MOTION COMPENSATION submodule. Several range gates about the aim point location will be coherently processed to remove sidelobe clutter by the COHERENT PROCESS SAMPLES submodule. Calibration of the samples with the Doppler frequencies corresponding to that of the aim point using ARC and internal calibration data will be achieved by the CALIBRATE submodule.

Since the aim point range will not always correspond to a range gate time, it will be necessary to interpolate the RCS at the aimpoint using data from several of the surrounding gates by the RANGE GATE INTERPOLATION submodule. Antenna gain effects are introduced into the processing by the COMPUTE BEAM WEIGHTING submodule. The beam weights corresponding to the aimpoint range and Doppler cell are then used by the COMPUTE SCATTERING COEFFICIENT submodule to compute the desired clutter scattering coefficient .

The above process will be performed for both monostatic and bistatic data. In addition, an ASSESS DATA QUALITY submodule will be active throughout this process to provide an indication of the quality of the data. Quantities such as external calibration factor variance from a calculated calibration factor based on pre and post pass internal calibration data, minimal ARC signal strength, excessive aircraft position errors, excessive aircraft velocity errors, excessive heading errors, excessive acceleration errors, and excessive transmitter power variations will be used to set a data quality flag and brought to the attention of the operator.

The PROCESS CLUTTER module contains nine submodules.

DESIGN PLAN
COMPUTER COMPATIBLE TAPE
INTERFACE SPECIFICATION
ELIN A003

CONTRACT: BISTATIC CLUTTER PHENOMENOLOGICAL
MEASUREMENT/MODEL DEVELOPMENT

CONTRACT NUMBER: F30602-86-C-0045

CONTRACT PERIOD: 1 APRIL 1986 TO 30 SEPTEMBER 1987

PREPARED BY: CATHERINE SANDERS-FOSTER

DATE: 17 AUGUST 1987

Prepared For:
ROME AIR DEVELOPMENT CENTER
GRIFFISS AIR FORCE BASE
NEW YORK 13441-5700

VERSION 5.0

TABLE OF CONTENTS

1.0 INTRODUCTION

- 1.1 PURPOSE OF DOCUMENT
- 1.2 TAPE CHARACTERISTICS
- 1.3 ORGANIZATION OF DOCUMENT

2.0 CCT FORMAT DEFINITION OVERVIEW

- 2.1 STANDARD RECORD FORMAT
- 2.2 RECORD TYPE
 - 2.2.1 PASS-HEADER RECORD
 - 2.2.2 ATTENUATION RECORDS
 - 2.2.3 ANTENNA PATTERN RECORDS
 - 2.2.4 AUXILIARY DATA RECORDS
 - 2.2.5 CHANNEL DATA RECORDS

3.0 CCT FORMAT DETAILED DEFINITION

- 3.1 PASS-HEADER RECORD DEFINITION
- 3.2 ATTENUATION RECORD DEFINITION
- 3.3 ANTENNA PATTERN RECORD DEFINITION
- 3.4 AUXILIARY DATA RECORD DEFINITION
- 3.5 CHANNEL DATA RECORD DEFINITION

APPENDIX A
APPENDIX B

ACRONYMS
LIST OF REQUIREMENTS

LIST OF FIGURES

NUMBER	TITLE
1	Computer Compatible Tape Format Definition
2	Computer Compatible Tape Size Calculations
3	Computer Compatible Tape Record Type Definition
4	Computer Compatible Tape Record Format
5	Computer Compatible Tape Pass-Header Record
6	Computer Compatible Tape Auxiliary Data Record
7	Computer Compatible Tape Channel Data Record
8	Computer Compatible Tape Channel 1 - 8 Sub-Record

LIST OF TABLES

Pass-Header Record Format

Attenuation Record Format

Antenna Pattern Record Format

Auxiliary Data Record Format

Channel Data Record Format

CMP DATA TAPE FORMAT DESCRIPTION

17 AUGUST 1987

1.0 INTRODUCTION

1.1 PURPOSE OF DOCUMENT

The Clutter Measurements Program (CMP), designed to collect bistatic clutter data for Hybrid Bistatic Radar Concept Evaluation, will generate pass data which will be stored on Computer Compatible Tape (CCT) after post processing. The recommended CCT format is described in this document.

A single data collection mission will consist of sixteen passes. Each pass will be contained on a separate set of CCT data tapes. Each CCT set will consist of about 2 1/2, 2400 ft. tapes. The information for each pass will include: (1) pass identification data, (2) calibration data, (3) pass characteristic data, (4) location data and (5) radar channel data.

1.2 TAPE CHARACTERISTICS

In order to make the CCT readable on most computer systems, the tape shall conform to level 3 of the ANSI standard (American National Standard X3.27-1978) for labeled magnetic tapes.

The characteristics of the tape are as follows:

9 tracks per tape

1600 bpi

1 file per pass (2 or 3 tapes)

Fixed length records

1964 bytes per record

Five record categories:

(1) Pass-Header record

(4) Auxiliary data records

(2) Attenuation records

(5) Channel data records

(3) Antenna Pattern records

1.3 ORGANIZATION OF DOCUMENT

The format of this computer compatible tape (CCT) will be discussed in the following manner. First the standard tape format will be discussed, followed by the standard record format and a general overview of each of the five

record types. Finally, each record type will be addressed separately, starting with a more specific overview. An exact definition for the contents of each record type will be given, including units, record sizes and any other applicable qualifications.

2.0 CCT FORMAT DEFINITION OVERVIEW

The flight information for each pass shall be stored on a set of Computer Compatible Tapes. Antenna Pattern calibration data obtained on other flights will also be written on the CCT so it will contain all information required for processing. The tapes will have all the standard ANSI labeled tape headers. The first block of information on the tape will be the Pass-Header record, followed by the Attenuation record, the Antenna Pattern records and the first Auxiliary Data record for the pass. One Auxiliary Data record will be written for each 0.1 seconds of the pass. Following each Auxiliary Data record will be 0.1 seconds of Channel Data records. Figure 1 illustrates the tape layout. Figure 2 details the size calculations and the space necessary to store the records for one pass. Seventy-six Mbytes of storage are required per pass, which is approximately 2 1/2, 2400 ft., 1600 BPI mag tapes per pass. The pass file on the tape shall be continued to the other tapes using ANSI file continuation labels.

2.1 STANDARD RECORD FORMAT

The standard fixed length record format will contain 1964 bytes. The first four bytes are the record header. The record header indicates the type of record that follows. Figure 3 lists the numbers associated with each record type. The next eight bytes will contain the common record number. The common record number is an integer*8 format. The remaining 1952 bytes will contain the data inherent to that particular record type. Figure 4 illustrates the generic record format.

2.2 RECORD TYPE

As indicated above, the five record types are: Pass-Header Record, Attenuation Record, Antenna Pattern Record, Auxiliary Data Record and Channel Data Record. In all five cases, the first twelve bytes contain the same information, the record type and the record number. However, this is where the similarity ends.

2.2.1 PASS-HEADER RECORD

The Pass-Header Record contains mission and pass identification information, ARC calibration information, synchronization information, Channel polarizations and attenuator settings. It contains mission information, such as number, title, date and time. It also contains pass information, such as number and time. It contains transmitter and receiver starting and ending waypoints, altitudes, boresight ranges and various angles. Pulse information is given, such as pulse lengths, sample intervals, range gate delays and number of range gates. ARC calibration information includes positions, power

Computer Compatible Tape Format Definition

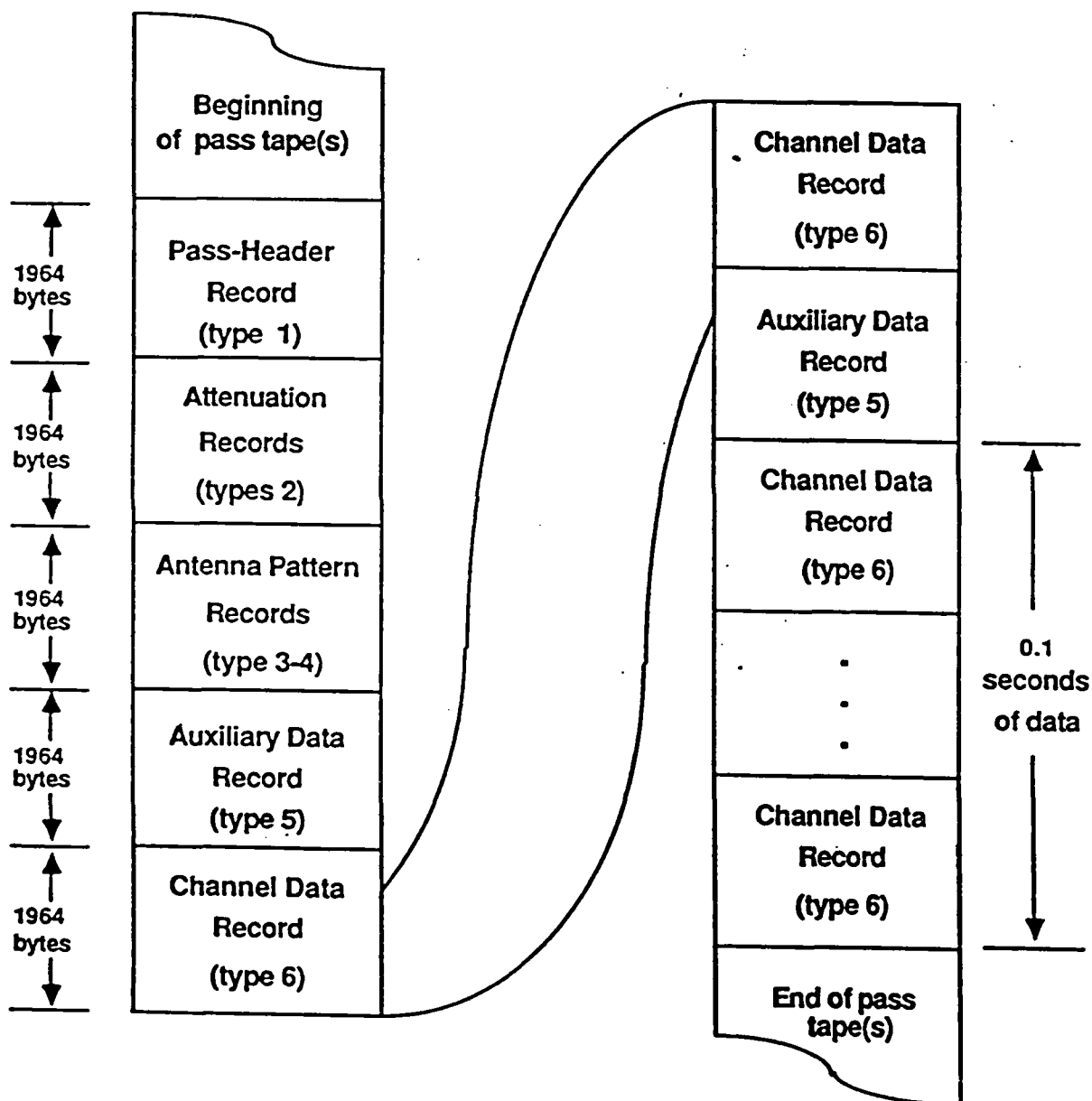


Figure 1

Computer Compatible Tape Size Calculations

Figure 2

Records for One Pass:

- 1 Pass-Header Record
- 1 Attenuation Record
- 40 Antenna Pattern Records
- 3000 Auxiliary Data Records
- 37500 Channel Data Records

40542 Total Records per Pass (1964 bytes per record)

Tape Size:

$$\frac{40542 \text{ REC}}{\text{PASS}} \times \frac{1964 \text{ BYTES}}{\text{REC}} \times \frac{1 \text{ MBYTE}}{1,048,576 \text{ BYTES}} = 75.94 \text{ MBytes per Pass}$$

Which Is 2 or 3, 2400 ft., 1600 BPI Mag Tapes per Pass.

Auxiliary Record Calculation:

$$\frac{5 \text{ MIN}}{\text{PASS}} \times \frac{10 \text{ AUX RECORDS}}{\text{SEC}} \times \frac{60 \text{ SEC}}{\text{MIN}} = 3000 \text{ Auxiliary Data Records}$$

Channel Data Record Calculation:

$$\frac{5 \text{ MIN}}{\text{PASS}} \times \frac{4000 \text{ PULSES}}{\text{SECOND}} \times \frac{\text{CHAN}}{\text{PULSE}} \times \frac{80 \text{ SAMP}}{\text{CHAN}} \times \frac{6 \text{ BIT}}{\text{SAMP}} \times \frac{\text{BYTE}}{8 \text{ BITS}} \times \frac{\text{REC}}{1920 \text{ BYTE}} \times \frac{60 \text{ SEC}}{\text{MIN}} = 37,500 \text{ Channel Data Records}$$

Computer Compatible Tape Record Type Definition

Type Number	Description
1	Pass-Header Record
2	Attenuation Record
3	Antenna Pattern Calibration Record 1
4	Antenna Pattern Calibration Record 2
5	Auxiliary Data Record
6	Channel Data Record

Figure 3

Computer Compatible Tape Record Format

BYTE

1 - 4

Record Type Indicator

Record
Header

5

bit 7

bit 0

6

bit 15

bit 8

7

bit 23

bit 16

8

bit 31

bit 24

9

bit 39

bit 32

10

bit 47

bit 40

11

bit 55

bit 48

12

bit 63

bit 56

Record
Number

13 - 1964

Record Data

Figure 4

gains, time delays, doppler offsets and another set of related angles. Clutter patch information is also included. Finally, the nominal geometry information is included in this record. The Pass-Header record format is illustrated in Figure 5.

2.2.2 ATTENUATION RECORD

The Attenuation Record contains six bit samples of receiver output for both in-phase and quadrature, in the form of $I^2 + Q^2$. Only post-pass attenuation records will be provided. Signal Power levels will also be included in these records. Up to five signal increments are possible and up to seventy-one attenuator settings for both in-phase and quadrature samples.

2.2.3 ANTENNA PATTERN RECORDS

The Antenna Pattern records contain the orientation pedestal angles, pitch, roll and yaw. There can be up to ten antenna patterns per plane, and two records per pattern. Each record contains the number of antenna patterns, ID number, antenna orientation, initial, final and delta azimuth and elevation angles, and the gain for each set of azimuth and elevation positions. There are a up to 10 azimuth and 30 elevation positions. If not all azimuth and elevation positions are used, the remainder of the matrix is filled with zeros.

2.2.4 AUXILIARY DATA RECORD

The Auxiliary Data Record contains additional information about the bistatic transmitter and the monostatic-bistatic receiver. This information includes: beacon coordinates, Aircraft true heading and altitude, velocity, bistatic and monostatic acceleration, and power meter readings, commanded antenna angles, and the delta of the commanded angles. Again, a large portion of the record is not used, as indicated in Figure 6.

2.2.5 CHANNEL DATA RECORD

The Channel Data Record consists of four sub-records(See Figures 7 & 8). Each sub-record is 488 bytes long. The first eight bytes are the pass pulse number. The remaining 480 bytes are divided into eight 60 byte parts, one for each channel. Each part contains eighty, six bit digital samples for one channel. The samples are alternated, one in-phase sample followed by one quadrature sample for each of forty gates. These samples represent the bulk of the collected data.

3.0 CCT FORMAT DETAILED DEFINITION

3.1 PASS-HEADER RECORD DEFINITION

The Pass-Header Record contains all of the mission and pass information necessary to identify the data taken from any pass in the experiment. This information includes mission number, title, date and time, and pass number and

Computer Compatible Tape Pass-Header Record

BYTE

1 - 4	Record Header
5 - 12	Record Number
13 - 16	Mission Number
17 - 76	Mission Title
77 - 82	Mission Date
83 - 86	Mission Time
87 - 90	Pass Number
91 - 94	Pass Time
95 - 110	Channel 1-8 Polarizations
111 - 142	Channel 1-8 Attenuator Settings
143 - 150	Channel Type
151 - 158	BS Range Gate Delay
159 - 162	BS Sample Interval
163 - 166	BS Pulse Length
167 - 170	BS Samples
171 - 178	BS Altitude
179 - 194	BS Start Map Waypt.(lat,long)
195 - 210	BS End Map Waypt.(lat,long)
211 - 218	BS Boresight Azimuth Angle

Figure 5

Computer Compatible Tape Pass-Header Record

BYTE

219 - 226	BS Boresight Elevation Angle
227 - 234	BS Boresight Range
235 - 242	BS Grazing Angle
243 - 250	BS Squint Angle
251 - 258	MS Range Gate Delay
259 - 262	MS Sample Interval
263 - 266	MS Pulse Length
267 - 270	MS Samples
271 - 278	MS Altitude
279 - 294	MS Start Map Waypt.(lat,long)
295 - 310	MS End Map Waypt.(lat,long)
311 - 318	MS Boresight Azimuth Angle
319 - 326	MS Boresight Elevation Angle
327 - 334	MS Boresight Range
335 - 342	MS Grazing Angle
343 - 350	MS Squint Angle
351 - 366	Start Clutter (lat,long)
367 - 382	End Clutter (lat,long)

Figure 5 (cont.)

Computer Compatible Tape Pass-Header Record

BYTE

383 - 390	Start Clutter Altitude
391 - 398	End Clutter Altitude
399 - 402	Number of ARCs
403 - 406	ARC ID
407 - 430	ARC Position (X,Y,Z)
431 - 446	ARC Position (lat,long)
447 - 454	ARC Altitude
455 - 456	ARC Receiver Polarization
457 - 460	ARC Time Delay
461 - 464	ARC Doppler Offset
465 - 466	ARC BS Transmitter Polarization
467 - 474	BS ARC Power Gain
475 - 482	BS Receiver Azimuth Angle
483 - 490	BS Receiver Elevation Angle
491 - 492	ARC MS Transmitter Polarization
493 - 500	MS ARC Power Gain
501 - 508	MS Recv.&Trans. Azimuth Angle
509 - 516	MS Recv.&Trans. Elevation Angle
517 - 1388	ARCs 2 through 10

Figure 5 (cont.)

Computer Compatible Tape Auxiliary Data Record

BYTE	
1 - 4	Record Header
5 - 12	Record Number
13 - 16	Major Count
17 - 20	Minor Count
21 - 44	BS Beacon Coordinate (X, Y, Z)
45 - 52	INS BS A/C Velocity (N/S)
53 - 60	INS BS A/C Velocity (E/W)
61 - 108	BS Acceleration
109 - 116	BS INS True Heading
117 - 124	BS INS Roll
125 - 132	BS INS Pitch
133 - 140	BS INS Yaw
141 - 148	Commanded BS Roll
149 - 156	Commanded BS Pitch
157 - 164	Commanded BS Yaw
165 - 172	Delta Commanded BS Roll
173 - 180	Delta Commanded BS Pitch
181 - 188	Delta Commanded BS Yaw
189 - 204	BS Power Meter
205 - 212	BS Radar Word
213 - 236	MS Beacon Coordinate (X,Y,Z)
237 - 244	INS BS A/C Velocity (N/S)

Figure 6

Computer Compatible Tape Auxiliary Data Record

BYTE

245 - 252	INS MS A/C Velocity (E/W)
253 - 300	MS Acceleration
301 - 308	MS INS True Heading
309 - 316	MS INS Roll
317 - 324	MS INS Pitch
325 - 332	MS INS Yaw
333 - 340	Commanded MS Roll
341 - 348	Commanded MS Pitch
349 - 356	Commanded MS Yaw
357 - 364	Delta Commanded MS Roll
365 - 372	Delta Commanded MS Pitch
373 - 380	Delta Commanded MS Yaw
381 - 396	MS Power Meter
397 - 404	MS Radar Word
405 - 1964	Not Used

Figure 6 (cont.)

Computer Compatible Tape Channel Data Record

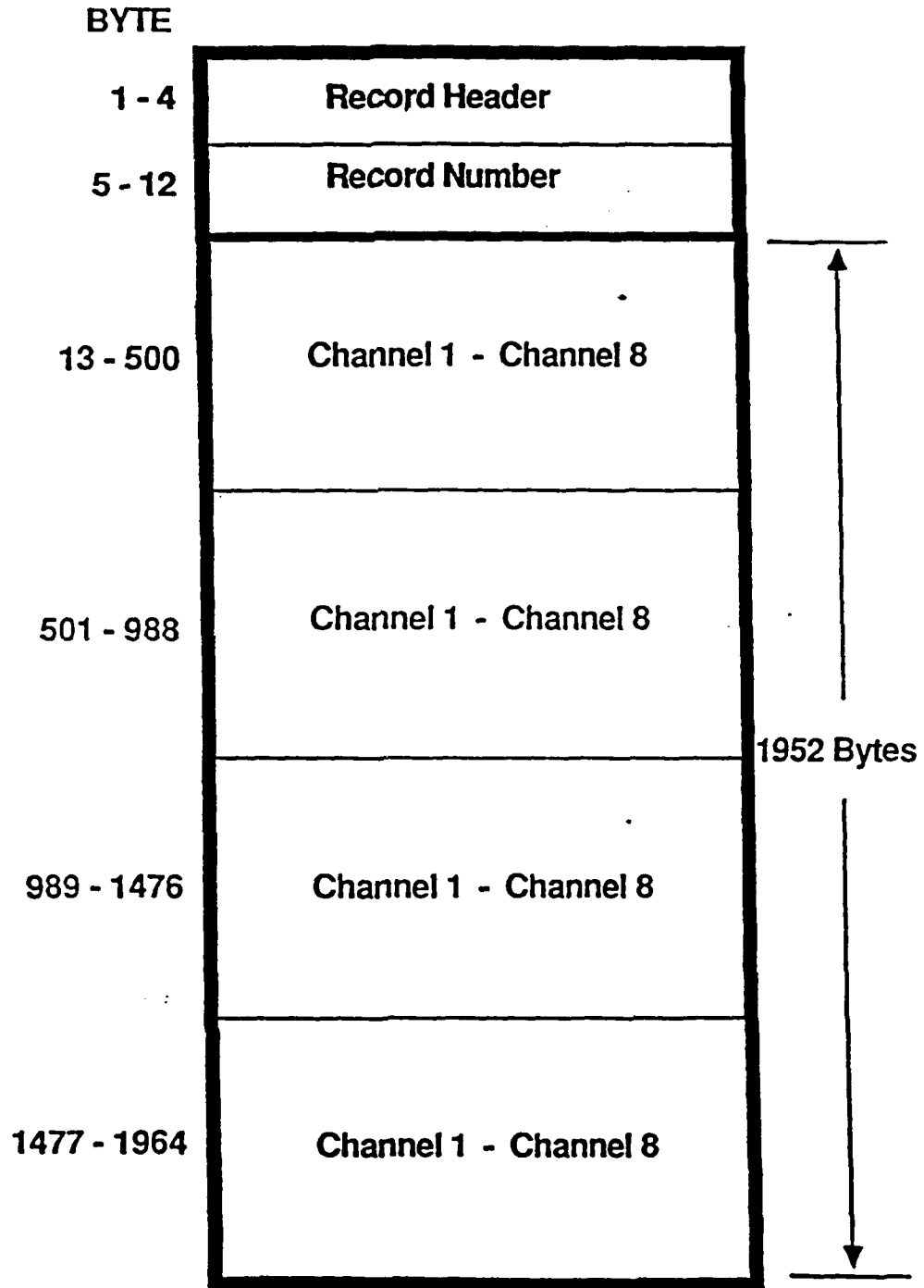


Figure 7

Computer Compatible Tape

Channel 1 - Channel 8

Sub-Record

BYTE	
1 - 8	Pass Pulse Number
9 - 68	Channel 1 - Alternate I & Q Samples for 40 range gates (80 Samples)
69 - 128	Channel 2
129 - 188	Channel 3
189 - 248	Channel 4
249 - 308	Channel 5
309 - 368	Channel 6
369 - 428	Channel 7
429 - 488	Channel 8

$$\frac{6 \text{ BITS}}{\text{SAMPLE}} \frac{80 \text{ SAMPLES}}{\text{CHANNEL}} \frac{1 \text{ BYTE}}{8 \text{ BITS}} = \frac{60 \text{ BYTES}}{\text{CHANNEL}}$$

Figure 8

time. Following the mission and pass information are the channel polarizations, the channel attenuator settings, the pulse information, the aircraft starting and ending positions, boresight angles and range, clutter patch information and finally ARC calibration information. The data components, their location in the Pass-Header Record, their data types and descriptions are as follows:

BYTES	PASS-HEADER RECORD FORMAT SUB-FIELD NAME	DATA FORMAT
13 - 16	Mission Number Range: 1 - 16,383	I4
17 - 76	Mission Title ASCII string	A60
77 - 82	Mission Date YYMMDD	A6
83 - 86	Mission Time (HHMM) At time of plane power up.	A4
87 - 90	Pass Number Range: 1 - 99	I4
91 - 94	Pass Time (HHMM) At major cycle zero time.	A4
95 - 110	Channel 1-8 Polarizations (H, V, -, as inputs)	8 A2
111 - 142	Channel 1-8 Attenuator Settings (dB)	8 I4
143 - 150	Channel Type (B=bistatic,M=monostatic)	8 A1
151 - 158	BS Range Gate Delay (nanosec)	I8
159 - 162	BS Sample Interval (nanosec)	I4
163 - 166	BS Pulse Length (nanosec)	I4
167 - 170	Number of Bistatic Samples	I4
171 - 178	BS Altitude (feet)	I8
179 - 186	BS Start Map Waypt. (Lat) (SDDD.MMM)	F8.3

187 - 194	BS Start Map Waypt. (Long) (SDDD.MMM)	F8.3
195 - 202	BS End Map Waypt. (Lat) (SDDD.MMM)	F8.3
203 - 210	BS End Map Waypt. (Long) (SDDD.MMM)	F8.3
211 - 218	BS Boresight Azimuth Angle (SDDD.M)	F8.3
219 - 226	BS Boresight Elevation Angle (SDDD.M)	F8.3
227 - 234	BS Boresight Range (feet)	I8
235 - 242	BS Grazing Angle (SDDD.MMM)	F8.3
243 - 250	BS Squint Angle (SDDD.MMM)	F8.3
251 - 258	MS Range Gate Delay (nanosec)	I8
259 - 262	MS Sample Interval (nanosec)	I4
263 - 266	MS Pulse Length (nanosec)	I4
267 - 270	MS Samples	I4
271 - 278	MS Altitude (feet)	I8
279 - 286	MS Start Map Waypt. (Lat) (SDDD.MMM)	F8.3
287 - 294	MS Start Map Waypt. (Long) (SDDD.MMM)	F8.3
295 - 302	MS End Map Waypt. (Lat) (SDDD.MMM)	F8.3
303 - 310	MS End Map Waypt. (Long) (SDDD.MMM)	F8.3
311 - 318	MS Boresight Azimuth Angle (SDDD.M)	F8.3
319 - 326	MS Boresight Elevation Angle (SDDD.M)	F8.3
327 - 334	MS Boresight Range (feet)	I8

335 - 342	MS Grazing Angle (SDDD.MMM)	F8.3
343 - 350	MS Squint Angle (SDDD.MMM)	F8.3
351 - 358	Start Clutter (Lat)(SDDD.MMM)	F8.3
359 - 366	Start Clutter (Long)(SDDD.MMM)	F8.3
367 - 374	End Clutter (Lat)(SDDD.MMM)	F8.3
375 - 382	End Clutter (Long)(SDDD.MMM)	F8.3
383 - 390	Start Clutter Altitude (feet)	I8
391 - 398	End Clutter Altitude (feet)	I8
399 - 402	Number of ARCs	I4
403 - 406	ARC Serial Number	I4
407 - 430	ARC Position (X,Y,Z)(feet)	3 I8
431 - 446	ARC Position (Lat,Long)	2 F8.3
447 - 454	ARC Altitude (feet)	I8
455 - 456	ARC Receiver Polarization (H,V)	A2
457 - 460	ARC Time Delay (nanosec)	I4
461 - 464	ARC Doppler Offset (Hz)	I4
465 - 466	ARC BS Transmitter Polariz.(H,V)	A2
467 - 474	BS ARC Power Gain (dB)	F8.3
475 - 482	BS Receiver Azimuth Angle (SDDD.MMM)	F8.3
483 - 490	BS Receiver Elevation Angle (SDDD.MMM)	F8.3
491 - 492	ARC MS Transmitter Polariz.(H,V)	A2
493 - 500	MS ARC Power Gain (dB)	F8.3
501 - 508	MS Recv.&Trans. Azimuth Angle (SDDD.MMM)	F8.3

509 - 516 MS Recv.&Trans. Elevation Angle F8.3
(SDDD.MMM)

517 - 1578 ARCs 2 through 10 (same format)

1578- 1964 Not Used

* note: If less than 10 ARCs are used, fill remaining matrix with zeros.

3.2 ATTENUATION RECORD

There is one post-pass attenuation record. This record contains up to five different Signal Generator Power Levels and six bit samples of receiver output for each signal increment and each attenuator setting, both in-phase and quadrature, squared and summed. The data components, their location in the Post-Pass Attenuation Record, their data types and descriptions are as follows:

POST-PASS ATTENUATION RECORD FORMAT

BYTES	SUB-FIELD NAME	DATA FORMAT
Signal Generator Power Level		
	CP(J) J = 1, 5 Signal Increments	
13 - 20	CP(1) dB	F8.3
21 - 28	CP(2) dB	F8.3
.	.	.
45 - 52	CP(5) dB	F8.3
	M(I, J) I = 0..70 Attenuator Settings J = 1..5 Signal Increments	
	6 Bit Sample of Receiver Output, both in-phase and quadrature, are squared and summed and stored in zero extended integer*4, in column major order	
53 - 56	M(0, 1)	I4
57 - 60	M(1, 1)	I4
61 - 64	M(2, 1)	I4
65 - 68	M(3, 1)	I4
.	.	.

333 - 336	M(70, 1)	I4
337 - 340	M(0, 2)	I4
341 - 344	M(1, 2)	I4
1469 - 1472	M(70, 5)	I4
1473 - 1964	Not Used	

3.3 ANTENNA PATTERN RECORDS

We expect up to ten antenna patterns for each plane, and two records per pattern. The record type indicates whether it is the first or second record. Included in these records are the number of antenna patterns, the ID number, the antenna orientations, and the initial, final and delta azimuth and elevation angles. The gain is written for each azimuth and elevation position. If the matrices are not filled with measured values, the empty elements are filled with zeros. The data components, their location in the Antenna Pattern Records, their data types and descriptions are as follows:

ANTENNA PATTERN RECORD FORMAT		
BYTES	SUB-FIELD NAME	DATA FORMAT
13 - 16	Number of Antenna Patterns Pattern per Pedestal Orientation	I4
17 - 20	Antenna Pattern ID Number (1 <= n <= 10)	A4
21 - 28	Antenna Orientation Pedestal Pitch degrees	F8.3
29 - 36	Antenna Orientation Pedestal Roll degrees	F8.3
37 - 44	Antenna Orientation Pedestal Yaw degrees	F8.3
45 - 52	Initial Azimuth Angle (SDDD.MMM)	F8.3
53 - 60	Final Azimuth Angle (SDDD.MMM)	F8.3
61 - 68	Delta Azimuth Angle (SDDD.MMM)	F8.3
69 - 76	Initial Elevation Angle (SDDD.MMM)	F8.3
77 - 84	Final Elevation Angle (SDDD.MMM)	F8.3

85 - 92	Delta Elevation Angle (SDDD.MMM)	F8.3
	AP (I, J) J = 1..10 Azimuth Position K = 1..30 Elevation Position	
93 - 100	AP(1, 1) dB	F8.3
101 - 108	AP(2, 1) dB	F8.3
...		
165 - 172	AP(10, 1) dB	F8.3
173 - 180	AP(1, 2) dB	F8.3
...		
1285 - 1292	AP(10, 15) dB	F8.3
1293 - 1298	Version Validation Date MMDDYY	A6
1299 - 1964	Not Used	

The above format is repeated for antenna pattern records. Again, the only difference is the record type in Bytes 1-4, indicating which antenna and which record.

3.4 AUXILIARY DATA RECORD DEFINITION

The auxiliary data record contains information about the two aircraft and UHF beacons necessary to process the information recorded. All of the data components are four or eight byte integer or four byte real variables. The data components, their location in the Auxiliary Record, their data types and descriptions are as follows:

AUXILIARY DATA RECORD FORMAT

BYTES	SUB-FIELD NAME	DATA FORMAT
13 - 16	Major Count (seconds)	I4
17 - 20	Minor Count (seconds)	I4
21 - 28	BS Beacon X Coordinate (feet)	I8
29 - 36	BS Beacon Y Coordinate (feet)	I8
37 - 44	BS Beacon Z Coordinate (feet)	I8
45 - 52	INS BS A/C N/S Velocity Knots (North = +, South = -)	F8.3
53 - 60	INS BS A/C E/W Velocity Knots (East = +, West = -)	F8.3
61 - 108	BS Acceleration (G's)	3 F16.6
109 - 116	BS INS True Heading (SDDD.M)	F8.3
117 - 124	BS INS Roll (SDDD.MMM)	F8.3
125 - 132	BS INS Pitch (SDDD.MMM)	F8.3
133 - 140	BS INS Yaw (SDDD.MMM)	F8.3
141 - 148	Commanded BS Roll (SDDD.MMM)	F8.3
149 - 156	Commanded BS Pitch (SDDD.MMM)	F8.3
157 - 164	Commanded BS Yaw (SDDD.MMM)	F8.3
165 - 172	Delta Commanded BS Roll (SDDD.MMM)	F8.3
173 - 180	Delta Commanded BS Pitch (SDDD.MMM)	F8.3
181 - 188	Delta Commanded BS Yaw (SDDD.MMM)	F8.3
189 - 204	BS Power Meter (dB)	F16.6
205 - 212	BS Radar Word (all blanks=OK)	A8
213 - 220	MS Beacon X Coordinate (feet)	I8
221 - 228	MS Beacon Y Coordinate (feet)	I8

229 - 236	MS Beacon Z Coordinate (feet)	I8
237 - 244	INS MS A/C N/S Velocity Knots (North = +, South = -)	F8.3
245 - 252	INS MS A/C E/W Velocity Knots (East = +, West = -)	F8.3
253 - 300	MS Acceleration (G's)	3 F16.6
301 - 308	MS INS True Heading (SDDD.M)	F8.3
309 - 316	MS INS Roll (SDDD.MMM)	F8.3
317 - 324	MS INS Pitch (SDDD.MMM)	F8.3
325 - 332	MS INS Yaw (SDDD.MMM)	F8.3
333 - 340	Commanded MS Roll (SDDD.MMM)	F8.3
341 - 348	Commanded MS Pitch (SDDD.MMM)	F8.3
349 - 356	Commanded MS Yaw (SDDD.MMM)	F8.3
357 - 364	Delta Commanded MS Roll (SDDD.MMM)	F8.3
365 - 372	Delta Commanded MS Pitch (SDDD.MMM)	F8.3
373 - 380	Delta Commanded MS Yaw (SDDD.MMM)	F8.3
381 - 396	MS Power Meter (dB)	F16.6
397 - 404	MS Radar Word (all blanks=OK)	A8
405 - 1954	Not Used	

3.5 CHANNEL DATA RECORD DEFINITION

The channel data record contains collected data for each channel and each pass in the experiment. All of the data components, except the pass pulse number, are six bit digital values, alternating between in-phase (I) and quadrature (Q) samples. The data components, their location in the Channel Data Record, their data types and descriptions are as follows:

CHANNEL DATA RECORD FORMAT

BYTES	SUB-FIELD NAME	DATA FORMAT
13 - 20	Pass pulse number	I8
21 - 80	Channel 1 I & Q Data	6 bit BCD

1 -	6 bits	I data for Range Gate 1	6 bit BCD
7 -	12 bits	Q data for Range Gate 1	6 bit BCD
13 -	18 bits	I data for Range Gate 2	6 bit BCD
19 -	24 bits	Q data for Range Gate 2	6 bit BCD
25 -	30 bits	I data for Range Gate 3	6 bit BCD
31 -	36 bits	Q data for Range Gate 3	6 bit BCD
.			
.			
469 -	474 bits	I data for Range Gate 40	6 bit BCD
475 -	480 bits	Q data for Range Gate 40	6 bit BCD
81 -	140	Channel 2 I & Q Data Using same format as bits 1-480	6 bit BCD
141 -	200	Channel 3 I & Q Data Using same format as bits 1-480	6 bit BCD
201 -	260	Channel 4 I & Q Data Using same format as bits 1-480	6 bit BCD
261 -	320	Channel 5 I & Q Data Using same format as bits 1-480	6 bit BCD
321 -	380	Channel 6 I & Q Data Using same format as bits 1-480	6 bit BCD
381 -	440	Channel 7 I & Q Data Using same format as bits 1-480	6 bit BCD
441 -	500	Channel 8 I & Q Data using same format as bits 1-480	6 bit BCD
501 -	508	Pass Pulse Number	18
509 -	988	Channel 1 through 8 I&Q Data Using same format as bytes 10-489	6 bit BCD
989 -	996	Pass Pulse Number	18
997 -	1476	Channel 1 through 8 I&Q Data Using same format as bytes 10-489	6 bit BCD
1477 -	1484	Pass Pulse Number	18
1485 -	1964	Channel 1 through 8 I&Q Data Using same format as bytes 10-489	6 bit BCD

APPENDIX A

Below is a list of abbreviations and acronyms used in this document.

ACRONYM	DEFINITION
ARC	Active Radar Calibrator
CCT	Computer Compatible Tape
MMDDYY	Month/Day/Year
BSXM	Bistatic Transmitter
MRBR	Monostatic-Bistatic Receiver
M _{SL}	Measured at Sea Level
A/C	Aircraft
Lat	Latitude
Long	Longitude
N/S	North/South
E/W	East/West
Accel	Acceleration
I	In-Phase
Q	Quadrature

LIST OF REQUIREMENTS

Regularity of Auxiliary Data with minimal flexibility,
1 Auxiliary record per 12 or 13 Channel Data records.

Provide an antenna pattern mesh, azimuth and elevation positions
define the mesh, not just random points.

The order of channels should be the same order they are recorded
and should be well defined.

The Clutter patch elevation means and boresight values should be
nominal.

The attenuation table indices should correspond to the settings.

All array elements on the CCT not containing values should be filled
with zeros. Along the same line, all measured values should be
placed in the upper left corner of the matrix.

Attenuator setting 1 should correspond to 1 dB or be well defined.

The ordering of records is important, those records which occur only
once per pass should be recorded first.

THIS PAGE INTENTIONALLY LEFT BLANK.

DESIGN PLAN
FLIGHT DATA PROCESSING
SOFTWARE FUNCTIONAL SPECIFICATION
ELIN A003

CONTRACT TITLE: BISTATIC CLUTTER PHENOMENOLOGICAL
MEASUREMENT/MODEL DEVELOPMENT

CONTRACT NUMBER: F30602-86-C-0045

CONTRACT PERIOD: 1 APRIL 1986 - 30 SEPTEMBER 1987

PREPARED BY: DAVID M. MAESCHEN

DATE: 15 JUNE 1987

Prepared for:
ROME AIR DEVELOPMENT CENTER
GRIFFISS AIR FORCE BASE
NEW YORK 13441-5700

SRS

TECHNOLOGIES

ADVANCED TECHNOLOGY DIVISION
17252 ARMSTRONG AVENUE
IRVINE, CALIFORNIA 92714
(714) 250-4206

1.0 INTRODUCTION

The Hybrid Bistatic Radar Clutter Measurements Program will collect calibrated monostatic and bistatic radar clutter data at L-band. Numerous missions over various terrains will be flown. Each mission will correspond to a matrix of scattering geometries while each pass will correspond to a specific geometry and represent about five minutes of data collection. There will be an external calibration pass with illuminating Active Radar Calibrators (ARCs) prior to each mission at a geometry chosen to avoid multipath effects on the ARC signals. Before and after each pass an internal receiver calibration will also be performed. Calibration for the bistatic and the monostatic radar antenna patterns will also be available from other flights made solely for this purpose.

During each pass, eight channels consisting of linearly polarized monostatic and bistatic clutter will be coherently sampled and recorded. Each channel will be sampled for forty range gates centered about the nominal aimpoint. The samples will be recorded as six bit digital in-phase and quadrature (I+Q) data. Position, velocity, and acceleration of each aircraft position are also recorded as auxiliary data.

The objective of Computer Compatible Tape (CCT) signal processing is to derive a time series of calibrated normalized surface scattering coefficients for later data analysis. Computation of the normalized surface scattering coefficient from the calibrated clutter power requires assumption of a scattering model. Initially a uniform scattering model independent of polarization and terrain will be used, for its simplicity, comparison with other data, and ease of recovery of the original data. Subsequent data analysis will utilize more sophisticated models. Estimates of the scattering coefficient will be retained along with all data necessary for later processing.

2.0 MISSION CCT SIGNAL PROCESSING

The structure of the signal processing procedure is briefly summarized here and in the flow chart below. Description of individual software modules are discussed in the following section. The external calibration processing will be performed first.

2.1 External calibration processing

The internal and external calibration are complementary. Internal calibration is performed to remove receiver nonlinearities and estimate power measured at the receiver input. External calibration will provide a known reference signal from an Active Radar Calibrator (ARC) located in the radar field of view. Internal calibration

will provide a power calibration curve for the digital samples, while external calibration will provide an absolute level at one point on the curve. Internal calibration will be performed first, and external calibration will scale the internally calibrated results to an absolute power level. If the internal and external calibrations are significantly different it will be a cause for concern which will have to be addressed during analysis.

The external calibration passes will be processed to derive a scale factor to convert measured clutter power to absolute clutter power. A window about each ARC will be searched and presumably the ARC will be detected. Its I and Q magnitude (I^2+Q^2) will be internally calibrated, and effects of antenna main beam gain, antenna patterns, transmit power, and transmitter and receiver ranges will also be removed. This measured magnitude will be compared to its expected magnitude. The average ratio of expected to measured magnitudes will form the scale factor.

It will be assumed this scale factor is independent of absolute clutter power level and geometry. The processing of the external calibration pass is similar to the other passes, but the scale factor determined from it will be used for all passes during the mission.

2.2 Retrieve invariant pass information

Before any pass is processed an internal calibration table and attenuation setting table are established from the pre and post pass measurements. These will be used to convert recorded I and Q samples to voltages at the receiver input, eliminating any receiver nonlinearities. Antenna patterns will be retrieved and stored for computation of beam weighted areas.

2.4 Process ARCs

The data will then be processed twice. Initially, selected time segments and range doppler cells will be examined for ARC detection. The ARC locations will provide an indication of the UHF/beacon positioning system accuracy, assuming the ARC remains in the ground clutter patch of interest. The ARC strengths during the external calibration passes will be used for calibration for the rest of the mission, as mentioned in Section 2.1.

After the ARCs have been processed, the calibration scale factor from the external calibration pass will be entered. This value will be used to scale the internal calibration table previously established.

2.5 Process clutter data

On the second pass though the CCT, all the clutter data will be processed for a normalized scattering coefficient time series. This will involve predicting the platform positions, locating the aimpoint range gate, calibrating the data, interpolating at the range gate, accumulating a number of time samples for each channel, doppler filtering them, and sampling the aimpoint doppler frequency bin.

Only the range doppler cell at the system aimpoint will be considered. A data reduction from 40 range gates and 64 pulses to 1 sample, a factor of 2560, will reduce the scattering coefficient data to about 2500 complex samples per channel per pass.

The monostatic transmitter and receiver are located at the bistatic receiver. Monostatic data will not be affected much by position errors, but both monostatic and bistatic data will be corrected for them. As near as possible, the monostatic and bistatic scattering areas processed will be centered on the system aimpoint. The difference between bistatic and monostatic range doppler cell geometries will not allow comparison of scattering coefficient data on a sample to sample basis.

The data upon which monostatic and bistatic processing is performed, antenna patterns, platform positions, ARC positions, aimpoint range-doppler, beam weighted areas, and channels are different, however their processing is similar.

2.6 Structured program definition

The command module program flow may be briefly encapsulated as follows.

For each clutter data collection pass

 Retrieve invariant pass information

 Process ARCs ?

 For each ARC

 Locate window about ARC

 For data

 Process data

 Search for ARC

 Next data

 Save time, location, and magnitude

 Next ARC

Compute calibration factor

Enter calibration factor

Save calibration factor and scale calibration table

For clutter data

Process data

Save time, data quality, positions, velocities,
complex scattering coefficient

Next data

Next pass

2.7 Process data functional definition

The "Process data" step shown above refers to computing the clutter scattering coefficient from a selected set of range-doppler cells. It is the most critical function performed by this software. Specifically it will perform the following functions.

Predict aircraft positions

Locate aimpoint range gate

Calibrate

Range gate interpolate

Motion compensate (optional)

Coherent process and sample

Compute beam weighted areas

Compute normalized scattering coefficient

Assess data quality

3.0 MODULE DEFINITION

The program has been separated into three basic modules, the Executive module, the Process ARCs module, and the Process clutter data module. Each of these modules has been divided into submodules which perform specific functions for those modules. These modules and submodules detail the program flow as defined in Section 2.

3.1 Executive module

The executive module of the program will access each CCT record and determine what processing to undertake. Header, pass, calibration, and pattern data will be used to initialize the program. Auxiliary records will be examined until the recorded time falls within a prescribed interval, possibly any interval. Then the auxiliary and channel records will be processed. If an end of file or end of tape condition is reached, the next file or tape will be accessed.

The channel data is stored in six bit digital words which will need to be unpacked prior to processing. A submodule will perform the bit manipulation necessary for this, for any sample and any channel.

The time, platform positions, velocities, normalized scattering coefficient, among other variables, will be saved for analysis.

The basic processing modules are described in more detail below.

3.2 Process ARCs

The Process ARCs module is composed of several submodules to detect the ARCs and compute an external calibration factor from the ARC magnitudes. Only if the ARCs are significantly above the competing clutter will they be of any use.

3.2.1 Locate window about ARC

This module utilizes the clutter patch position, ARC positions, ARC range doppler offsets, and platform velocities to compute the approximate time and location of the ARCs in the recorded data. A time window and a range doppler window is computed about each ARC to search. A time window of 6 seconds, and a range doppler window of 10 range gates and 1 doppler bin should be adequate.

3.2.2 Process data

This module replicates the functions of the process data module below. It computes the clutter scattering coefficient from a selected set of range-doppler cells. Several range doppler cells will be coherently processed for ARC detection, and the cells processed will be offset from the system aimpoint by the builtin device time delays and phase shifts. The ARC magnitude is converted to a normalized clutter coefficient appropriate for a discrete.

3.2.3 Search for ARC

The selected set of range doppler cells within the time window will be searched for the maximum return which exceeds the clutter by a 20 db threshold. For those ARCs detected, the time, location, and magnitude is noted. The location is only significant as the difference between calculated and detected positions, and the magnitude is significant for external calibration passes. ARC information available on multiple channels of the monostatic or bistatic system will be averaged.

3.2.4 Compute calibration factor

As described in Section 2.1, this module will compute the external calibration scale factor, the mean ratio of expected to measured magnitude of the ARCs. This value from the external calibration pass will be used to scale the internal calibration table.

3.3 Process clutter data

The process clutter data module is composed of a number of submodules to correct for platform positioning errors and compute the normalized clutter scattering coefficient for a selected range doppler cell.

3.3.1 Predict aircraft positions

The aircraft and aimpoint positions will be calculated from the auxiliary data. The altitude of each aircraft may be derived from the altimeter data corrected for barometric pressure for better accuracy. Other than altitude, the receiver is slaved to the transmitter and all position corrections are made to the receiver position. For this reason the aimpoint will be assumed to be fixed relative to the transmitter and all position errors assumed to be due to the receiver. These may be smoothed and extrapolated between samples using a Kalman filter.

3.3.2 Locate aimpoint range gate

Using the position information, the aimpoint time delay $t = (|r1|+|r2|)/c$ will be computed, where $r1$ and $r2$ are the transmitter and receiver ranges respectively, and c the speed of light. The range gate will be taken to lie between the aimpoint time delay t and $t + dt$, where dt is the pulse duration. Positioning errors measured by the ARCs may also be accounted for here, by interpolating between ARC measured locations and correcting the range gate selected. In general, the range gates sampled will not correspond to the aimpoint sample and interpolation between range gate samples will be necessary. The monostatic data corresponding to the same aimpoint as the bistatic data will be selected and processed similarly.

3.3.3 Calibrate

Initially, this module processes the pre and post pass calibration measurements and attenuator information to produce tables for calibration for conversion of digital samples to received power. External calibration scale factor computed above, Section 2.1, will then convert this received power to absolute clutter power scattered. The calibration curves will, in general, be nonlinear.

Having located the aimpoint range gate, the samples within and around the gate will be calibrated. The attenuation will be removed and the pre and post pass internal calibration measurements with interpolation may be used. It will be assumed the phase errors are independent of signal strength, and calibration of signal magnitude is sufficient. Signal phase will be retained for coherent processing.

3.3.4 Range gate interpolate

After calibration of the samples, interpolation will be used to estimate the scattered power in the I+Q channels at the computed range gate.

3.3.5 Motion compensate

For coherent processing it may be necessary to perform motion compensation of the data due to fine scale platform motion. The INS velocity and acceleration data on the auxiliary records may be used in the computation of motion smaller than the pulse duration, and the resulting position offsets, dr , used for phase correction. Phase correction for fine scale motion may be done by scaling each complex sample by $\exp(-ik*dr)$.

3.3.6 Coherent process and sample

For coherent processing, 64 complex aimpoint time samples corresponding to 128 ms or 7.8125 Hz will be accumulated and doppler filtered by Fast Fourier Transform. The complex doppler sample nearest to or interpolated about the aimpoint will be selected. The sample selected will be different for the monostatic and bistatic radars due to different doppler frequency shifts at beam center in the out-of-plane cases.

3.3.7 Compute beam weighted area

This module processes the antenna patterns, and computes the constants, K and I , for the geometry and range doppler cell of interest. These, together with transmit power, will be used to convert calibrated clutter power to normalized scattering coefficient for the uniform scattering model.

$$K = \frac{L_t L_r G_t G_r \lambda^2}{(4\pi)^2}$$

$$I = \int_{A_c} \frac{f_t(x,y) f_r(x,y)}{R_t^2 R_r^2} dx dy$$

$$\sigma_{pq}^o = \frac{P_{c,q}}{P_{t,p} K I}$$

λ	Wavelength
A_c	Clutter area
$L_t L_r$	Transmitter and receiver losses
$G_t G_r$	Transmitter and receiver gains
$f_t f_r$	Transmitter and receiver antenna patterns
$R_t R_r$	Transmitter and receiver ranges
$P_{c,q}$	Clutter power q polarization
$P_{t,p}$	Transmit power p polarization

3.3.8 Compute normalized scattering coefficient

Each calibrated coherent sample will be converted to a complex normalized scattering coefficient by this module, initially utilizing a uniform scattering model. The receive power will be normalized by the transmit power and the beam weighted area as shown in Section 3.3.7. All variables necessary for later, possibly dynamic, modeling using statistical models will be retained for post processing.

3.3.9 Assess data quality

Data quality will be assessed throughout the processing by this module. A number of quantities will be computed and compared to a previously selected value range. For each quantity, a corresponding bit will be set in a data quality flag when the quantity lies outside this range. This will provide an indication of when and why the data may be suspect. Such quantities as an external magnitude calibration scale factor outside a 3 db range (relative to the internal calibration) or ARCs less than 20db above competing clutter, positions errors greater than 100 feet, velocity errors greater than 10 knots, heading errors greater than 1 degree, accelerations of greater than 0.1 g, and transmit power changes of greater than 100 Watts, will be used.

4.0 CONCLUSION

The signal processing software has been described. At the end of this processing a computed time series of calibrated normalized scattering coefficients will then be available for analysis.

DISTRIBUTION LIST

ROBERT F. OGDONIK RADC/OCTM	8
RADC/DOVL GRIFFISS AFB NY 13441	1
RADC/DAP GRIFFISS AFB NY 13441	2
ADMINISTRATOR DEF TECH INF CTR ATTN: DTIC-DDA CAMERON STA BG 5 ALEXANDRIA VA 22304-6145	5
Director DMAAC (Attn: RE) 3200 S. Second St. St Louis MO 63118-3399	1
AFCSA/SAMI Attn: Miss Griffin 10363 Pentagon Wash DC 20330-5425	1
SAF/AQSC Pentagon 4D-267 Wash DC 20330-1000	1
Fleet Analysis Center Attn: GIDEP Operations Center Code 30G1 (E. Richards) Corona CA 91720	1
HQ AFSC/DLAE ANDREWS AFB DC 20334-5000	1
HQ AFSC/XRT Andrews AFB MD 20334-5000	1

HQ AFSC/XRK 1
ANDREWS AFB MD 20334-500

HQ SAC/NRI 1
OFFUTT AFB NE 68113-5001

DTEA/RQEE 1
ATTN: LARRY G.MCMANUS
2501 YALE STREET SE
Airport Plaza, Suite 102
ALBUQUERQUE NM 87106

HQ TAC/DOA 1
LANGLEY AFB VA 23665-5001

HQ TAC/DRCC 1
LANGLEY AFB VA 23665-5001

HQ TAC/DRCA 1
LANGLEY AFB VA 23665-5001

AFWL/NTAAB 1
Attn: Dr Carl E. Baum
Kirtland AFB NM 87117-6008

ASD/AFALC/AXAE 1
Attn: W. H. Dungey
Wright-Patterson AFB OH 45433-6533

ASD/ENAMW 1
Wright-Patterson AFB OH 45433-6503

ASD/ENAMA 1
Wright-Patterson AFB OH 45433

AFIT/LDEE 1
BUILDING 640, AREA B
WRIGHT-PATTERSON AFB OH 45433-6583

AFWAL/MLPO 1
Attn: G. H. Griffith
Wright-Patterson AFB OH 45433-6533

AFWAL/MLPO 1
WRIGHT-PATTERSON AFB OH 45433-6533

AFWAL/FIES/SURVIAC 1
WRIGHT-PATTERSON AFB OH 45433

AAMRL/HE 1
WRIGHT-PATTERSON AFB OH 45433-6573

2750 ABW/SSLT 1
Bldg 262
Post 11S
Wright-Patterson AFB OH 454433

1843EIG/EIEM 1
HICKAM AFB HI 96854

AUL/LSE 1
MAXWELL AFB AL 36112-5564

HQ AFSPACECOM/XPYS 1
ATTN: DR. WILLIAM R. MATOUSH
PETERSON AFB CO 80914-5001

3280TTG/BISS 1
Attn: TSgt Kirk
Lackland AFB TX 78236

HQ Air Training Command 1
TTOI
Randolph AFB TX 78150-5001

HQ ATC/TTOK 1
Randolph AFB TX 78150-5001

Defense Communications Engineering Ctr 1
Technical Library
1860 Wiehle Avenue
Reston VA 22090-5500

COMMAND CONTROL AND COMMUNICATIONS DIV 2
DEVELOPMENT CENTER
MARINE CORPS DEVELOPMENT & EDUCATION COMMAND
ATTN: CODE DIOA
QUANTICO VA 22134-5080

U.S. Army Strategic Defense Command 1
Attn: DASD-H-MPL
P.O. Box 1500
Huntsville AL 35807-3801

COMMANDING OFFICER 1
NAVAL AVIONICS CENTER
LIBRARY - D/765
INDIANAPOLIS IN 46219-2189

COMMANDER 1
NAVAL OCEAN SYSTEMS CENTER
ATTN: TECHNICAL LIBRARY, CODE 9642B
SAN DIEGO CA 92152-5000

COMMANDER (CODE 3433) 1
ATTN: TECHNICAL LIBRARY
NAVAL WEAPONS CENTER
CHINA LAKE, CALIFORNIA 93555-6001

SUPERINTENDENT (CODE 1424) 1
NAVLA POST GRADUATE SCHOOL
MONTEREY CA 93943-5000

COMMANDING OFFICER 2
NAVAL RESEARCH LABORATORY
ATTN: CODE 2627
WASHINGTON DC 20375-5000

SPACE & NAVAL WARFARE SYSTEMS COMMAND 1
PMW 153-3DP
ATTN: R. SAVARESE
WASHINGTON DC 20363-5100

CDR, U.S. ARMY MISSILE COMMAND 2
REDSTONE SCIENTIFIC INFORMATION CENTER
ATTN: AMSMI-RD-CS-R (DOCUMENTS)
REDSTONE ARSENAL AL 35898-5241

Advisory Group on Electron Devices 2
Hammond John/Technical Info Coordinator
201 Varick Street, Suite 1140
New York NY 10014

UNIVERSITY OF CALIFORNIA/LOS ALAMOS 1
NATIONAL LABORATORY
ATTN: DAN BACA/REPORT LIBRARIAN
P.O. BOX 1663, MS-P364
LOS ALAMOS NM 87545

RAND CORPORATION THE/LIBRARY 1
HELPER DORIS S/HEAD TECH SVCS
P.O. BOX 2138
SANTA MONICA CA 90406-2138

AEDC LIBRARY (TECH REPORTS FILE) 1
MS-100
ARNOLD AFS TN 37389-9998

USAG 1
Attn: ASH-PCA-CRT
Ft Huachuca AZ 85613-6000

JTFPMO 2
Attn: Technical Director
1500 Planning Research Drive
McLean VA 22102

HQ ESC/CWPP 1
San Antonio TX 78243-5000

AFEWC/ESRI 4
SAN ANTONIO TX 78243-5000

485 EIG/EIER (DMO) 2
GRIFFISS AFB NY 13441-6348

ESD/AVS 1
ATTN: ADV SYS DEV
HANSCOM AFB MA 01731-5000

ESD/TCD-2 1
ATTN: CAPTAIN J. MEYER
HANSCOM AFB MA 01731-5000

DIRECTOR 1
NSA/CSS
ATTN: T513/TDL (DAVID MARJARUM)
FORT GEORGE G MEADE MD 20755-6000

DIRECTOR 1
NSA/CSS
ATTN: W166
FORT GEORGE G MEADE MD 20755-6000

DIRECTOR 1
NSA/CSS
ATTN: R-8316 (MR. ALLEY)
FORT GEORGE G MEADE MD 20755-6000

DIRECTOR 1
NSA/CSS
ATTN: R24
FORT GEORGE G MEADE MD 20755-6000

DIRECTOR 1
NSA/CSS
ATTN: R21
9800 SAVAGE ROAD
FORT GEORGE G MEASDE MD 20755-6000

DIRECTOR 1
NSA/CSS
ATTN: R31
FORT GEORGE G MEADE MD 20755-6000

DIRECTOR 1
NSA/CSS
ATTN: R5
FORT GEORGE G MEADE MD 20755-6000

DIRECTOR
NSA/CSS
ATTN: R8
FORT GEORGE G MEADE MD 20755-6000

1

DIRECTOR
NSA/CSS
ATTN: R9
FORT GEORGE G MEADE MD 20755-6000

1

DIRECTOR
NSA/CSS
ATTN: S21
FORT GEORGE G MEADE MD 20755-6000

1

DIRECTOR
NSA/CSS
ATTN: V33 (S. Friedrich)
FORT GEORGE G MEADE MD 20755-6000

1

DIRECTOR
NSA/CSS
ATTN: W07
FORT GEORGE G MEADE MD 20755-6000

1

DIRECTOR
NSA/CSS
ATTN: W3
FORT GEORGE G MEADE MD 20755-6000

1

DIRECTOR
NSA/CSS
ATTN: R523
FORT GEORGE G MEADE MD 20755-6000

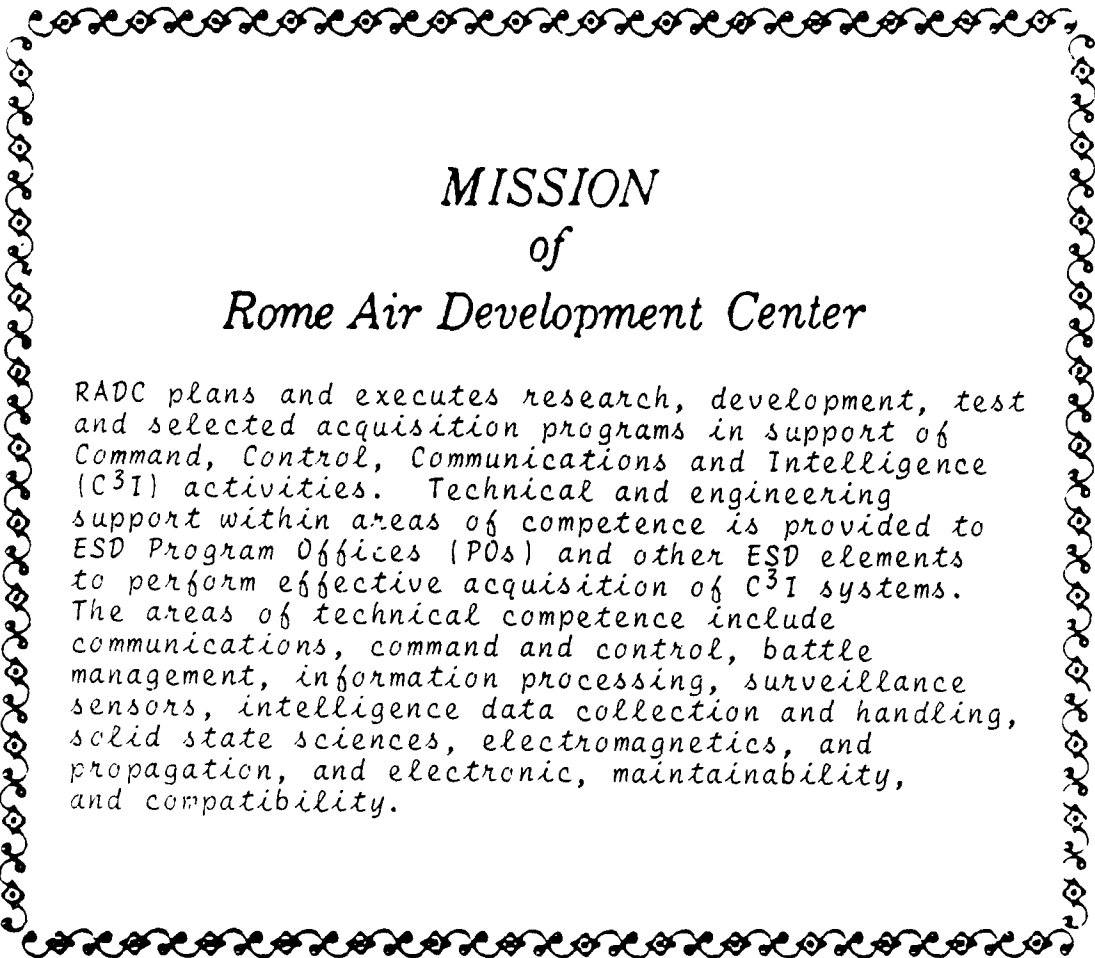
2

DIRECTOR
NSA/CSS
ATTN: R53 (JOHN C. DAVIS)
9800 SAVAGE ROAD
FORT GEORGE G MEADE MD 20755-6000

1

SRS Technologies
ATTN: C. Hightower
17252 Armstrong Ave
Irvine CA 92714

5



*MISSION
of
Rome Air Development Center*

RADC plans and executes research, development, test and selected acquisition programs in support of Command, Control, Communications and Intelligence (C³I) activities. Technical and engineering support within areas of competence is provided to ESD Program Offices (POs) and other ESD elements to perform effective acquisition of C³I systems. The areas of technical competence include communications, command and control, battle management, information processing, surveillance sensors, intelligence data collection and handling, solid state sciences, electromagnetics, and propagation, and electronic, maintainability, and compatibility.